Modelling and Characterisation of the Pyrolysis of Secondary Refuse Fuel Briquettes and Biomass Materials

Yi Liu

Ph.D. Thesis 2010

Modelling and Characterisation of the Pyrolysis of Secondary Refuse Fuel Briquettes and Biomass Materials

by

Yi Liu

A thesis submitted for the award of the degree of Doctor of Philosophy

This research programme was carried out in collaboration with EB Nationwide Limited, Progressive Energy Limited, Cardiff University and Welsh Energy Research Centre (WERC)

Faculty of Advanced Technology
University of Glamorgan

Submitted July 2010

R11

Certificate of Research

This is to certify that, except where specific reference is made, the work described in this thesis is the result of the candidate. Neither this thesis, nor any part of it, has been presented, or is currently submitted, in candidature for any degree at any other University.

Signed 

Candidate

Date 16th July 2010

Abstract

This research was established due to an increase of interest in renewable energy sources and utilisation of various wastes and biomass. Gasification is currently one of the most promising thermal-chemical conversion techniques for recovering energy from waste, and the pyrolytic behaviour of secondary refuse fuel (SRF) briquettes and biomass-derived fuels is the starting point for the process. The purpose of this study was to evaluate the pyrolytic characteristics of SRF briquettes and biomass materials, suggest a kinetic model for simulating the pyrolytic process and obtaining the kinetic parameters, and then predict the yield of volatile products in pyrolysis.

Knowledge of the chemical composition, the thermal behaviour and the reactivity of SRF briquettes and their blends with other materials, such as biomass and plastic during pyrolysis is very important for the effective design operation of gasification units. The kinetics of the pyrolysis of simulated SRF briquettes, SRF briquettes and pulverised biomass samples was successfully modelled by a scheme consisting of two independent general order parallel reactions of the main components which were hemicellulose, cellulose, lignin and plastic. The kinetic parameters estimated through the model were comparable with those reported in the literature. In this research, activation energy values varied between 30 – 70 kJ/mol for lignin pyrolysis, 96 – 137 kJ/mol for hemicellulose and cellulose pyrolysis, and about 260 kJ/mol for plastic pyrolysis.

Biomass has a very high volatile content. Adding biomass into SRF briquettes could increase the volatile yield. Increasing the plastic content of SRF briquettes could increase the volatile yield, the derivative thermogravimetric (DTG) peak height and the repeatability of pyrolysis. Inorganic component could shift the cellulose pyrolysis to a lower temperature and cause the hemicellulose pyrolysis and the cellulose pyrolysis highly overlapped, but it could have a positive effect by acting as catalysts and lower the activation energy in the pyrolysis of hemicellulose and cellulose. Molasses used as a binder could improve the DTG peak height and restrain the curve shifting effect of inorganic component on the hemicellulose and cellulose pyrolysis, but couldn't restrain the lignin pyrolysis at low temperatures during the hemicellulose

and cellulose pyrolysis. Molasses could restrain the effect of the lignin pyrolysis at high temperatures on the plastic pyrolysis. Mechanical biological treatment (MBT) process could highly improve the volatile yield and improve the DTG peak height of SRF briquettes.

Key words: Pyrolysis, Gasification, Secondary refuse fuel (SRF) briquette, Municipal solid waste (MSW), Biomass, Hemicellulose, Cellulose, Lignin, Derivative thermogravimetric (DTG) analysis, Pyrolytic characteristics, Volatile yield, Peak temperature, Activation energy

Acknowledgements

This work has been carried out at the Faculty of Advanced Technology, University of Glamorgan.

First of all, I would like to thank my supervisors Professor Steven Wilcox and Dr. Chee Tan, and Professor John Ward. Their guidance and support have been excellent in all respects.

I would also like to thank my colleagues at the Faculty of Advanced Technology. Many thanks are also to Mr. Gareth Betteney, Senior Technical Officer at the faculty for his kind help and guidance during the experiment.

Finally and most important, I would like to thank my parents for all their encouragement and support.

Porth, July 2010
Yi Liu

Contents

List of Figures

List of Tables

Nomenclature

Symbols

a	result value
a_{mean}	mean result value
e	error
E_a	activation energy, J/mol
k_S	reaction rate coefficient
$k_{S,0}$	pre-exponential factor; frequency factor
$m_{A,t=\infty}$	final ash mass, g
m_S	sample mass, g
$m_{S,0}$	initial mass of dry sample, g
m_t	measured mass, g
n	reaction order
R^2	regression coefficient
r_A	ash mass generation rate, g/s
r_S	sample mass loss rate, g/s
r_t	measured mass loss rate, g/s
T	sample temperature, K
x	constant remaining mass fraction
y	volatile yield

Abbreviations

BMW	biodegradable municipal waste
CV	calorific value
DTG	derivative thermogravimetric
MBT	mechanical biological treatment
MFC	melamine faced chipboard
MSW	municipal solid waste

PAH polycyclic aromatic hydrocarbon

PCDD polychlorinated dibenzodioxin

PCDF polychlorinated dibenzofuran

PE polyethylene

PP polypropylene

PS polystyrene

RCA re-crystallised alumina

RDF refuse-derived fuel

RWE *Rheinisch-Westfälisches Elektrizitätswerk* (a German electric power and natural gas public utility company)

SRF secondary refuse fuel; solid recovered fuel; solid residual fuel

TG thermogravimetric; thermogravimetry

TGA thermogravimetric analysis

Chapter One Introduction

1.1 Motivation

The UK faces a period of unparalleled change in its approach to waste management. In addition to wider environmental and sustainability considerations, the need to meet targets under Article 5 of the EU Landfill Directive relating to the diversion of biodegradable municipal waste (BMW) from landfill represents a particular challenge. The Government announced on 8th September 2010 that they would meet the 2010 Landfill Directive target. In England 14.6 million tonnes of BMW was sent to landfill in 2009 compared to the target for 2010 of about 21.7 million tonnes [1]. The data showed that England was landfilling considerably less waste than its 2010 target. In Wales 0.52 million tonnes of BMW was sent to landfill in 2009 compared to the target for 2010 of about 0.71 million tonnes [2]. While data were still being collated from Scotland and Northern Ireland, the government expressed confidence that it would meet the 2010 target set under the EU Landfill Directive [1]. However, there are two further EU waste targets to be met in 2013 and 2020, and failure to meet the next target could result in an EU penalty of £180 million [3].

One route to divert BMW from landfill is to process unsorted municipal solid waste (MSW) using a mechanical biological treatment (MBT) process, which combines the mechanical sorting of MSW with some kind of biological treatment. The MBT process removes recyclables such as metals and glass with mechanical sorting techniques such as screening and shredding, and diverts bulky inert material to landfill. The remaining organic portion of MSW is BMW which is then treated biologically such as composting or anaerobic digestion. The MBT residue of MSW is about 40% of the original volume and has significant energy value (about 17 GJ/tonne). Therefore, it can be used as a secondary refuse fuel (SRF), also known as solid recovered fuel or solid residual fuel. The introduction of MBT plants offers a more cost-effective route to meet recycling targets.

Although 60% of the original volume of MSW can be reduced through MBT process, landfill of SRF is not efficient due to its significant energy value. It is theoretically

possible to incinerate SRF, but a preferred option is to extract this available energy source using gasification because the process is more efficient, emissions are lower and the amount of residual material (ash and frit) to be landfilled is reduced. This process route is considered by many as a more socially acceptable option. Waste gasification technology also has potential for the co-production of other streams, such as hydrogen (which could be used as a petrol/diesel substitute in vehicles or for fuel cell combined heat and power units), or methanol (used as a chemical feedstock). This process can be implemented at large scale and could provide an option for landfill for 10 – 16 million tonnes per annum of material expected nationally. Approximately 50% of the energy of SRF is biomass and hence the gas produced is "green" to this extent by helping to displace fossil fuels.

Currently there are no suitable commercial technologies available to gasify raw SRF and a manufacturing route is required so that this material can be easily fed into such an energy conversion system. A typical and well-accepted route is to produce fuel briquettes, although the biggest problem is that of prime material variability which can require the use of coal or other material to stabilise the heat content. Experience in Europe and in particular Germany has highlighted that briquetted sorted waste has been successfully gasified since 1992 with an annual output of 120,000 tonnes [4]. This would be an ideal process route for the manipulation of residual material from MBT operations into a useful product – SRF briquettes.

Pyrolysis is thermal decomposition occurring in the absence of oxygen. It is always the first step in the gasification process to partition the briquette into volatiles and char. Pyrolysis is crucial because volatiles are subsequently converted into the ultimate product in a very short time. Today, any major technology development is almost always supported by design calculation schemes. Pyrolytic models apply conservation of mass, momentum, energy, and species to the pyrolytic process. In a general model, five processes (external heat transfer, internal heat transfer, reaction kinetics, internal mass transfer and external mass transfer) are comparable. The kinetic study is one of the most important aspects in understanding SRF briquette pyrolysis. This is important to design and simulate the reactor, to predict the reaction behaviour and to optimise the operating conditions.

The pyrolytic kinetics of SRF briquette is complicated, as it involves a large number of reactions in parallel and series [5]. The thermogravimetric (TG) technique is used for studying the pyrolytic process, since although it has a relative value with respect to establishing reaction mechanisms, it is an essential tool for the determination of the kinetic behaviour and hence for process design and control. Due to the different chemical compositions of the raw materials and experimental methods, such as operating conditions and data analysis, substantial differences in the reported kinetic parameters can be observed [5]. The reactions involved in pyrolysis are complex and involve both endothermic and exothermic processes. SRF briquettes are chemically and physically heterogeneous and their components have different reactivity and yield different product spectra. Although the broad outlines of chemistry are known, understanding of the thermodynamics and the kinetics is inadequate for the development of fundamental models [6].

SRF has a skewed distribution in terms of its composition. It is likely that the plastic fraction is a disproportionately high fraction. This has an impact in terms of both processing and fuel preparation. In this research, a number of simulated SRF briquettes with compositions of differing paper/plastic ratios and at varying extruding temperatures, SRF briquettes derived from waste and pulverised raw biomass materials were tested to investigate the thermal behaviour at the laboratory scale. This research aims to use a pyrolytic kinetic model to determine the pyrolytic characteristics of simulated SRF briquettes, SRF briquettes and pulverised raw biomass materials through thermogravimetric analysis (TGA) in order to optimise the gasification process of SRF briquettes.

1.2 Overview of thesis

The thesis consists of a total of seven chapters. Chapter One gives a brief introduction to the gasification technology of SRF briquettes. This involves motivation and overview of thesis. Chapter Two reviews the current treatment of MSW and related work, and contains a section where new contributions to the research field are discussed. Chapter Three describes the experimental equipment and methodology and the sample composition of simulated SRF briquettes, SRF briquettes and pulverised

raw biomass materials. Chapter Four presents the experimental results of TG and derivative thermogravimetric (DTG) analysis. Chapter Five discusses pyrolytic kinetic models and describes the pyrolytic kinetic results. Chapter Six gives a further description of the results and compares the pyrolytic characteristics of all samples. Chapter Seven provides a short discussion in addition to conclusions and suggestions for future work.

Chapter Two Background

Today's society has a throwaway culture, producing vast quantities of waste. Approximately 434 million tonnes of waste were generated in 2005 in the UK from a variety of sectors [7], as shown in Figure 2.1, according to the Environment Agency.

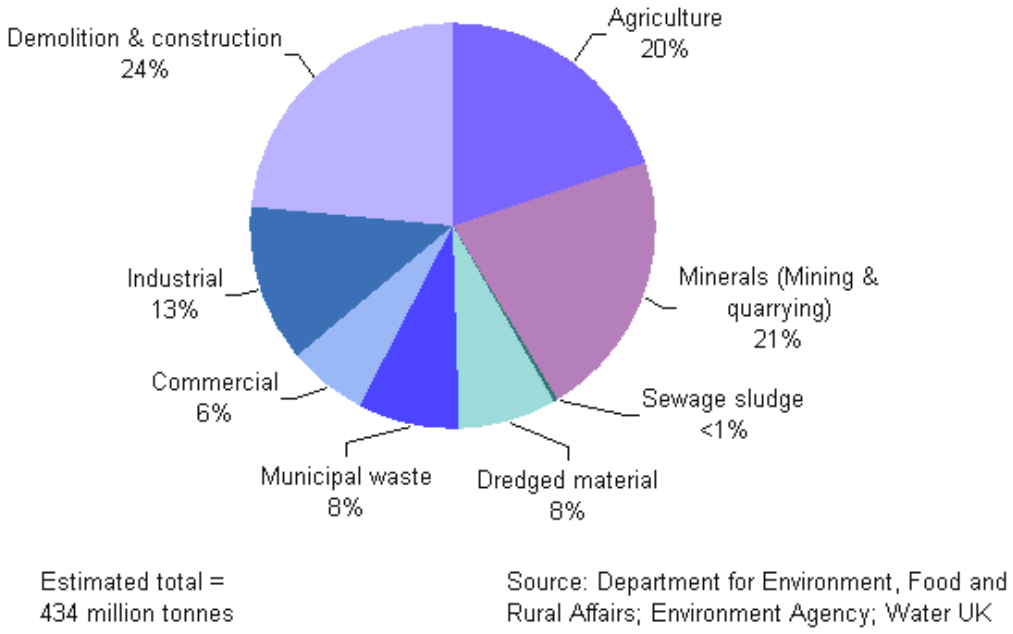

Figure 2.1 Estimated overall UK waste arisings by sector for 2005.

Municipal solid waste includes paper, containers, tin cans, plastics, aluminium cans, food scraps and sewage. It is the solid component of the waste stream arising from the household waste placed at the kerbside for council collection and the waste collected by councils from municipal parks and gardens, street sweepings, council engineering works and public council bins. In developed countries, MSW generation is in the range 0.95 – 1.45 kg per person day. These wastes are composed of a mixture of lignocellulosic materials (around 65 – 95%), plastic (around 6 – 16%), metals (around 4 – 8%), and inorganic ash components [8]. Household waste makes up about 85 – 90% of the total MSW content for the majority of local authorities in the UK [9]. MSW increased year on year until 2005 and constitutes about 8% of the total arisings (about 36 million tonnes for 2005 across the UK as shown in Figure 2.1). Although it is currently decreasing slowly, MSW presents a growing problem for local authorities particularly as new legislation is introduced. The total amount of MSW produced in

Wales increased from 1.39 million tonnes in 1996/1997 to 1.94 million tonnes in 2004/2005 [9] and decreased slightly to 1.79 million tonnes in 2007/2008 [10].

2.1 Management and legislation of municipal solid waste

The heterogeneous nature of traditional MSW means that effective recycling of commingled waste can be complex due to the required mechanical separation of materials. Consequently the disposal routes in the early 21st century still rely heavily on landfill. In light of European Legislative requirements with regard to landfill and diminishing availability of capacity, the disposal of MSW is the subject of much current and forthcoming activity, and in particular is the focus of much governmental attention.

MSW is recognised to comprise 60 – 70% biodegradable matter. Its detailed composition is reported to vary with locality, season, socio-economics, and changes in consumption and packaging. The primary variability is seasonal, due to garden waste arisings [7]. Plastics usually account for about 7% of the total MSW by weight and much more by volume [11]. In Western Europe 6 – 10% of MSW (or 9.3 million tonnes) was composed of plastics in 1992 and the largest part (72%) was disposed of by landfill [12]. During the last 20 years, there has been a substantial increase in the use of plastic packaging.

The EU Landfill Directive was adopted on 26 April 1999 and came into force on the 16 July 1999. The obligatory target meant that by 2010 the UK and other countries in the EU had to reduce the biodegradable fraction of MSW sent to landfill to 75% of the 1995 level. Subsequently, waste targets for England and Wales were introduced in 2000 and 2002, respectively, which focused on recycling, composting and energy from waste technologies for the recovery and disposal of MSW [9], and the UK has met the 2010 target. Similarly, the EU targets require the BMW landfill will have to be further reduced to 50% by 2013 and to 35% by 2020.

In recent years the burden that waste puts on the environment has been widely publicised. To address the earth's dwindling resources and the growing mountains of

waste, many countries have introduced statutory waste minimisation and recovery targets. The general public are generally more concerned with the effects that waste has on the environment [9]. Waste management has climbed the political agenda over the last ten years; it has been recognised that continued generation of waste, poor recycling and significant use of landfill is not sustainable. In 2004, environmental measurement techniques have already shown that the current demand on the earth's resources is not sustainable [13]. The need for sustainable waste and energy management is widely recognised and this is increasingly reflected in policy and regulatory arrangements.

Over the years, many of solid fuel based combustion systems have been converted to gaseous or petroleum-based fuels due to flexibility, ease of use, availability and compactness. Sometimes this occurs without serious concern as to the economics of operation. With the present changes in cost of gaseous and liquid hydrocarbon fuels, the overall economics are being affected and this together with environmental considerations has resulted in increased interest in alternate sources of energy [14]. Advanced technologies which can produce useful energy both efficiently and in an environmentally responsible way are therefore of much interest. A report in 2005 [7] has estimated that residual waste arisings in the UK even after high levels of recycling could in principle provide approximately 17% of the UK electricity demand. Consequently, open dumping of waste material not only occupies a large space, presents an eyesore and could cause potential health and environmental hazards, but is also a waste of a valuable energy resource. The utilisation of waste material as a fuel source is therefore important [15].

2.2 Main components of municipal solid waste

The main components of MSW are lignocellulosic materials including paper and other biomass materials, and plastics.

2.2.1 Paper

Coated printing and writing paper is one of the principal materials contributing to MSW. Since such waste paper has a high calorific value (CV) of about 11 MJ/kg, its

conversion to marketable fuels has become a worthy goal from not only an economic but also an environmental standpoint [16]. Paper is composed of cellulose fibres, natural impurities such as lignins, and "artificial" impurities, such as residual chemicals such as sulphites which can not be washed out during processing, or such chemicals as alum that have been added during final processing. Cellulose is a polymer of the sugar glucose and is used by plants to produce cell walls. Lignin is the combined glue that holds plant cells together and comprises 20 – 30% of wood, and only 1% of cotton fibres [17].

2.2.2 Biomass

The term "biomass" refers to all organic materials that originate from plants, and is traditionally used as an energy source especially for cooking and heating, particularly in developing countries [18]. Biomass is not well-defined. It can generally be defined as any hydrocarbon material which mainly consists of carbon, hydrogen, oxygen and nitrogen [19], and its composition may vary depending on origin, physical location, age, season and other factors. Biomass can be categorized into wastes (such as sewage sludge, refuse-derived fuel (RDF)), herbaceous (such as grasses, stalks, and straw), aquatic (such as kelp), woody (hardwood and softwood), as well as derivatives (such as paper).

There are nine main sources of energy on Earth: solar, biomass, wind, wave, hydro, tidal, geothermal, nuclear and fossil. Although the first six are generally called renewable sources of energy, as they are not depleted over human timescales [15], energy needs to be utilized properly and people need to be energy conscious and treat conservation of energy more important than finding an alternative form of energy. Biomass material constitutes the greatest proportion of waste materials, and currently biomass and waste are widely recognised as important sources of sustainable energy. Biomass is recognized as the third largest primary energy resource in the world after coal and oil [20-23]. The chemical and physical properties of biomass in each of these categories fall over a broad range and it is quite clear that the category alone cannot be used as a means of predicting behaviour [24]. Almost all biomass is composed of three main components, namely cellulose, hemicellulose and lignin, in addition to extractives, water and mineral matter [23]. Cotton is almost pure α-cellulose which is

a polysaccharide having the general formula $(C_6H_{10}O_5)_n$ and an average molecular weight range of 300,000 – 500,000 (the ratio of the mass of the molecule to 1/12 of the mass of carbon 12) [19]. The structure of hemicellulose is similar to that of cellulose except that its polymers generally contain 50 – 200 units, fewer than those of cellulose, are soluble in dilute alkali, and exhibit a branched rather than a linear structure. Hemicelluloses are known to be less thermally stable than celluloses in view of its molecular structure [16]. Lignins are highly branched, substituted, mononuclear aromatic polymers in the cell walls of certain biomass, especially woody species, and are often bound to adjacent cellulose fibres to form a lignocellulosic complex. This complex and the lignins along are often quite resistant to conversion by microbial systems and many chemical agents. The lignin content on a dry basis is generally in the range from 20% to 40% by weight in both softwoods and hardwoods and from 10% to 40% by weight in various herbaceous species, such as bagasse, corncobs, peanut shells, rice hulls and straws [25]. The composition of the organic matter of biomass does not vary much, e.g., wood typically contains cellulose:hemicellulose:lignin in 2:1:1 ratio. Wheat straw and reed canary grass have similar compositions whilst willow has a noticeably lower amount of hemicellulose but higher levels of cellulose and lignin [26]. However, variations in moisture content and ash content are especially large [27]. The concentration of the ash due to the inorganic content changes from less than 1% in softwoods to 15% in herbaceous biomass and agricultural residues [19].

Cotton fibres and wood are the most important raw materials used to produce cellulose for industry [8]. A tree produces an average of 13.7 g of cellulose daily [28]. Cellulose is synthesized mainly in plants and constitutes about 40% carbon [29]. Compared to lignite that is the second most abundant biopolymer [8], all biomass materials show an improved quality, having lower moisture, ash and sulfur contents, while a higher volatile content and CVs [23]. The components of cellulose, hemicellulose and lignin behave independently, and biomass behaviour can be predicted based on a knowledge of the pure component behaviour [30]. However, Caballero argued that the interactions between cellulose, hemicellulose and lignin may vary or partially vary the pyrolytic kinetic behaviour of lignocellulosic materials [31].

In view of the world-wide increase in energy demand, the high costs of fossil fuels and disposal, as well as the environmental concern about levels of CO_2 in the atmosphere, the use of biomass to provide partial substitution of fossil fuels for steam and power generation is of growing importance [23]. The equivalent energy substitution for low temperature drying applications and high temperature heat treatment applications works out to be 1 l of diesel being substituted by about 3 kg and 3.3 kg of biomass, respectively [14]. Considering the biomass price of £25/t and the fossil fuel price of £0.30/l, it would result in the biomass fuel cost amount to about 25% of the fossil fuel cost and about 2400 kl of fossil fuel could be saved by using about 7300 t of biomass and a net saving of 6300 t of CO_2 [14].

Gasification of biomass is considered as one of the viable means for overcoming the so-called "energy crisis". It has many advantages from an ecological point of view. It is well known and accepted that thermochemical processing of biomass has more important differences with respect to the processing of coal. Biomass is much more reactive than coal, it pyrolyses very quickly and its ash content is usually very low [32]. Compared with coal, biomass has lower sulphur dioxide and nitrogen dioxide emissions along with the CO_2 savings. It also has other pollutants in much lower concentrations, and a much higher volatile matter content, which determines a lower char yield [33]. In some industrial heat applications fossil fuels can be totally replaced by technology using only biomass as the fuel [14]. The benefit on the environment is significant. Biomass is also an attractive fuel for power generation. Although it is getting increased attention as a potential source of renewable energy, biomass is not yet competitive with fossil fuels. Fossil fuels contribute to the major part of world's total energy consumption. According to the World Energy Assessment report, 80% of the world's primary energy consumption is provided by fossil fuel, 14% by renewables (out of which biomass contributes 9.5%) and 6% by nuclear energy sources [34]. Recently the developed countries in Europe in particular have promoted the importance of biomass energy [35-43] mainly owing to three targets: economic and social development of countryside, elimination of wastes and reduction of CO_2 emissions.

Bio-energy is now accepted as having the potential to provide the major part of the projected renewable energy provisions of the future. There are three main routes to

providing these bio-fuels – physical conversion, biological conversion and thermal conversion [44]. Biochemical conversion methods are based on the conversion of biomass into alcohols or oxygenated products by biological activity. Thermochemical processes involve the pyrolysis, liquefaction, gasification and supercritical fluid extraction methods [19].

2.2.3 Plastic

Plastic waste can be considered as an additional resource of energy and as a chemical raw material. Since plastic is a rich source of hydrocarbons, it can play a vital role in coal liquefaction processes, so that chemical treatment of waste plastics is gaining importance, particularly when incorporated with coal to get the benefit of the hydrogen rich character of the polymeric plastics, thereby enhancing the coal conversion to liquid fuels [45, 46]. Mixed plastics consist of various plastic types, which have different physical-chemical properties. Thus, according to the type of plastics in a plastic mixture, the quality of oil product obtained is affected [47]. Polyethylene (PE) is a common polymer, widely used in industry (pipes, cable isolation, containers, bottles for example) [8]. The polymer fraction in domestic refuse comes to 7 – 8% by weight and encompasses about 77% polyolefines such as PE or polypropylene (PP), 12% polystyrene (PS), 5% polyvinyl chloride and 6% other polymers [48].

2.3 Waste treatment

A sustainable energy future requires not only renewable resources but also advanced energy technology. Most modern waste treatment systems aim to treat wastes as "cleanly" as possible and are designed according to the priority list [49] of: (1) avoidance, (2) recycling, (3) conversion to energy and (4) landfilling.

2.3.1 Landfilling, incineration and recycling

The most common ways to treat solid waste are landfilling, incineration and materials recycling [50]. There are economic, social and environmental factors that should be allowed for when choosing appropriate waste management options. Finnveden et al

[51] used a life cycle assessment tool to quantify emissions, energy use and financial costs to compare different alternative waste treatment strategies, and their results suggested the environmental preference of recycling over incineration over landfilling.

For many years strategic landfilling has been the most common method of disposal for the majority of MSW. However, the combined burden of increasing quantities of wastes and environmental legislation in Europe limits the wastes that can be disposed to landfill. Waste generation and destruction is an important problem from an economic as well as environmental point of view, and as a result the search for alternative solid waste management options has led to an increase in the number of thermal treatment plants operating.

In the late sixties and seventies of the 20th century there was a tremendous worldwide drive towards MSW incineration. However, a lack of technical knowledge led to serious emission problems [52]. In particular, the small amount of chlorine containing polymers causes serious problems in incineration [48]. The development and better understanding of combustion technology throughout the eighties has led to a new generation of large-scale highly effective MSW incinerators/thermal processing units meeting stringent emission limit guidelines [53-55]. MSW incineration has significant benefits [55, 56]. The volume of MSW is reduced to a fraction of its original size (85 – 90% reduction by volume). The waste reduction is immediate and not dependent on long biological break-down reaction times. Incineration facilities can be constructed closer to MSW sources or collection points, reducing transportation costs. Using heat recovery technology, the cost of the operation can be offset by energy sales. Gaseous discharges to air can be controlled to meet environmental legislative limit values. However, incineration does have its problems [55]. Some materials should not be incinerated because they are more valuable for recycling, or they are non-combustible or their by-products may give rise to harmful emissions. Poor operating practices and the presence of chlorine in the MSW may lead to emissions containing highly toxic dioxins and furans. The control of metal emissions may be difficult for inorganic waste containing heavy metals, such as arsenic, cadmium, chromium, copper, lead, mercury and nickel. Incinerators require high capital costs and trained operators leading to moderately high operating costs. Supplementary fuels are required to achieve a necessary high combustion temperature.

With respect to the method of recycling, for example, plastics can be practically recycled either mechanically towards a new plastic with a lower grade application, i.e., physical recycling, or chemically to obtain chemical raw materials or fuel oil, i.e., chemical recycling [47]. However, due to the limited economic benefits of separation and recycling and the questionable quality of recycled product if poor state-of-the-art technologies are employed [57], resource recovery in the form of heat and power production has gained favour in the past thirty years for the waste reduction [58]. There are three main thermal processes available for converting MSW to a more useful energy form – combustion, gasification and pyrolysis [44].

2.3.2 Combustion

Scientifically, the terms combustion and incineration have the same definition which basically refers to the burning of substances during an extremely rapid chemical oxidation process. Both of these terms have been used interchangeably in waste incineration documents. However, combustion is generally used more often in the area for steam or power generation, and incineration is used more often when referring to waste destruction [59].

Combustion is an attractive alternative for waste treatment since, together with the energy generation, about 90% reduction by volume is reached [8]. The combustion technology is widely available commercially to provide hot water and/or electricity. In combustion, oxidation is substantially complete in one process. The useful product of combustion is heat, which must be used immediately for hot water and/or power generation, as the storage of heat is not a viable option. Moreover, overall efficiencies of biomass combustion are rather low at typically 15% for small plants up to 30% for large plant. However, the costs of combustion are only currently competitive [44]. Due to the possibility of contaminant emissions during waste combustion, it is necessary to control the process. Atmospheric pollution from biomass and waste combustion processes has received much attention. Atmospheric contaminants can be produced in different ways, depending on the type of refuse treated [60]: fly-ashes and entrained particles, evaporation of metals, formation of compounds derived from Cl, N, F or S and products of incomplete combustion. Among the hazardous products

resulting from unsuitable combustion conditions, polycyclic aromatic hydrocarbons (PAHs), polychlorinated dibenzodioxins (PCDDs) and polychlorinated dibenzofurans (PCDFs) have received a lot of attention [8].

2.3.3 Gasification

Various gasification processes are under development, so that biomass conversion by this route is gaining more attention. Unlike combustion, gasification is a process of partial oxidation which converts carbonaceous solid fuels into synthesis gas, a mixture of CO and H_2 that is a raw material for chemicals, as well as a fuel for producing electricity and heat. The cheapest gasification medium is air but oxygen/steam gasification and hydrogenation are also used [61]. Gasification has the best fuel flexibility of any of the advanced technologies for power generation [62]. Coal gasification has been well established, and some woody biomass gasifiers are in commercial use [63].

Gasification is an efficient and advanced technology for extracting the energy from biomass and has received increasing attention in the past two decades. Current technology has already operated well with biomass and other low-value feedstocks, and with high-ash residues [62]. Biomass gasification is applicable to deal with all kinds of biomass residues produced in the food processing industry, agriculture, forest industry [64]. The primary advantages of biomass gasification technology are environmental protection and energy saving [64]. The energy efficiency in case of gasification is higher than that of combustion [18], and the overall efficiency of conversion of biomass to energy using gasification is estimated as 75 – 80% [61]. Moreover, it is possible to install small, low-cost and efficient gasifier-engine coupled systems, which permit biomass wastes to be used in situ, and thus, to eliminate much of the storage and transportation to power plants [65]. Biomass gasification can convert dispersed biomass waste to good quality fuels. It converts the intrinsic chemical energy of the carbon in the biomass into a combustible gas that can be standardised in its quality and is easier and more versatile to use than the original biomass. The gas can be used to power gas engines and gas turbines, or used as a chemical feedstock to produce liquid fuels [61]. Several studies have been made on

gasification of biomass and biomass residues for applications in direct heating, power generation, methanol and ammonia production [66-69].

Experiments have verified that the gasification method can be adapted to a wide variety of solid fuels. Thermal energy conversion of MSW through gasification technology has been gaining importance as an alternative fuel source and MSW gasification is under development due to the pressure on biomass reserves. The gas produced from RDF pellets is low in tar content with high carbon monoxide and hydrogen contents when compared with the gas produced from conventional fuel wood chips. The global energy content of the product gas generated from RDF pellets is very close to that of wood chips [70].

Wastes are generally difficult to process, because they are heterogonous, which gives rise to fluctuations in quality, availability and composition. The use of coal or lignite can help to provide stable gasification conditions and prevent problems due to seasonal fluctuations in waste quantities. Therefore, waste/biomass co-gasification with coal could be a versatile technology that can benefit from different fuel compositions to reduce the problems of wastes availability and composition variations. However, the technology of co-gasification is not mature enough and very few projects worldwide involve co-gasification at an industrial scale [71].

Gasification occurs in a number of sequential steps [44]: (1) drying to evaporate moisture; (2) pyrolysis, also known as devolatilisation, to give gas, vaporised tars or oils and a solid char residue; (3) gasification or partial oxidation of the solid char, pyrolytic tars and pyrolytic gases.

When fuel briquettes are heated to 300 – 500°C in the absence of an oxidising agent, they pyrolyse to solid char, condensable hydrocarbons or tar, and gases. The relative yields of gas, liquid and char depend mostly on the rate of heating and the final temperature. Generally in gasification, pyrolysis proceeds at a much quicker rate than gasification and the latter is thus the rate controlling step. The gas, liquid and solid products of pyrolysis then react with the oxidising agent – usually air [44].

The product from gasification is fuel gas whose composition or quality is influenced by many factors such as feed composition, water content, reaction temperature, and the extent of oxidation of the pyrolytic products [44]. By varying the gasification medium, three types of product gas with different CVs can be produced. Low CV gas of 4 – 6 MJ/m^3 can be produced using air or steam/air and can be used directly in combustion or as an engine fuel. Medium CV gas of 12 – 18 MJ/m^3 can be produced using oxygen and steam, and high CV gas of 40 MJ/m^3 can be produced using hydrogen and hydrogenation. Both medium CV gas and high CV gas can be utilised as feedstock for subsequent conversion into basic chemical, principally methane and methanol [61].

The product gas from gasification consists of a mixture of carbon monoxide, carbon dioxide, methane, hydrogen and water vapour. The main reactions taking place in gasification are summarised below [61]:

Partial oxidation

$$C + \frac{1}{2}O_2 \rightleftharpoons CO \qquad dH = -268 \text{ MJ/kmol}$$

Complete oxidation

$$C + O_2 \rightleftharpoons CO_2 \qquad dH = -406 \text{ MJ/kmol}$$

Water gas reaction

$$C + H_2O \rightleftharpoons CO + H_2 \qquad dH = 118 \text{ MJ/kmol}$$

Water gas shift reaction

$$CO + H_2O \rightleftharpoons CO_2 + H_2 \qquad dH = -42 \text{ MJ/kmol}$$

Methane formation

$$CO + 3H_2 \rightleftharpoons CH_4 + H_2O \qquad dH = -88 \text{ MJ/kmol}$$

Commercial gasifiers are nowadays facing economic and other non-technical barriers, since the energy from gasification gas has to be competitive with natural gas which is abundant and cheap [32].

Supercritical water gasification is a special gasification process. The reaction generally takes place at the temperature over 600°C and a pressure higher than the

critical point of water. With temperature higher than 600°C, water becomes a strong oxidant, and oxygen in water can be transferred to the carbon atoms of the briquettes. As a result of the high density, carbon is preferentially oxidised into CO_2 but also low concentrations of CO are formed. The hydrogen atoms of water and of the briquettes are set free and form H_2. The gas product consists of hydrogen, CO_2, CH_4 and CO [72].

2.3.4 Pyrolysis

Pyrolysis is a process of thermal degradation at the moderate temperature in the absence of oxygen, leading to the formation of solid charcoal, liquid oil and gas in different proportions, depending on the operation conditions [73]. Pyrolysis can be used as an independent process for the production of useful energy (fuels) and/or chemicals. It is also present in the initial stages of a gasification or combustion process [74], and is followed by partial or total oxidation of the primary products, respectively. Conventional pyrolysis consists of the irreversible thermal decomposition of organic components [19].

In pyrolysis, polymeric materials are heated to a high temperature, so their macromolecular structures are broken down into smaller molecules and a wide range of hydrocarbons are firmed. These pyrolytic products can be divided into a gas fraction, a liquid fraction and solid residues, and can be used as fuel oil or petrochemical raw material. For recycling of waste plastics, pyrolysis as a chemical recycling method is becoming a promising alternative, in order to recover fuel oil and hydrocarbon feedstock [11, 75-77]. As an advantage of this process, pyrolysis can treat all thermoplastic mixtures consisting of various types of plastics, without separation or treatment [78]. Biomass fuels represent a promising route for the production of charcoal, medium heating value gases and condensable organic components (tars), through pyrolytic conversion. The gases are mainly CO, CO_2, H_2 and C_1-C_2 hydrocarbons. Tars contain more than a hundred compounds: major products from cellulose include levoglucosan and furfural, from hemicellulose include furan derivatives, and from lignin include phenolic compounds [79]. Primary decomposition of biomass material (< 400°C) consists of a degradation process, whereas the secondary thermolysis (> 400°C) involves an aromatisation process [80].

Pyrolysis has received increased interest, since the process conditions can be optimised to maximise the production of chars, liquids or gases. The physical conditions of biomass pyrolysis, such as temperature, heating rate and residence time, have been shown to have a profound effect on the product yields and composition [81]. Even among different samples of the same type, the behaviour of pyrolysis under different conditions can be widely variable [62]. The lower process temperature and the longer vapour residence time favour the production of charcoal. The higher temperature and the longer residence time increase the conversion to gas. The moderate temperature and the short vapour residence time are optimum for producing liquids [62]. The high heating rate of up to 10^4 °C/s at the temperature < 650°C with rapid quenching favours the formation of liquid products and minimise char and gas formation; these process conditions are often referred to as 'flash pyrolysis'. The high heating rate to the temperature > 650°C tends to favour the formation of gaseous products at the expense of liquids. The heating values of the products are functions of the initial composition of biomass. Heating values of the chars obtained from pyrolysis are comparable with those of lignite and coke, and the heating values of liquids are comparable with those of oxygenated fuels, such as methanol and ethanol, which are much lower than those of petroleum fuels. The heating value of gases is comparable with those of producer gas or coal gas and is much lower than that of natural gas [82]. For highly cellulosic biomass feedstock, the liquid fraction usually contains acids, alcohols, aldehydes, ketones, esters, heterocyclic derivatives and phenolic compounds [25]. The pyrolytic liquids are complex mixtures of oxygenated aliphatic and aromatic compounds [83]. The tars contain native resins, intermediate carbohydrates, phenols, aromatics, aldehydes, their condensation products and other derivatives [19]. Inorganic compounds, especially potassium, calcium, sodium, silicon, phosphorus and chlorine, are the main components of the ash in biomass. The concentrations of ash range from less than 1% in softwoods to 15% in herbaceous biomass and agricultural residues. During biomass pyrolysis, these inorganics, especially potassium and calcium, catalyse biomass decomposition and char-forming reactions [84].

Pyrolysis at high temperature plays an important role as a first and fast step in gasification processes since it is well known that the pyrolytic condition strongly

determines the yield of char and its reactivity in the process [85]. Pyrolysis consists of very complex reactions during which both chemical (endothermic and exothermic reactions, such as bond breaking and recombination) and physical (softening and resolidification) changes occur due to thermal effects [86].

2.4 Briquettes

SRF is prepared from non-hazardous waste and composed of a variety of materials. It consists largely of organic and polymeric components of MSW such as plastics and biodegradable waste. SRF is different from classical RDF. To qualify for SRF, RDF must comply with a series of environmental and process-relevant standards such as minimum requirements concerning the contents of some critical trace elements (mercury, thallium, cadmium), corroding capacity and net CV. SRF represents a significant potential storable source of indigenous energy and produces lower greenhouse gas emissions than conventional fuels [87].

Compared to unsorted MSW, SRF has a lower moisture content, a higher CV and a more homogeneous form, and burns more efficiently [87]. However, raw SRF as well as raw biomass is still poor quality fuels, since the majority of them comprise particles in loose form, which makes them unsuitable for direct use for gasification. Furthermore, their bulk density or heating value per unit volume is much lower, and they are dirty during handling and storage, burn too fast and are smoky. Densification is a process by which loose particles are compressed together into a larger, more compact form, referred to as briquettes, with or without the use of a binder. Briquetting of SRF is a viable technology and can provide a relatively high-quality alternative source of fuel. Making use of SRF in briquette in co-firing makes ignitability easy and increases the burning rate of low grade coals. The advantages of briquetted fuel include: the convenience of storage and transport, the ease of charging the furnace, increase in CV, improvement of gasification characteristics, reduction of entrained particulate emissions, uniformity in size and shape, and good substitution for natural fuels [88].

In order to obtain mechanically strong briquettes, the briquetting pressure and the time applied during the operation must be adjusted properly. Under pressures below an optimum value, firm briquettes cannot be obtained. However, application of excessively high pressures also causes negative effects on the mechanical strength [19]. High pressures and the use of binders can add to the briquette production costs significantly. Albeit with poor durability in the case of straw [89], briquettes can be manufactured without any binder. In general, briquetted fuel made from different processes or materials differs in handling and combustion behaviour [88]. Each SRF briquette requires different optimum condition to prepare. Generally, the quality of briquettes improves as die pressure, dwell time and binder content increase [90]. Briquettes at intermediate moisture content perform better. High moisture in the briquettes not only prevents their application for thermo-chemical conversion processes, but also results in swelling and disintegration of the briquettes. However, a limited amount of moisture is beneficial as the steam generated causes a steam gasification reaction leading to better gas quality [91].

The storage of biomass briquettes during period of high humidity will not create any problem [91]. The sawdust briquettes have the best handling characteristics in terms of storage and lack of deterioration [90]. Since briquettes of pure sawdust are not a good conductor of heat, by adding small quantity of burnt engine oil, thermal conductivity of sawdust improves and heat penetrates up to the centre of briquettes. Thus, uniform temperature distribution exists and better quality briquettes are obtained [92]. Starch and molasses are good binders because of their availability and low price. For rice husks, water rather than molasses is a good binding agent [90].

The main factors affecting the properties of briquettes include solid fuel size, binder/additive ratio, water addition mixing procedure, curing time and extruding temperature [33]. Compression strength and water resistance are two of the most important properties required in the preparation of good fuel briquettes and have been extensively used as the selection criteria [93] for most adequate briquettes. They are closely associated to the amount and the type of minerals and organic composition of the raw materials [94]. Three tests can be used to characterise the mechanical behaviour of briquettes: impact resistance, water resistance and compression resistance. Impact resistance (or drop resistance or shattering resistance) test is

considered to be a general diagnosis of briquette strength. Briquettes are dropped from specific height and the weight retained as the fraction of the initial weight is taken. It simulates the impact forces at which a briquette may be subjected to when it is transferred between conveyors or dropped into cargo and storage areas [33, 95]. Because the binders used are water-soluble and the briquettes can be porous, the resistance against water absorption and disintegration must also be tested. The test is designed to simulate severe weathering conditions, which fuel briquettes might encounter during transportation and outdoor storage. The water resistance is the fraction of water absorbed by a briquette when immersed in water at specific temperature for a specific period of time [33, 95]. Compression resistance (or crushing resistance or hardness) is the maximum crushing load, which a briquette can withstand before cracking or breaking [33, 93, 95]. It is determined by diametrical compression test in which a single briquette is placed between two flat, parallel plates and an increasing load is applied at a constant rate until the briquette fails by cracking or braking [95].

For coal briquettes, biomass may behave as a binder during briquetting. Some coals tend to form an enormous amount of dust leading serious environmental problems and utilisation of coal dust to produce briquettes is one of the important techniques. However, it is difficult to obtain strong coal dust briquettes without using any binding agent. Biomass can be used as a binder in the production of coal briquettes, as it has fibrous structure and contains oily or sticky components, which facilitate to form a more dense bulk [96]. The mechanical strength of briquettes can be improved by adding some biomass material. Paper mill waste improves the impact resistance of briquettes. Sawdust and paper mill waste increase compression resistance of briquettes. Water resistance of briquettes can be augmented by adding olive refuse, cotton refuse, pine cone, and paper mill waste [97].

2.5 Thermogravimetric analysis and kinetic studies

The need to develop models which predict the behaviour of SRF briquettes and biomass-derived fuels when they are subjected to a heating process in a furnace or a gasifier confers great interest on the pyrolytic kinetic study. The analysis of complex

chemical equilibriums helps to identify the temperature ranges corresponding to stability domains of certain molecules. In fact, temperature is an important parameter in cracking reactions [98]. TGA is a method by which the weight loss of a sample is recorded against temperature under controlled heating rate and gas atmosphere. When the heating rate is low and the cracking of primary products is negligible, TGA is one of the techniques used to study the primary reactions in the decomposition of solids and has been widely used to study the thermal decomposition of polymers and other materials. DTG curves are derived from TG curves and have been widely applied to biomass to evaluate pyrolytic kinetics [19]. The interpretation of experimental data can provide information on the composition of materials, the order of reactions, the number of different processes that take place, and the corresponding kinetic constants [99]. However, the yields of gas and tar cannot be separated, as thermogravimetry (TG) can only measure weight loss [99].

The design of the thermochemical process for the conversion of SRF briquettes and biomass-derived fuels and proper equipment requires knowledge of several process features, such as governing mechanisms, significant parameters and their effect on the process and kinetic studies [100]. An understanding of the pyrolytic processes of SRF briquettes and biomass-derived fuels is important not only for optimisation of boilers and large scale furnaces, but also for many other applications including determining forest fire behaviour and predicting the resistance of buildings to fire [101]. Due to the presence of homogeneous and heterogeneous reactions occurring consecutively along with heat, mass and momentum transfer operations occurring simultaneously during the pyrolytic process, little work has been reported in the literature on the mechanistic modelling of such extreme complex kinetics [74].

One rationale for the modelling of complicated organic reactions by simplified reaction schemes is that a partial reaction in the scheme may correspond in reality to a group of reactions. A partial reaction may be the average of several parallel reactions or the slower step in a sequence of consecutive reactions [102]. A kinetic model is necessary to predict the reaction behaviour as well as product range distribution. Fast pyrolysis occurs in a time of few seconds. Therefore, not only chemical reaction kinetics but also heat and mass transfer processes, as well as phase transition phenomena, play important roles [44].

Pyrolysis of lignocellulosic materials has been simulated by two parallel reactions and a third reaction for the secondary interactions between charcoal and volatiles [103]. The most used mechanisms usually comprise parallel reactions for the decomposition of the volatile fractions of pseudo-components. These are pseudo-components owing to the difficulty in separating the effects of the different contributions [104]. Each pseudo-component acts as if there were no interactions. In the majority of cases, the number of pseudo-components or temperature zones is three and coincides with hemicellulose, cellulose and lignin [105].

The pyrolytic process of lignocellulosic materials can be divided into three non-interacting mass-loss events. In the first event, the moisture is removed and it lasts up to 200°C. In the second event, between 250°C and 390°C, the lightest volatile compounds are evolved. This event is usually identified in literature as hemicellulose and cellulose decomposition. It is generally assumed that hemicellulose and cellulose decompose independently of one another, the former associated with the shoulder of the rate curve and the latter with the peak [104]. Decomposition of hemicellulose starts at the temperature above 200°C and full pyrolysis will occur by 350°C, with the major products being H_2O, CO_2, CO and char, as well as traces or low molecular weight organics. Pure cellulose has a comparatively slower decomposition process at the temperature in excess of 250°C, and the rate of thermal decomposition only becomes more rapid above 300°C [26]. Cellulose pyrolysis occurs in a relatively narrow temperature interval [106]. The third event, above 390°C, is usually identified as lignin decomposition, and this process occurs slowly and over a broad temperature range [107].

Although the components of lignocellulosic material interact chemically or physically, and cause the lignocellulosic material to behave in its own unique way during its thermal degradation, two or three peaks in the DTG analysis can be assigned to hemicellulose, cellulose and lignin, and their identity is maintained [31]. Cellulose is, by far, the most studied component. For experiments at moderate temperature, the cellulose pyrolysis involves three groups of processes. The first is an intramolecular dehydration to form anhydrocelluloses and this process is slightly endothermic and occurs at around 220°C. The second competes with the first to produce levoglucosan

(around 280°C and is more endothermic). The final process involves a great number of reactions with scissions C-C, C-O and radicalary reactions to form gases or volatile compounds, principally from anhydrocellulose decomposition [31]. The cellulose pyrolysis is globally endothermic and the endothermicity mainly reflects a latent heat requirement for vaporising the primary tar decomposition products. Exothermicity in biomass pyrolysis is associated with the formation of char [105, 108]. Hemicellulose converts to furanoses and furans via intermediates [109]. Lignin does not present an intermediate compound. Lignin undergoes a slight decomposition at a very low temperature, and during the initial stages of decomposition it is less stable than cellulose [110]. This initial instability of lignin is probably due to the scission of lateral groups that form the lignin polymer [31]. However, lignin is usually considered the most stable biomass compounds [31] and it converts to mononuclear and condensed aromatic and phenolic compounds [109] at a higher temperature. The lignin pyrolytic process is considered to be globally exothermic [105].

In several cases of biomass pyrolysis, dynamic measurements and the corresponding kinetic analyses are examined at one heating rate, generally below 10 °C/min, as thermal lag may be established between the sample and the controlling thermocouple owing to sample thermal inertia and/or reaction energetics [105]. Process simulations showed that the pseudo-components which are hemicellulose and cellulose, decompose independently of one another [105]. Activation energies vary between 80 and 116 kJ/mol for hemicellulose, 195 – 286 kJ/mol for cellulose, and 18 – 65 kJ/mol for lignin [105, 111]. At higher heating rates, the impact of thermal lag is larger and appears as reduced values of activation energies and pre-exponential factors [105].

During plastic pyrolysis, the polymeric structure is broken down, producing smaller intermediate groups, which can further react and produce smaller hydrocarbon molecules, liquids and gases [112-114]. Temperature has a vital role in the degradation of polymeric materials. From the mechanistic point of view, de-polymerisation results from the scissions or cleavages of some weak linkages having energy less than 243 kJ/mol, which result in the formation of free radicals [115].

A kinetic study of MSW pyrolysis [116] was carried out at heating rates of between 1.5 and 200 °C/min using a first order reaction kinetic model and showed that the

overall process of MSW pyrolysis is governed by two independent reactions: (a) decomposition of the cellulose fraction around 310 – 380°C with the mean values of the pre-exponential factor of 2.92×10^{9} s^{-1} and the activation energy of 135.9 kJ/mol, and (b) decomposition of the other fraction in the range 200 – 500°C with the mean values of the pre-exponential factor of 1.13 s^{-1} and the activation energy of 26.8 kJ/mol. At the temperature above 840°C, the decomposition of calcium carbonate ($CaCO_3$) present in the ash takes place. The dispersion of the kinetic constant is due more to the sample heterogeneity than to an important gap between the actual temperature and that measured by the thermocouple, and the dispersion of the first process is lower than that of the second process, which is logical taking into account the MSW composition.

MSW pyrolysis produces a variety of nitrogenated compounds. Kraft lignin pyrolysis produces sulphur compounds. Almond shells and cellulose pyrolysis produces higher yields of oxygenated compounds. Lignin pyrolysis produces a significant fraction of high molecular weight PAHs with mutagenic character [8].

The cellulose and lignin content in biomass is one of the important parameter to evaluate the pyrolytic characteristics. For the biomass with a higher cellulose content, the pyrolytic rate is faster. While, the biomass with a higher lignin content gives a slower pyrolytic rate [117]. Biomass reactivity during combustion is also higher when the lignin content is low. Evaluation of the lignin content is useful to predict biomass thermal behaviour and the quality of pyrolytic products obtained. Biomass of low lignin content produces a lighter pyrolytic product, which may be considered a better bio-oil for use as a fuel [118].

The peak height in DTG analysis is directly proportional to the reactivity, and the peak temperature is inversely proportional to the reactivity [119]. Many biomass samples are highly contaminated by inorganic salts which shift cellulose decomposition to a lower temperature and therefore, the DTG peaks of the cellulose and hemicellulose highly overlap each other [102]. Minerals have a positive effect on biomass pyrolysis by acting as catalysts and increase the reactivity by lowering the

peak temperature. However, minerals appear to hinder the overall process in the case of coals and increase activation energy values [119].

Several comparisons of pyrolytic characteristics with some biomass materials and coal have been published. The DTG curves of hardwoods and softwoods are similar, apart from a higher overlap between the hemicellulose and the cellulose zones for softwoods. Based on the characteristic reaction temperature, softwoods show a lower reactivity of hemicellulose components than hardwoods, and both hemicellulose and cellulose zones of softwoods are wider [111]. A maximum weight loss takes place due to the removal of the volatile matter and the release of tars in the temperature range between 432°C and 440°C for sawdust and coal-sawdust and higher (500 – 507°C) for coal [33]. The order of the reaction determined for sewage sludge is much higher than that of acacia wood, bagasse and rice husk, whereas the activation energy is lower. Rice husk and sewage sludge yield higher amounts of secondary char due to the catalytic effect of the inorganics present in higher amounts in the samples [19]. Cotton residue has higher reactivity than waste wood [119]. The thermochemical reactivity of biomass is higher than that of coal [119]. Gasification of almond shell indicates the significance of extra- and/or intra-particle thermal resistances for particles larger than 1 mm in diameter [120]. Changes in operational conditions, including heating rate (4, 10 and 20 °C/min); temperature/time programs with intermediate isothermal heating; gas flow rate and the type of gas (argon and carbon dioxide), during apple-pulp pyrolysis doesn't seem to have any effect on the course of apple-pulp pyrolysis, and they have no influence on the char yield [121]. The chemical additive (phosphoric acid) has a greater effect on the cellulose decomposition, causing a decrease in the temperature for maximum weight loss, and this is ascribed to their well-known catalytic effect for dehydration reactions, particularly during cellulose dehydration [121]. The yields of liquid and gaseous products from pyrolysis of the solid waste and black liquor samples increase with increasing temperature [122]. The pyrolytic kinetics of wheat straw and corn stalks under rapid heating (25 – 70 °C/min) show the same qualitative behaviour, however, in the second case, larger volatile yields are obtained, probably as a result of a lower ash content [123].

Sodium, potassium, calcium, magnesium, iron, phosphorus, aluminium and silicon are the major elements present in biomass fuel ash; cobalt, chromium, copper, manganese,

nickel, sulphur and zinc are present in smaller amounts. On demineralisation, the active surface area increases, and liquid yield increases and gas yield decreases for all biomass. Demineralisation increases the volatile yield, initial decomposition temperature and rate of pyrolysis for most of the kinds of biomass. However, rice husk, groundnut shell and coir pith are exceptions and show an increase in char yield on demineralisation due to their high potassium (and/or zinc) content in combination with a high lignin content [124].

2.6 New contributions to the research field

Gasification is currently one of the most promising thermal-chemical conversion techniques for recovering energy from waste, and the pyrolytic behaviour of SRF briquettes and biomass-derived fuels is the starting point for the process. Due to very different physical properties and chemical compositions of SRF and biomass materials and different experimental methods, the reported kinetic parameters are substantially different in the literature. Although the broad outlines of chemistry are known, understanding of the thermodynamics and kinetics is still inadequate. Therefore it is a difficult task to develop a global model and it is essential to understand how SRF and biomass materials behave. In this research, the pyrolytic characteristics of simulated SRF briquettes made of paper and plastic representing the two main components of MSW were examined. Experimental investigations were undertaken in order to show whether important interactions exist between lignocellulosic materials and plastics. Gasification can be adapted to a wide variety of solid fuels. Gasification technology has already operated well with biomass, and MSW gasification is under development. Fuel materials are heterogonous and give rise to fluctuations in the quality, availability and composition of fuels. Therefore, the pyrolytic characteristics of several SRF briquettes and biomass materials were examined in order to show whether important interactions exist between hemicellulose, cellulose and lignin of the lignocellulosic materials in the solid phase during the pyrolytic process.

The aim of this research is to get a deeper insight into the characteristics and the kinetics of the pyrolysis, and in this way to aid the development of biomass and MSW

gasification processes. In this research, the pyrolytic behaviour of various briquettes and biomass materials were studied. Chapter Three deals with experimental apparatus and methodology. The pyrolysis processes of three groups of samples, which were simulated SRF briquettes (paper and plastic blends), SRF briquettes and pulverised raw biomass samples, were investigated. Simulated SRF briquettes were made with compositions of differing paper/plastic ratios and at varying extruding temperatures. SRF briquettes were made from different waste materials including ecodeco, dried sewage, RDF, raw MSW, molasses, sawdust, paper and plastic. Pulverised raw biomass samples were sawdust, borage meal, oat husk, MFC wood, willow, miscanthus, rape straw and wheat straw. To overcome the thermal lag effect, a slow heating rate of 5 °C/min from ambient up to 750°C was used, so that the sample could have a fairly uniform known temperature throughout its volume. Pure nitrogen with a constant flow rate of 9 l/min was used as a carrier gas in the furnace to prevent the presence of oxygen in the pyrolysis zone and to reduce the secondary reaction effects by removing volatile products from the hot zone, and primary reactions took place almost exclusively. Therefore, the yields of the products obtained from the pyrolytic process were mainly due to the solid decomposition (primary reactions). Chapter Four describes the experimental results of the TG and DTG curves obtained in this research. The pyrolytic characteristics of each sample is represented and compared with other samples. Chapter Five derives a simplified general order pyrolytic kinetic model and demonstrates that a first order kinetic model is unsuitable. The kinetic parameters, such as activation energy, pre-exponential factor and reaction order were acquired through a general order ash rise model. There are several postulations in this chemical reaction kinetic model: the temperature inside the sample was uniform; both internal and external mass transfer was very fast; and the pyrolytic system reached a macroscopic chemical equilibrium during the slow temperature rise. Chapter Six gives a further description of the DTG profiles and the pyrolytic kinetics of the samples. The reactivity and the interaction between the components of each sample are discussed. This is the major contribution to the research field. Chapter Seven provides a short discussion and conclusions of this research and suggestions for future work.

In this research, the following aspects were considered:

• Experimental investigation of the pyrolytic characteristics of simulated SRF briquettes, SRF briquettes and pulverised biomass materials.

• Qualitative assessment of the interactions between components of the samples during pyrolysis.

• Acquisition of the kinetic parameters of the primary pyrolytic reactions of the samples.

• Comparison of the results presented in this research with those reported in the literature.

• Analysis and discussion of the difference in the pyrolytic process between the samples.

• Qualitative comparison of the contents of the samples such as cellulose, hemicellulose, lignin, and ash, and the discussion of their effects.

• Identification of the factors which affect the pyrolysis of the samples.

Chapter Three Experimental Apparatus and Methodology

This chapter describes the experimental equipment used to obtain the pyrolytic characteristics of simulated SRF briquettes, SRF briquettes and pulverised biomass, the composition of the sample materials and the method adapted in the pyrolysis tests.

3.1 Pyrolytic experimental system

Pyrolysis tests were undertaken using the TGA technique with a specially designed thermo-balance rig (Carbolite STF 151/-/450) shown in Figures 3.1 and 3.2. The samples were heated in an electrically heated vertical tube furnace which was controlled by a digital temperature programmer (Eurotherm 2408). The silicon carbide furnace heating element had a maximum operating temperature of 1500°C and was mounted around the outside of a 70 mm diameter mullite work-tube which acted as the heated test section. The work-tube was partially sealed both at the bottom and top by separate plates. The bottom plate contained an off-centre gas inlet to provide a controlled ingress of pure nitrogen as an inert atmosphere. Pure nitrogen was used as an inert purge gas, not only to prevent the presence of air in the furnace, but also to remove the gaseous and condensable products that evolved during pyrolysis and so prevent volatile products from remaining close to the devolatilising particles in the furnace. This ensured an inert atmosphere during the run and reduced the secondary reaction effects within the hot solid residue.

A centrally located, hollow, re-crystallised alumina (RCA) sheath passed freely through the bottom end-plate. The top of the sheath was fixed to a 57 mm diameter circular holder for mounting the sample in the hot section of the furnace. The other end of the sheath was then placed on an electronic balance (Sartorius LP620S Analytical Balance) with its maximum capacity of 620 g. The instantaneous mass of the solid was determined to a resolution of 0.001 g, while the sample underwent thermal decomposition, when subjected to a linear rise in the furnace temperature.

Adequate clearance was incorporated between the sheath and the bottom end-plate to avoid errors in the measurement of the mass due to friction between these two components. A 1.5 mm diameter mineral insulated N-type thermocouple was inserted into the sample and the leads were led out through the sheath and connected to a second temperature controller (Eurotherm 2416) to measure the sample temperature. A computer was connected to the Eurotherm 2416, the Eurotherm 2408 and the Sartorius LP620S Analytical Balance to concurrently record the sample temperature, the furnace temperature and the instantaneous solid mass respectively with a sampling interval of 10 s. The data were subsequently processed to yield solid mass and sample temperature vs. time profiles and a solid mass vs. sample temperature profile over the duration of a test. All tests were carried out at atmospheric pressure, and an atmosphere of pure nitrogen was supplied from an oxygen free nitrogen bottle to the inlet of the test section at a constant flow rate of 9 l/min. This flow rate together with air infiltration through the clearance between the bottom end-plate and the sheath resulted in oxygen levels in the centre of the mullite work-tube of less than 0.1% by volume.

Figure 3.1 Photograph of pyrolysis test rig.

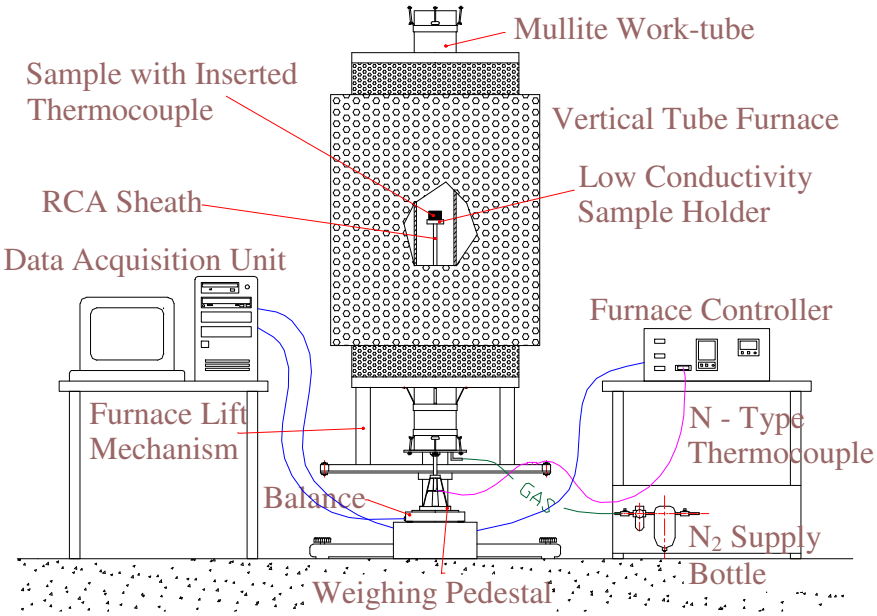

Figure 3.2 Schematic of specially designed thermobalance.

To avoid damage to the element and the work-tube at the start of a test, the manufacturer's maximum recommended permissible heating rate is 40 °C/min. In this research, the furnace was heated slowly from ambient at a rate of 5 °C/min up to a temperature of 750°C when the pyrolytic process completed.

3.2 Materials and methods

Tests of SRF briquettes involved a number of materials with a varying plastic/non-plastic fraction. To simulate SRF briquettes, the non-plastic fraction was represented by shredded office-grade paper. Paper was chosen as it is an organic-based substance, and for the purpose of the experiment it can be considered as lignocellulosic materials which are present in large quantities in MSW. Polyolefines such as PE or PP largely exist in plastic waste and therefore, regrind PP supplied by Plastex was used to prepare SRF briquettes to simulate the plastic fraction.

There were three groups of samples: (1) simulated SRF briquettes; (2) SRF briquettes; and (3) pulverised biomass, which were produced by Cardiff University as part of two research projects: design and testing of secondary refuse fuel briquettes to enable hydrogen production and energy recovery via gasification; Welsh Energy Research Centre biomass, waste to energy and underground gasification of coal.

The briquettes were produced by Cardiff University with a single-screw industrial extruder which was capable of producing 15mm diameter cylindrical briquettes. A photograph of this equipment is shown in Figure 3.3. Material was fed through the inlet and was heated and compressed as it passed along an extruder screw located inside the heating collars. The briquettes were discharged and cut by hand at the die face. The cylindrical briquettes produced for this research were not very uniform. Although the diameters were set to be 15 mm, Tables 3.2 and 3.7 show the actual diameters of the briquettes were between 11 and 21 mm.

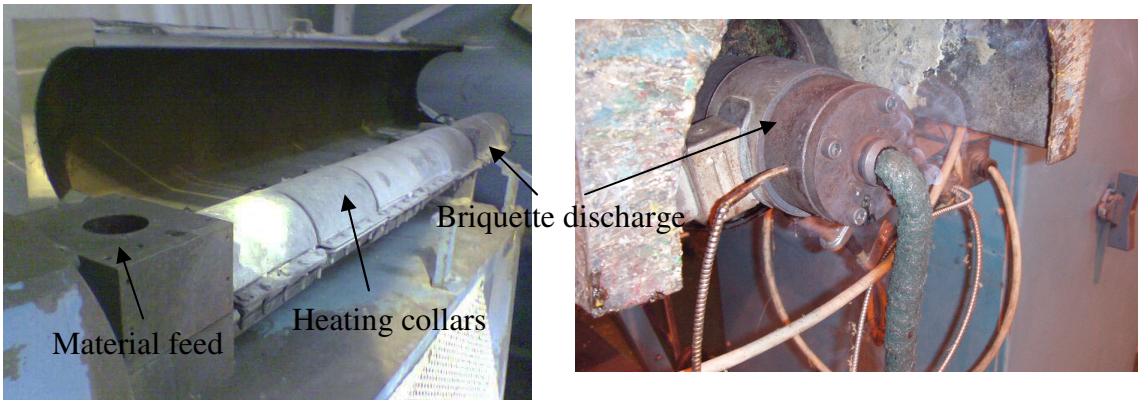

Figure 3.3 Briquette producing equipment.

3.2.1 Simulated SRF briquettes

PP was mixed with paper in ratios by mass of 20% PP and 80% paper to 60% PP and 40% paper. These cylindrical briquettes were produced in the equipment shown in Figure 3.3. A 100% compressed paper briquette was also produced by Cardiff University to compare with the other simulated SRF briquettes. The paper material was first shredded into 20 mm fragments and compressed into blocks using a Ruf two-stage piston-driven briquetting press, working at 150 MPa. A specially shaped receiving die shaped the compressed materials into blocks with dimensions of 60 mm × 100 mm × 150 mm. These blocks were cut into cuboids with dimensions of 15 mm square cross sections with different length using a bandsaw [125]. An image of a cuboidal paper briquette and a cylindrical simulated SRF briquette is shown in Figure 3.4. Seven simulated SRF briquettes for the tests are described in Table 3.1, and these briquettes were considered to be composition consistency acceptable compared to waste materials due to the heterogeneous composition nature of MSW.

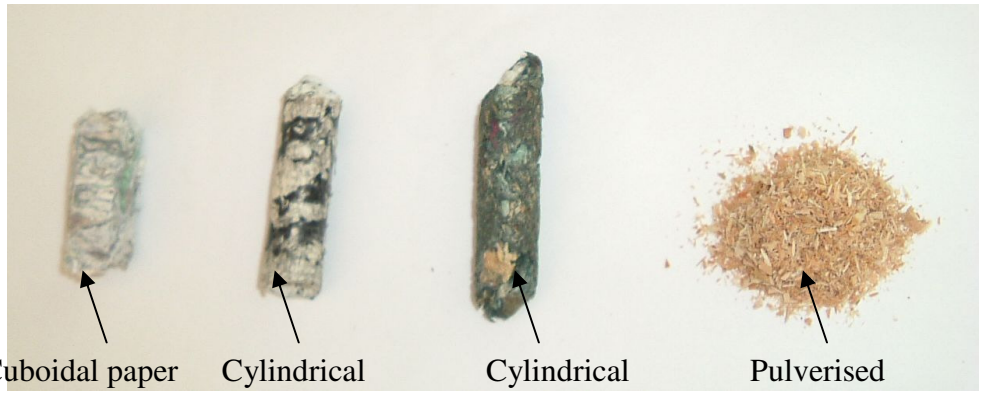

Figure 3.4 Samples' images.

Table 3.1 Simulated SRF briquettes

Sample code	Description
0PP	Compressed paper block
2PP	20% PP and 80% paper extruded at 125°C
4PP	40% PP and 60% paper extruded at 125°C
6PPa	60% PP and 40% paper extruded at 125°C
6PPb	60% PP and 40% paper extruded at 150°C
6PPc	60% PP and 40% paper extruded at 200°C
6PPd	60% PP and 40% paper extruded at 250°C

The pyrolysis test of the simulated SRF briquettes was to examine the repeatability of the pyrolytic process of each briquette above and to simulate the pyrolysis of the SRF briquettes made from real waste materials. Paper and PP were blended to represent two major components of SRF. The simulated SRF briquettes with the varying amount of plastic were tested to investigate the interactions between paper and plastic. Since plastic is a rich source of hydrocarbons and briquette "binding" is dominated by the plastic component, the effects of the amount of plastic in briquettes were studied. For further evaluation of the performance of the paper and PP blends, different extruding temperatures were also studied.

There were three groups of pyrolysis tests of the simulated SRF briquettes: (1) paper briquette; (2) briquettes of paper and plastic blend with varying ratios by mass; and (3) briquettes of paper and plastic blend with varying extruding temperatures.

(1) Pyrolysis of paper briquette (briquette 0PP shown in Table 3.1)
Seven pyrolysis tests of single segment cuboidal paper briquette were undertaken. The repeatability of the pyrolysis of paper, as a lignocellulosic material, was examined and the pyrolytic process of hemicellulose, cellulose and lignin was studied.

(2) Pyrolysis of paper and plastic blend briquettes extruded at 125°C with varying mass ratios of 20% PP and 80% paper (2PP), 40% PP and 60% paper (4PP), and 60% PP and 40% paper (6PPa)
Six pyrolysis tests of briquette 2PP, five pyrolysis tests of briquette 4PP and four pyrolysis tests of briquette 6PPa were undertaken. The repeatability of the pyrolysis of the lignocellulose and plastic blend briquette was examined, and the interactions between lignocellulose and plastic were studied in order to simulate the pyrolysis of SRF briquettes.

(3) Pyrolysis of 60% PP and 40% paper blend briquettes extruded at 125°C (6PPa), at 150°C (6PPb), at 200°C (6PPc) and at 250°C (6PPd)
Four pyrolysis tests of briquettes 6PPa and 6PPc, and five pyrolysis tests of briquettes 6PPb and 6PPd were undertaken. The repeatability of the pyrolysis of the lignocellulose and plastic blend briquette was examined, and the effect of the extruding temperature on the pyrolytic process was studied.

These three groups of tests are shown in Table 3.2. A single briquette segment with different initial mass pyrolysed in each test.

Table 3.2 Tests of simulated SRF briquettes

Sample	Number of tests	Segment length (mm)	Diameter (mm)	Initial mass (g)
0PP	7	/	/	12.0-26.0
2PP	6	41-79	13-19	5.9-14.8
4PP	5	48-57	14-18	7.1-8.8
6PPa	4	46-85	14-19	5.9-10.7
6PPb	5	47-49	12-19	6.4-7.2
6PPc	4	46-49	14-19	6.2-7.8
6PPd	5	47-49	11-17	4.0-5.2

The proximate analysis and the CVs of the simulated SRF briquettes provided by Cardiff University and the CV of paper from the literature are shown in Table 3.3. Table 3.4 shows the proximate analysis on a dry basis.

Table 3.3 Proximate analysis (% by mass) and CVs of simulated SRF briquettes

Sample code	CV (MJ/kg)	Moisture	Volatiles	Ash	Fixed carbon
0PP	11.0 [16]	4.40	73.20	13.40	9.00
2PP	21.0	2.65	78.55	13.65	5.15
4PP	24.2	2.75	80.45	11.65	5.15
6PPa	31.5	1.05	84.65	8.05	6.25
6PPd	31.1	0.75	87.05	10.70	1.50

Table 3.4 Proximate analysis (% by mass) of dry simulated SRF briquettes

Sample code	Volatiles	Ash	Fixed carbon
0PP	76.57	14.02	9.41
2PP	80.69	14.02	5.29
4PP	82.72	11.98	5.30
6PPa	85.55	8.14	6.31
6PPd	87.71	10.78	1.51

Table 3.3 shows that the CV of paper was much lower than that of paper and plastic blend briquettes. The briquettes with higher amounts of plastic had higher CVs. The 60% PP and 40% paper blend briquette extruded at 250°C had a slightly lower CV than that extruded at 125°C. This indicated that the extruding temperature didn't apparently affect the CV of the briquettes very much.

Table 3.4 shows the paper briquette had the lowest volatile content and the highest ash content. The briquette with a higher amount of plastic had a higher volatile content and a lower ash content. It also shows the briquette made at higher extruding temperature had a higher volatile content and a higher ash content. This is because lignocellulose has lower decomposition temperature than plastic. At high temperature such as 250°C, the decomposition of paper took place, some volatile matter was lost, and hence the reaction increases the ash content during the briquetting process. Therefore, briquette 6PPd had a higher volatile content and a higher ash content than briquette 6PPa. Briquette 6PPd had lower fixed carbon than briquette 6PPa and this indicated that high extruding temperature could increase volatile content.

3.2.2 SRF briquettes

The SRF briquettes were prepared from real waste materials including ecodeco, RDF, MBT processed RDF, raw MSW, sawdust, tar, molasses, RDF, sewage sludge, paper and PE. The sawdust was purchased from a pet shop, and consisted of unseasoned wood chips. The tar was obtained from a gasification process. It constituted 85% carbon and 15% hydrogen by molecular weight, and it also contained a trace amount of oxygen, nitrogen and sulphur. The compositions of ecodeco, MBT processed RDF and raw MSW are shown in Table 3.5. These three materials contained a large amount of paper and plastic. MBT processed RDF contained the highest paper content and the lowest plastic content. Ecodeco contained the highest plastic content and a high paper content of 35.1%. Raw MSW contained the lowest paper content of 24.0%. The proximate analysis by mass of ecodeco provided by Cardiff University shows: moisture 2.50%, volatiles 71.60%, ash 14.40% and fixed carbon 11.50%. The proximate analysis of dry ecodeco was: volatiles 73.44%, ash 14.77% and fixed carbon 11.79%. The volatiles of ecodeco were lower than those of paper and plastic. The ash content of ecodeco was higher than that of paper and plastic.

Table 3.5 Compositions (% by mass) of ecodeco, MBT processed RDF and raw MSW

Source: Progressive Energy Limited

Category	Ecodeco	MBT processed RDF	Raw MSW
Paper/card	35.1	55.0	24.0
Putrescibles	2.1	0.0	30.0
Glass	0.9	1.0	8.0
Fines	20.3	0.0	6.0
Ferrous	2.2	0.0	4.0
Non-ferrous		0.0	1.0
Dense plastic	23.0	5.0	10.0
Plastic film	0.0	4.0	0.0
Textiles	14.0	5.0	4.0
Miscellaneous combustibles	1.6	30.0	13.0
Miscellaneous non-combustibles	0.8	0.0	0.0
Dry lower heating value (MJ/kg)	16.5	17.4	/

Table 3.6 SRF briquettes

Sample code	Description
SRF1	Briquetted from 100% ecodeco at 125°C
SRF2	Briquetted from 100% ecodeco at 150°C
SRF3	Briquetted from 80% ecodeco and 20% sawdust
SRF4	Briquetted from 65% ecodeco, 10% sawdust, 15% paper and 10% PE
SRF5	Briquetted from RDF
SRF6	Briquetted from MBT processed RDF
SRF7	Briquetted from raw MSW
SRF8	Briquetted from RDF and molasses mixtures
SRF9	Briquetted from 50% standard dried sewage sludge and 50% tar

Nine SRF briquettes prepared for the pyrolysis tests in this research are described in Table 3.6. An image of a cylindrical SRF briquette is shown in Figure 3.4. There were four groups of pyrolysis tests of the SRF briquettes undertaken: (1) ecodeco briquettes

with varying extruding temperatures; (2) briquettes of ecodeco, biomass and plastic blend; (3) RDF briquettes with or without MBT process; and (4) other SRF briquettes.

(1) Ecodeco briquettes with varying extruding temperatures

The pyrolysis tests of the briquettes with the extruding temperature of 125°C (briquette SRF1 shown in Table 3.6) and at 150°C (SRF2) were undertaken. In the pyrolysis of briquette SRF1, there were four tests of small briquette multi segments and four tests of a single briquette segment. The repeatability of the pyrolytic process of both the small briquette multi segments and the single briquette segment was examined. The difference in the pyrolytic behaviour of the briquettes between the multi segments tests and the single segment tests was also examined. In the pyrolysis of briquette SRF2, there was one test with small briquette multi segments and five tests with a single briquette segment. The repeatability of the pyrolytic process of the single briquette segment was examined. The difference between the multi segments tests and the single segment tests was also examined. Meanwhile, the effect of the extruding temperature was also studied.

(2) Ecodeco briquettes blended with biomass or with biomass and plastic

One pyrolysis test of SRF briquette blended with 80% ecodeco and 20% sawdust (SRF3), and one pyrolysis test of SRF briquette blended with 65% ecodeco, 10% sawdust, 15% paper and 10% PE (SRF4) were undertaken. The effects of adding biomass and plastic on the pyrolytic characteristics of SRF briquettes were studied.

(3) RDF briquettes

One pyrolysis test of RDF briquette (SRF5) and one pyrolysis test of MBT processed RDF briquette (SRF6) were undertaken. The improvement of the pyrolytic characteristics of SRF briquettes through the MBT process was studied.

(4) Other SRF briquettes

One pyrolysis test of raw MSW briquette (SRF7) was undertaken and the pyrolytic characteristics of the briquette made from the waste material were studied. One pyrolysis test of RDF and molasses blend briquette (SRF8) was undertaken. Molasses is usually used as a binder, and in this research the effect of adding molasses on the pyrolytic characteristics of SRF briquettes was studied. One pyrolysis test of two

briquette segments of 50% standard dried sewage sludge and 50% tar blend (SRF9) was undertaken to examine the pyrolytic characteristics of SRF briquettes made from specific waste materials.

These four groups of tests are shown in Table 3.7. All tests started with different initial mass.

Table 3.7 Tests of SRF briquettes

Sample	Number of tests	Segment length (mm)	Diameter (mm)	Initial mass (g)
SRF1	4(multi-segment)	/	12-17	14.9-17.4
	4	33-47		3.9-8.2
SRF2	1(multi-segment)	/	13-20	15.3
	5	45-50		6.6-8.7
SRF3	1	75	15-17	14.1
SRF4	1	74	15-17	13.2
SRF5	1	92	14-15	15.2
SRF6	1	71	16-17	15.0
SRF7	1	54	14-15	10.3
SRF8	1	32	21	14.9
SRF9	1(two-segment)	26; 29	16	15.9

3.2.3 Pulverised biomass

Eleven raw biomass materials pulverised for the pyrolysis tests in this research are shown in Table 3.8, and the pyrolysis tests were carried out by three groups: (1) wood materials; (2) willow materials; and (3) other biomass materials. An image of the pulverised pet shop sawdust is shown in Figure 3.4.

Table 3.8 Pulverised biomass samples

Sample code	Description
PB1a	Pet shop sawdust
PB1b	RWE standard sawdust
PB2	Pulverised MFC wood
PB3a	Pulverised willow (inger 1)
PB3b	Pulverised willow (discovery 3)
PB4	Pulverised borage meal
PB5	Pulverised oat husk
PB6	Pulverised miscanthus giganteus
PB7	Pulverised miscanthus goliath
PB8	Pulverised rape straw
PB9	Pulverised wheat straw

(1) Wood materials

Three pyrolysis tests of the pet shop sawdust (sample PB1a shown in Table 3.8) and the RWE standard sawdust (PB1b) and two pyrolysis tests of the pulverised MFC wood (PB2) were undertaken to study the pyrolytic characteristics of wood materials. The repeatability of the pyrolytic process and the difference in the pyrolytic characteristics of these three wood materials were examined.

(2) Willow materials

Two pyrolysis tests of pulverised willow (inger 1) (PB3a) and pulverised willow (discovery 3) (PB3b) were undertaken. The difference in the pyrolytic characteristics of these two willow materials was studied.

(3) Other biomass

Two pyrolysis tests of pulverised borage meal (PB4), pulverised oat husk (PB5), pulverised miscanthus giganteus (PB6), pulverised miscanthus goliath (PB7), pulverised rape straw (PB8) and pulverised wheat straw (PB9) were undertaken to study the difference in the pyrolytic characteristics of these biomass materials.

These three groups of tests are shown in Table 3.9. All tests started with different initial mass.

Table 3.9 Tests of pulverised biomass samples

Sample	Number of tests	Initial mass (g)
PB1a	3	2.0
PB1b	3	2.7-2.9
PB2	2	3.6-4.2
PB3a	2	3.7-4.7
PB3b	2	3.2-3.4
PB4	2	7.2-7.4
PB5	2	4.0-5.3
PB6	2	4.9
PB7	2	3.4-3.7
PB8	2	2.3-2.8
PB9	2	2.2-2.9

The proximate analysis and the CVs of the pulverised biomass samples provided by Cardiff University are shown in Table 3.10. Table 3.11 shows the proximate analysis on a dry basis. Table 3.10 shows that biomass materials in this research had similar CV except that the CVs of RWE standard sawdust (PB1b), borage meal (PB4) and sawdust (PB1a) were lower than the others. This indicated that the category of biomass alone couldn't be used to predict CVs of the biomass briquettes. In fact, the moisture content played an important role. Table 3.10 shows that the sample with a high moisture content had a low CV. Sample PB1b contained 44.80% moisture, but it had been dried by Cardiff University and most of the moisture had been removed before the pyrolysis experiment was carried out.

Table 3.11 shows that the ash content of biomass materials was much lower than that of waste materials, except borage meal (PB4) which had even a higher ash content than paper. Two sawdust samples (PB1a and PB1b), rape straw (PB8) and wheat straw (PB9) had high volatiles.

Table 3.10 Proximate analysis (% by mass) and CVs of pulverised biomass samples

Sample code	CV (MJ/kg)	Moisture	Volatiles	Ash	Fixed carbon
PB1a	14.1	28.87	62.83	0.17	8.13
PB1b	11.1	44.80	48.30	0.20	6.70
PB2	17.9	7.77	70.00	1.30	20.93
PB3a	17.5	10.23	72.03	1.47	16.27
PB3b	17.6	8.85	74.70	1.20	15.25
PB4	14.0	13.93	57.10	15.10	13.87
PB5	17.1	7.77	73.33	4.50	14.40
PB6	17.9	6.60	74.40	1.90	17.10
PB7	17.6	7.43	74.80	2.69	15.08
PB8	18.1	10.17	83.43	3.20	3.20
PB9	18.3	7.87	80.13	2.57	9.43

Table 3.11 Proximate analysis (% by mass) of dry pulverised biomass samples

Sample code	Volatiles	Ash	Fixed carbon
PB1a	88.33	0.23	11.43
PB1b	87.50	0.36	12.14
PB2	75.89	1.41	22.70
PB3a	80.25	1.63	18.12
PB3b	81.95	1.32	16.73
PB4	66.34	17.54	16.11
PB5	79.45	4.88	15.67
PB6	79.66	2.03	18.31
PB7	80.81	2.91	16.29
PB8	92.81	3.56	3.63
PB9	86.98	2.79	10.24

Chapter Four Experimental Results

This chapter presents the experimental results of the pyrolytic characteristics of the simulated SRF briquettes, the SRF briquettes and the pulverised biomass, which include sample temperature vs. time, TG and DTG profiles.

Figure 4.1 shows the furnace temperature vs. time profile of a pyrolysis test. In the about first 60 min, the furnace temperature rise was lower than 5 °C/min and due to the temperature control, the furnace temperature rise waved between low and high rates. After about 60 min, the furnace temperature rise became stable and stayed at 5 °C/min. After the furnace temperature increased to 750°C, it stayed at 751°C for about 5 min and then was kept at 750°C.

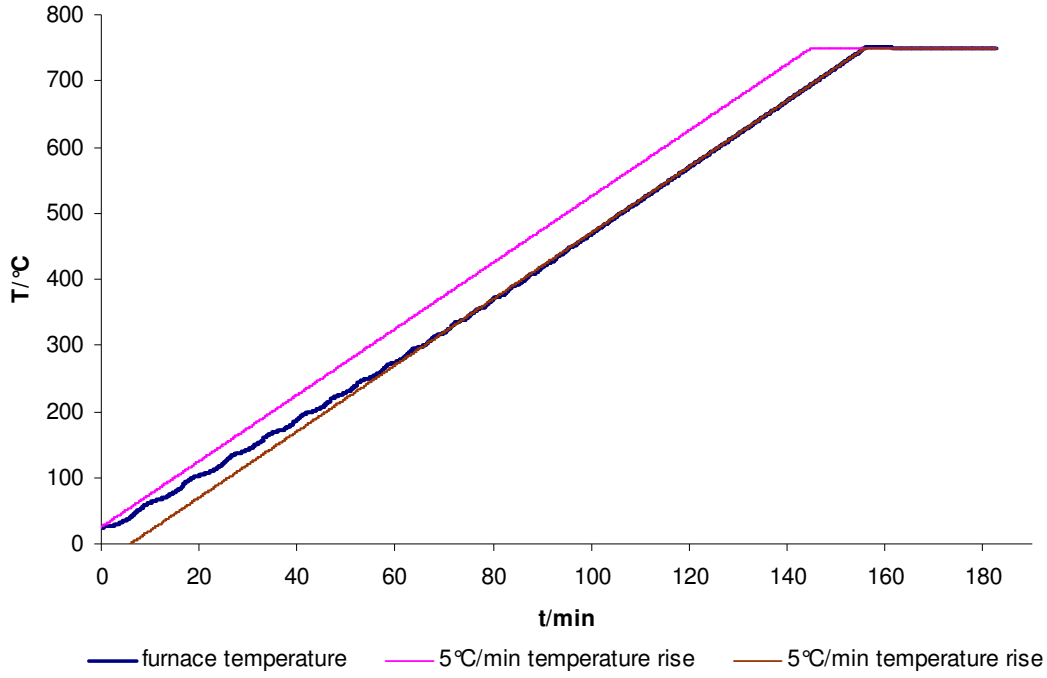

Figure 4.1 Furnace temperature vs. time profile.

In order to examine the repeatability of a pyrolytic process, error analysis was calculated with the equation below, and the errors of both minimum and maximum values are shown in the table in the following TG and DTG profiles.

$$e = \frac{a - a_{mean}}{a_{mean}} \times 100\%$$

where

e is error,

a is result value,

a_{mean} is mean result value.

4.1 Pyrolytic characteristics of simulated SRF briquettes

Simulated SRF briquettes were prepared with the compositions of varying paper/plastic ratios at varying extruding temperatures. The pyrolysis tests of the simulated SRF briquettes were carried out by three groups: (1) pyrolysis of paper briquette; (2) pyrolysis of briquettes with varying paper/PP ratios; and (3) pyrolysis of briquettes with varying extruding temperatures.

4.1.1 Pyrolytic characteristics of cuboidal paper briquette

Seven pyrolysis tests started with different initial sample mass of 20.255 g, 23.361 g, 13.468 g, 11.802 g, 15.321 g, 20.774 g and 11.692 g, respectively. Figure 4.2 shows the sample temperature vs. time profile of the pyrolysis tests of the cuboidal paper briquette (0PP). When the briquette's inside temperature was below 150°C in the beginning of each test, it experienced a lower heating rate than 5 °C/min. This was mainly because the electric furnace needed a large amount of energy to start and therefore, the furnace temperature experienced a slower heating rate than the set rate in the beginning. There was also temperature difference between the furnace temperature and the briquette's inside temperature. The moisture content of 4.40% in the paper briquette also delayed briquette temperature rise by absorbing heat for moisture vaporisation. As a lignocellulosic material, the paper briquette contained hemicellulose, cellulose and lignin. When the briquette temperature increased over 150°C, the temperature rise became faster, but it was still lower than the furnace temperature, as the pyrolysis of hemicellulose and cellulose was endothermic. Between 300°C and 450°C, the briquette temperature increased very fast. This indicated that exothermic pyrolysis of lignin took place and the endothermicity of the pyrolysis of hemicellulose and cellulose was offset within this temperature range. Above 450°C, the temperature rise became slower and close to 5 °C/min. Figure 4.2 shows when tests 1, 3, 5 and 6 continued, the briquette temperature continued increasing to over 750°C, which was higher than the set final furnace temperature.

This indicated the exothermic pyrolysis of lignin in the paper briquette took place over a broad temperature range. When the pyrolysis of lignin was completed, the sample temperature dropped to the furnace temperature of 750°C. At the end of the tests under the high temperature, the exothermic decomposition of calcium carbonate ($CaCO_3$) also took place to form calcium oxide (CaO) and carbon dioxide (CO_2). Figure 4.2 shows these seven curves had very similar distinguishing features at specific temperature ranges, except that the briquette temperature rise in some tests was lower than that in other tests between 300°C and 450°C.

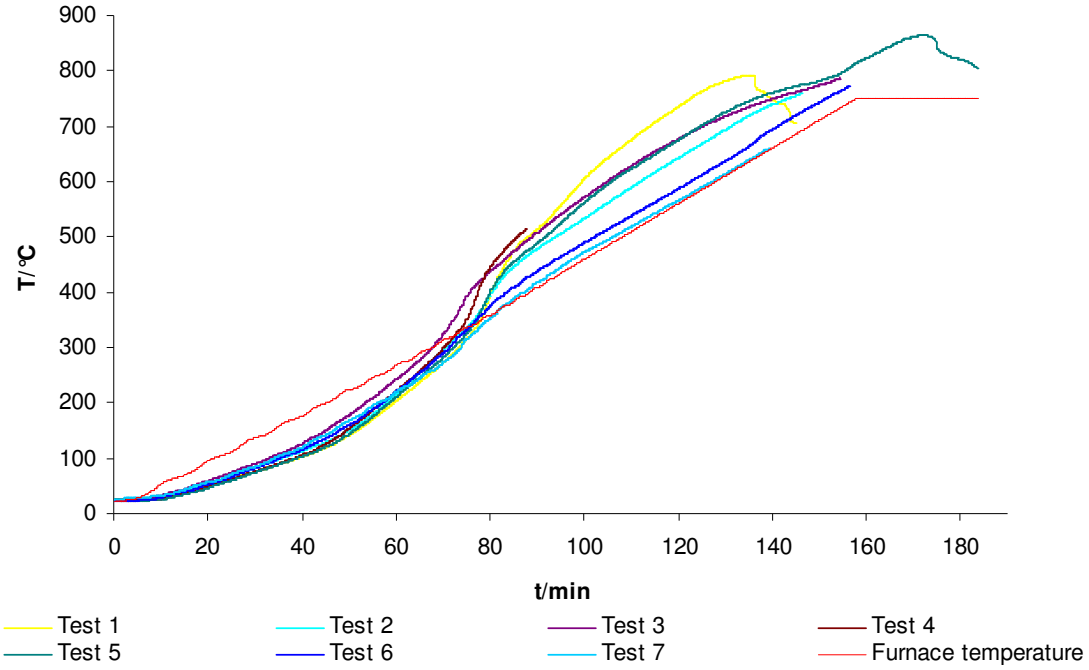

Figure 4.2 Briquette 0PP's temperature vs. time profile.

Figure 4.3 shows the TG curve of the pyrolysis tests of the cuboidal paper briquette. The briquette temperature increased from room temperature, and the mass loss was only moisture vaporisation in the beginning and proceeded slowly until the residual mass fraction reached around 93%. As the moisture content was only about 4.40% as shown in Table 3.3, this indicated some light volatiles might be released from paper under 250°C and a small amount of lignin might pyrolyse slowly at this low temperature. When the residual mass fraction fell below 93%, the mass change proceeded rapidly and the main pyrolytic process occurred. When the residual mass fraction fell below 40%, the mass change proceeded slowly again, and the pyrolysis was mainly the decomposition of lignin which was slow and lasted until the end of the test. At the end of the test, the exothermic decomposition of calcium carbonate took

place. There were backward curves in the end of tests 1 and 5 because of the temperature drop during the pyrolytic process. The distinguishing features of these seven TG curves at the specific mass remaining fraction were quite similar, and this indicated that the composition of the paper briquette (moisture, volatile, and ash contents) was quite constant. Figure 4.3 also shows that more than a quarter of the sample mass had not pyrolysed by the end of the test and therefore was considered to be inert component which was ash including calcium carbonate. The ash contained a large amount of inorganic component, some of which could affect the pyrolytic process by shifting cellulose decomposition to a lower temperature. As the inorganic component might vary in the paper briquette sample, the TG curve shifting effect varied in these seven tests.

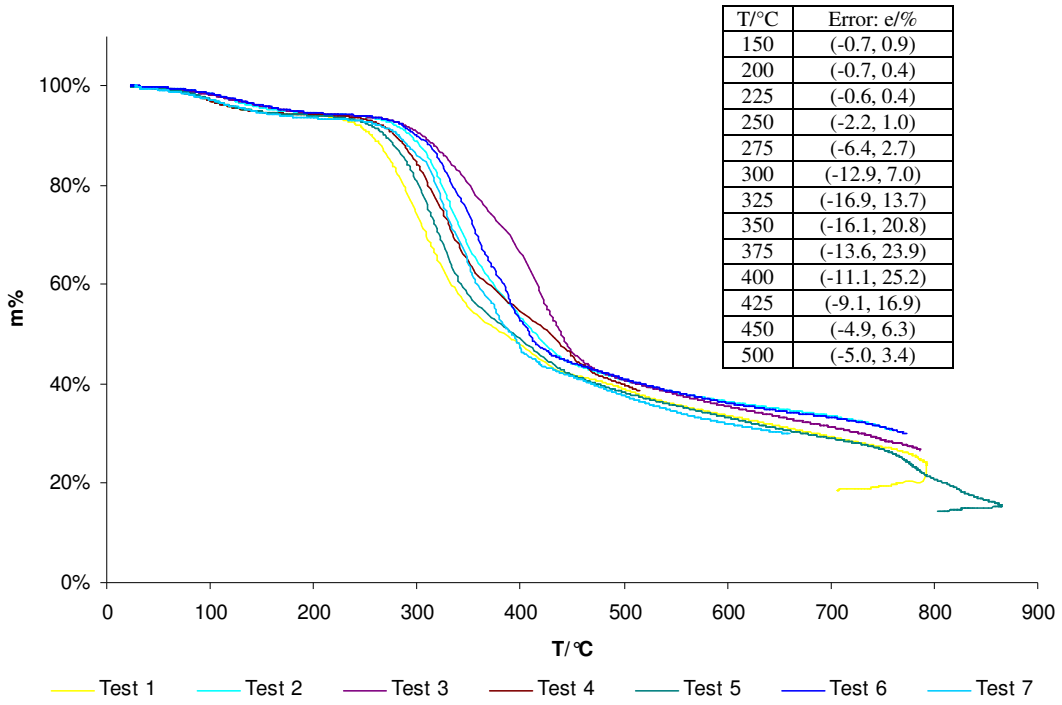

Figure 4.3 TG profile of briquette 0PP.

Figure 4.4 shows the DTG curve of the pyrolysis tests of the cuboidal paper briquette. Two different zones can be distinguished in the curve. The moisture vaporisation was the first zone as a small mass loss event with the maximum rate at between 110°C and 150°C. The thermal decomposition started in the second zone with the maximum mass loss rate at between 310°C and 355°C except the test 3 whose maximum mass loss rate was at 388°C. The main pyrolytic process involved the decomposition of hemicellulose, cellulose and lignin, and was essentially completed at between 430°C and 480°C. The main pyrolytic process was followed by a slow further mass loss,

which was the decomposition of lignin up to the final temperature. The curve shifting can also be seen in the DTG profile in Figure 4.4, and it widened the peak of the curve and reduced the maximum mass loss rate. Test 5 had the highest maximum mass loss rate and tests 3 and 6 had the lowest maximum mass loss rate. The reaction kinetic study is discussed in the next chapter. The error analysis shows that the error of DTG profile was much larger than that of TG profile.

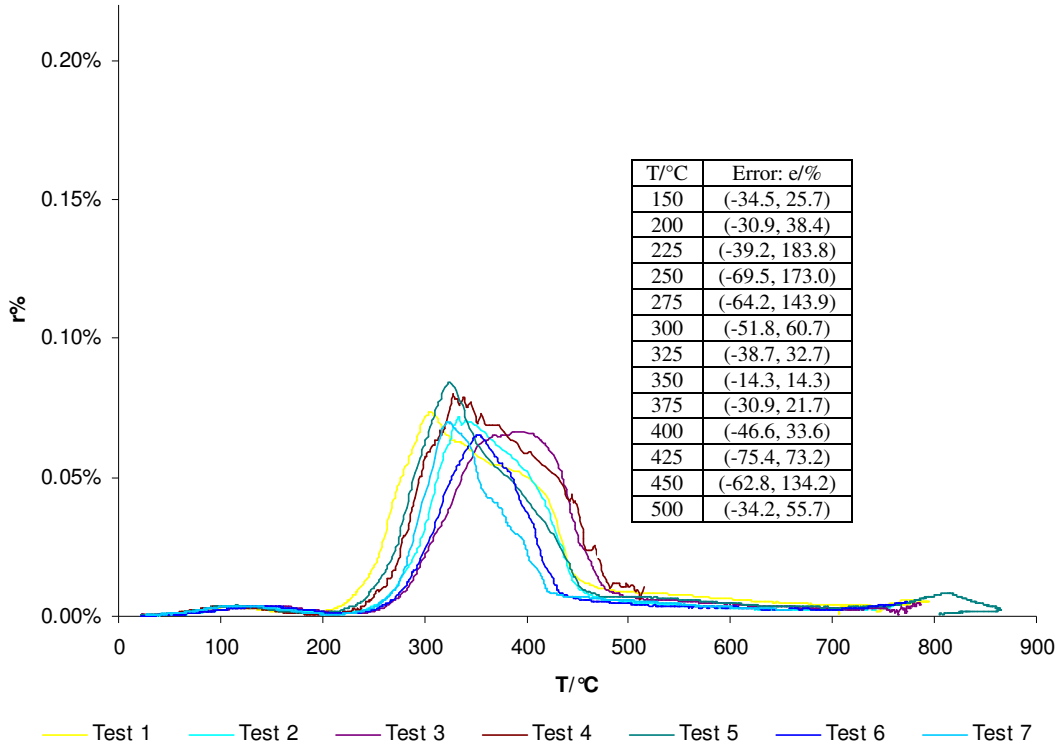

T/°C	Error: e/%
150	(-34.5, 25.7)
200	(-30.9, 38.4)
225	(-39.2, 183.8)
250	(-69.5, 173.0)
275	(-64.2, 143.9)
300	(-51.8, 60.7)
325	(-38.7, 32.7)
350	(-14.3, 14.3)
375	(-30.9, 21.7)
400	(-46.6, 33.6)
425	(-75.4, 73.2)
450	(-62.8, 134.2)
500	(-34.2, 55.7)

Figure 4.4 DTG profile of briquette 0PP.

The overall pyrolytic process of the paper briquette consisted of a moisture vaporisation zone and a thermal decomposition zone. Hemicellulose decomposition was associated with the shoulder of the thermal decomposition zone in the DTG profile, and cellulose decomposition was associated with the peak at about 330°C. The temperature of cellulose decomposition could be shifted to a lower temperature due to the effect of the inorganic component. The pyrolysis of hemicellulose and cellulose was slightly endothermic. The pyrolysis of lignin was exothermic, started at a very low temperature, occurred slowly, and was over a broad temperature range. At the temperature range of 300 – 450°C, the effect of lignin decomposition was significant. At the temperature above 700°C, the exothermic decomposition of calcium carbonate took place.

4.1.2 Pyrolytic characteristics of briquettes with varying paper/plastic ratios

The pyrolysis of the paper and PP blend briquette extruded at 125°C with varying ratios by mass of 20% PP and 80% paper (2PP), 40% PP and 60% paper (4PP), and 60% PP and 40% paper (6PPa) was carried out. Six pyrolysis tests of briquette 2PP started with different initial sample mass of 14.822 g, 12.119 g, 7.213 g, 5.904 g, 7.099 g and 8.733 g, respectively. Five pyrolysis tests of briquette 4PP started with different initial sample mass of 7.243 g, 8.831 g, 7.440 g, 7.099 g and 7.502 g, respectively. And four pyrolysis tests of briquette 6PPa started with different initial sample mass of 6.629 g, 5.902 g, 6.892 g and 6.979 g, respectively.

Figures 4.5, 4.6 and 4.7 show the sample temperature vs. time profile of the pyrolysis tests of briquettes 2PP, 4PP and 6PPa, respectively. Same as the pyrolysis tests of the paper briquette, the temperature of the inside of the briquettes 2PP, 4PP and 6PPa in the beginning of the tests experienced a lower heating rate than 5 °C/min. When the briquette temperature increased over 150°C, the temperature rise became faster, but it was still slower than the furnace temperature, as the pyrolysis of hemicellulose and cellulose was endothermic. Figure 4.5 shows between 330°C and 420°C, the temperature of briquette 2PP increased faster. This indicated that the effect of lignin decomposition was significant. Figure 4.6 shows the effect of lignin decomposition of briquette 4PP was significant between 350°C and 440°C. As the pyrolytic process continued, the plastic decomposition took place. At the temperature between 420°C and 480°C, the temperature rise became slow, and this indicated that the pyrolysis of plastic was endothermic. It can be observed that the curve shifting effect was less when the briquettes contained a higher plastic fraction, as the briquette with a higher plastic fraction contained less inorganic component.

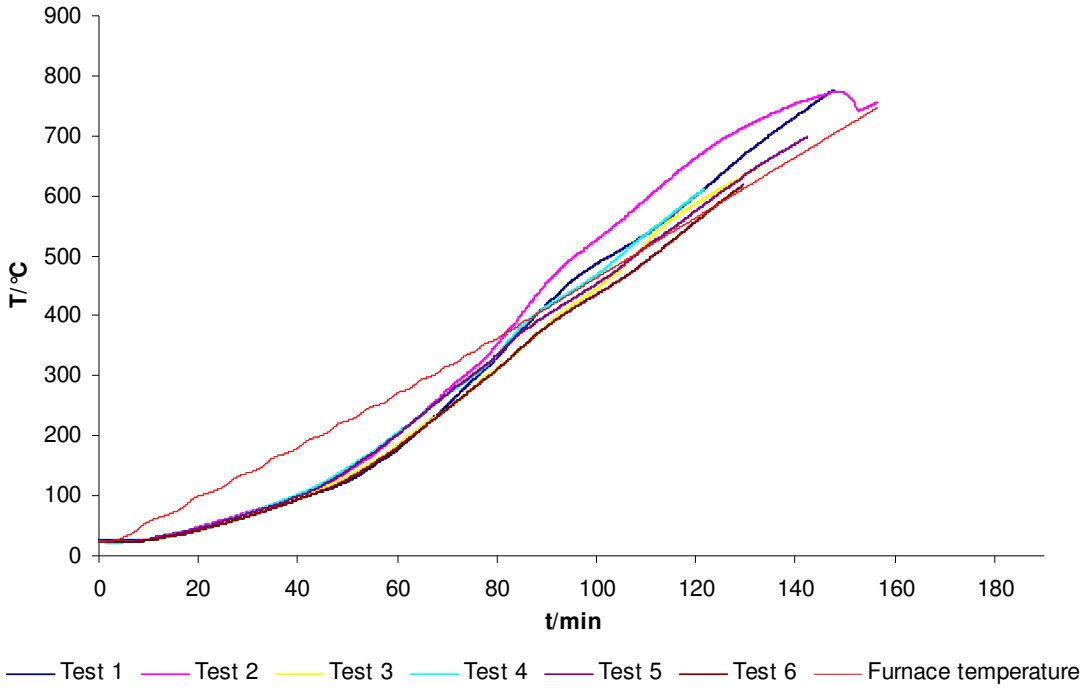

Figure 4.5 Briquette 2PP's temperature vs. time profile.

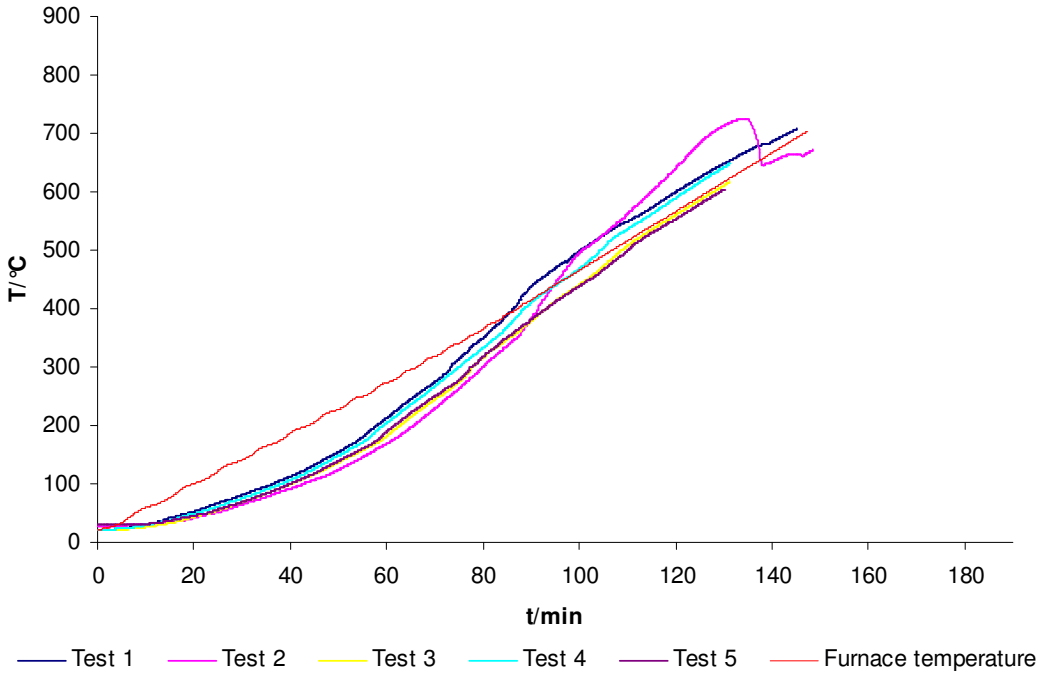

Figure 4.6 Briquette 4PP's temperature vs. time profile.

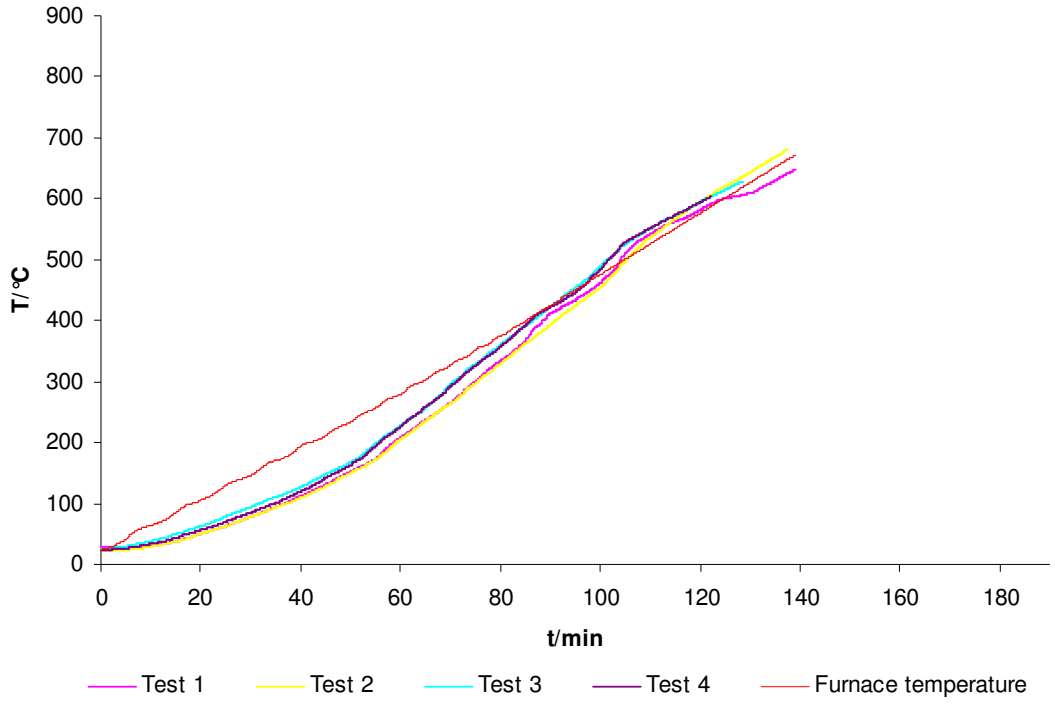

Figure 4.7 Briquette 6PPa's temperature vs. time profile.

Figures 4.8, 4.9 and 4.10 show the TG curve of the pyrolysis tests of briquettes 2PP, 4PP and 6PPa, respectively. Similar to the pyrolysis of the paper briquette, the briquette temperature of paper and plastic blend increased from room temperature, and when the mass loss was only moisture vaporisation it proceeded slowly. The decomposition of lignin also took place slowly at the low temperature. Figure 4.8 shows when the residual mass fraction in the pyrolysis of briquette 2PP fell below 93%, the mass change proceeded rapidly and the main pyrolysis occurred. When the residual mass fraction fell below 28%, the mass change proceeded slowly again and the pyrolysis was mainly the decomposition of lignin. Figure 4.9 shows the pyrolysis of briquette 4PP proceeded fast within the range of the residual mass fraction between 94% and 25%, and Figure 4.10 shows the pyrolysis of briquette 6PPa proceeded fast within the range of the residual mass fraction between 96% and 23%. Compared to the other simulated SRF briquettes, briquette 6PPa contained a higher plastic content and had a more apparent mass loss rate change in the end of the main pyrolytic process at about 500°C. It can be observed that, the briquette containing a higher plastic content released more volatiles in the pyrolytic process. Volatiles were mainly the products of decomposition of hemicellulose and cellulose. The curve shifting was effected by the inorganic component, and the error analysis shows the curve was more

repeatable and shifted less during the main pyrolytic process between 300°C and 500°C when the briquette had a higher plastic content.

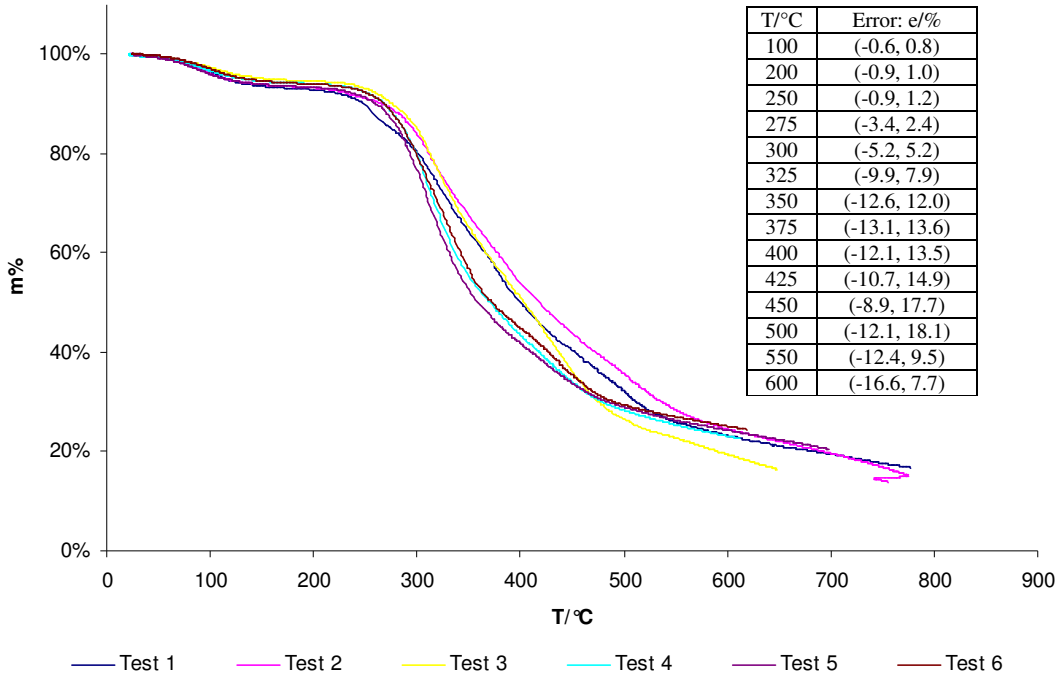

T/°C	Error: e/%
100	(-0.6, 0.8)
200	(-0.9, 1.0)
250	(-0.9, 1.2)
275	(-3.4, 2.4)
300	(-5.2, 5.2)
325	(-9.9, 7.9)
350	(-12.6, 12.0)
375	(-13.1, 13.6)
400	(-12.1, 13.5)
425	(-10.7, 14.9)
450	(-8.9, 17.7)
500	(-12.1, 18.1)
550	(-12.4, 9.5)
600	(-16.6, 7.7)

Figure 4.8 TG profile of briquette 2PP.

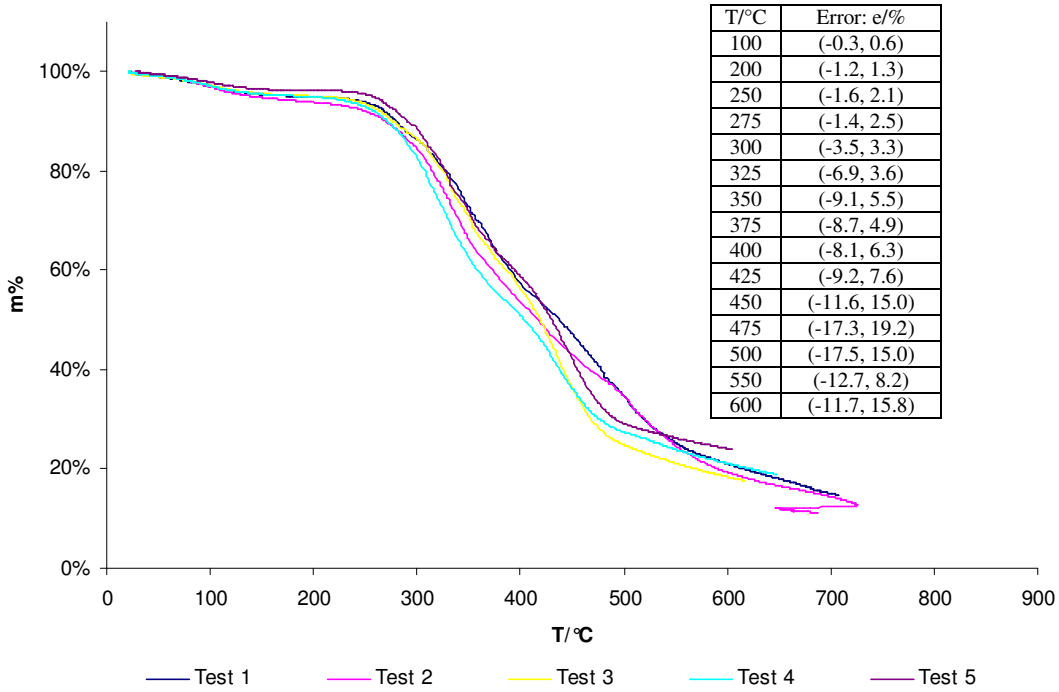

T/°C	Error: e/%
100	(-0.3, 0.6)
200	(-1.2, 1.3)
250	(-1.6, 2.1)
275	(-1.4, 2.5)
300	(-3.5, 3.3)
325	(-6.9, 3.6)
350	(-9.1, 5.5)
375	(-8.7, 4.9)
400	(-8.1, 6.3)
425	(-9.2, 7.6)
450	(-11.6, 15.0)
475	(-17.3, 19.2)
500	(-17.5, 15.0)
550	(-12.7, 8.2)
600	(-11.7, 15.8)

Figure 4.9 TG profile of briquette 4PP.

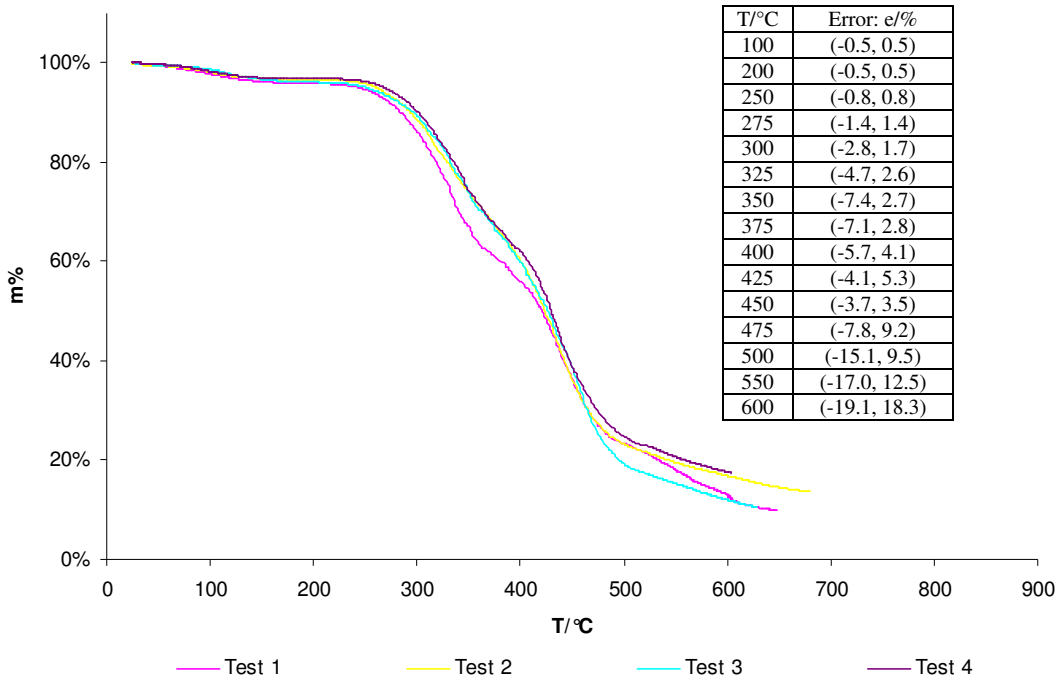

T/°C	Error: e/%
100	(-0.5, 0.5)
200	(-0.5, 0.5)
250	(-0.8, 0.8)
275	(-1.4, 1.4)
300	(-2.8, 1.7)
325	(-4.7, 2.6)
350	(-7.4, 2.7)
375	(-7.1, 2.8)
400	(-5.7, 4.1)
425	(-4.1, 5.3)
450	(-3.7, 3.5)
475	(-7.8, 9.2)
500	(-15.1, 9.5)
550	(-17.0, 12.5)
600	(-19.1, 18.3)

Figure 4.10 TG profile of briquette 6PPa.

Figure 4.11 shows the DTG curve of the pyrolysis of briquette 2PP. Two different zones can be distinguished. The moisture vaporisation was the first zone as a small mass loss event with the maximum rate at 110°C. The thermal decomposition started in the second zone with the maximum mass loss rate at between 320°C and 340°C except test 2 whose maximum mass loss rate was at 370°C. Following the second zone, there was a small mass loss event representing the pyrolysis of plastic. The main pyrolytic process was essentially completed at between 510°C and 610°C and it was followed by the slow further lignin pyrolysis up to the final temperature. Curve shifting existed in tests 1 and 2, and it lowered the mass loss rate and caused the second and third events highly overlapped. At the temperature above 700°C, the decomposition of calcium carbonate took place.

Figure 4.12 shows the DTG curve of the pyrolysis of briquette 4PP. Three different zones can be distinguished. The moisture vaporisation was the first zone as a small mass loss event with the maximum rate at 110°C. The thermal decomposition started in the second zone with the maximum mass loss rate at between 330°C and 340°C. The third zone represented the pyrolysis of plastic with the maximum rate at between 440°C and 455°C. The second and third zones in tests 1 and 2 overlapped, and this might be the effect of the inorganic component. The main pyrolytic process was

essentially completed at between 520°C and 610°C and it was followed by the slow further lignin pyrolysis up to the final temperature.

Figure 4.13 shows the DTG curve of the pyrolysis of briquette 6PPa. Three different zones can be distinguished. The moisture vaporisation was the first zone as a small mass loss event with the maximum rate at between 100°C and 115°C. The thermal decomposition started in the second zone with the maximum mass loss rate at between 330°C and 350°C. The third zone represented the pyrolysis of plastic with the maximum rate at between 445°C and 460°C. The main pyrolytic process was essentially completed at between 520°C and 560°C and it was followed by the slow further lignin pyrolysis up to the final temperature.

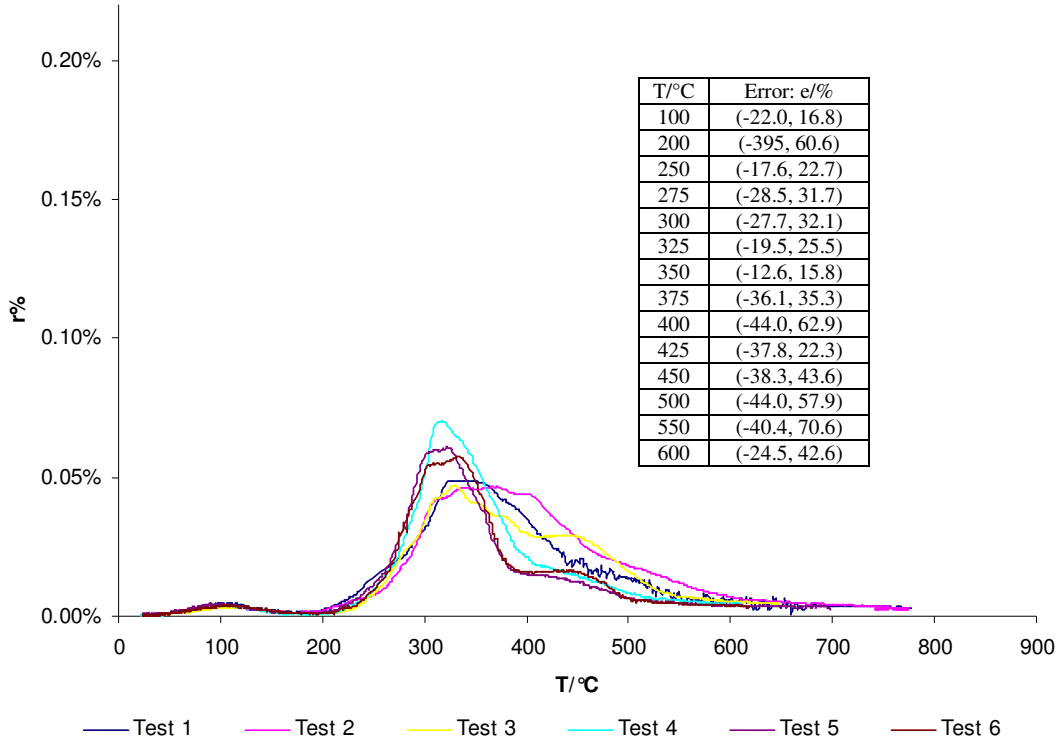

T/°C	Error: e/%
100	(-22.0, 16.8)
200	(-395, 60.6)
250	(-17.6, 22.7)
275	(-28.5, 31.7)
300	(-27.7, 32.1)
325	(-19.5, 25.5)
350	(-12.6, 15.8)
375	(-36.1, 35.3)
400	(-44.0, 62.9)
425	(-37.8, 22.3)
450	(-38.3, 43.6)
500	(-44.0, 57.9)
550	(-40.4, 70.6)
600	(-24.5, 42.6)

Figure 4.11 DTG profile of briquette 2PP.

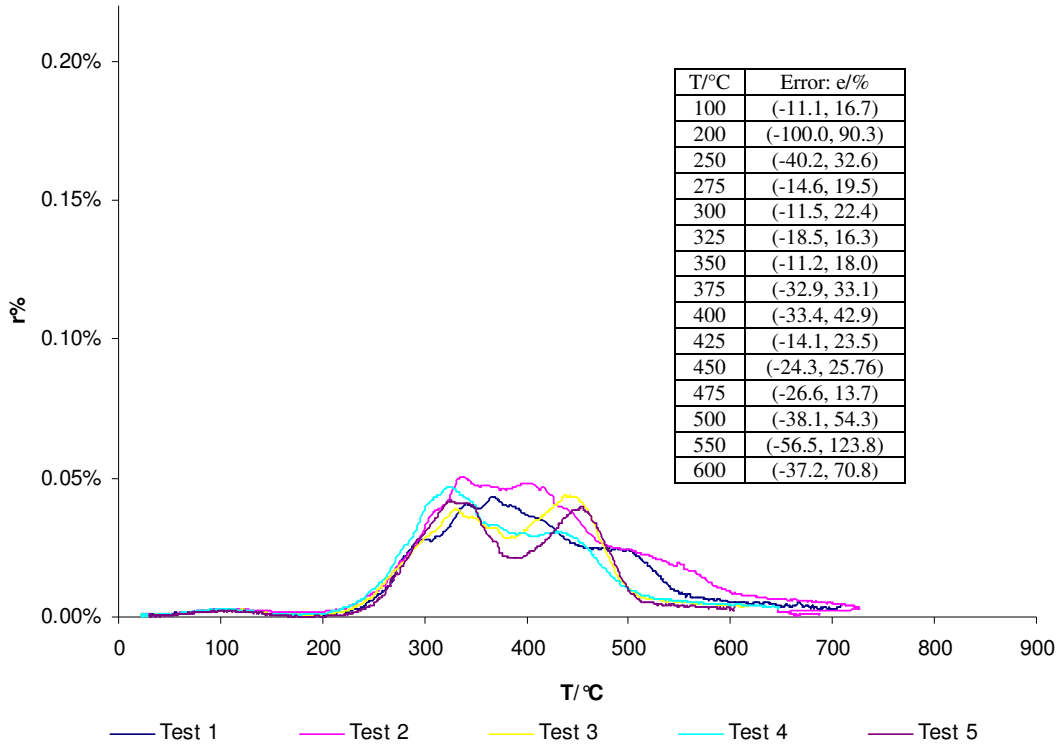

T/°C	Error: e/%
100	(-11.1, 16.7)
200	(-100.0, 90.3)
250	(-40.2, 32.6)
275	(-14.6, 19.5)
300	(-11.5, 22.4)
325	(-18.5, 16.3)
350	(-11.2, 18.0)
375	(-32.9, 33.1)
400	(-33.4, 42.9)
425	(-14.1, 23.5)
450	(-24.3, 25.76)
475	(-26.6, 13.7)
500	(-38.1, 54.3)
550	(-56.5, 123.8)
600	(-37.2, 70.8)

Figure 4.12 DTG profile of briquette 4PP.

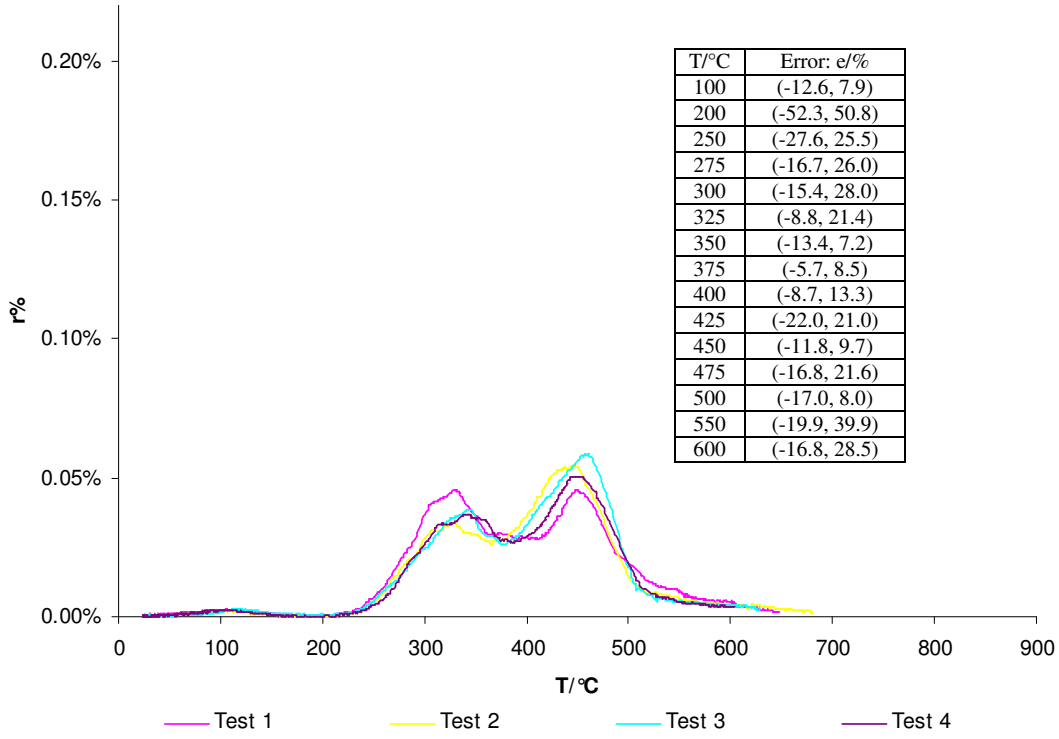

T/°C	Error: e/%
100	(-12.6, 7.9)
200	(-52.3, 50.8)
250	(-27.6, 25.5)
275	(-16.7, 26.0)
300	(-15.4, 28.0)
325	(-8.8, 21.4)
350	(-13.4, 7.2)
375	(-5.7, 8.5)
400	(-8.7, 13.3)
425	(-22.0, 21.0)
450	(-11.8, 9.7)
475	(-16.8, 21.6)
500	(-17.0, 8.0)
550	(-19.9, 39.9)
600	(-16.8, 28.5)

Figure 4.13 DTG profile of briquette 6PPa.

The overall pyrolytic process of the paper and PP blend briquettes consisted of a moisture vaporisation zone and two thermal decomposition zones. The first thermal decomposition zone was the pyrolysis of lignocellulose including hemicellulose, cellulose and lignin with the peak temperature at about 330°C corresponded to the thermal decomposition zone of the pyrolysis of the paper briquette. The second thermal decomposition zone was associated with the pyrolysis of plastic with the peak temperature at about 450°C as well as the pyrolysis of lignin. The pyrolysis of plastic was endothermic. The pyrolysis of lignocellulose and the pyrolysis of plastic proceeded independently. As a rich source of hydrocarbons, plastic enhanced the repeatability of the pyrolytic process. This can be seen from the error analysis of the DTG profiles. The briquette with a higher plastic fraction released more volatiles and the curve shifting was less affected. At the temperature above 700°C, the exothermic decomposition of calcium carbonate took place.

4.1.3 Pyrolytic characteristics of briquettes with varying extruding temperatures

The pyrolysis of the briquettes of 20% PP and 80% paper by mass with varying extruding temperatures at 125°C (6PPa), 150°C (6PPb), 200°C (6PPc) and 250°C (6PPd) was carried out. Four pyrolysis tests of briquette 6PPa started with different initial sample mass of 6.629 g, 5.902 g, 6.892 g and 6.979 g, respectively. Five pyrolysis tests of briquette 6PPb started with different initial sample mass of 6.990 g, 6.872 g, 6.436 g, 7.212 g and 7.152 g, respectively. Four pyrolysis tests of briquette 6PPc started with different initial sample mass of 7.080 g, 7.423 g, 6.236 g and 7.793 g, respectively. And five pyrolysis tests of briquette 6PPd started with different initial sample mass of 5.184 g, 4.283 g, 4.942 g, 4.294 g and 4.028 g, respectively.

Figures 4.7, 4.14, 4.15 and 4.16 show the sample temperature vs. time profile of the pyrolysis tests of briquettes 6PPa, 6PPb, 6PPc and 6PPd, respectively. Compared to the other simulated SRF briquettes, the curves of briquettes 6PPa, 6PPb, 6PPc and 6PPd had very similar distinguishing features in the endothermic pyrolysis of hemicellulose and cellulose, the exothermic pyrolysis of lignin, and the endothermic pyrolysis of plastic, and were more repeatable.

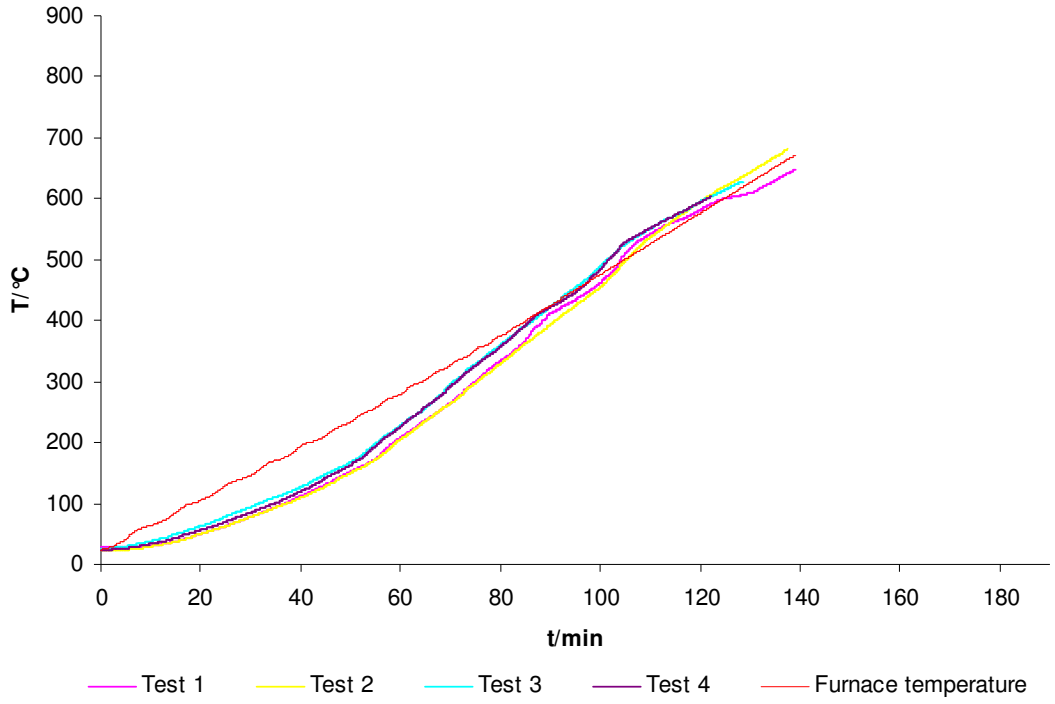

Figure 4.7 Briquette 6PPa's temperature vs. time profile.

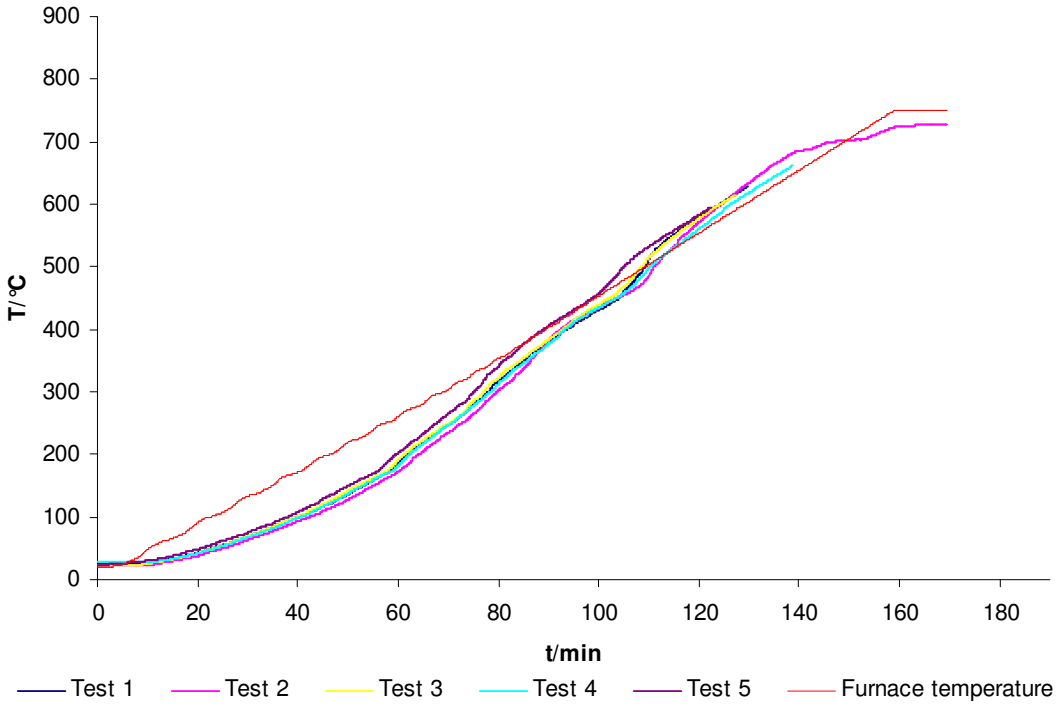

Figure 4.14 Briquette 6PPb's temperature vs. time profile.

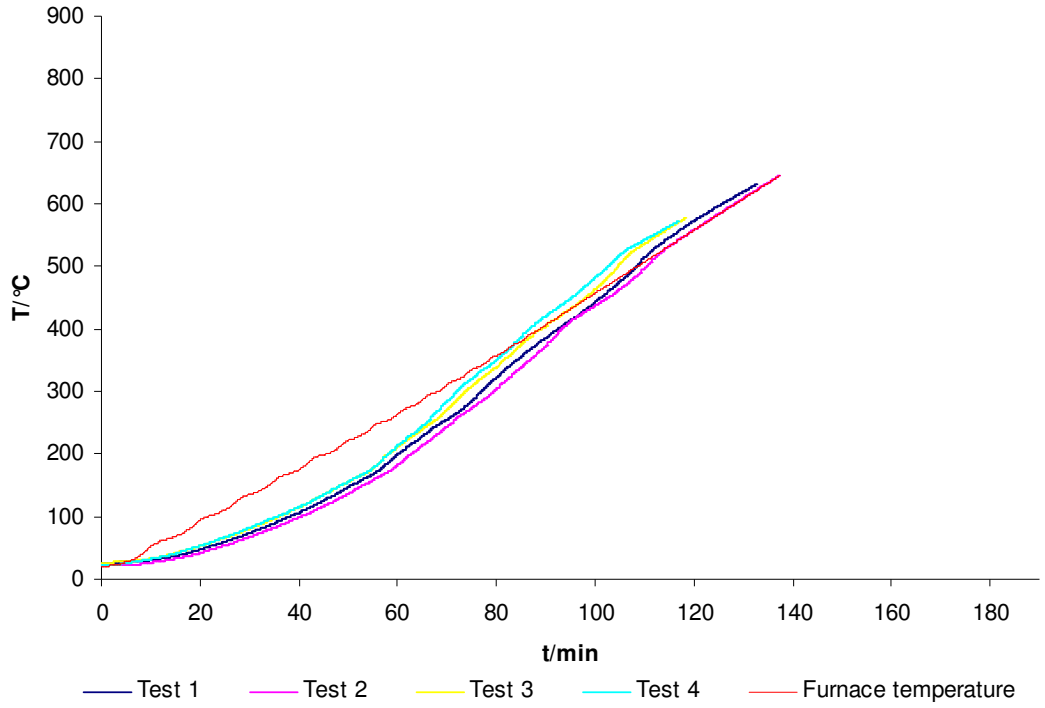

Figure 4.15 Briquette 6PPc's temperature vs. time profile.

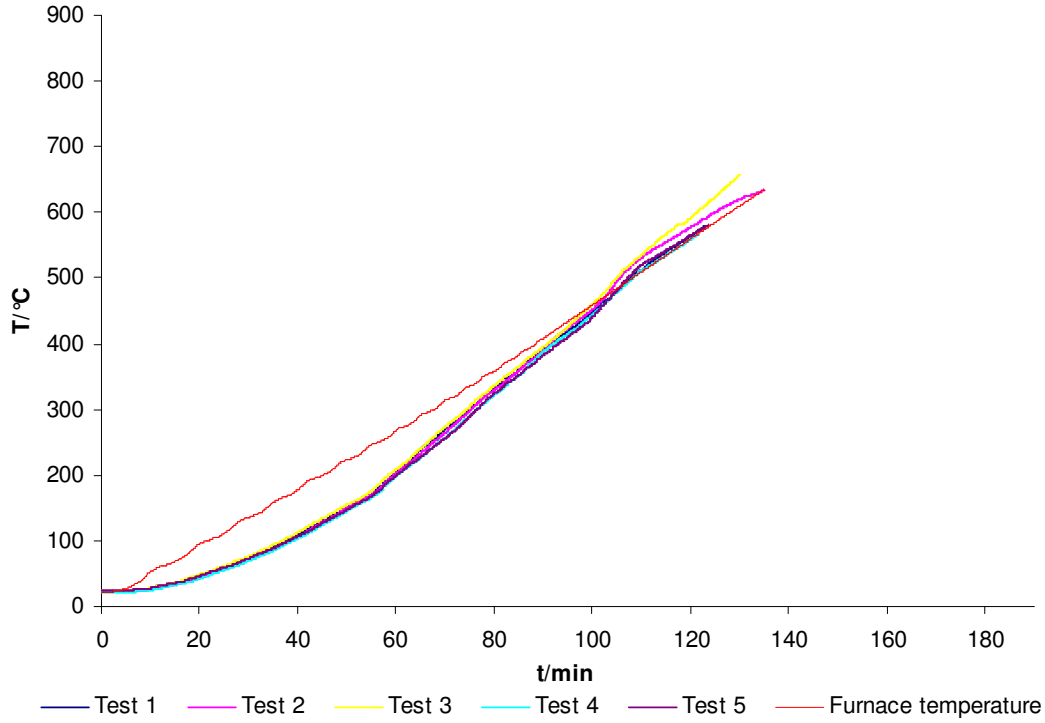

Figure 4.16 Briquette 6PPd's temperature vs. time profile.

Figures 4.10, 4.17, 4.18 and 4.19 show the TG curve of the pyrolysis tests of briquettes 6PPa, 6PPb, 6PPc and 6PPd, respectively. The main pyrolytic process which was mainly the pyrolysis of hemicellulose, cellulose and plastic, started when

the residual mass fraction fell below 96% and finished at about 500°C. There was an apparent mass loss rate change when the main pyrolytic process finished. The lignin pyrolysis continued slowly until the end of the test. The TG curves were more repeatable than the other lower plastic content simulated SRF briquettes.

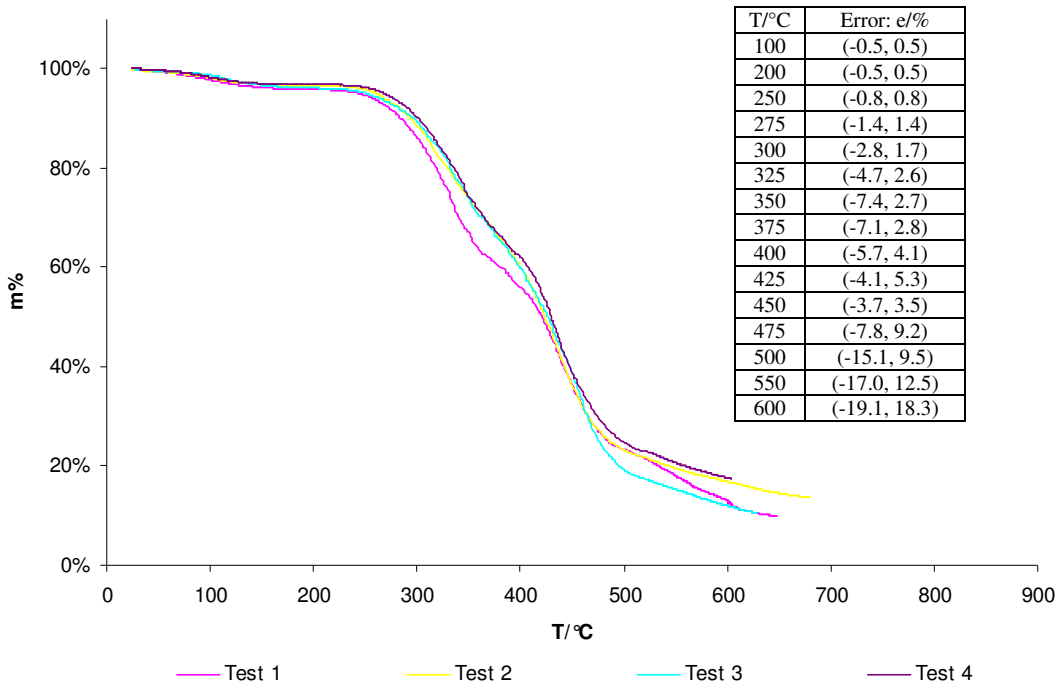

T/°C	Error: e/%
100	(-0.5, 0.5)
200	(-0.5, 0.5)
250	(-0.8, 0.8)
275	(-1.4, 1.4)
300	(-2.8, 1.7)
325	(-4.7, 2.6)
350	(-7.4, 2.7)
375	(-7.1, 2.8)
400	(-5.7, 4.1)
425	(-4.1, 5.3)
450	(-3.7, 3.5)
475	(-7.8, 9.2)
500	(-15.1, 9.5)
550	(-17.0, 12.5)
600	(-19.1, 18.3)

Figure 4.10 TG profile of briquette 6PPa.

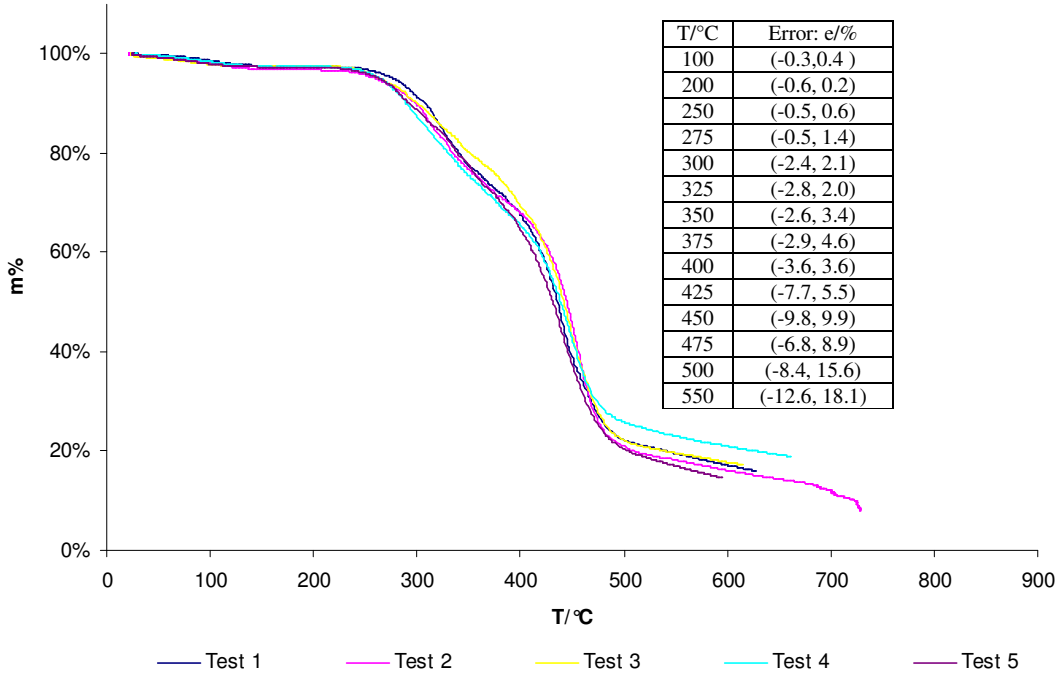

T/°C	Error: e/%
100	(-0.3,0.4)
200	(-0.6, 0.2)
250	(-0.5, 0.6)
275	(-0.5, 1.4)
300	(-2.4, 2.1)
325	(-2.8, 2.0)
350	(-2.6, 3.4)
375	(-2.9, 4.6)
400	(-3.6, 3.6)
425	(-7.7, 5.5)
450	(-9.8, 9.9)
475	(-6.8, 8.9)
500	(-8.4, 15.6)
550	(-12.6, 18.1)

Figure 4.17 TG profile of briquette 6PPb.

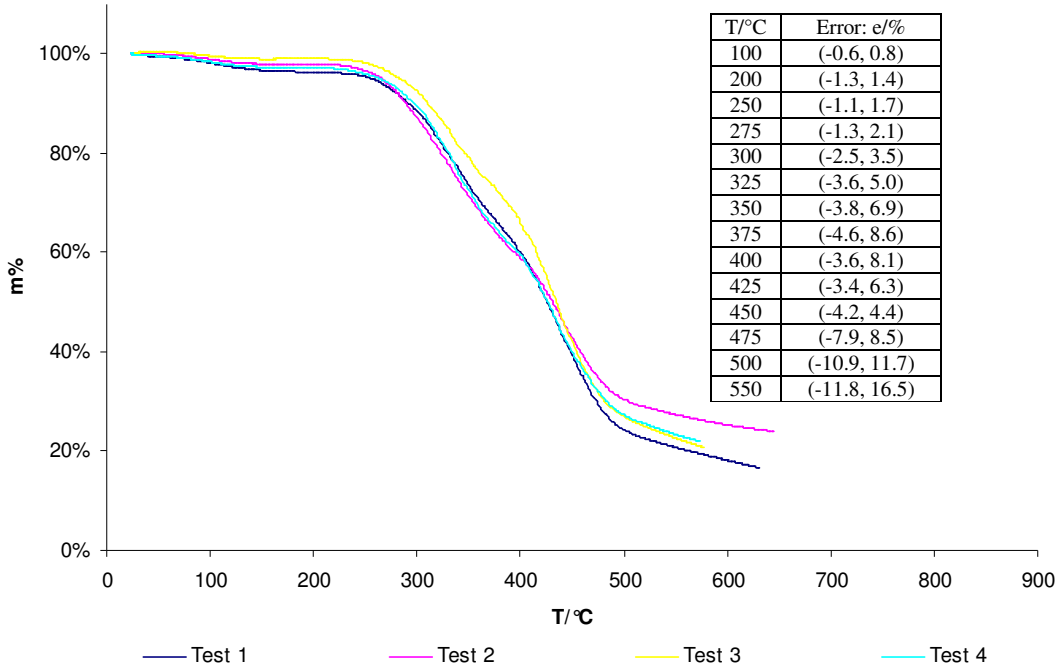

T/°C	Error: e/%
100	(-0.6, 0.8)
200	(-1.3, 1.4)
250	(-1.1, 1.7)
275	(-1.3, 2.1)
300	(-2.5, 3.5)
325	(-3.6, 5.0)
350	(-3.8, 6.9)
375	(-4.6, 8.6)
400	(-3.6, 8.1)
425	(-3.4, 6.3)
450	(-4.2, 4.4)
475	(-7.9, 8.5)
500	(-10.9, 11.7)
550	(-11.8, 16.5)

Figure 4.18 TG profile of briquette 6PPc.

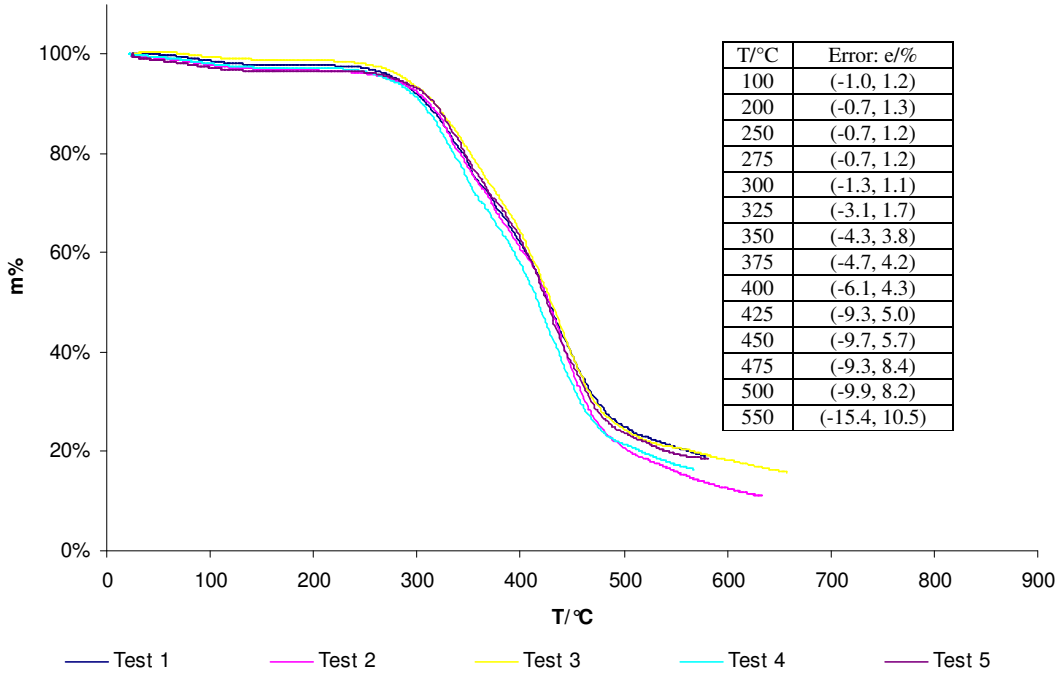

T/°C	Error: e/%
100	(-1.0, 1.2)
200	(-0.7, 1.3)
250	(-0.7, 1.2)
275	(-0.7, 1.2)
300	(-1.3, 1.1)
325	(-3.1, 1.7)
350	(-4.3, 3.8)
375	(-4.7, 4.2)
400	(-6.1, 4.3)
425	(-9.3, 5.0)
450	(-9.7, 5.7)
475	(-9.3, 8.4)
500	(-9.9, 8.2)
550	(-15.4, 10.5)

Figure 4.19 TG profile of briquette 6PPd.

The DTG curve of the pyrolysis of briquette 6PPa with the extruding temperature of 125°C shown in Figure 4.13 has been discussed in Section 4.1.2.

Figure 4.20 shows the DTG curve of the pyrolysis of briquette 6PPb with the extruding temperature of 150°C. Three different zones can be distinguished. The moisture vaporisation was the first zone as a small mass loss event with the maximum rate at between 95°C and 110°C. The thermal decomposition started in the second zone with the maximum mass loss rate at between 300°C and 330°C. The third zone represented the pyrolysis of plastic with the maximum rate at between 455°C and 465°C. The main pyrolysis process was essentially completed at 530°C and it was followed by the slow further lignin pyrolysis up to the final temperature. The pyrolytic process of briquette 6PPb had good repeatability especially in the peak height and the peak temperature of these two thermal decomposition zones.

Figure 4.21 shows the DTG curve of the pyrolysis of briquette 6PPc with the extruding temperature of 200°C. Three different zones can be distinguished. The moisture vaporisation was the first zone as a small mass loss event with the maximum rate at between 105°C and 110°C. The thermal decomposition started in the second zone with the maximum mass loss rate at between 330°C and 340°C. The third zone represented the pyrolysis of plastic with the maximum rate at between 445°C and 460°C. The main pyrolytic process was essentially completed at 530°C and it was followed by the slow further lignin pyrolysis up to the final temperature. The error analysis shows that the repeatability of the pyrolysis of briquette 6PPc was a little better than that of briquette 6PPb, and this indicated that the high extruding temperature could produce more uniform briquettes. But the extruding temperature of 200°C was close to the thermal decomposition temperature of lignin and therefore, it changed briquette's chemical properties and pyrolytic characteristics.

Figure 4.22 shows the DTG curve of the pyrolysis of briquette 6PPd with the extruding temperature of 250°C. Three different zones can be distinguished. The moisture vaporisation was the first zone as a small mass loss event with the maximum rate at 95°C. The thermal decomposition started in the second zone with the maximum mass loss rate at between 345°C and 365°C. The third zone represented the pyrolysis of plastic with the maximum rate at 445°C. The main pyrolytic process was essentially completed at 530°C and it was followed by the slow further lignin pyrolysis up to the final temperature. The error analysis shows that increasing the extruding temperature from 150°C to 250°C didn't improve the repeatability of the

pyrolysis of briquette much, however the high extruding temperature of 250°C could change briquette's chemical properties and pyrolytic characteristics more than the high extruding temperature of 200°C.

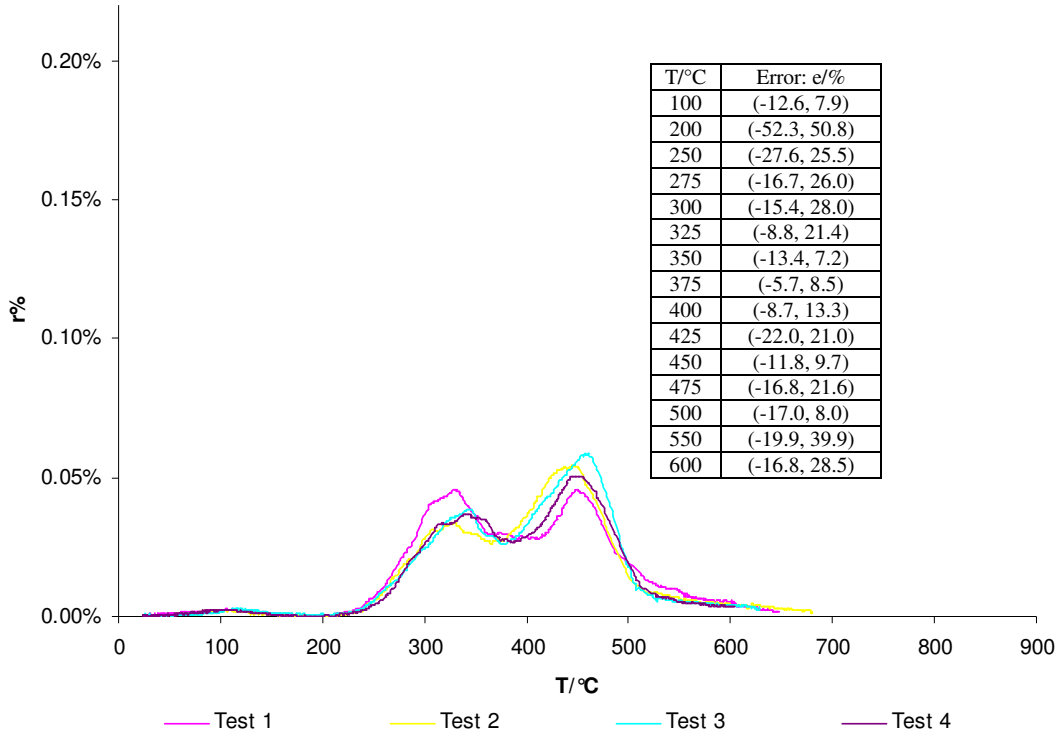

T/°C	Error: e/%
100	(-12.6, 7.9)
200	(-52.3, 50.8)
250	(-27.6, 25.5)
275	(-16.7, 26.0)
300	(-15.4, 28.0)
325	(-8.8, 21.4)
350	(-13.4, 7.2)
375	(-5.7, 8.5)
400	(-8.7, 13.3)
425	(-22.0, 21.0)
450	(-11.8, 9.7)
475	(-16.8, 21.6)
500	(-17.0, 8.0)
550	(-19.9, 39.9)
600	(-16.8, 28.5)

Figure 4.13 DTG profile of briquette 6PPa.

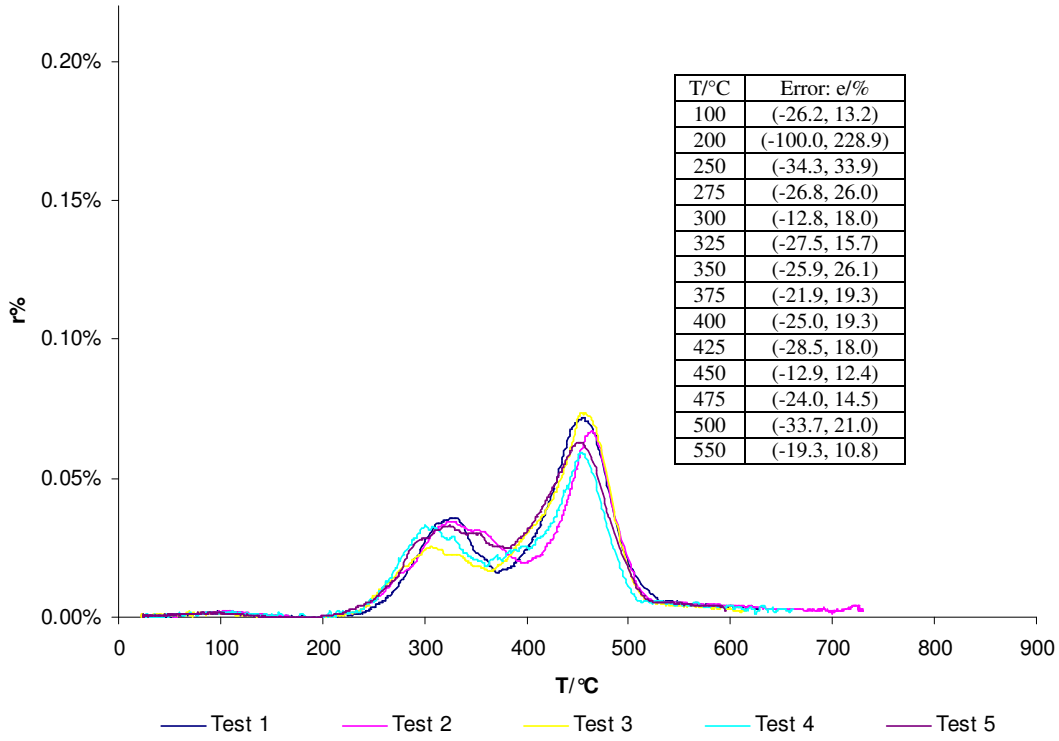

T/°C	Error: e/%
100	(-26.2, 13.2)
200	(-100.0, 228.9)
250	(-34.3, 33.9)
275	(-26.8, 26.0)
300	(-12.8, 18.0)
325	(-27.5, 15.7)
350	(-25.9, 26.1)
375	(-21.9, 19.3)
400	(-25.0, 19.3)
425	(-28.5, 18.0)
450	(-12.9, 12.4)
475	(-24.0, 14.5)
500	(-33.7, 21.0)
550	(-19.3, 10.8)

Figure 4.20 DTG profile of briquette 6PPb.

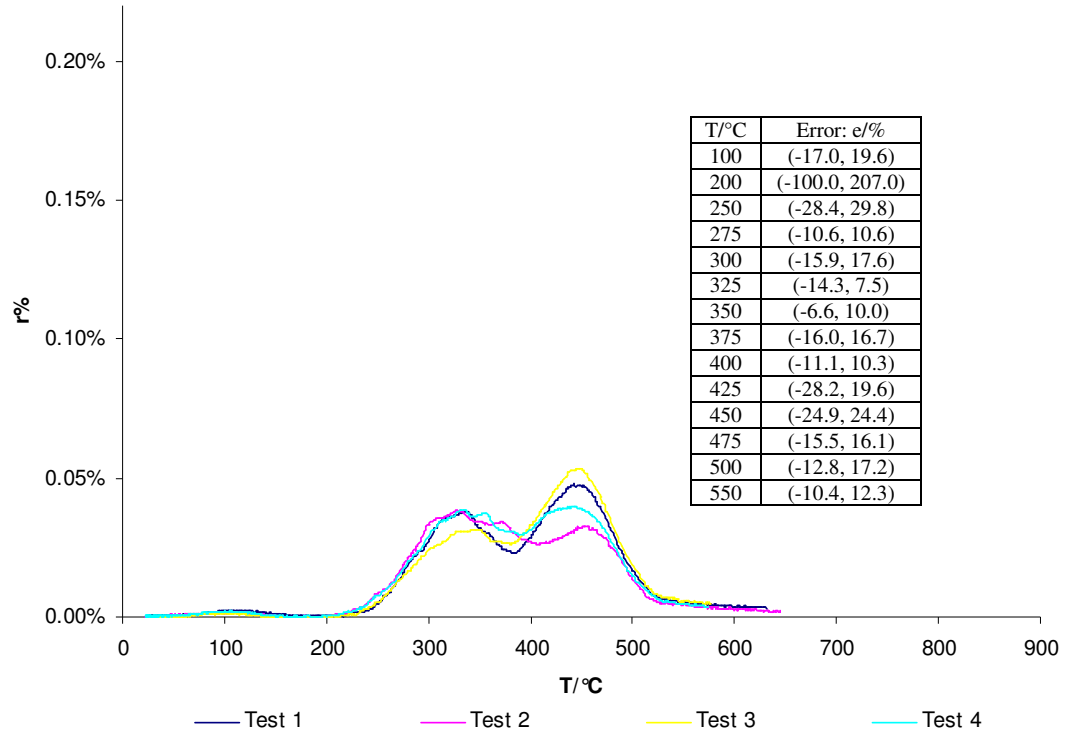

T/°C	Error: e/%
100	(-17.0, 19.6)
200	(-100.0, 207.0)
250	(-28.4, 29.8)
275	(-10.6, 10.6)
300	(-15.9, 17.6)
325	(-14.3, 7.5)
350	(-6.6, 10.0)
375	(-16.0, 16.7)
400	(-11.1, 10.3)
425	(-28.2, 19.6)
450	(-24.9, 24.4)
475	(-15.5, 16.1)
500	(-12.8, 17.2)
550	(-10.4, 12.3)

Figure 4.21 DTG profile of briquette 6PPc.

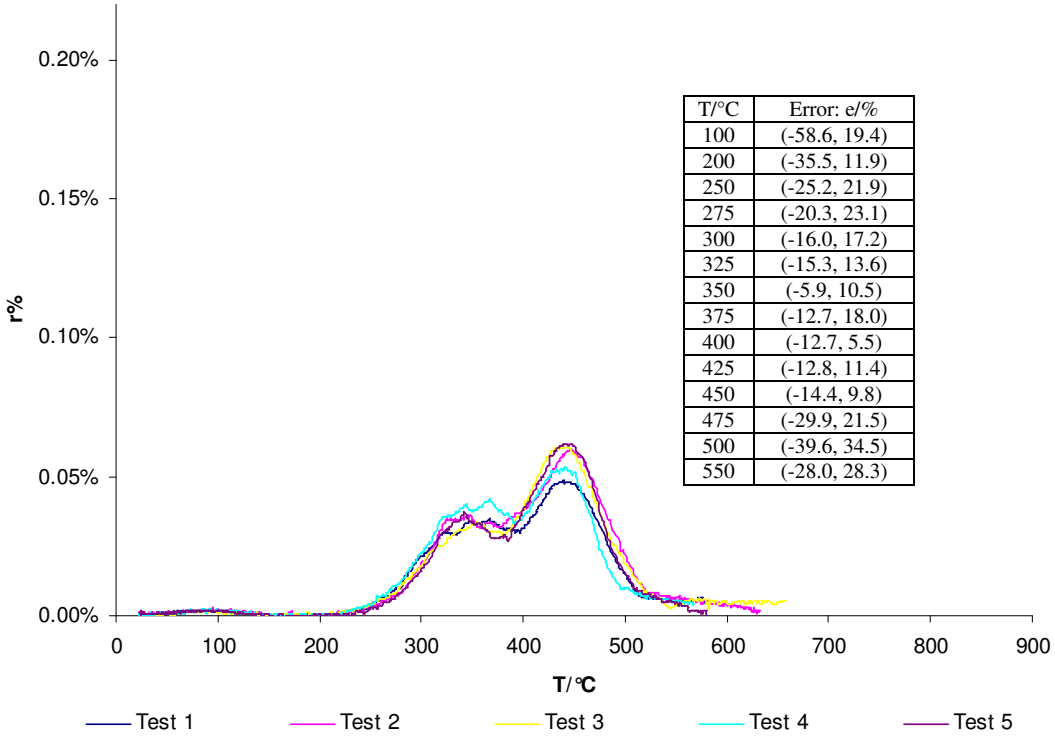

T/°C	Error: e/%
100	(-58.6, 19.4)
200	(-35.5, 11.9)
250	(-25.2, 21.9)
275	(-20.3, 23.1)
300	(-16.0, 17.2)
325	(-15.3, 13.6)
350	(-5.9, 10.5)
375	(-12.7, 18.0)
400	(-12.7, 5.5)
425	(-12.8, 11.4)
450	(-14.4, 9.8)
475	(-29.9, 21.5)
500	(-39.6, 34.5)
550	(-28.0, 28.3)

Figure 4.22 DTG profile of briquette 6PPd.

This group of tests showed that the overall pyrolytic process of paper and plastic blend briquettes consisted of a moisture vaporisation zone and two thermal

decomposition zones. The peak temperature of the pyrolysis of lignocellulose was at about 330°C and the peak temperature of the pyrolysis of plastic was at about 450°C. The pyrolysis of lignocellulose and the pyrolysis of plastic proceeded independently. Briquettes produced at different extruding temperatures had different pyrolytic characteristics. Higher extruding temperature could produce more uniform briquette. However, the pyrolysis of lignin took place at a low temperature and when the extruding temperature was too high, the chemical properties of lignocellulose in the briquette were changed and the quality of the briquette was lowered. The pyrolysis tests showed 150°C was the optimum extruding temperature to produce simulated SRF briquettes.

4.1.4 Summary

The overall pyrolytic process of simulated SRF briquettes consisted of three temperature zones. The first zone was a moisture vaporisation event up to 180°C. The second and third zones were associated with three independent mass loss events. The first event evolving light volatile compounds started at 220°C. This event was identified as hemicellulose and cellulose decomposition and was slightly endothermic. Hemicellulose decomposition was associated with the shoulder of the DTG curve and cellulose decomposition was associated with the peak at about 330°C. The second event with the maximum mass loss rate at about 450°C was associated with heavy volatile compounds. This event was identified as plastic decomposition. Plastic decomposition completed by 530°C and was endothermic. The third event was identified as lignin decomposition, which started at a very low temperature, occurred slowly and was over a broad temperature range. Lignin decomposition was exothermic, and its effect was significant at the temperature range of 300 – 450°C. The pyrolysis of lignocellulose and the pyrolysis of plastic proceeded independently. At the temperature above 700°C, the exothermic decomposition of calcium carbonate took place.

The paper briquette contained a large amount of inert ash which contained inorganic component. When the simulated SRF briquette contained a higher plastic fraction, the ash content in the briquette became lower. The inorganic component affected the pyrolytic process by shifting the cellulose decomposition to a lower temperature and

lowered the repeatability of the pyrolytic process. Plastic as a rich source of hydrocarbons played a vital role in the pyrolytic process of the simulated SRF briquettes by enhancing the repeatability of the process. This can be seen both from the sample temperature vs. time profiles and from the error analysis of the DTG profiles.

The extruding temperature affected the pyrolysis of the simulated SRF briquettes. The 60% PP and 40% paper blend briquette extruded at 150°C (6PPb) had good repeatability of the pyrolytic process. This indicated that the extruding temperature of 150°C was high enough to produce uniform briquettes, and was also low enough in order not to destroy the chemical structure of lignocellulosic materials. High extruding temperature could break down the molecules of lignocellulose, increased the ash content and therefore, degraded the briquette.

The pyrolysis tests of the simulated SRF briquettes showed the pyrolytic process was quite repeatable and the pyrolytic characteristics of the briquettes were reliable. In order to produce desirable SRF briquettes through an optimum method, some SRF briquettes made from waste materials were tested to investigate the pyrolytic characteristics in Section 4.2.

4.2 Pyrolytic characteristics of SRF briquettes

The SRF briquettes in this research were prepared from waste materials including ecodeco, RDF, MBT processed RDF, raw MSW, sawdust, tar, molasses, sewage sludge, paper and PE. The pyrolysis tests of the SRF briquettes were carried out by four groups: (1) pyrolysis of ecodeco briquettes with varying extruding temperatures; (2) pyrolysis of ecodeco briquettes blended with biomass or with biomass and plastic; (3) pyrolysis of RDF briquette and MBT processed RDF briquette; and (4) pyrolysis of other SRF briquettes.

4.2.1 Pyrolytic characteristics of ecodeco briquettes with varying extruding temperatures

The pyrolysis of the ecodeco briquettes with varying extruding temperatures at 125°C (SRF1) and 150°C (SRF2) was carried out. Eight pyrolysis tests of briquette SRF1 started with different initial sample mass of 17.374 g, 14.877 g, 15.727 g, 16.562 g, 8.194 g, 8.020 g, 5.790 g and 3.912 g, respectively. Tests 1 – 4 were multi segments tests, and tests 5 – 8 were single segment tests. Six pyrolysis tests of briquette SRF2 started with different initial sample mass of 15.328 g, 8.168 g, 6.928 g, 7.539 g, 8.732 g and 7.830 g, respectively. Test 1 was a multi segments test, and tests 2 – 6 were single segment tests.

Figures 4.23 and 4.24 show the sample temperature vs. time profile of the pyrolysis tests of briquettes SRF1 and SRF2, respectively. In tests 1 – 4 of briquette SRF1 and test 1 of briquette SRF2, the thermocouple was inserted into the centre of the segments. The recorded briquette temperature was lower than the actual pyrolytic temperature of the outside segments due to the thermal inertia. Therefore, the sample temperature rise profile of the multi segments tests in Figures 4.23 and 4.24 were behind those of the single segment tests. This indicated that the thermal conductivity of the ecodeco briquette was low. However, when the extruding temperature changed from 125°C to 150°C, the thermal conductivity of the ecodeco briquette was improved. In the kinetics analysis in Chapter Five, only the results of the single segment tests are studied.

Between 430°C and 500°C, the briquette temperature rise became slower, and this indicated that the global endothermic process took place. Lignin decomposition was exothermic, and its effect was offset by the endothermicity of plastic decomposition, as the ecodeco material contained 23.0% plastic as shown in Table 3.5.

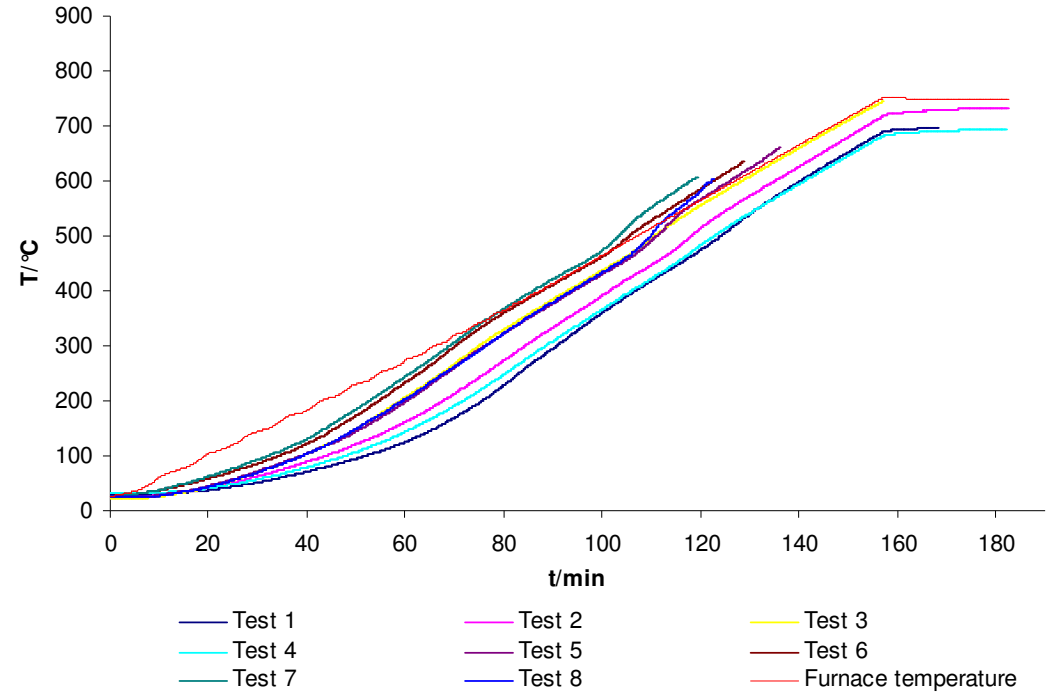

Figure 4.23 Briquette SRF1's temperature vs. time profile.

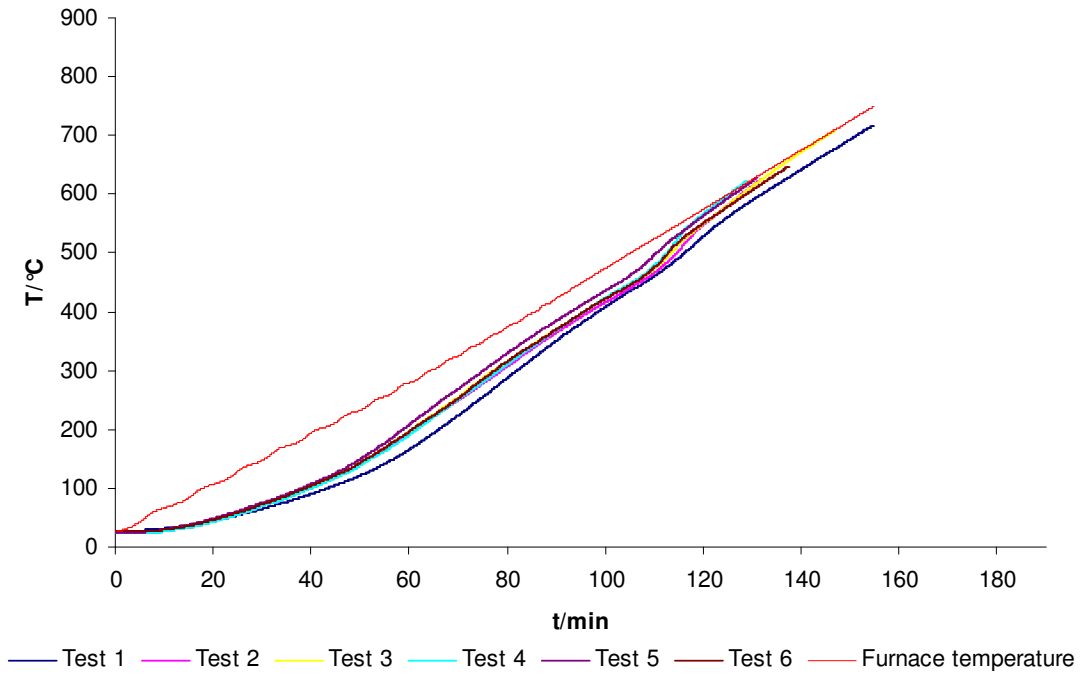

Figure 4.24 Briquette SRF2's temperature vs. time profile.

Figures 4.25 and 4.26 show the TG curve of the pyrolysis tests of briquettes SRF1 and SRF2, respectively. The main pyrolytic process which was mainly the pyrolysis of hemicellulose, cellulose and plastic, started when the residual mass fraction fell below 96% and finished at about 500°C. The lignin pyrolysis continued slowly until the end

of the test. The error analysis shows that the ecodeco briquette extruded at 150°C had better repeatability than that extruded at 125°C.

T/°C	Error: e/%	Error: e/% (tests 5-8)
100	(-1.2, 1.7)	(-1.4, 1.5)
175	(-1.3, 2.2)	(-1.5, 2.0)
200	(-3.1, 2.9)	(-1.5, 2.1)
225	(-6.9, 4.3)	(-1.5, 2.2)
250	(-10.3, 5.6)	(-1.8, 2.1)
275	(-12.7, 6.7)	(-3.8, 2.1)
300	(-11.6, 8.7)	(-6.3, 3.0)
325	(-11.3, 5.9)	(-9.9, 3.9)
350	(-11.0, 7.4)	(-11.6, 6.7)
375	(-12.8, 8.9)	(-12.1, 7.4)
400	(-16.9, 11.3)	(-13.1, 8.0)
425	(-19.1, 14.7)	(-14.6, 10.0)
450	(-19.3, 13.5)	(-13.1, 12.4)
475	(-13.4, 17.4)	(-11.1, 14.2)
500	(-11.1, 18.8)	(-9.6, 14.8)
550	(-11.5, 19.1)	(-9.8, 14.6)

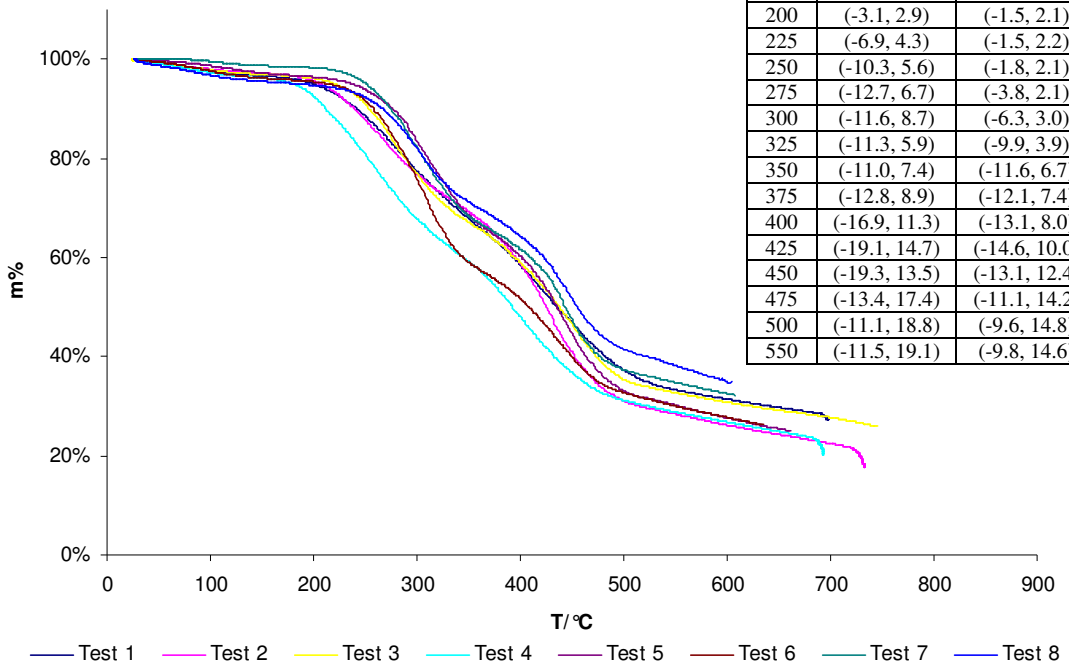

Figure 4.25 TG profile of briquette SRF1.

T/°C	Error: e/% (tests 2-6)
150	(-0.5, 0.5)
200	(-0.6, 0.6)
250	(-1.6, 1.1)
275	(-1.9, 1.7)
300	(-2.3, 2.0)
325	(-2.9, 3.4)
350	(-5.5, 4.7)
375	(-6.9, 5.5)
400	(-8.5, 6.8)
425	(-10.0, 7.4)
450	(-10.1, 11.2)
475	(-8.5, 10.8)
500	(-7.6, 8.0)
550	(-8.9, 9.3)

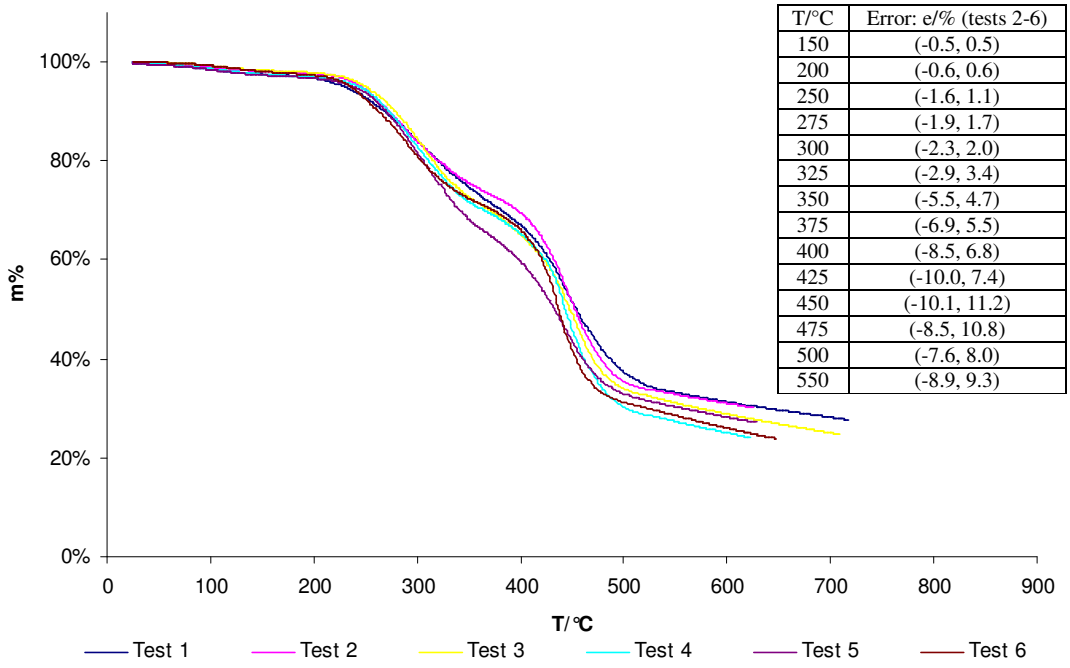

Figure 4.26 TG profile of briquette SRF2.

Figure 4.27 shows the DTG curve of the pyrolysis of briquette SRF1. Three different zones can be distinguished in the single segment tests 5 – 8. The moisture vaporisation was the first zone as a small mass loss event with the maximum rate at between 100°C and 110°C. The second zone was mainly the pyrolysis of hemicellulose and cellulose with the maximum mass loss rate at between 260°C and 310°C. Compared to the DTG curve of the simulated SRF briquettes, this second zone of the single segment tests was shifted to the lower temperature by about 40°C. This was because the ecodeco briquette was made from waste materials contained a large amount of inorganic component. The third zone mainly represented the pyrolysis of plastic with the maximum rate at between 400°C and 460°C. Compared to the DTG curve of the simulated SRF briquettes again, the third zone of the single segment tests wasn't shifted. The main pyrolytic process was essentially completed at 520°C and it was followed by the slow further lignin pyrolysis up to the final temperature.

Figure 4.27 shows that the thermal decomposition temperature range of the multi segments tests was broader than the single segment tests. This was because the sample size had an influence due to more ease of volatile evolution through the single segment and the effect of heat transfer. The SRF briquette had poor thermal conductivity and therefore, there was a temperature gradient along the briquette during the heating process. The temperature gradient was even more significant in the multi segments. When the thermocouple was inserted into the multi segments to measure temperature, the measured temperature was lower than the outside briquette temperature. Therefore, when the pyrolysis of outside segments took place, the lower inside briquette temperature was recorded. This caused the displacement of the DTG curve to the lower temperature in the beginning of the mass loss events. Diffusion also played an important role in the pyrolytic process. When volatiles were produced inside the briquette, it took time to escape from inside to outside before they were removed by nitrogen. The temperature was recorded when the volatiles removed by nitrogen, not actually when the reaction took place. This caused the displacement of the DTG curve to the higher temperature during the mass loss events. Therefore the multi segments tests had a broader temperature range of the DTG profile and the single segment test was more practicable in this research due to the poor thermal conductivity and the low diffusion coefficient.

Figure 4.28 shows the DTG curve of the pyrolysis of briquette SRF2. Three different zones can be distinguished. The moisture vaporisation was the first zone as a small mass loss event with the maximum rate at between 110°C and 130°C. The second zone was the pyrolysis of hemicellulose and cellulose with the maximum mass loss rate at between 290°C and 310°C. This second zone was shifted to the lower temperature by about 30°C, compared to the pyrolysis of lignocellulose in the simulated SRF briquettes. The third zone represented the pyrolysis of plastic with the maximum rate at between 440°C and 450°C. The main pyrolysis process was essentially completed at 540°C and it was followed by the slow further lignin pyrolysis up to the final temperature.

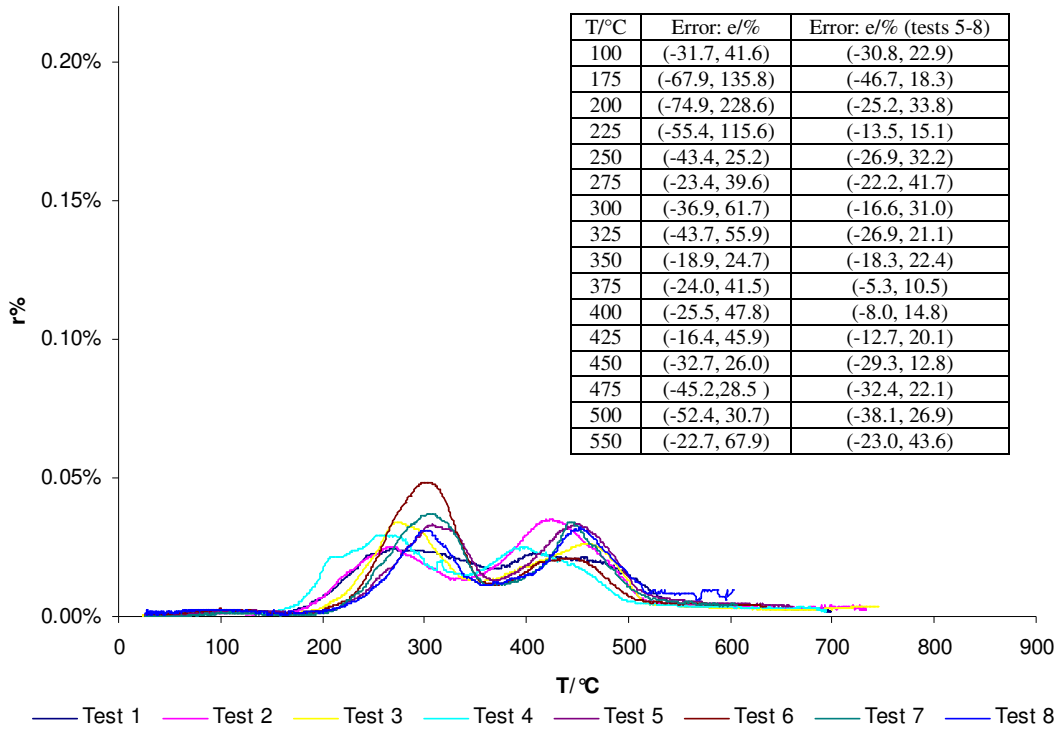

T/°C	Error: e/%	Error: e/% (tests 5-8)
100	(-31.7, 41.6)	(-30.8, 22.9)
175	(-67.9, 135.8)	(-46.7, 18.3)
200	(-74.9, 228.6)	(-25.2, 33.8)
225	(-55.4, 115.6)	(-13.5, 15.1)
250	(-43.4, 25.2)	(-26.9, 32.2)
275	(-23.4, 39.6)	(-22.2, 41.7)
300	(-36.9, 61.7)	(-16.6, 31.0)
325	(-43.7, 55.9)	(-26.9, 21.1)
350	(-18.9, 24.7)	(-18.3, 22.4)
375	(-24.0, 41.5)	(-5.3, 10.5)
400	(-25.5, 47.8)	(-8.0, 14.8)
425	(-16.4, 45.9)	(-12.7, 20.1)
450	(-32.7, 26.0)	(-29.3, 12.8)
475	(-45.2,28.5)	(-32.4, 22.1)
500	(-52.4, 30.7)	(-38.1, 26.9)
550	(-22.7, 67.9)	(-23.0, 43.6)

Figure 4.27 DTG profile of briquette SRF1.

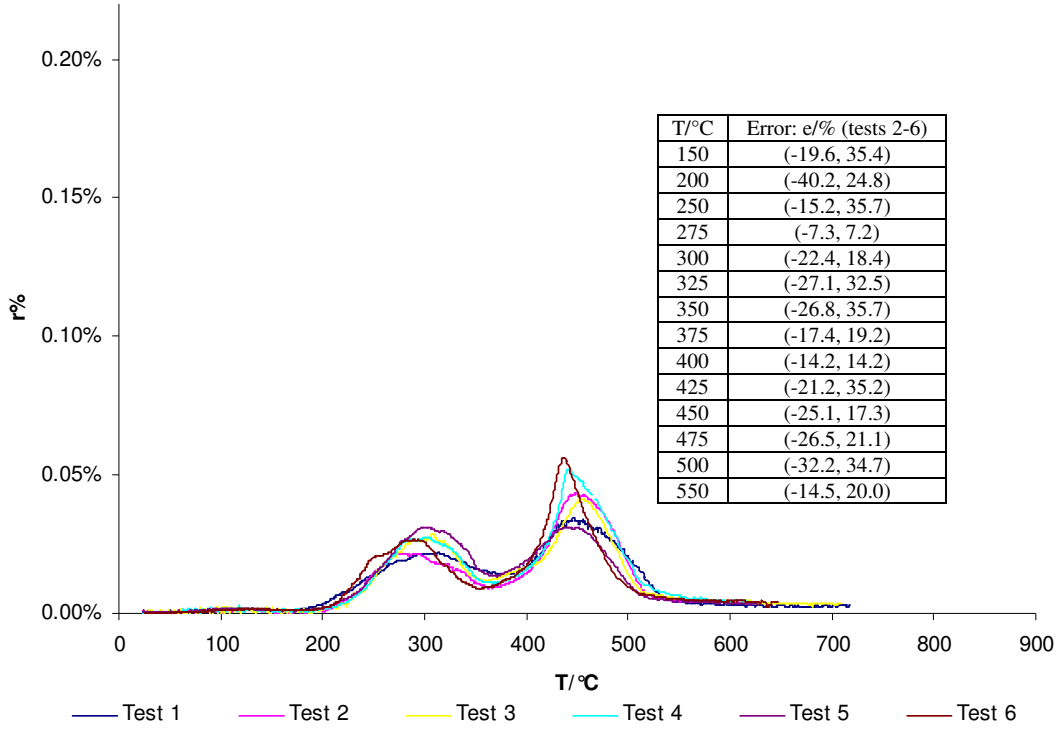

T/°C	Error: e/% (tests 2-6)
150	(-19.6, 35.4)
200	(-40.2, 24.8)
250	(-15.2, 35.7)
275	(-7.3, 7.2)
300	(-22.4, 18.4)
325	(-27.1, 32.5)
350	(-26.8, 35.7)
375	(-17.4, 19.2)
400	(-14.2, 14.2)
425	(-21.2, 35.2)
450	(-25.1, 17.3)
475	(-26.5, 21.1)
500	(-32.2, 34.7)
550	(-14.5, 20.0)

Figure 4.28 DTG profile of briquette SRF2.

This group of pyrolysis tests showed that the ecodeco briquettes had poor thermal conductivity, and by increasing the extruding temperature, the range of the data narrowed and the thermal conductivity of the briquette was improved. Ecodeco briquettes contained a large amount of inorganic component which shifted the DTG curve of the pyrolysis of cellulose to a lower temperature. However, the DTG curve of plastic pyrolysis of the ecodeco briquettes was at the same temperature range as that of the simulated SRF briquettes. The pyrolysis of lignocellulose and the pyrolysis of plastic proceeded independently in the pyrolytic process of the ecodeco briquettes.

4.2.2 Pyrolytic characteristics of ecodeco briquettes blended with biomass or with biomass and plastic

The pyrolysis of the briquette of 80% ecodeco and 20% sawdust blend (SRF3) and the briquette of 65% ecodeco, 10% sawdust, 15% paper and 10% PE blend (SRF4) was carried out with different initial sample mass of 14.088 g and 13.249 g, respectively. The briquettes' composition showed briquette SRF3 contained 15% ecodeco and 10% sawdust more than briquette SRF4 and briquette SRF4 contained 15% paper and 10% PE more than briquette SRF3. Table 3.5 shows that ecodeco contained 35% paper and

23% plastic. The proximate analysis shows that ecodeco contained 14.4% ash and paper contained 13.4% ash. A simple calculation based on the above data would conclude that briquette SRF4 contained more lignocellulose and plastic and less ash than briquette SRF3.

Figure 4.29 shows the sample temperature vs. time profile of the pyrolysis tests of briquettes SRF3 and SRF4. Since briquette SRF4 contained more lignocellulose and plastic than briquette SRF3 and the pyrolytic process of hemicellulose, cellulose and plastic were endothermic, the temperature rise profile of briquette SRF4 was behind that of briquette SRF3 during the main pyrolytic process. Below 390°C, the pyrolytic process was mainly the pyrolysis of hemicellulose and cellulose and therefore, the curve of briquette SRF4 was behind briquette SRF3. When the pyrolysis of hemicellulose and cellulose nearly finished at about 390°C and the pyrolysis of plastic was about to start, the curve of briquette SRF4 became closer to briquette SRF3 due to the exothermic pyrolysis of lignin. When the endothermic pyrolysis of plastic started, the temperature rise of briquette SRF4 became slow again, until the pyrolysis of plastic finished.

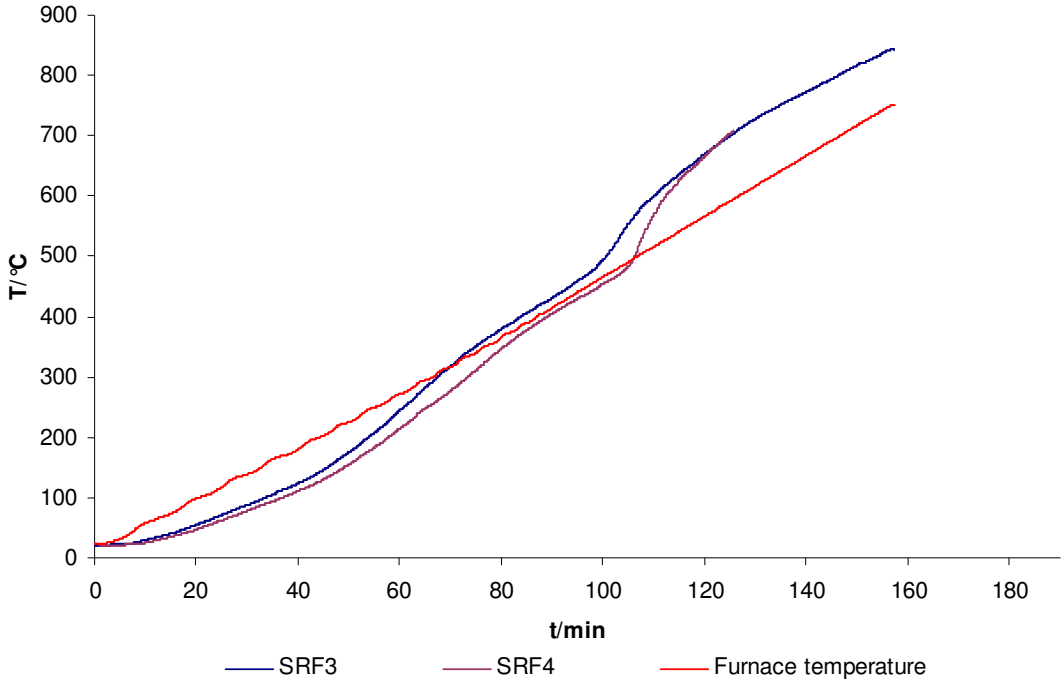

Figure 4.29 Temperature vs. time profiles of briquettes SRF3 & SRF4.

Figure 4.30 shows the TG curve of the pyrolysis tests of briquettes SRF3 and SRF4. The main pyrolytic process started when the residual mass fraction fell below 96%

and finished at about 500°C when the residual mass fraction became 37%. The pyrolysis of hemicellulose and cellulose of briquette SRF3 was faster than that of briquette SRF4. This was because briquette SRF3 contained more ash than briquette SRF4 and therefore, contained more inorganic component which acted as catalysts and increased the reaction rate. Briquette SRF4 contained more plastic than briquette SRF3 and therefore, the plastic pyrolysis of briquette SRF4 between 400°C and 490°C was faster than that of briquette SRF3. This also indicated that the inorganic component didn't catalyse the plastic pyrolysis. When the temperature was higher than 500°C, the lignin pyrolysis continued slowly until the end of the test. The lignin pyrolysis of briquette SRF3 was faster than that of briquette SRF4. This indicated that the inorganic component could catalyse the lignin pyrolysis.

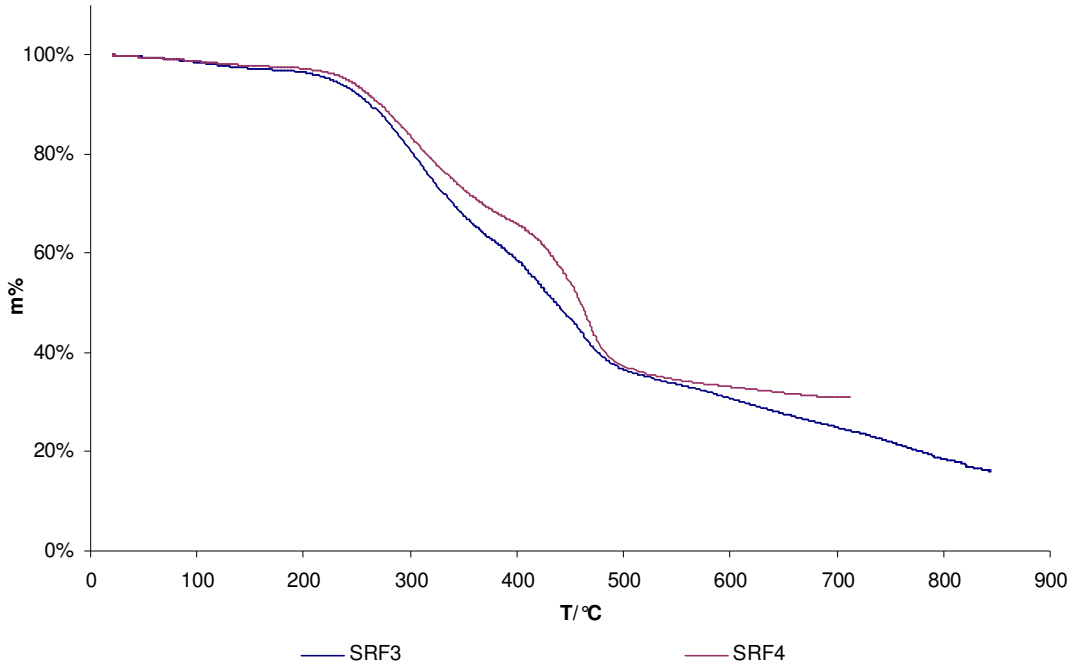

Figure 4.30 TG profiles of briquettes SRF3 & SRF4.

Figure 4.31 shows the DTG curve of the pyrolysis of briquettes SRF3 and SRF4. Three different zones can be distinguished. The moisture vaporisation was the first zone as a small mass loss event with the maximum rate at 130°C. The second zone was mainly hemicellulose and cellulose decomposition with the maximum mass loss rate at about 300°C. The peak temperature was shifted to the lower temperature by 30°C, due to the inorganic component in the briquettes. The curve shifted by 10°C less than the 100% ecodeco briquettes (SRF1 and SRF2). The third zone represented the pyrolysis of plastic with the maximum rate at a higher temperature than the

simulated SRF briquettes. SRF4 contained PE component and the simulated SRF briquettes contained PP component. This indicated that PP pyrolysed at a lower temperature than PE. The main pyrolytic process was essentially completed by 580°C and it was followed by the slow further lignin pyrolysis up to the final temperature.

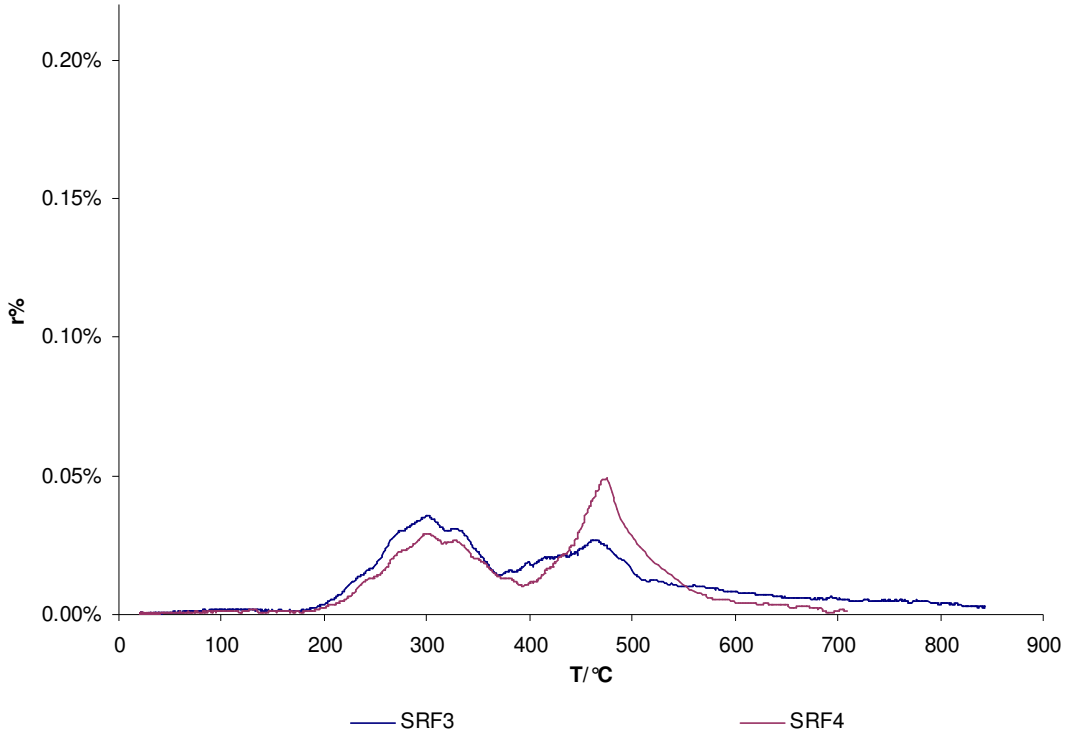

Figure 4.31 DTG profiles of briquettes SRF3 & SRF4.

This group of pyrolysis tests showed that ecodeco material was able to be blended with biomass and plastic to produce briquettes. Ecodeco had a high inorganic content which shifted the curve of cellulose pyrolysis to a lower temperature. However, the inorganic component didn't shift the curve of plastic pyrolysis. The inorganic component could act as catalysts and increased the reaction rate of the pyrolysis of hemicellulose, cellulose and lignin, but they couldn't catalyse the plastic pyrolysis. The pyrolysis of lignocellulose and the pyrolysis of plastic proceeded independently.

4.2.3 Pyrolytic characteristics of RDF briquette and MBT processed RDF briquette

The pyrolysis of the RDF briquette (SRF5) and the MBT processed RDF briquette (SRF6) was carried out with different initial sample mass of 15.156 g and 14.996 g, respectively.

Figure 4.32 shows the sample temperature vs. time profile of the pyrolysis tests of briquettes SRF5 and SRF6. The MBT processed RDF briquette (SRF6) contained 55% paper and 9% plastic and therefore, the curve of hemicellulose and cellulose pyrolysis of briquette SRF6 was similar to the paper briquette and between 400°C and 550°C the profile showed the pyrolytic characteristics of plastic. At high temperature where plastic pyrolysis finished, the exothermic lignin pyrolysis continued and the exothermic decomposition of calcium carbonate also took place. Therefore, the sample temperature became higher than the set final furnace temperature of 750°C. When the lignin pyrolysis and the decomposition of calcium carbonate were completed, the sample temperature dropped to the furnace temperature of 750°C. Figure 4.32 shows that the RDF briquette (SRF5) experienced a slow temperature rise.

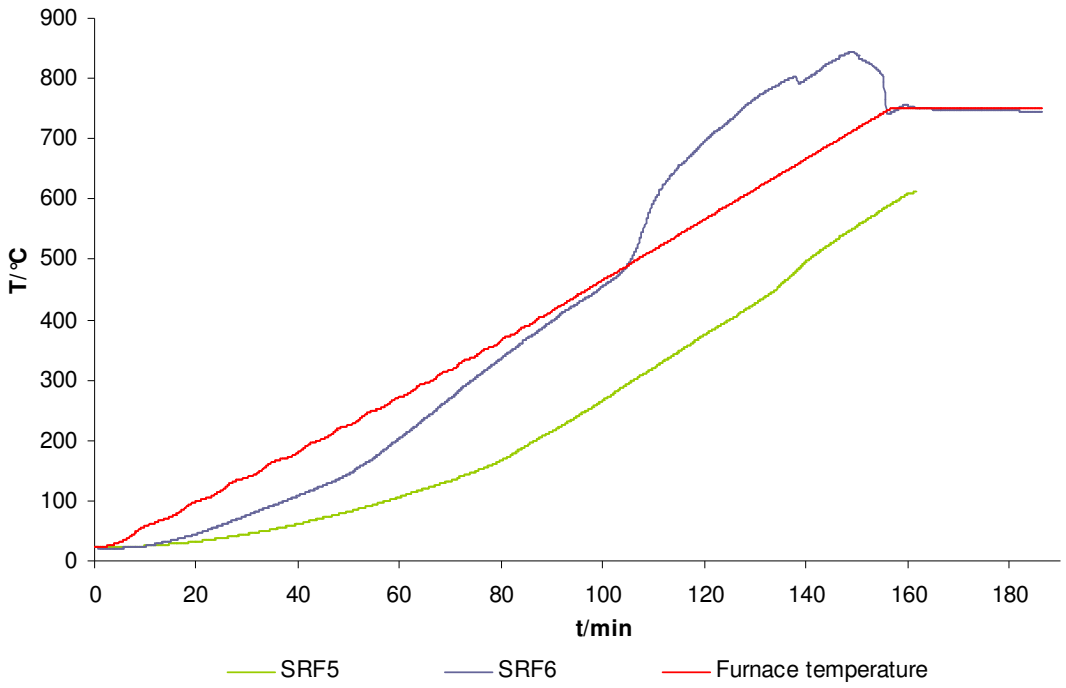

Figure 4.32 Temperature vs. time profiles of briquettes SRF5 & SRF6.

Figure 4.33 shows the TG curve of the pyrolysis tests of briquettes SRF5 and SRF6. The curve of briquette SRF6 shows the pyrolytic characteristics of main components more clearly than that of briquette SRF5. This indicated that the MBT process could improve the quality of RDF briquettes.

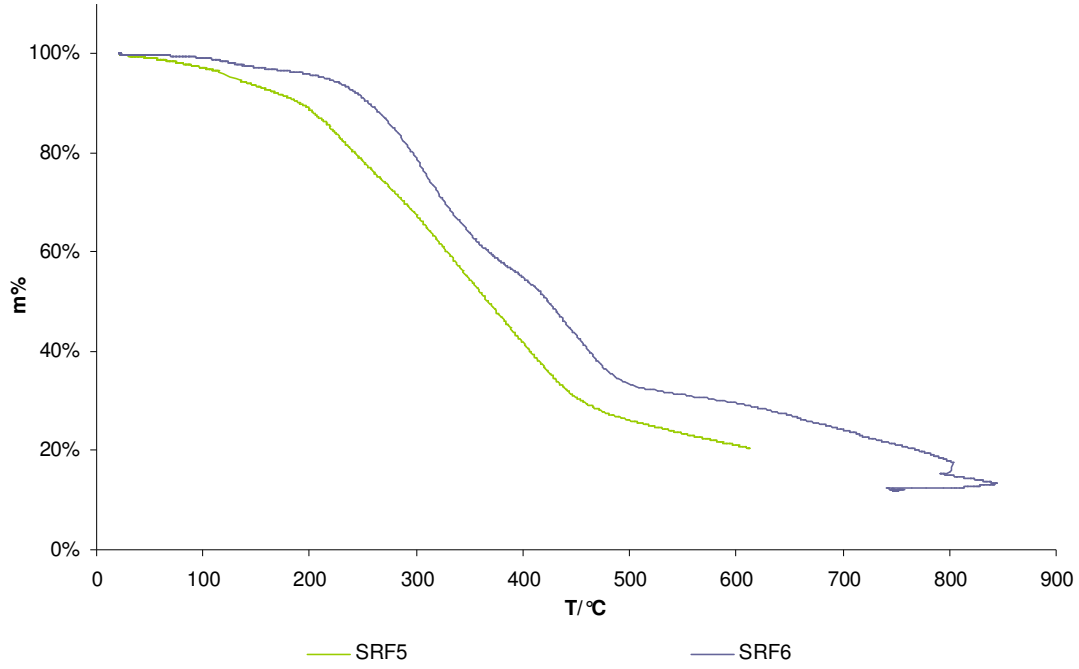

Figure 4.33 TG profiles of briquettes SRF5 & SRF6.

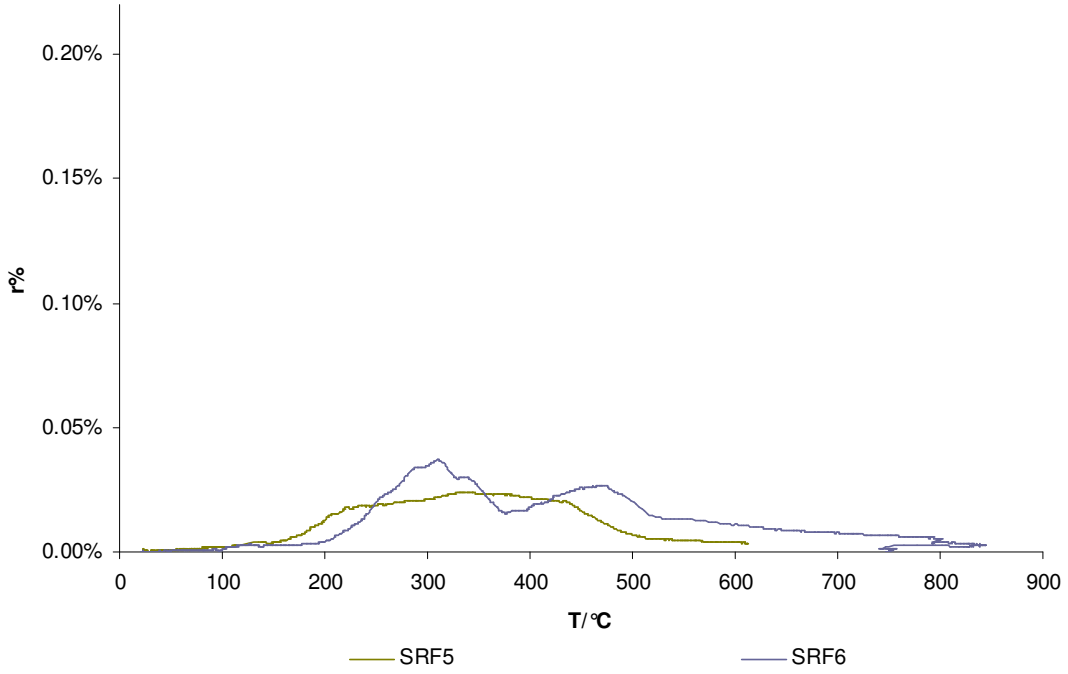

Figure 4.34 DTG profiles of briquettes SRF5 & SRF6.

Figure 4.34 shows the DTG curve of the pyrolysis of briquettes SRF5 and SRF6. The RDF briquette (SRF5) showed very poor pyrolytic characteristics. The MBT processed RDF briquette (SRF6) however showed improved pyrolytic characteristics. The peak of the cellulose pyrolysis of briquette SRF6 was shifted to 310°C by 20°C and this might be the effect of the inorganic component.

This group of tests showed that the RDF briquette had very poor pyrolytic characteristics and the quality of RDF briquettes could be significantly improved by introducing an MBT process prior to the briquetting process. The pyrolysis of lignocellulose and the pyrolysis of plastic proceeded independently in the pyrolysis of the MBT processed RDF briquette.

4.2.4 Pyrolytic characteristics of other SRF briquettes

The pyrolysis of the raw MSW briquette (SRF7), the briquette of RDF and molasses blend (SRF8) and the briquette of 50% standard dried sewage sludge and 50% tar blend (SRF9) was carried out with different initial sample mass of 10.307 g, 14.900 g and 15.879 g, respectively.

Figure 4.35 shows the sample temperature vs. time profile of the pyrolysis tests of briquettes SRF7, SRF8 and SRF9. Briquette SRF9 experienced a slow temperature rise.

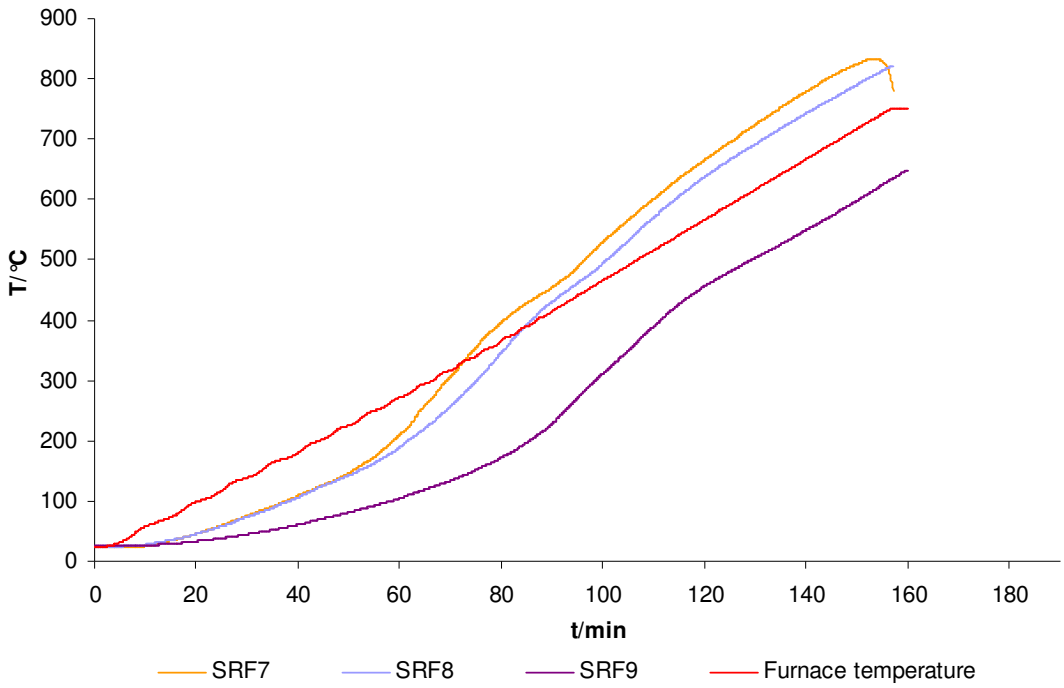

Figure 4.35 Temperature vs. time profiles of other SRF briquettes.

Figure 4.36 shows the TG curve of the pyrolysis tests of briquettes SRF7, SRF8 and SRF9. Briquette SRF9 made from 50% standard dried sewage sludge and 50% tar

contained the lowest volatile content and therefore, it was not suitable to produce SRF briquettes. Briquette SRF8 made from RDF and molasses binder also contained a low volatile content, compared to the MBT processed RDF briquette in Figure 4.33.

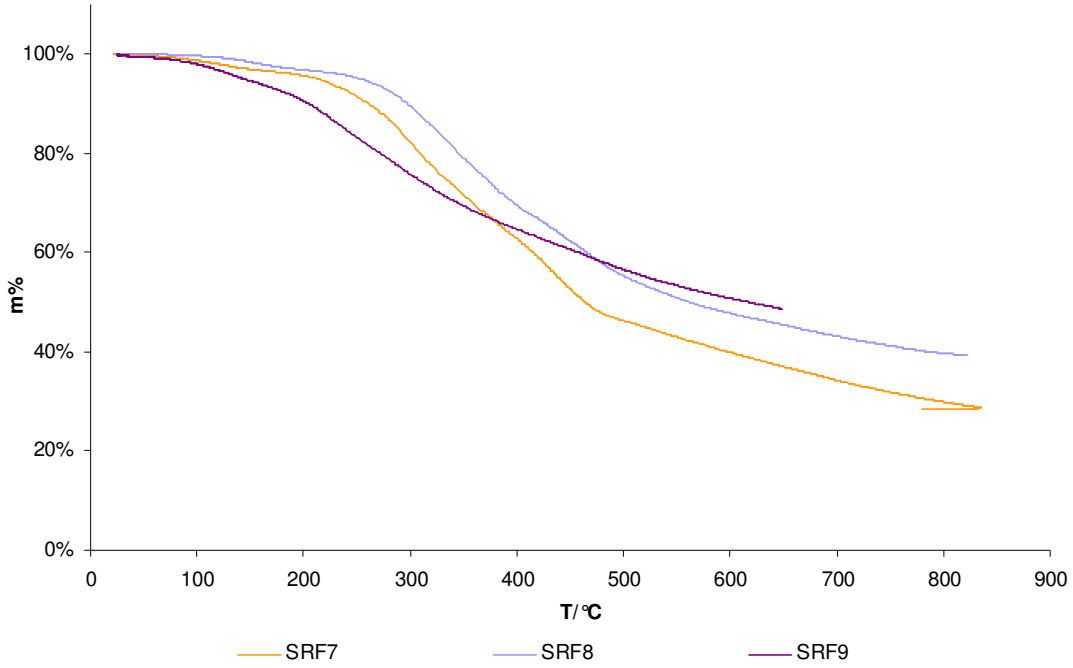

Figure 4.36 TG profiles of other SRF briquettes.

Figures 4.37 shows the DTG curve of the pyrolysis of briquettes SRF7, SRF8 and SRF9. It shows the raw MSW briquette (SRF7) and the RDF and molasses blend briquette (SRF8) contained a small amount of plastic. It was interesting that the peak temperature of the cellulose pyrolysis of briquette SRF8 was not shifted. This indicated that the binder molasses could restrain the curve shifting effect of the inorganic component. In the pyrolysis test of briquette SRF9, the peak of the DTG curve started 70°C lower than cellulose pyrolysis and was wide with no peak of plastic pyrolysis. This indicated that sewage sludge and tar contained volatiles lighter than cellulose and no plastic. The curve was also affected by a large amount of inorganic component particularly from sewage sludge.

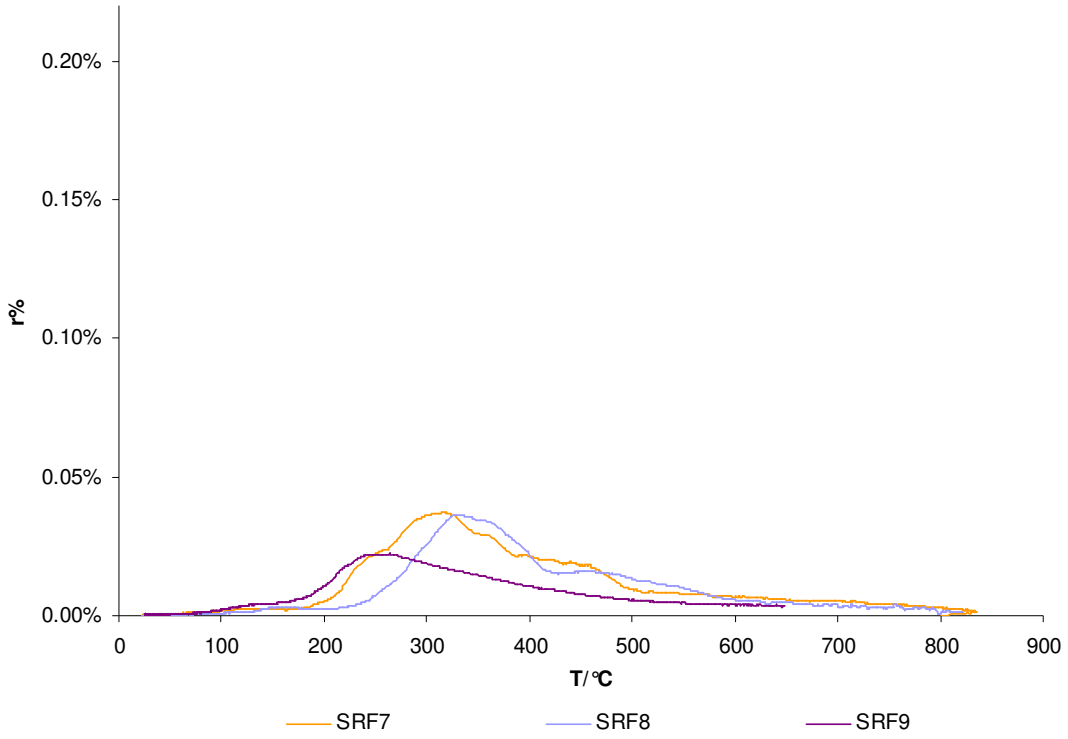

Figure 4.37 DTG profiles of other SRF briquettes.

This group of pyrolysis tests showed that the standard dried sewage sludge and tar material couldn't be used to produce SRF briquettes without any other materials or treatment. Molasses as a binder could restrain the curve shifting effect of the inorganic component. The pyrolysis of lignocellulose and the pyrolysis of plastic proceeded independently in the pyrolytic process of the SRF briquettes.

4.2.5 Summary

Same as the simulated SRF briquettes, the overall pyrolytic process of the SRF briquettes consisted of three independent mass loss events as well as a moisture vaporisation event. The first event was hemicellulose and cellulose decomposition and was slightly endothermic. Hemicellulose decomposition was associated with the shoulder of the DTG curve and cellulose decomposition was associated with the peak at about 330°C, which was affected by the briquette's inorganic component. The second event was plastic decomposition with the maximum mass loss rate at about 450°C and was endothermic, and it wasn't affected by the inorganic component. The pyrolysis of different types of plastics was similar, but took place at slightly different temperature. PP pyrolysed at a lower temperature than PE. The third event was lignin

decomposition, which started at very low temperature, occurred slowly, took place over a broad temperature range, and was exothermic. The pyrolysis of lignocellulose and the pyrolysis of plastic proceeded independently in the pyrolytic process of the SRF briquettes. The inorganic component could act as catalyst and increase the reaction rate of the hemicellulose, cellulose and lignin pyrolysis, but it couldn't catalyse the plastic pyrolysis. A further analysis of the catalysis of inorganic component is studied in Chapter Five where activation energies are discussed.

The pyrolysis tests of the SRF briquettes showed that the ecodeco briquettes had poor thermal conductivity, and by increasing the extruding temperature from 125°C to 150°C, the thermal conductivity of the briquettes was improved. Ecodeco material could be blended with biomass and plastic to produce SRF briquettes. RDF couldn't be used to produce SRF briquettes without any treatment and an MBT process prior to briquetting was needed to improve the quality of the briquettes. Standard dried sewage sludge and tar materials couldn't be used to produce SRF briquettes without any other materials or treatment. Molasses as a binder could restrain the curve shifting effect of the inorganic component.

In order to examine the difference of pyrolytic characteristics between different types of biomass, some pulverised biomass materials are investigated in Section 4.3.

4.3 Pyrolytic characteristics of pulverised biomass

The pyrolysis tests of eleven pulverised biomass materials were carried out by three groups in this research: (1) pyrolysis of wood materials; (2) pyrolysis of willow materials; and (3) pyrolysis of other biomass materials.

4.3.1 Pyrolytic characteristics of pulverised wood materials

The pyrolysis of the pet shop sawdust (PB1a), the RWE standard sawdust (PB1b) and the pulverised MFC wood (PB2) was carried out. Three pyrolysis tests of sample PB1a started with initial sample mass of 2.000 g. Three pyrolysis tests of sample PB1b started with different initial sample mass of 2.654 g, 2.888 g and 2.899 g,

respectively. And two pyrolysis tests of sample PB2 started with different initial sample mass of 3.570 g and 4.194 g, respectively.

Figures 4.38 and 4.39 show the sample temperature vs. time profile of the pyrolysis tests of the sawdust samples (PB1a and PB1b) and the pulverised MFC wood sample (PB2), respectively. During the sawdust pyrolysis between 250°C and 460°C and the pulverised MFC wood pyrolysis between 250°C and 570°C, the sample temperature rise was fast. This indicated the exothermic effect of the lignin decomposition. During the sawdust pyrolysis above 460°C and the MFC wood pyrolysis above 570°C, the sample temperature rise was slow. This indicated the pyrolysis of lignin was completed.

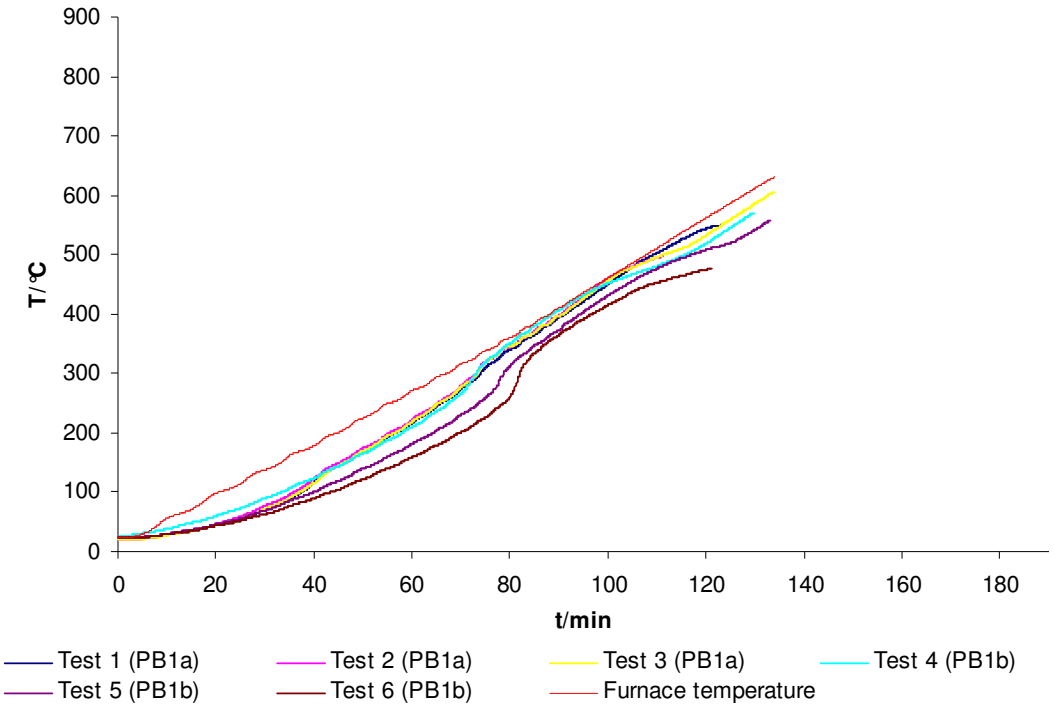

Figure 4.38 Temperature vs. time profiles of samples PB1a & PB1b.

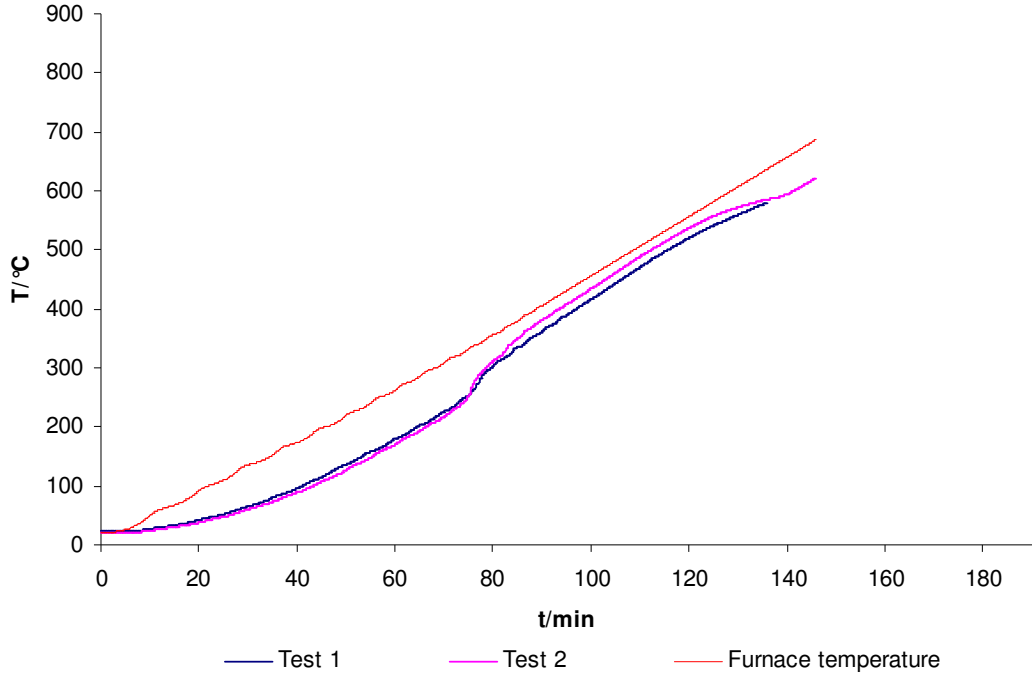

Figure 4.39 Sample PB2's temperature vs. time profile.

Figures 4.40 and 4.41 show the TG curve of the pyrolysis tests of samples PB1a and PB1b and sample PB2, respectively. The pyrolytic process was completed at between 480°C and 590°C. There was very little ash generated in the tests and no exothermic decomposition of calcium carbonate took place.

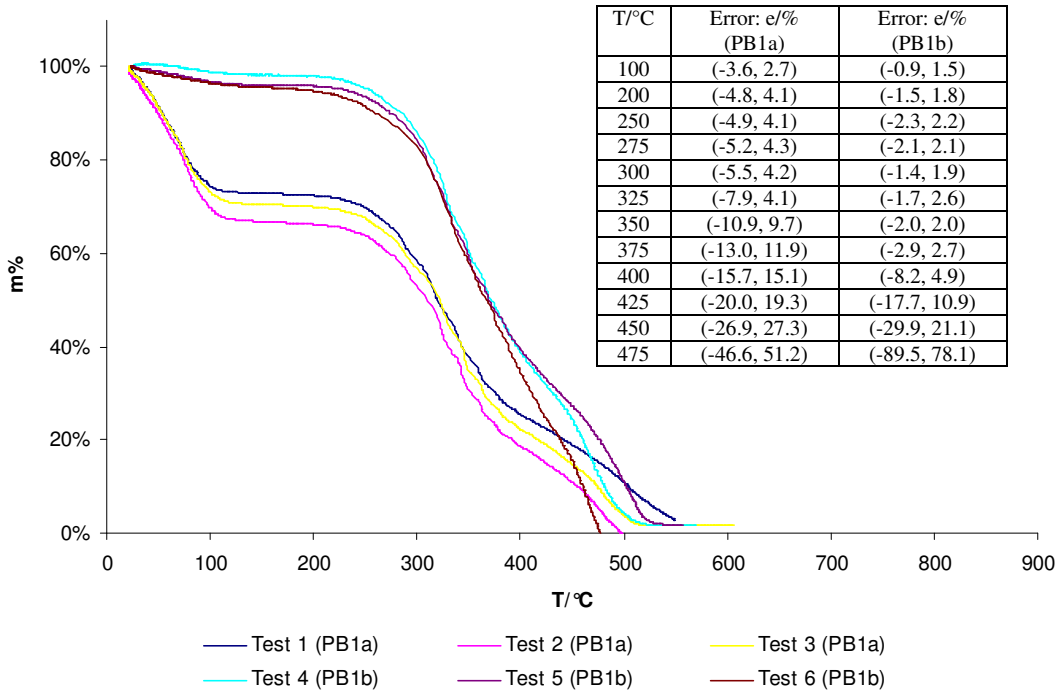

T/°C	Error: e/% (PB1a)	Error: e/% (PB1b)
100	(-3.6, 2.7)	(-0.9, 1.5)
200	(-4.8, 4.1)	(-1.5, 1.8)
250	(-4.9, 4.1)	(-2.3, 2.2)
275	(-5.2, 4.3)	(-2.1, 2.1)
300	(-5.5, 4.2)	(-1.4, 1.9)
325	(-7.9, 4.1)	(-1.7, 2.6)
350	(-10.9, 9.7)	(-2.0, 2.0)
375	(-13.0, 11.9)	(-2.9, 2.7)
400	(-15.7, 15.1)	(-8.2, 4.9)
425	(-20.0, 19.3)	(-17.7, 10.9)
450	(-26.9, 27.3)	(-29.9, 21.1)
475	(-46.6, 51.2)	(-89.5, 78.1)

Figure 4.40 TG profiles of samples PB1a & PB1b.

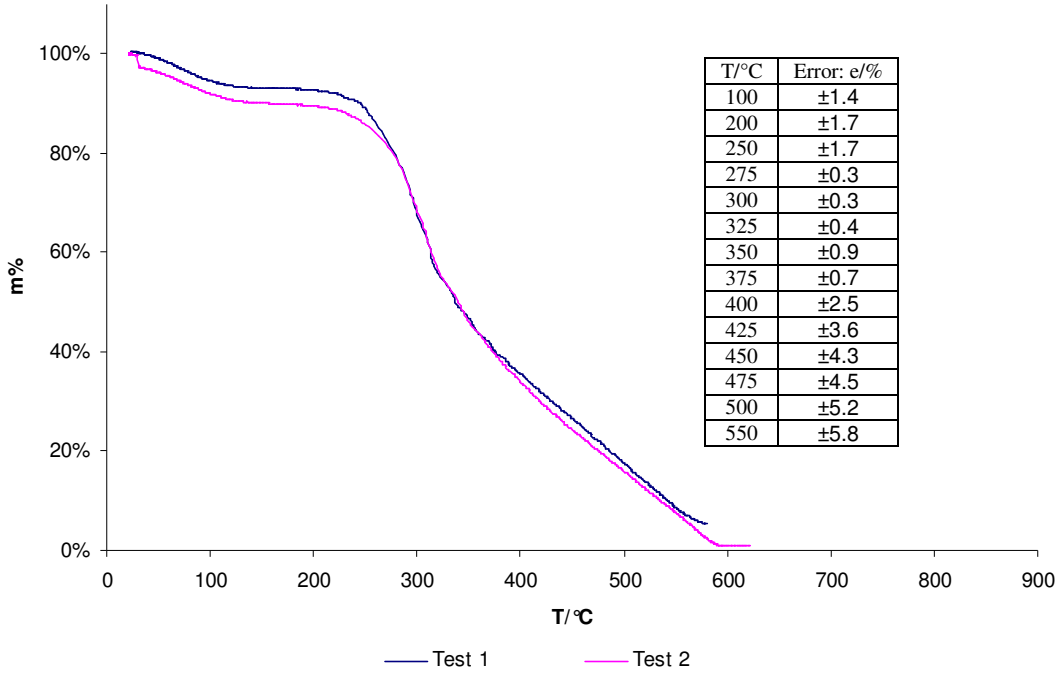

T/°C	Error: e/%
100	±1.4
200	±1.7
250	±1.7
275	±0.3
300	±0.3
325	±0.4
350	±0.9
375	±0.7
400	±2.5
425	±3.6
450	±4.3
475	±4.5
500	±5.2
550	±5.8

Figure 4.41 TG profile of sample PB2.

Figure 4.42 shows the DTG curve of the pyrolysis tests of the sawdust samples (PB1a and PB1b). Three different zones can be distinguished. The moisture vaporisation was the first zone with the maximum rate at between 80°C and 90°C. The second zone was the pyrolysis of hemicellulose and cellulose with the maximum mass loss rate at between 305°C and 315°C, as well as lignin decomposition. The pyrolysis of lignin continued in the third zone with the maximum rate at between 460°C and 490°C. Compared to both the simulated SRF briquettes and the SRF briquettes, the peak of the lignin pyrolysis of the sawdust materials was large, and this indicated that sawdust contained more lignin. The main pyrolytic process was essentially completed at between 490°C and 550°C. The sawdust materials contained very little ash and no decomposition of calcium carbonate took place. However, the curve of hemicellulose and cellulose pyrolysis shifted to the lower temperature by 20°C. This was because pulverised samples had smaller thermal inertia than briquette samples.

Figure 4.43 shows the DTG curve of the pyrolysis tests of the pulverised MFC wood sample (PB2). Three different zones can be distinguished. The moisture vaporisation was the first zone with the maximum rate at 85°C. The second zone was the pyrolysis of hemicellulose and cellulose with the maximum mass loss rate at 285°C as well as lignin decomposition. The pyrolysis of lignin continued in the third zone with the

maximum rate at 470°C. Compared to both the simulated SRF briquettes and the SRF briquettes, the peak of the lignin pyrolysis of pulverised MFC wood was large, and this indicated that MFC wood material contained a high lignin content. The main pyrolytic process was essentially completed at 590°C. The MFC wood material contained very little ash and no decomposition of calcium carbonate took place. The curve of hemicellulose and cellulose pyrolysis shifted to the lower temperature by 45°C. This was because of the smaller thermal inertia of the pulverised sample than that of the briquette sample.

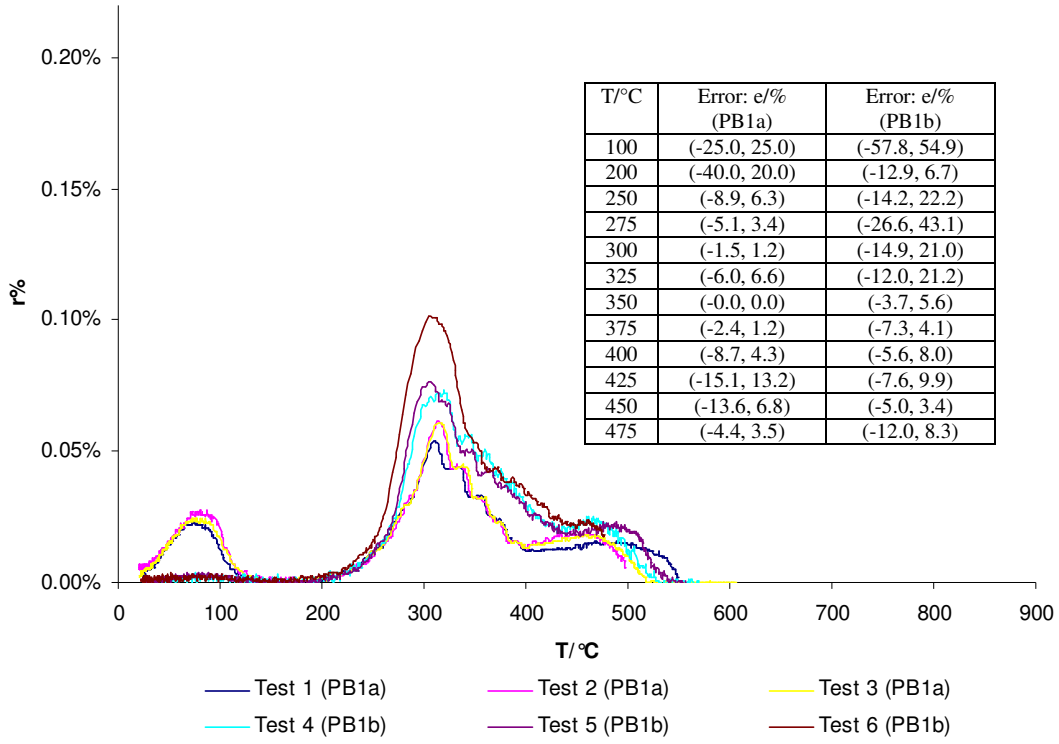

T/°C	Error: e/% (PB1a)	Error: e/% (PB1b)
100	(-25.0, 25.0)	(-57.8, 54.9)
200	(-40.0, 20.0)	(-12.9, 6.7)
250	(-8.9, 6.3)	(-14.2, 22.2)
275	(-5.1, 3.4)	(-26.6, 43.1)
300	(-1.5, 1.2)	(-14.9, 21.0)
325	(-6.0, 6.6)	(-12.0, 21.2)
350	(-0.0, 0.0)	(-3.7, 5.6)
375	(-2.4, 1.2)	(-7.3, 4.1)
400	(-8.7, 4.3)	(-5.6, 8.0)
425	(-15.1, 13.2)	(-7.6, 9.9)
450	(-13.6, 6.8)	(-5.0, 3.4)
475	(-4.4, 3.5)	(-12.0, 8.3)

Figure 4.42 DTG profiles of samples PB1a & PB1b.

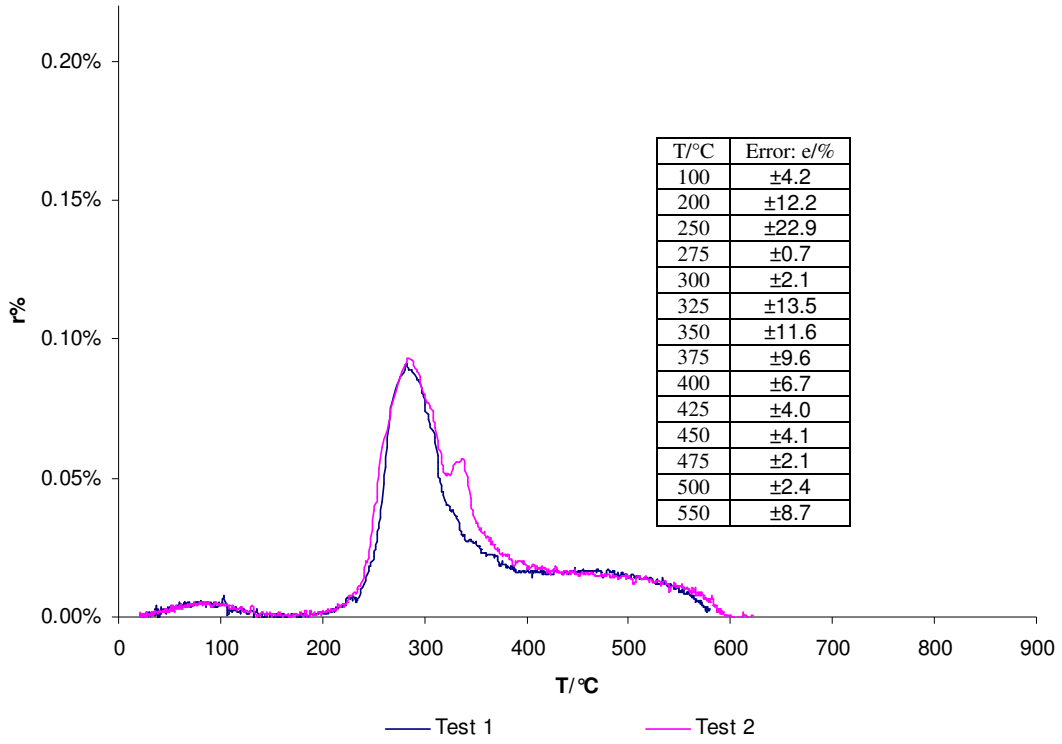

T/°C	Error: e/%
100	±4.2
200	±12.2
250	±22.9
275	±0.7
300	±2.1
325	±13.5
350	±11.6
375	±9.6
400	±6.7
425	±4.0
450	±4.1
475	±2.1
500	±2.4
550	±8.7

Figure 4.43 DTG profile of sample PB2.

This group of tests showed that the pyrolysis of the pulverised wood materials was quite repeatable. Wood materials contained a large amount of moisture and lignin and no plastic. They contained very little ash, and no calcium carbonate. The pyrolytic process was completed by 590°C.

4.3.2 Pyrolytic characteristics of pulverised willow materials

The pyrolysis of the pulverised willow inger 1 (PB3a) and the pulverised willow discovery 3 (PB3b) was carried out. Two pyrolysis tests of sample PB3a started with different initial sample mass of 4.720 g and 3.722 g, respectively. And two pyrolysis tests of sample PB3b started with different initial sample mass of 3.448 g and 3.194 g, respectively.

Figure 4.44 shows the sample temperature vs. time profile of the pyrolysis tests of samples PB3a and PB3b. Between 230°C and 500°C, the sample temperature rise was fast. This indicated the exothermic effect of the lignin decomposition. Above 500°C, the sample temperature rise was slow, and this indicated the pyrolysis of lignin was completed.

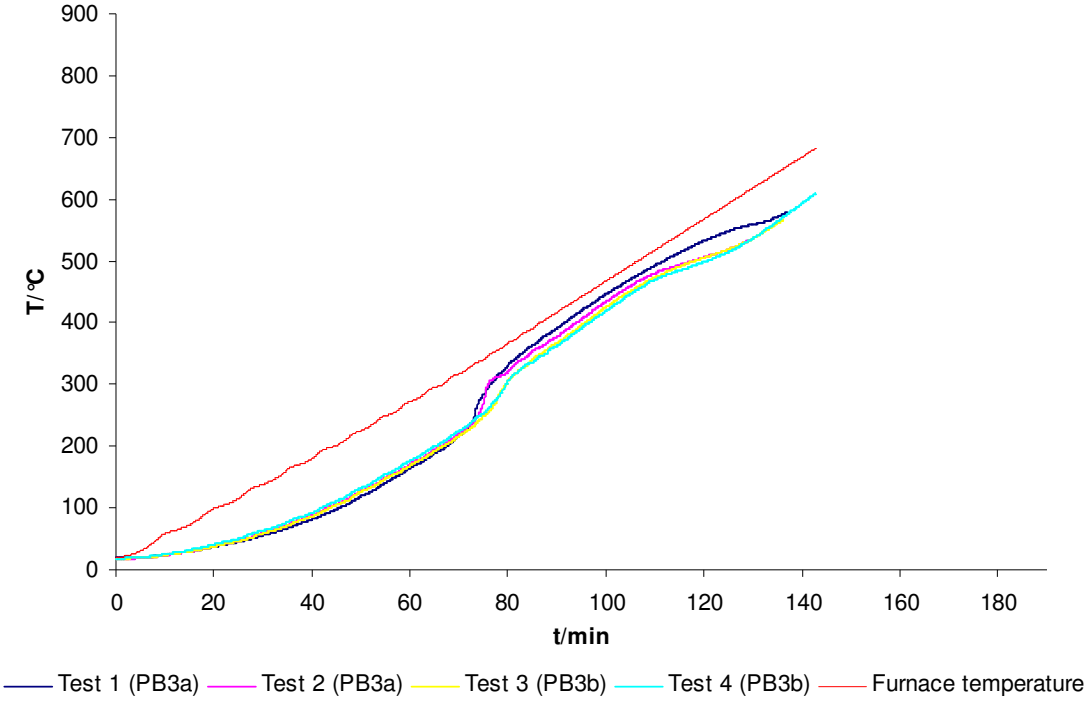

Figure 4.44 Temperature vs. time profiles of samples PB3a & PB3b.

Figure 4.45 shows the TG curve of the pyrolysis tests of samples PB3a and PB3b. The pyrolytic process was completed at between 530°C and 570°C. There was a small amount of ash produced in the tests and no exothermic decomposition of calcium carbonate took place.

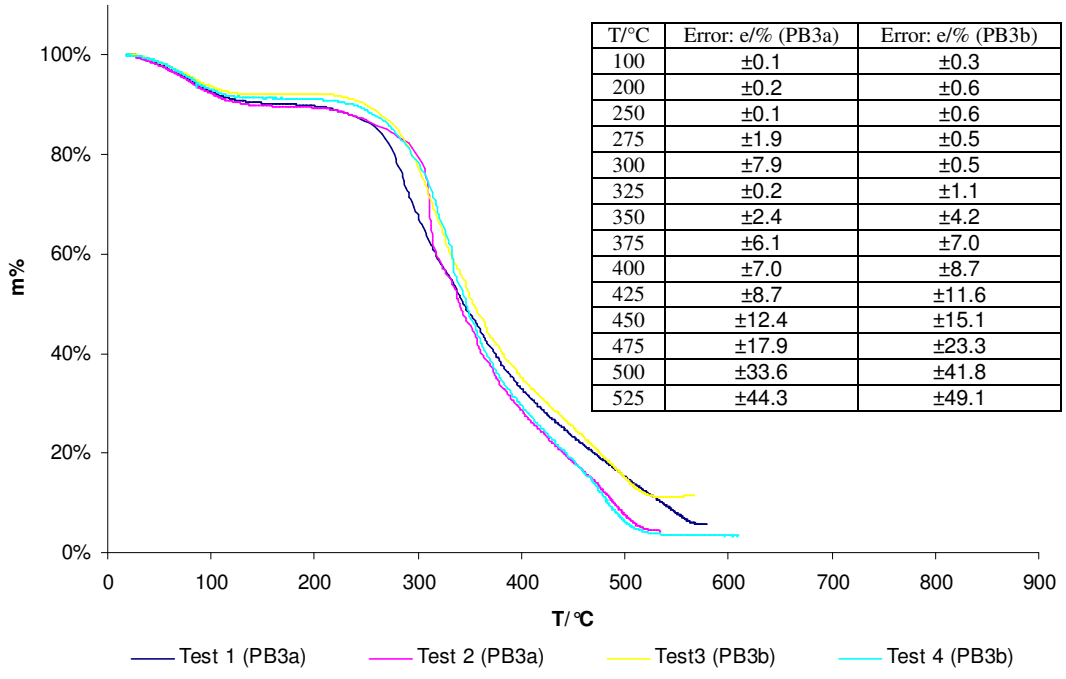

T/°C	Error: e/% (PB3a)	Error: e/% (PB3b)
100	±0.1	±0.3
200	±0.2	±0.6
250	±0.1	±0.6
275	±1.9	±0.5
300	±7.9	±0.5
325	±0.2	±1.1
350	±2.4	±4.2
375	±6.1	±7.0
400	±7.0	±8.7
425	±8.7	±11.6
450	±12.4	±15.1
475	±17.9	±23.3
500	±33.6	±41.8
525	±44.3	±49.1

Figure 4.45 TG profiles of samples PB3a & PB3b.

Figure 4.46 shows the DTG curve of the pyrolysis tests of samples PB3a and PB3b. Two different zones can be distinguished. The moisture vaporisation was the first zone with the maximum rate at 90°C. The second zone was hemicellulose and cellulose decomposition with the maximum mass loss rate at between 280°C and 310°C as well as lignin decomposition. The curve of the cellulose pyrolysis was shifted to the lower temperature by about 20°C due to the smaller thermal inertia of the pulverised sample. The pyrolysis of lignin took place over a broad temperature range and continued after the second zone. The pyrolytic process was essentially completed at between 530°C and 570°C. Compared to the pulverised wood materials, the willow materials contained less lignin. Two willow materials had quite similar pyrolytic characteristics.

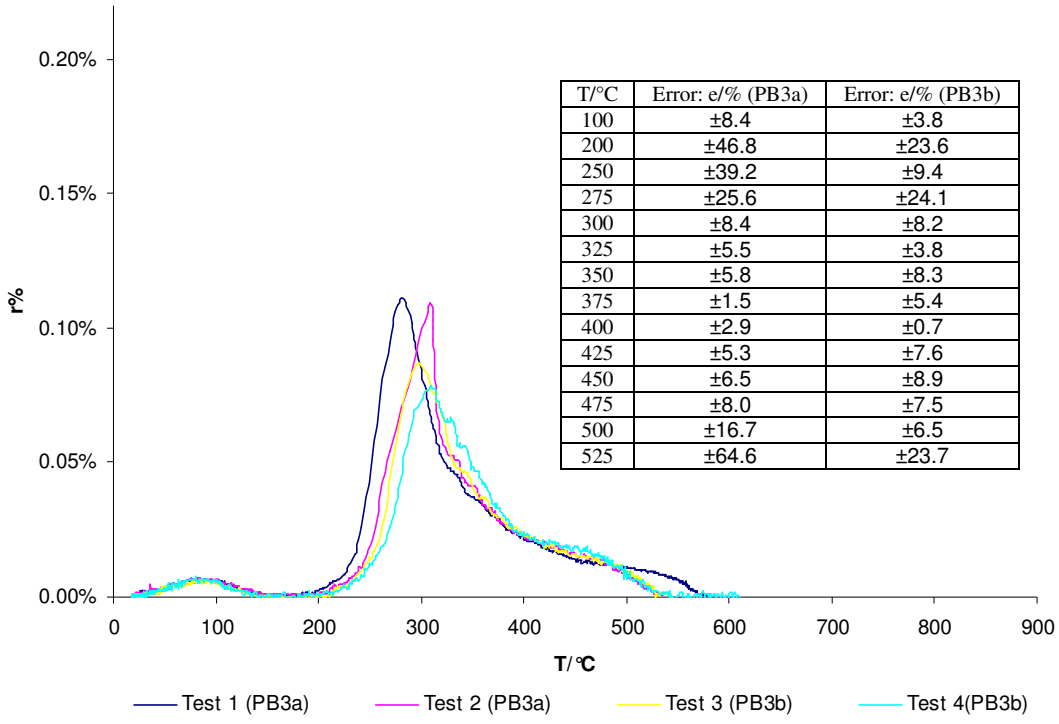

T/°C	Error: e/% (PB3a)	Error: e/% (PB3b)
100	±8.4	±3.8
200	±46.8	±23.6
250	±39.2	±9.4
275	±25.6	±24.1
300	±8.4	±8.2
325	±5.5	±3.8
350	±5.8	±8.3
375	±1.5	±5.4
400	±2.9	±0.7
425	±5.3	±7.6
450	±6.5	±8.9
475	±8.0	±7.5
500	±16.7	±6.5
525	±64.6	±23.7

Figure 4.46 DTG profiles of samples PB3a & PB3b.

This group of tests showed that the pyrolysis of the willow materials was quite repeatable. Willow materials contained very little ash, no plastic, and no calcium carbonate. The pyrolytic process was completed by 570°C.

4.3.3 Pyrolytic characteristics of other pulverised biomass materials

The pyrolysis of the pulverised borage meal (PB4), the pulverised oat husk (PB5), the pulverised miscanthus giganteus (PB6), the pulverised miscanthus goliath (PB7), the pulverised rape straw (PB8) and the pulverised wheat straw (PB9) was carried out. Two pyrolysis tests of sample PB4 started with different initial sample mass of 7.150 g and 7.449 g, respectively. Two pyrolysis tests of sample PB5 started with different initial sample mass of 4.025 g and 5.262 g, respectively. Two pyrolysis tests of sample PB6 started with different initial sample mass of 4.899 g and 4.922 g, respectively. Two pyrolysis tests of sample PB7 started with different initial sample mass of 3.654 g and 3.437 g, respectively. Two pyrolysis tests of sample PB8 started with different initial sample mass of 2.767 g and 2.340 g, respectively. And two pyrolysis tests of sample PB9 started with different initial sample mass of 2.188 g and 2.931 g, respectively.

Figures 4.47 – 4.52 show the sample temperature vs. time profile of the pyrolysis tests of samples PB4, PB5, PB6, PB7, PB8 and PB9, respectively. All curves show the exothermic effect of the lignin decomposition. When the pyrolysis of lignin was completed, the sample temperature rise became slow. However, different biomass materials had their own pyrolytic temperature ranges.

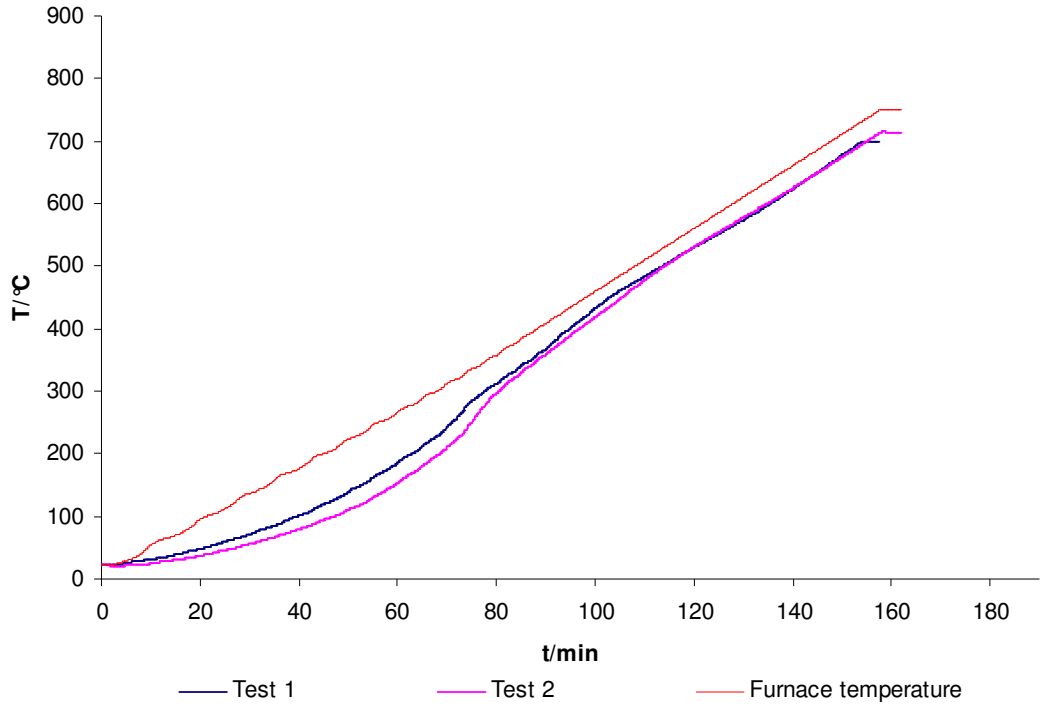

Figure 4.47 Sample PB4's temperature vs. time profile.

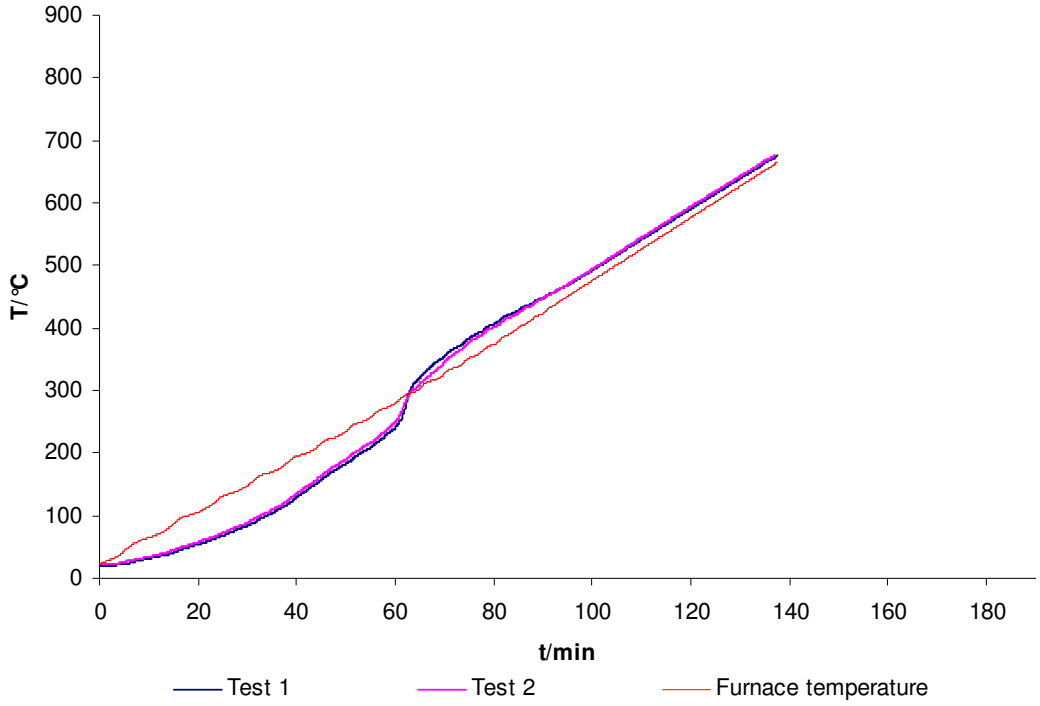

Figure 4.48 Sample PB5's temperature vs. time profile.

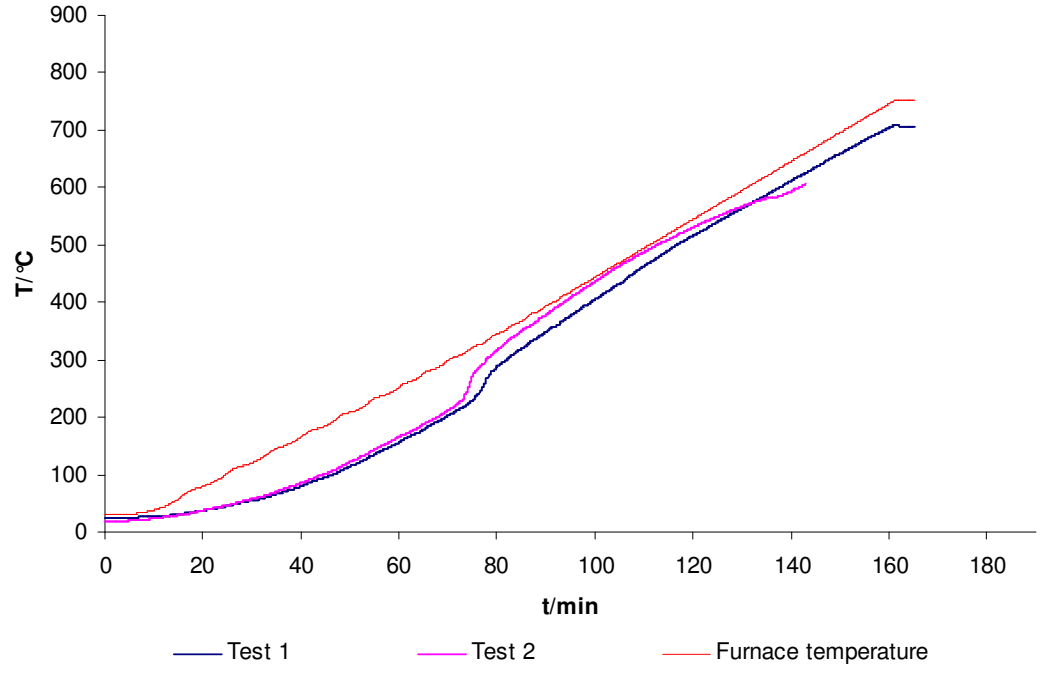

Figure 4.49 Sample PB6's temperature vs. time profile.

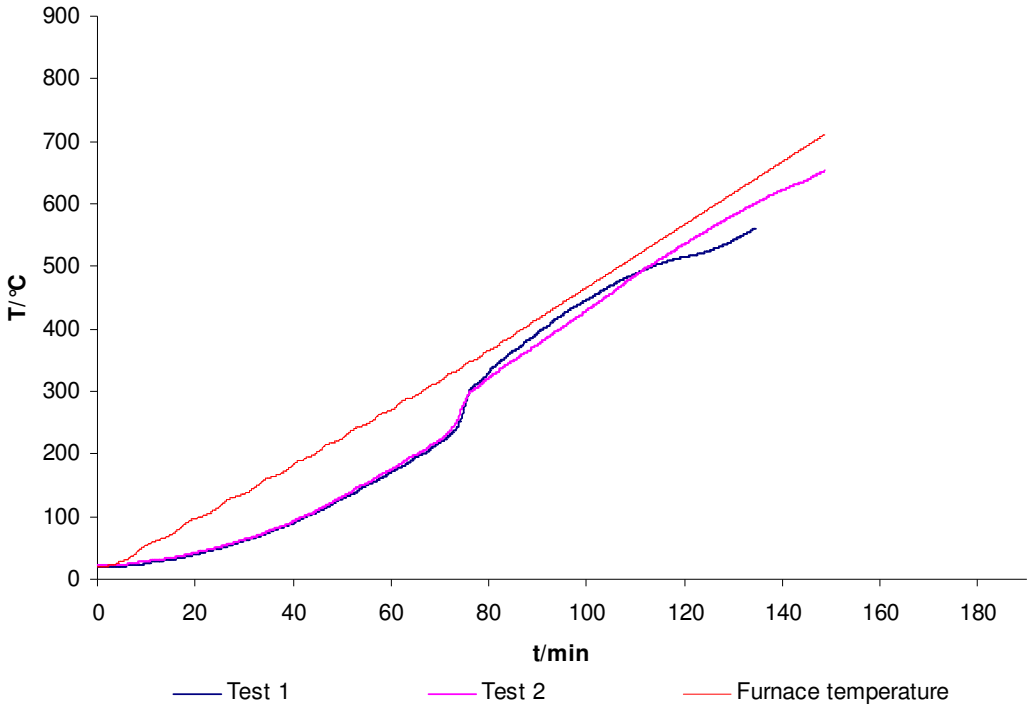

Figure 4.50 Sample PB7's temperature vs. time profile.

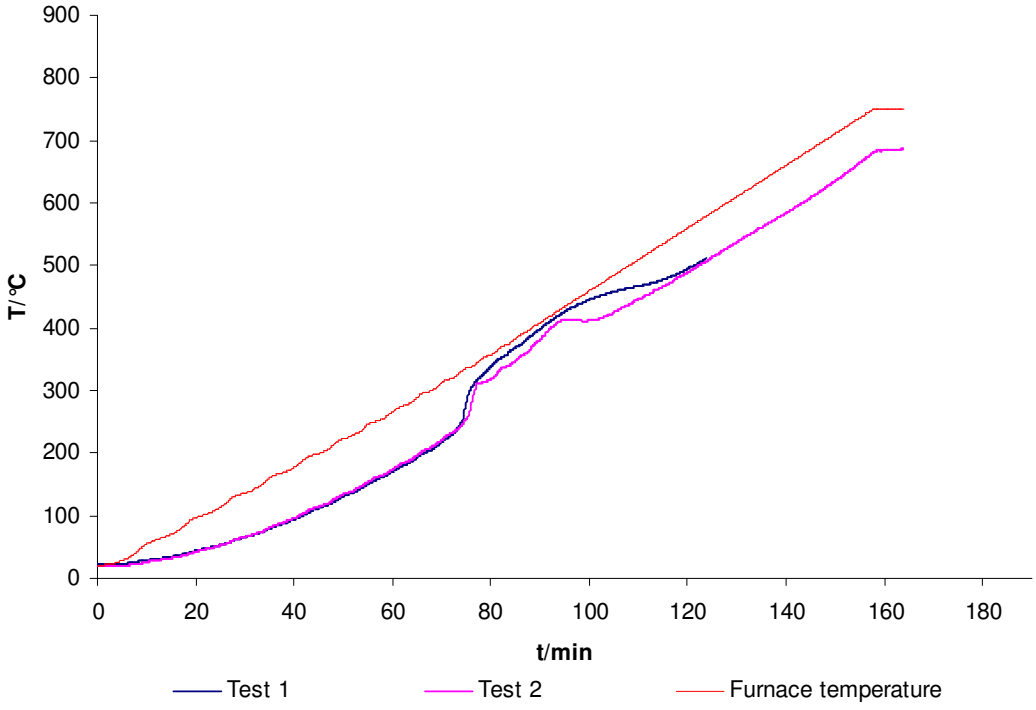

Figure 4.51 Sample PB8's temperature vs. time profile.

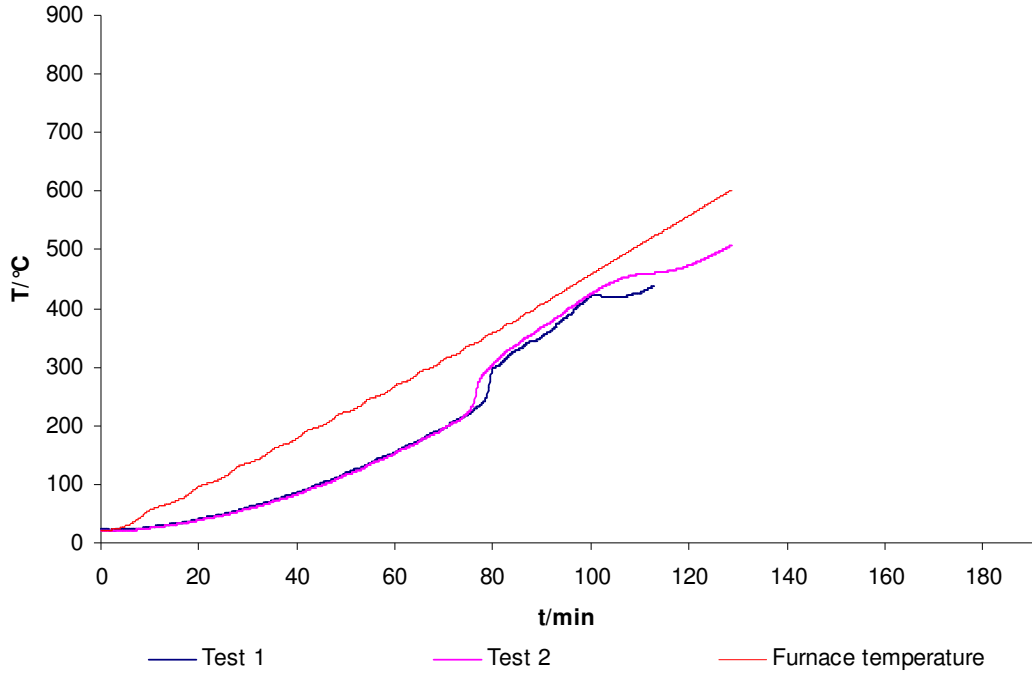

Figure 4.52 Sample PB9's temperature vs. time profile.

Figures 4.53 – 4.58 show the TG curve of the pyrolysis tests of samples PB4, PB5, PB6, PB7, PB8 and PB9, respectively. Figure 4.53 shows the moisture vaporisation event was overlapped with the thermal decomposition event in the pyrolysis of the pulverised borage meal due to the large amount of moisture in the sample. All pyrolysis tests were not quite repeatable at the end of each test. This indicated that the lignin content varied in the same material. Figures 4.53 – 4.55 show that the borage meal, the oat husk and the miscanthus giganteus had a lower volatile content than the other biomass materials.

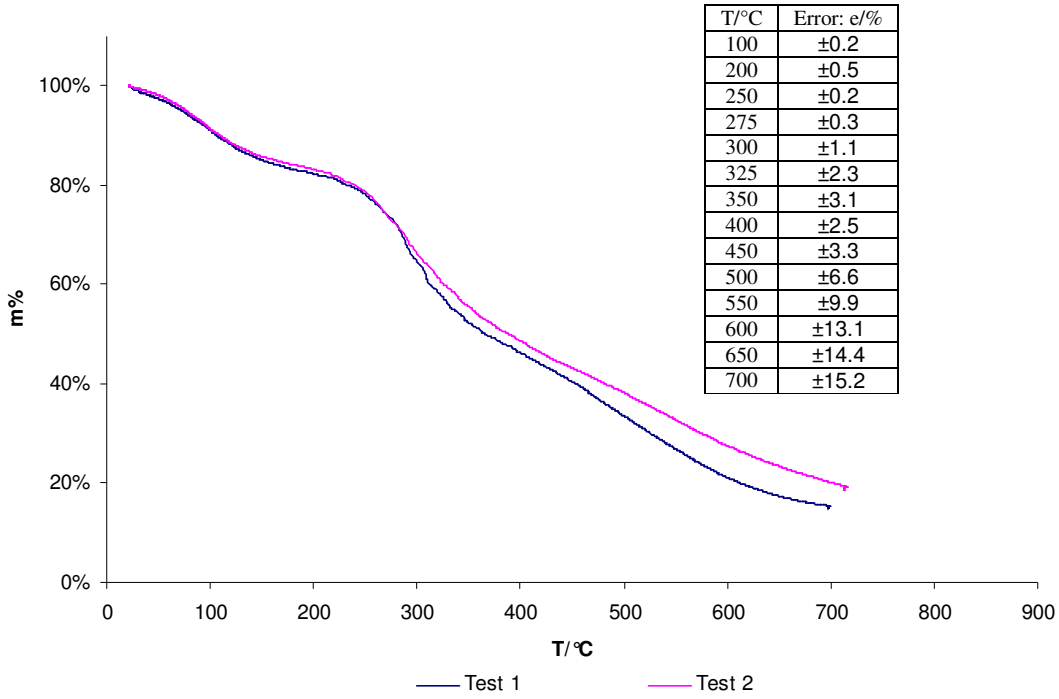

T/°C	Error: e/%
100	±0.2
200	±0.5
250	±0.2
275	±0.3
300	±1.1
325	±2.3
350	±3.1
400	±2.5
450	±3.3
500	±6.6
550	±9.9
600	±13.1
650	±14.4
700	±15.2

Figure 4.53 TG profile of sample PB4.

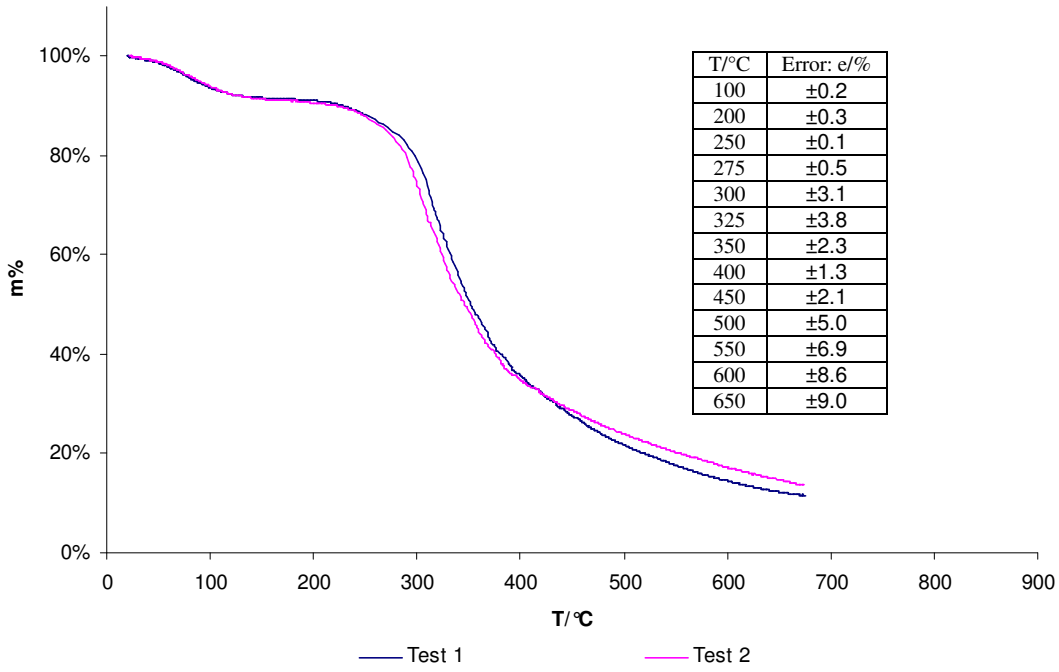

T/°C	Error: e/%
100	±0.2
200	±0.3
250	±0.1
275	±0.5
300	±3.1
325	±3.8
350	±2.3
400	±1.3
450	±2.1
500	±5.0
550	±6.9
600	±8.6
650	±9.0

Figure 4.54 TG profile of sample PB5.

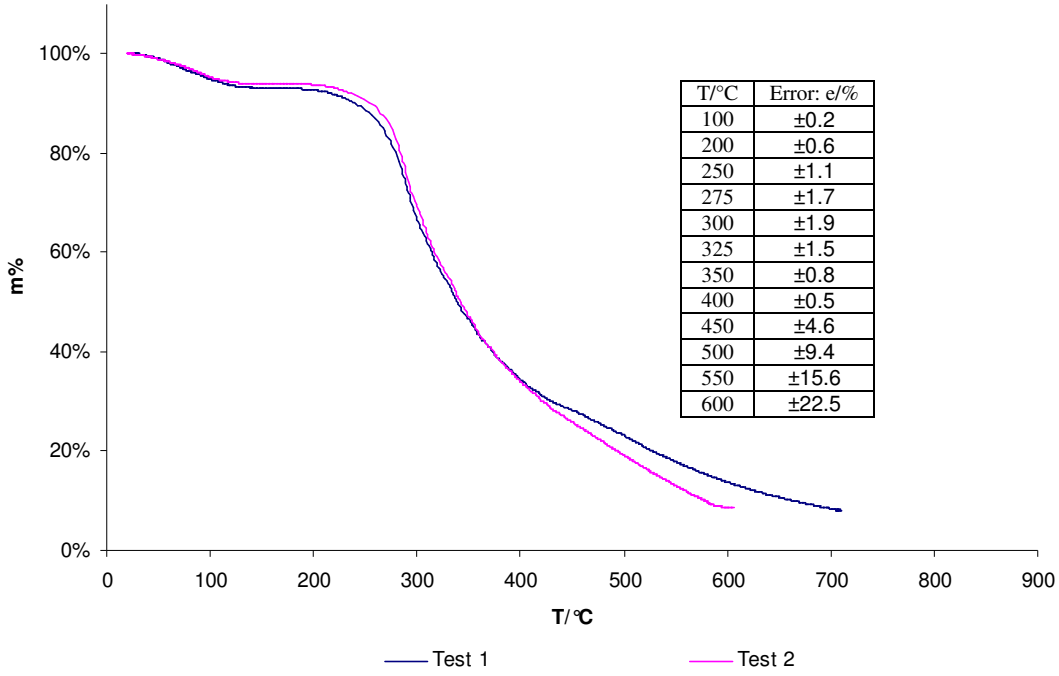

T/°C	Error: e/%
100	±0.2
200	±0.6
250	±1.1
275	±1.7
300	±1.9
325	±1.5
350	±0.8
400	±0.5
450	±4.6
500	±9.4
550	±15.6
600	±22.5

Figure 4.55 TG profile of sample PB6.

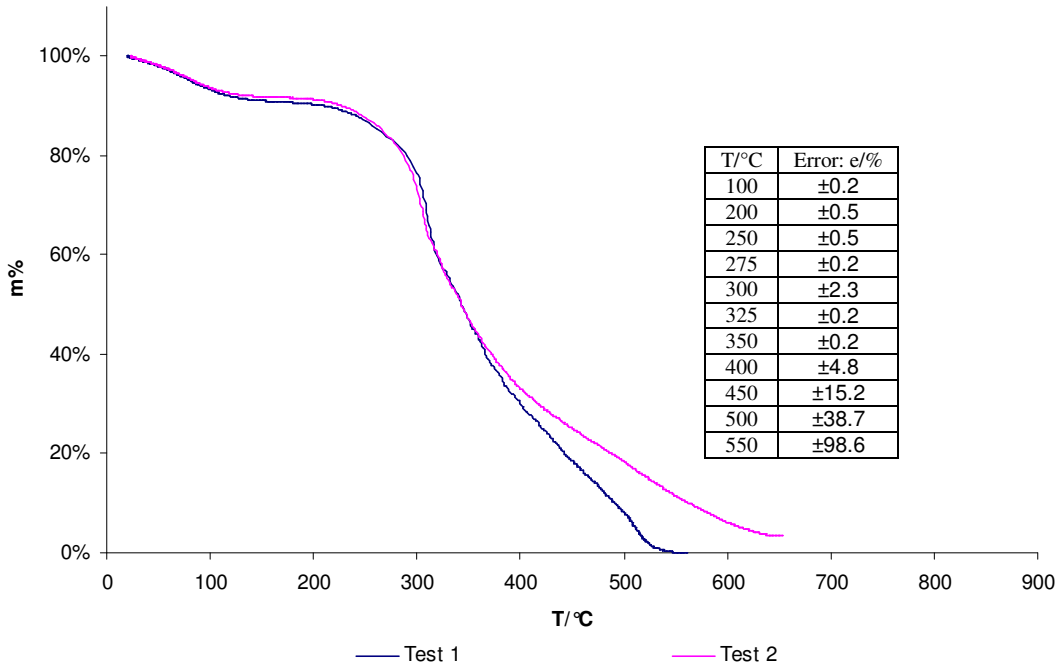

T/°C	Error: e/%
100	±0.2
200	±0.5
250	±0.5
275	±0.2
300	±2.3
325	±0.2
350	±0.2
400	±4.8
450	±15.2
500	±38.7
550	±98.6

Figure 4.56 TG profile of sample PB7.

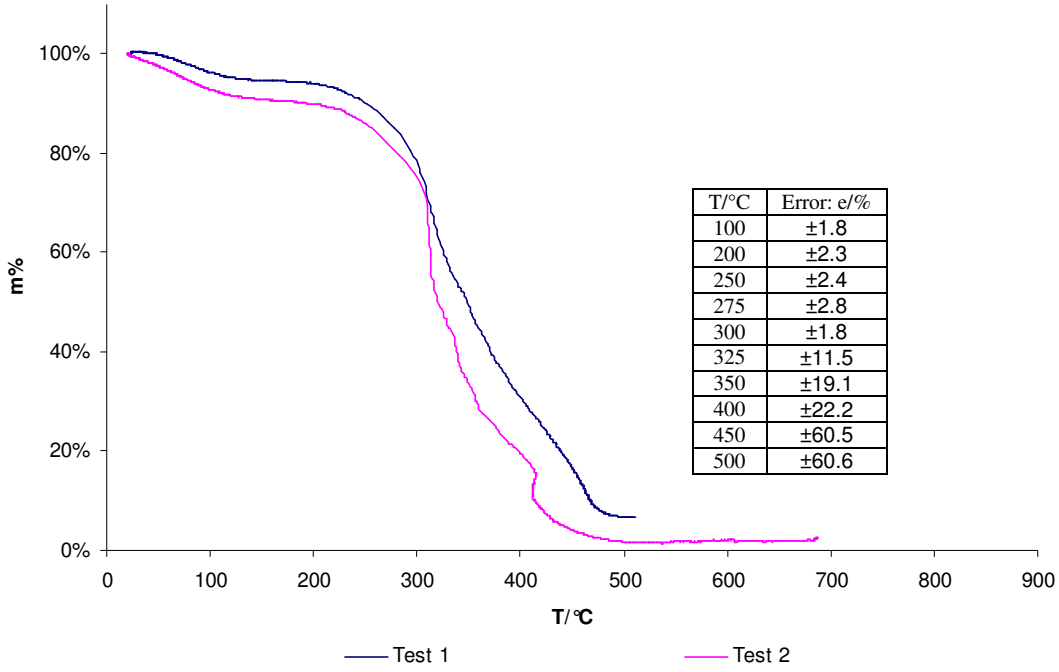

T/°C	Error: e/%
100	±1.8
200	±2.3
250	±2.4
275	±2.8
300	±1.8
325	±11.5
350	±19.1
400	±22.2
450	±60.5
500	±60.6

Figure 4.57 TG profile of sample PB8.

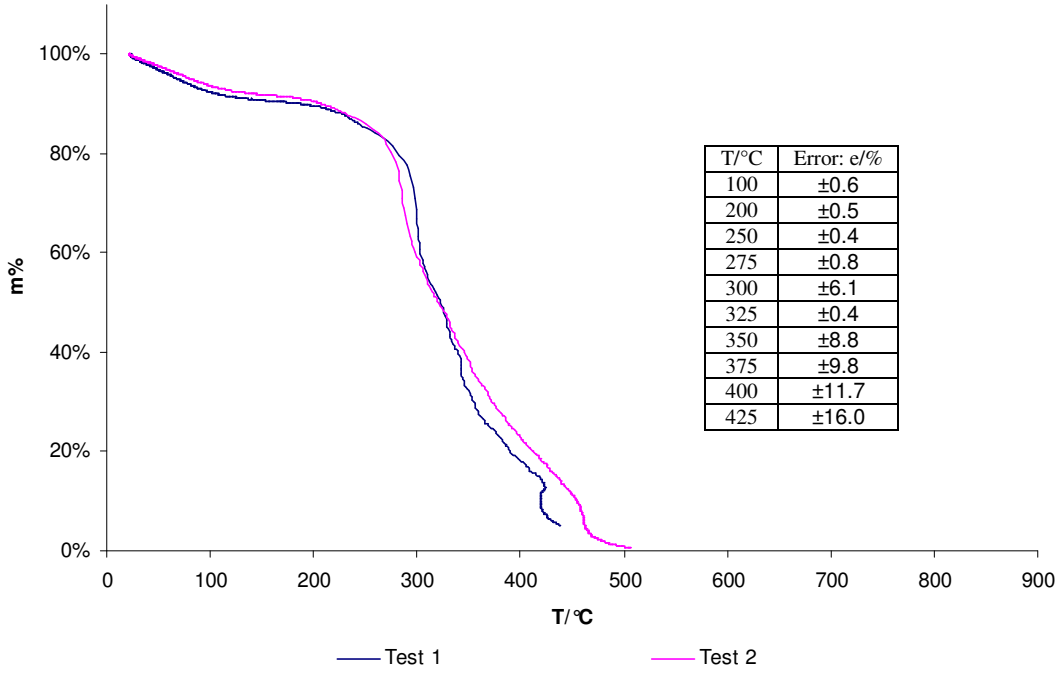

T/°C	Error: e/%
100	±0.6
200	±0.5
250	±0.4
275	±0.8
300	±6.1
325	±0.4
350	±8.8
375	±9.8
400	±11.7
425	±16.0

Figure 4.58 TG profile of sample PB9.

Figure 4.59 shows the DTG curve of the pyrolysis tests of the pulverised borage meal sample PB4. Two different zones can be distinguished. The moisture vaporisation was the first zone with the maximum rate at 105°C. The second zone was hemicellulose and cellulose decomposition with the maximum mass loss rate at between 270°C and

280°C as well as lignin decomposition. The proximate analysis in Table 3.1 shows that the borage meal had the highest ash content among the biomass samples. This could explain why the peak of DTG curve of sample PB4 was very low compared to the other biomass samples. The curve of cellulose pyrolysis was shifted to the lower temperature by 55°C, and this was due to both the effect of inorganic component and the effect of the smaller thermal inertia than briquettes. The slow further lignin pyrolysis continued up to the final temperature. At the temperature above 700°C, the exothermic decomposition of calcium carbonate took place.

Figure 4.60 shows the DTG curve of the pyrolysis tests of the pulverised oat husk sample PB5. Two different zones can be distinguished. The moisture vaporisation was the first zone with the maximum rate at 95°C. The second zone was hemicellulose and cellulose decomposition with the maximum mass loss rate at between 295°C and 305°C as well as lignin decomposition. The curve of cellulose pyrolysis was shifted to the lower temperature by 30°C due to both the effect of inorganic component and the effect of the smaller thermal inertia than briquettes. The slow further lignin pyrolysis continued up to the final temperature, and no decomposition of calcium carbonate took place.

Figure 4.61 shows the DTG curve of the pyrolysis tests of the pulverised miscanthus giganteus sample PB6. Two different zones can be distinguished. The moisture vaporisation was the first zone with the maximum rate at 90°C. The second zone was hemicellulose and cellulose decomposition with the maximum mass loss rate at 280°C as well as lignin decomposition. The curve of cellulose pyrolysis was shifted to the lower temperature by 50°C due to both the effect of inorganic component and the effect of the smaller thermal inertia than briquettes. The slow further lignin pyrolysis continued over a broad temperature range, and no decomposition of calcium carbonate took place.

Figure 4.62 shows the DTG curve of the pyrolysis tests of the pulverised miscanthus goliath sample PB7. Two different zones can be distinguished. The moisture vaporisation was the first zone with the maximum rate at 95°C. The second zone was hemicellulose and cellulose decomposition with the maximum mass loss rate at between 295°C and 305°C as well as lignin decomposition. The curve of

hemicellulose and cellulose pyrolysis was shifted to the lower temperature by 30°C due to both the effect of inorganic component and the effect of the smaller thermal inertia than briquettes. The slow further lignin pyrolysis continued up to the final temperature, and no decomposition of calcium carbonate took place.

Figure 4.63 shows the DTG curve of the pyrolysis tests of the pulverised rape straw sample PB8. Although the TG curve of PB8 in Figure 4.57 was not quite repeatable, the repeatability of the DTG curve was quite good. Two different zones can be distinguished. The moisture vaporisation was the first zone with the maximum rate at 85°C. The second zone was hemicellulose and cellulose decomposition with the maximum mass loss rate at between 300°C and 315°C as well as lignin decomposition. The curve of hemicellulose and cellulose pyrolysis was shifted to the lower temperature by 20°C due to both the effect of inorganic component and the effect of the smaller thermal inertia than briquettes. The lignin pyrolysis finished at 500°C and no decomposition of calcium carbonate took place.

Figure 4.64 shows the DTG curve of the pyrolysis tests of the pulverised wheat straw sample PB9. Two different zones can be distinguished. The moisture vaporisation was the first zone with the maximum rate at 90°C. The second zone was hemicellulose and cellulose decomposition with the maximum mass loss rate at between 280°C and 300°C as well as lignin decomposition. The curve of hemicellulose and cellulose pyrolysis was shifted to the lower temperature by 40°C due to both the effect of inorganic component and the effect of the smaller thermal inertia than briquettes. The lignin pyrolysis finished by 500°C and no decomposition of calcium carbonate took place.

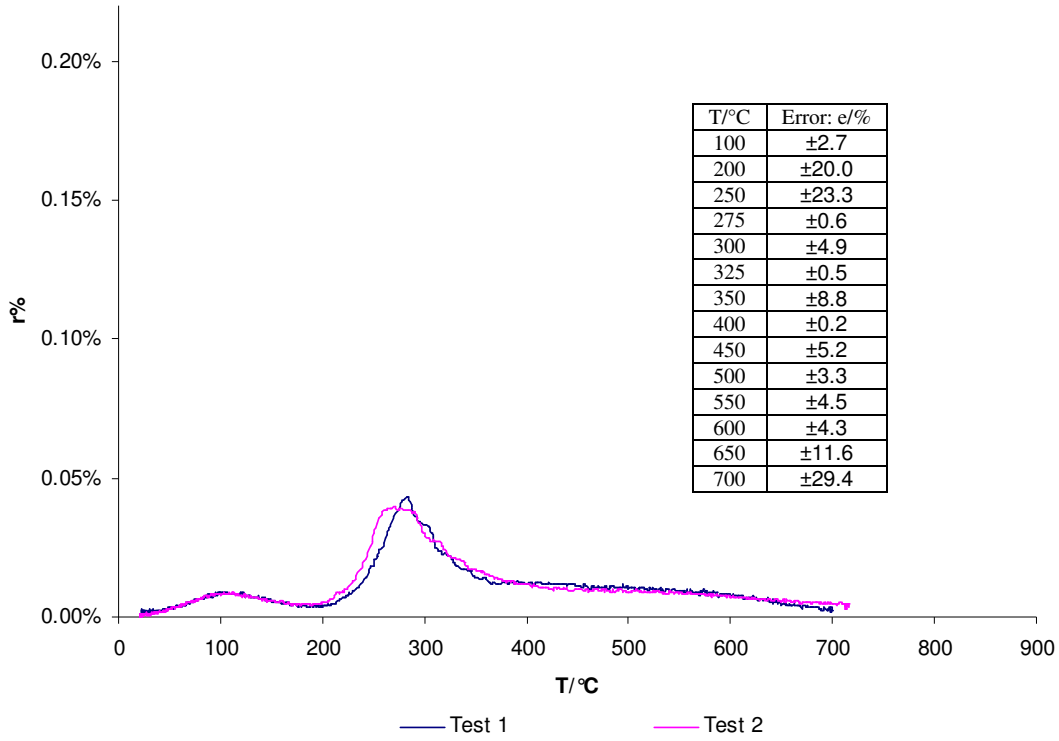

T/°C	Error: e/%
100	±2.7
200	±20.0
250	±23.3
275	±0.6
300	±4.9
325	±0.5
350	±8.8
400	±0.2
450	±5.2
500	±3.3
550	±4.5
600	±4.3
650	±11.6
700	±29.4

Figure 4.59 DTG profile of sample PB4.

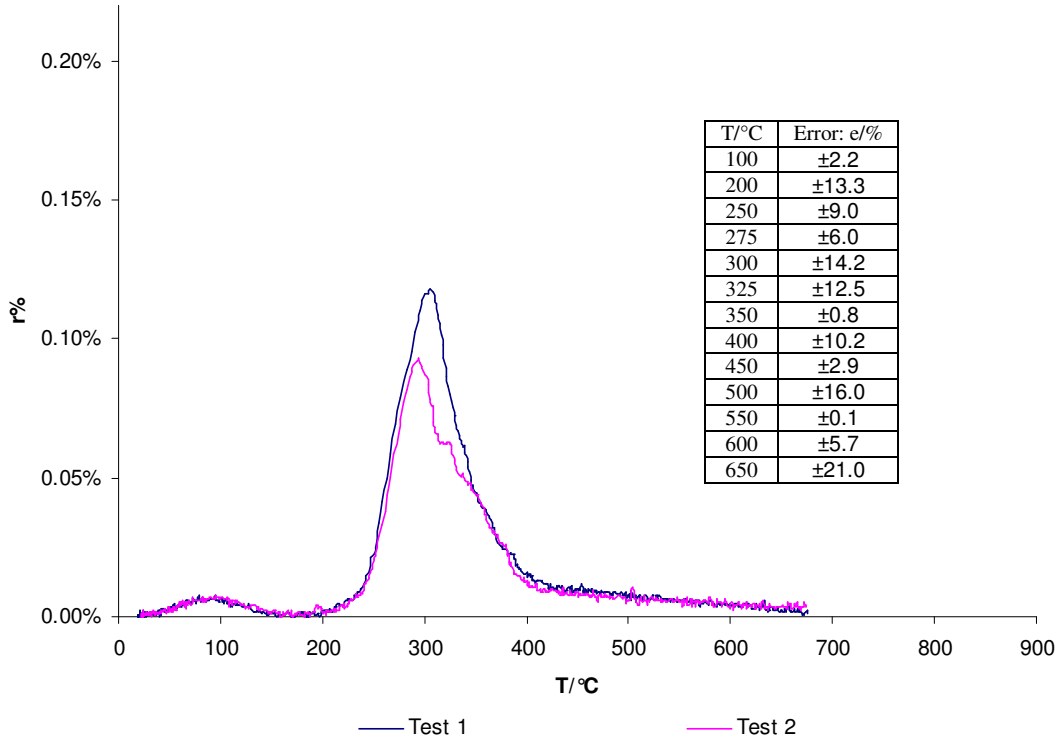

T/°C	Error: e/%
100	±2.2
200	±13.3
250	±9.0
275	±6.0
300	±14.2
325	±12.5
350	±0.8
400	±10.2
450	±2.9
500	±16.0
550	±0.1
600	±5.7
650	±21.0

Figure 4.60 DTG profile of sample PB5.

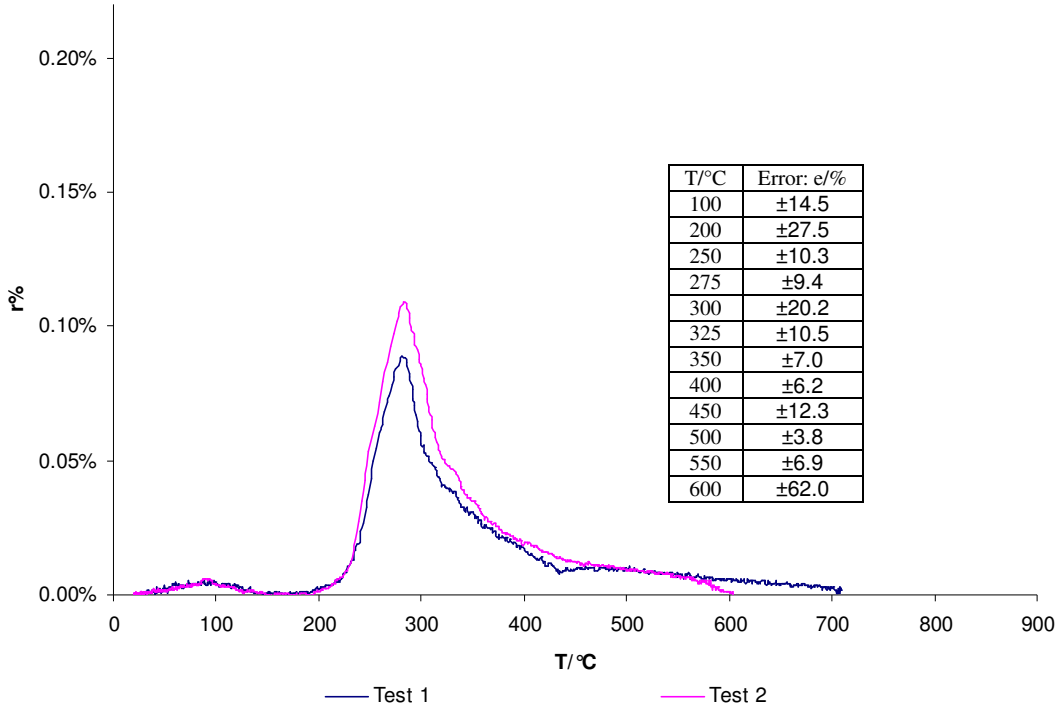

T/°C	Error: e/%
100	±14.5
200	±27.5
250	±10.3
275	±9.4
300	±20.2
325	±10.5
350	±7.0
400	±6.2
450	±12.3
500	±3.8
550	±6.9
600	±62.0

Figure 4.61 DTG profile of sample PB6.

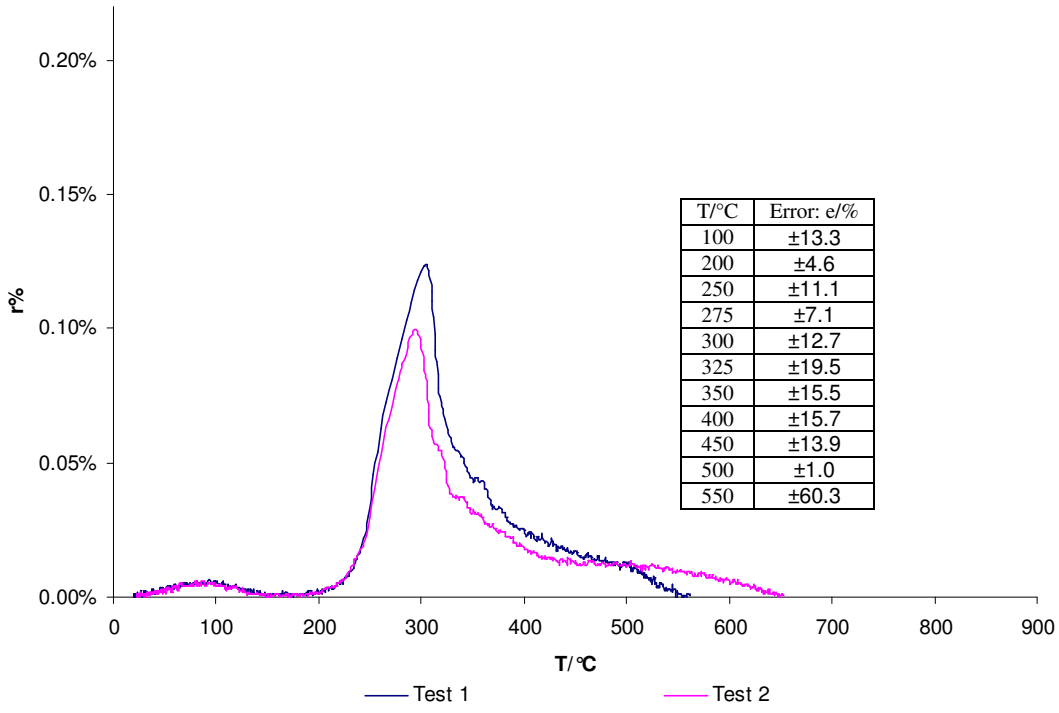

T/°C	Error: e/%
100	±13.3
200	±4.6
250	±11.1
275	±7.1
300	±12.7
325	±19.5
350	±15.5
400	±15.7
450	±13.9
500	±1.0
550	±60.3

Figure 4.62 DTG profile of sample PB7.

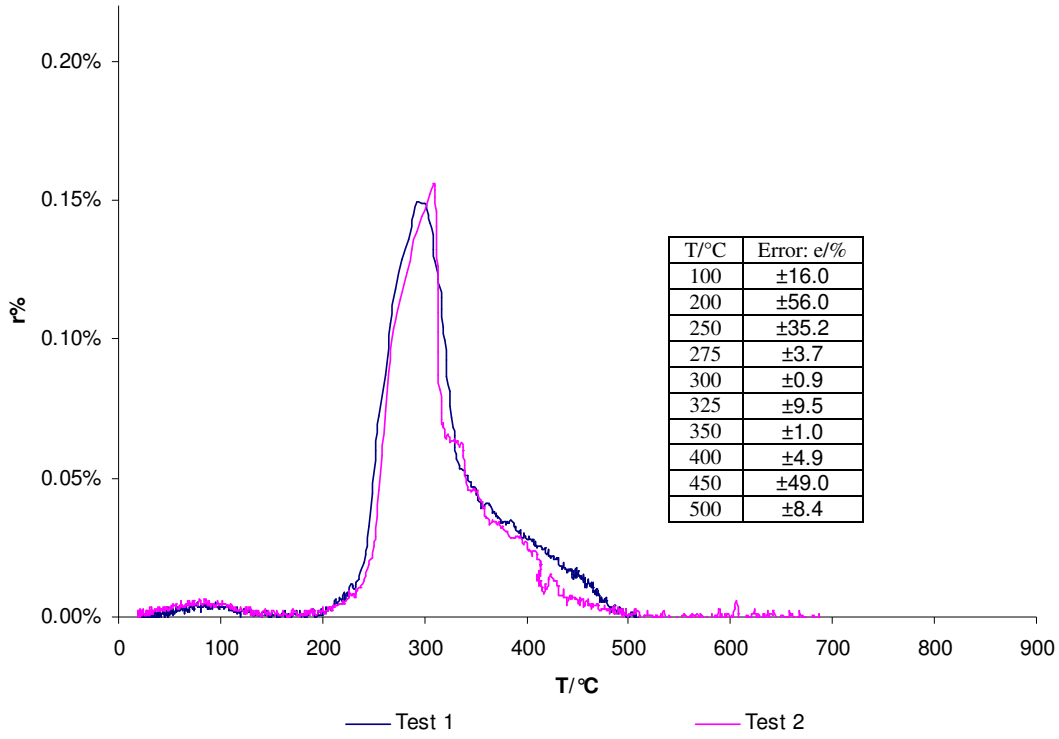

Figure 4.63 DTG profile of sample PB8.

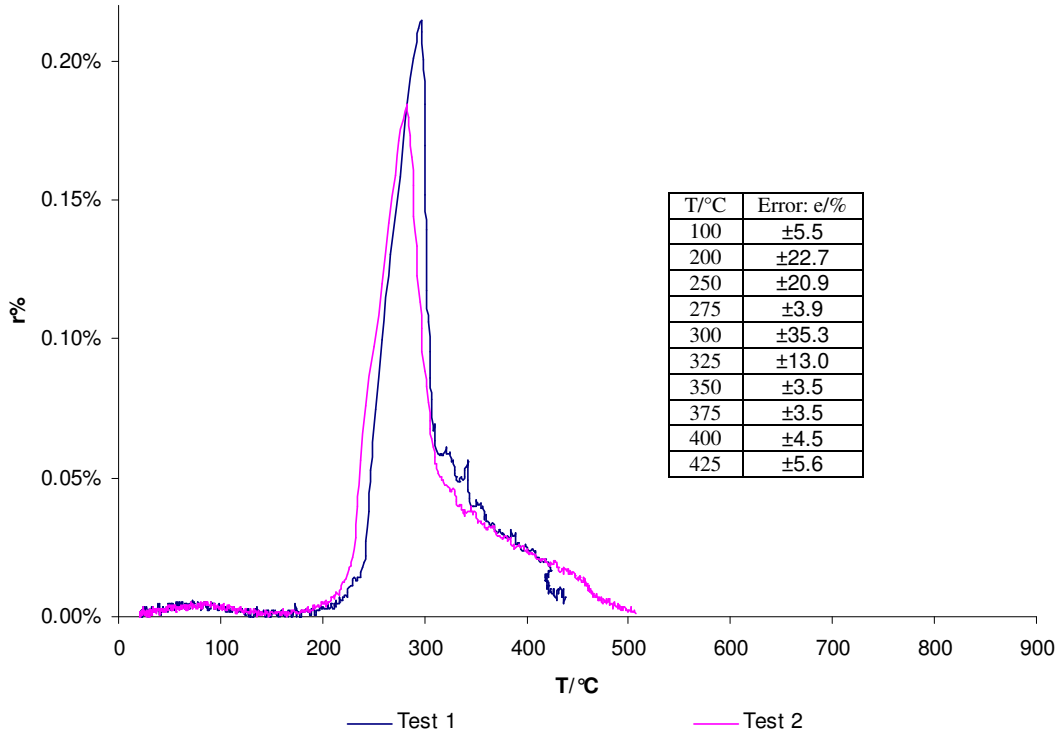

Figure 4.64 DTG profile of sample PB9.

This group of tests showed that the pyrolysis of the biomass materials was quite repeatable, especially the peak temperature and the pyrolytic process in the low

temperature. At the high temperature the lignin pyrolysis wasn't quite repeatable. No biomass materials contained plastic. Biomass materials contained very little ash, except the borage meal, the oat husk and the miscanthus giganteus which contained a relatively high ash content. In the end of the pyrolysis of the pulverised borage meal, the decomposition of calcium carbonate took place. The curve of hemicellulose and cellulose pyrolysis of all materials shifted to a lower temperature due to both the effect of inorganic component and the effect of the smaller thermal inertia than briquettes.

4.3.4 Summary

The overall pyrolytic process of most of the pulverised biomass consisted of two independent mass loss events as well as a moisture vaporisation event. The first event was hemicellulose and cellulose decomposition and was slightly endothermic. The hemicellulose decomposition was associated with the shoulder of the DTG curve and the cellulose decomposition was associated with the peak. The curve of the hemicellulose and cellulose pyrolysis shifted to a lower temperature. This was because of the smaller thermal inertia of pulverised samples than that of briquette samples. The second event was lignin decomposition, which started at very low temperature, occurred slowly, took place over a broad temperature range, and was exothermic. Biomass materials had a relatively high amount of moisture and very low ash. However, the borage meal had a high ash content. The oat husk and the miscanthus giganteus had a relatively high ash content. The wood materials contained relatively high lignin. The pyrolysis of the pulverised biomass was quite repeatable except the DTG curve of the lignin pyrolysis at high temperature. The pyrolysis tests showed that different types of biomass had different pyrolytic characteristics.

To further investigate the pyrolytic characteristics of the simulated SRF briquettes, the SRF briquettes and the pulverised biomass materials, a kinetic study is addressed in Chapter Five.

Chapter Five Kinetic Studies

Sophisticated models are unsuitable for design and prediction purposes, particularly given the difficulties of establishing and incorporating basic physical and chemical phenomena. Also, the lack of reliable experimental data on the thermodynamics of the pyrolysis of the simulated SRF briquettes, the SRF briquettes and the pulverised biomass materials makes it difficult to select appropriate models [6].

An increase in particle sizes or heating rates can cause a small displacement of a DTG profile to a higher temperature [23]. The pyrolysis of small particles (< 2 mm) of biomass is controlled entirely by reaction kinetics. For the size in the range of 2 – 50 mm, the pyrolysis is controlled by both heat transfer and chemical reactions. Above 50 mm, the pyrolysis is completely heat transfer controlled. The heat transfer is related to the gas flow condition, the gas diffusivity and the internal pore structure of samples [6, 126]. However, Ahuja et al. argued that the effect of sample size is sometimes misconstructed as a heating rate effect. The effect of the sample size is an internal mass transfer effect, and reactions are primarily concerned with the tar fraction of the volatiles [127].

5.1 Kinetic models

In the initial kinetic analysis of this research, a simplified model was used, which postulated that the rates of internal heat transfer, internal mass transfer and external mass transfer were all very fast. When the rate of internal heat transfer was very fast, the temperature inside the sample would be essentially uniform and therefore, the reaction zone would extend throughout the sample. Also, when the rates of internal mass transfer and external mass transfer were very fast, the reaction rate would be independent of position, and the overall controlling factor is the intrinsic reaction kinetics [6]. This simplified model also postulated that, although temperatures increased, the system reached a macroscopic chemical equilibrium state for the particular values of the temperature at one standard atmosphere.

A one-stage multi-reaction kinetic model assumed to consist of hypothesized chemical equations is shown below

$$\text{Sample} \xrightarrow{\Delta} \text{Volatile} \uparrow + \text{Ash}\,.$$

The first mass loss event in a DTG curve was a moisture vaporisation event followed by a pyrolytic process. In this kinetic study, only the pyrolytic process was studied. The pyrolytic process was assumed as one reaction or two non-interacting parallel reactions depending on the number of the thermal decomposition zones from the DTG profile rather than on the number of pseudo-components in the pyrolytic process, such as hemicellulose, cellulose, lignin and plastic. This was because the lignin pyrolysis taking place slowly over a broad temperature range was merged into the hemicellulose and cellulose pyrolysis and the plastic pyrolysis and therefore, it was very difficult to separate the lignin pyrolysis from these thermal decomposition zones. The hemicellulose pyrolysis and the cellulose pyrolysis were treated as one reaction, as the first was associated with the shoulder of the first thermal decomposition zone of the DTG curve and the latter was associated with the peak and they were difficult to separate.

In the following calculation, *m* represents mass and *r* represents mass reaction rates. *S*, *V*, and *A* are used as subscripts to represent *Sample*, *Volatile* and *Ash*, respectively.

This kinetic model is described as

$$r_S = k_S \cdot {m_S}^n \tag{1}$$

where

r_S is sample mass loss rate,

k_S is reaction rate coefficient,

m_S is sample mass,

n is reaction order.

The Arrhenius equation is used in the above chemical equation,

$$k_S = k_{S,0} \cdot e^{-\frac{E_a}{RT}} \tag{2}$$

where

T is sample temperature,

E_a is activation energy independent of T,
$k_{S,0}$ is pre-exponential factor independent of T.

In the Collision Theory of the Reaction Rate, activation energy is the minimum collision energy per mole of collisions that brings about a reaction between two colliding reactant particles, and it represents an energy barrier that the reactants must get over in order to become products. It determines the temperature dependence on the reaction rate. Higher activation energy means that the reaction rate more relies on the temperature. Pre-exponential factor, also known as frequency factor, is related to the frequency of collisions and the orientation of the reacting molecules, and indicates how many collisions have the correct orientation to lead to products.

Substitute Equation (2) into Equation (1) and it can be obtained

$$r_S = k_{S,0} \cdot e^{-\frac{E_a}{RT}} \cdot {m_S}^n . \tag{3}$$

Equation (3) can also be expressed as

$$\ln r_S = n \ln m_S - \frac{E_a}{RT} + \ln k_{S,0} . \tag{4}$$

A linear regression analysis of the values of $\ln m_S$, $-\frac{1}{RT}$ and $\ln r_S$ is used to acquire the values of n, E_a and $\ln k_{S,0}$ or $k_{S,0}$. But first, it is necessary to get the values of sample mass m_S and sample mass loss rates r_S.

Inorganic component is part of the sample composition, and ash is one of the reaction products. In the literature, ash is usually treated as a constant component of the sample. However, in this research, it was postulated that ash increased proportionally to the sample mass during the pyrolytic process. Two models, a constant ash model in the literature and an ash rise model in this research are compared in Section 5.2 by applying the data of pyrolysis test 2 of the ecodeco briquette extruded at 150°C (SRF2). The result shows that the ash rise model is better than the constant ash model.

5.1.1 Constant ash model

In the constant ash model, the sample mass can be obtained,

$$m_S = m_t - m_{A,t=\infty} \tag{5}$$

where

m_t is measured mass,

$m_{A,t=\infty}$ is final ash mass when the pyrolytic process is completed.

The sample mass loss rate and the measured mass loss rate are same,

$$r_S = r_t \tag{6}$$

where

r_t is measured mass loss rate.

The values of $m_{A,t=\infty}$, m_t and r_t are all known. Therefore, the values of m_S and r_S are known. Using the values of m_S and r_S and linear regression Equation (4), the kinetic parameters can be obtained.

5.1.2 Ash rise model

In the following calculation, *x* represents a constant remaining mass fraction. In the ash rise model, the constant remaining mass fraction *x* can be expressed as

$$x = \frac{m_{A,t=\infty}}{m_{S,0}} \tag{7}$$

where

$m_{S,0}$ is initial mass of dry sample after the moisture vaporisation process.

The constant remaining mass fraction *x* can also be expressed as

$$x = \frac{r_A}{r_S} \tag{8}$$

where

r_A is ash mass generation rate, and can be expressed as

$$r_A = r_S - r_t \,. \tag{9}$$

From Equations (7 – 9), the values of sample mass loss rates r_S can be obtained,

$$r_S = \frac{m_{S,0}}{m_{S,0} - m_{A,t=\infty}} \cdot r_t \,. \tag{10}$$

The values of $m_{S,0}$, $m_{A,t=\infty}$ and r_t are all known. Therefore, the values of r_S are known. Using the values of r_S and Equation (11) below, the values of sample mass m_S can be obtained. The calculation starts at $m_{S,0}$ and $r_{S,t=0}$.

$$m_{S,t+10\text{s}} = m_{S,t} - r_{S,t} \cdot 10 \text{ s}. \tag{11}$$

Using the values of m_S and r_S and linear regression Equation (4), the kinetic parameters can be obtained.

5.1.3 First order kinetic model

First order kinetic models were used to extract kinetic parameters from experimental data on the pyrolysis of solid fuels in several papers [23, 65, 99, 100, 128-134]. In the first order kinetic model, the reaction order *n* is 1 and therefore, Equations (3 and 4) can be expressed as

$$\frac{r_S}{m_S} = k_{S,0} \cdot e^{-\frac{E_a}{RT}} \tag{12}$$

and

$$\ln \frac{r_S}{m_S} = -\frac{E_a}{RT} + \ln k_{S,0}. \tag{13}$$

The values of sample mass m_S and sample mass loss rate r_S can be obtained either through the constant ash model or through the ash rise model. A linear regression analysis of the values of $\ln \frac{r_S}{m_S}$ against $-\frac{1}{RT}$ is used to acquire the values of E_a and $\ln k_{S,0}$ or $k_{S,0}$.

In Section 5.2, the first order kinetic model and the general order kinetic model are compared. The result shows that the general order kinetic model is better.

5.2 Comparison of general order ash rise kinetic model with other models

In this study, a first order constant ash kinetic model, a first order ash rise kinetic model, a general order constant ash kinetic model and a general order ash rise kinetic model were used to obtain the kinetic parameters for briquette SRF2 and the results are compared below by applying the data from test 2 of briquette SRF2.

In the constant ash model, Equation (5) was used to obtain the data of sample mass m_S against sample temperature *T* from the data of measured mass m_t against sample temperature *T*. The result is shown by the green curve in Figure 5.1. The sample mass loss rate r_S is the same as the measured mass loss rate r_t as described in Equation (6), and is shown by the pink curve in Figure 5.2.

In the ash rise model, Equations (10 and 11) were used to obtain the data of sample mass loss rate r_S and sample mass m_S against sample temperature *T* from the data of measured mass loss rate r_t and measured mass m_t against sample temperature *T*. The results are shown by the blue curve in Figures 5.1 and 5.2.

In Figure 5.1, the blue curve shows the derived sample mass against sample temperature profile in which the ash mass generated during the pyrolytic process was removed. The constant remaining mass fraction was a global factor for the whole pyrolytic process and was assumed to be the same value in every reaction zone. In the beginning of the pyrolytic process, the ash mass was zero and therefore, the derived sample mass was equal to the measured mass. As the pyrolysis continued, the derived sample mass curve moved away from the measured mass curve following a constant gradient during the process. In the end of the test, there was only ash left. The final measured mass was only the final ash mass and therefore, the final sample mass was zero.

In Figure 5.2, the blue curve shows the derived sample mass loss rate against sample temperature. The measured mass loss rate was the combination of the sample mass

loss rate and the ash mass generation rate. Therefore, the sample mass loss rate was higher than the measured mass loss rate.

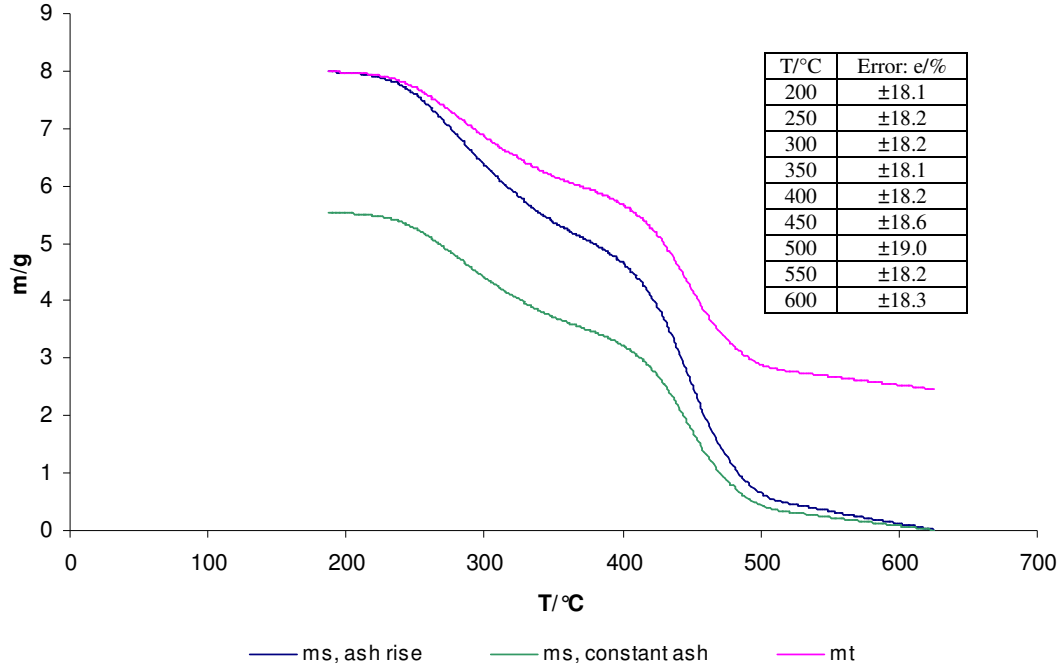

T/°C	Error: e/%
200	±18.1
250	±18.2
300	±18.2
350	±18.1
400	±18.2
450	±18.6
500	±19.0
550	±18.2
600	±18.3

Figure 5.1 Derived sample mass and measured mass vs. briquette temperature in test 2 of briquette SRF2.

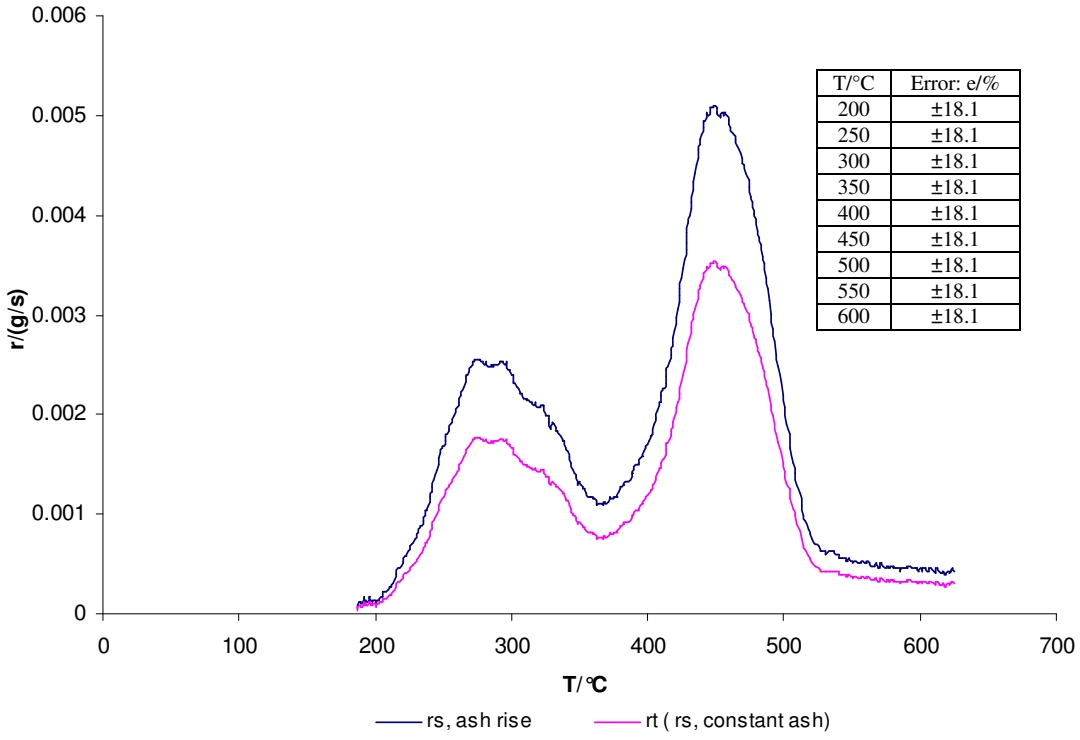

T/°C	Error: e/%
200	±18.1
250	±18.1
300	±18.1
350	±18.1
400	±18.1
450	±18.1
500	±18.1
550	±18.1
600	±18.1

Figure 5.2 Derived sample mass loss rate and measured mass loss rate vs. briquette temperature in test 2 of briquette SRF2.

The error analysis between the ash rise model and the constant ash model are shown in Figures 5.1 and 5.2. Figure 5.1 shows that the error of the derived sample mass between these two models was quite constant. In Figure 5.2, the error of the derived sample mass loss rates between these two models remained constant, and this because the derived sample mass curve moves away from the measured mass curve at a constant gradient in the ash rise model and the sample mass loss rate is equal to the measured mass loss rate in the constant ash model.

Two thermal decomposition zones were found in Figure 5.2 and therefore, the pyrolytic process of briquette SRF2 was treated as two non-interacting parallel reactions. The first peak from 187°C to 367°C in Figure 5.2 was treated as the first reaction, and the second peak from 368°C to 528°C was treated as the second reaction.

In the first order kinetic model, a linear regression analysis of $\ln\frac{r_S}{m_S}$ against $-\frac{1}{RT}$ are shown in Figures 5.3 and 5.7 for the constant ash model and in Figures 5.4 and 5.8 for the ash rise model to obtain the values of the activation energy E_a and the pre-exponential factor $k_{S,0}$. Figure 5.3 shows the linear regression of the first thermal decomposition zone in the pyrolytic process of briquette SRF2 in test 2 in the constant ash model. The curve started from the left side, moved to the right during the reaction, and finished at the top right. The activation energy E_a was the slope of the regression line and $\ln k_{S,0}$ was the intercept on axis $\ln\frac{r_S}{m_S}$. Therefore, the kinetic parameters were $E_{a,1} = 39.7$ kJ/mol and $k_{S,0,1} = 1.049\ \text{s}^{-1}$, and the regression coefficient R^2_1 was 66.1%. Similarly, Figure 5.4 shows the linear regression of the first thermal decomposition zone in the pyrolytic process of briquette SRF2 in test 2 in the ash rise model. The kinetic parameters were $E_{a,1} = 39.7$ kJ/mol and $k_{S,0,1} = 1.043\ \text{s}^{-1}$, and the regression coefficient R^2_1 was 66.1%.

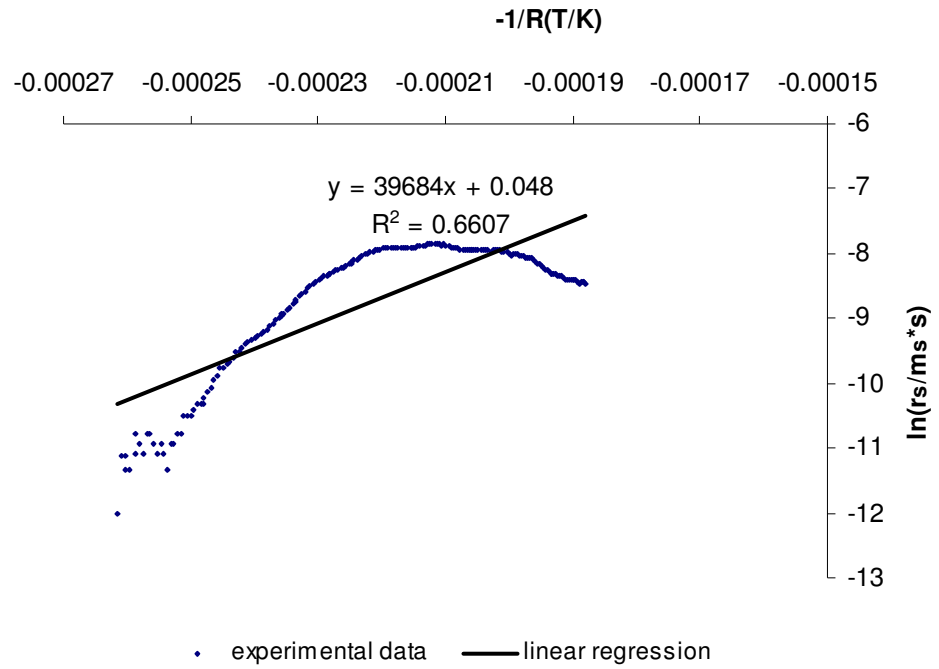

Figure 5.3 Linear regression analysis of the first reaction in test 2 of briquette SRF2 via first order constant ash kinetic model.

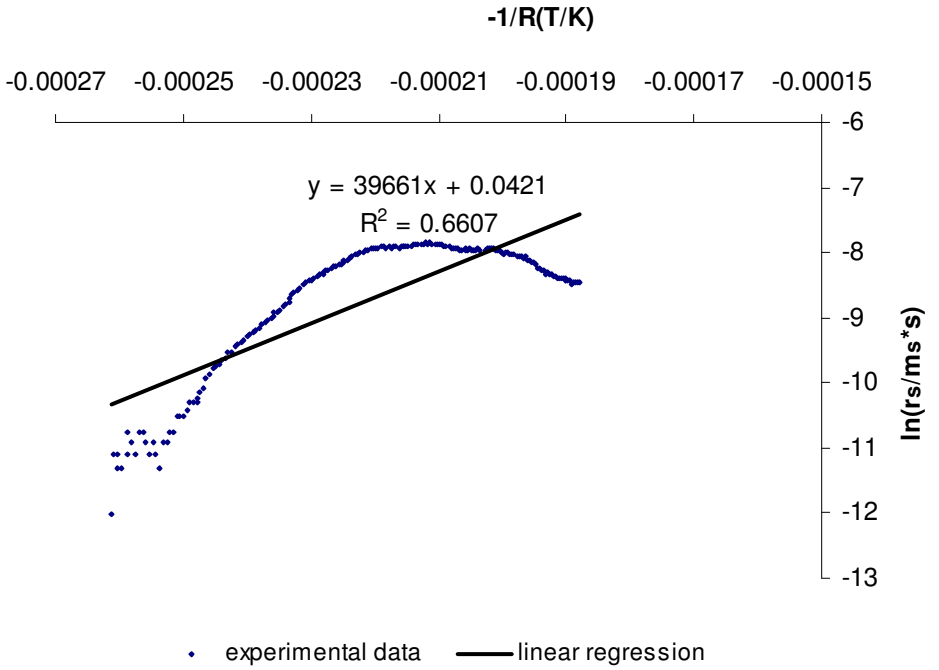

Figure 5.4 Linear regression analysis of the first reaction in test 2 of briquette SRF2 via first order ash rise kinetic model.

In the general order kinetic model, a linear regression analysis of $\ln m_S$, $-\frac{1}{RT}$ and $\ln r_S$ shown in Figures 5.5 and 5.9 for the constant ash model was used to obtain the

values of n_S, E_a and $k_{S,0}$. Figure 5.5 shows the linear regression of the first thermal decomposition zone in the pyrolytic process of briquette SRF2 in test 2 for the constant ash model. The linear regression curve in three-dimensions should fit in a plane. The curve started from the bottom right in Figure 5.5 (a), moved to the left during the reaction, and finished at the top left. The reaction order n was the coefficient of the item $\ln m_S$, the activation energy E_a was the coefficient of the item $-\frac{1}{RT}$ and $\ln k_{S,0}$ was the intercept on axis $\ln r_S$. Figure 5.5 shows the linear regression fit the experimental data very well, and the regression coefficient R^2_1 was 97.9%. The kinetic parameters were $n_1 = 14.3$, $E_{a,1} = 130.2$ kJ/mol and $k_{S,0,1} = 0.609$. Similarly, in the ash rise model, the kinetic parameters obtained in Figures 5.6 were $n_1 = 14.3$, $E_{a,1} = 129.5$ kJ/mol and $k_{S,0,1} = 4.35\times10^{-3}$, and the regression coefficient R^2_1 was 98.0%.

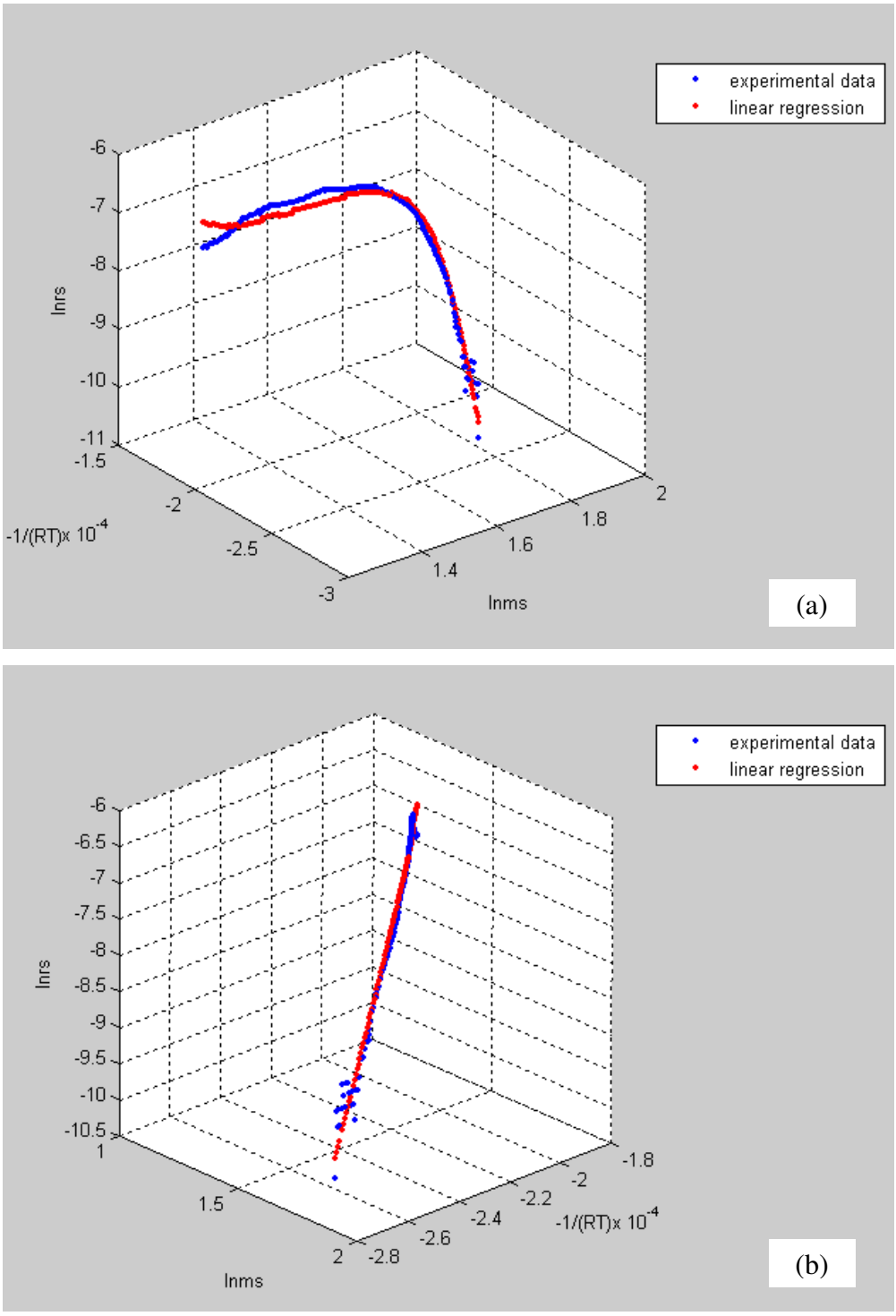

Figure 5.5 Linear regression analysis of the first reaction in test 2 of briquette SRF2 via general order constant ash kinetic model.

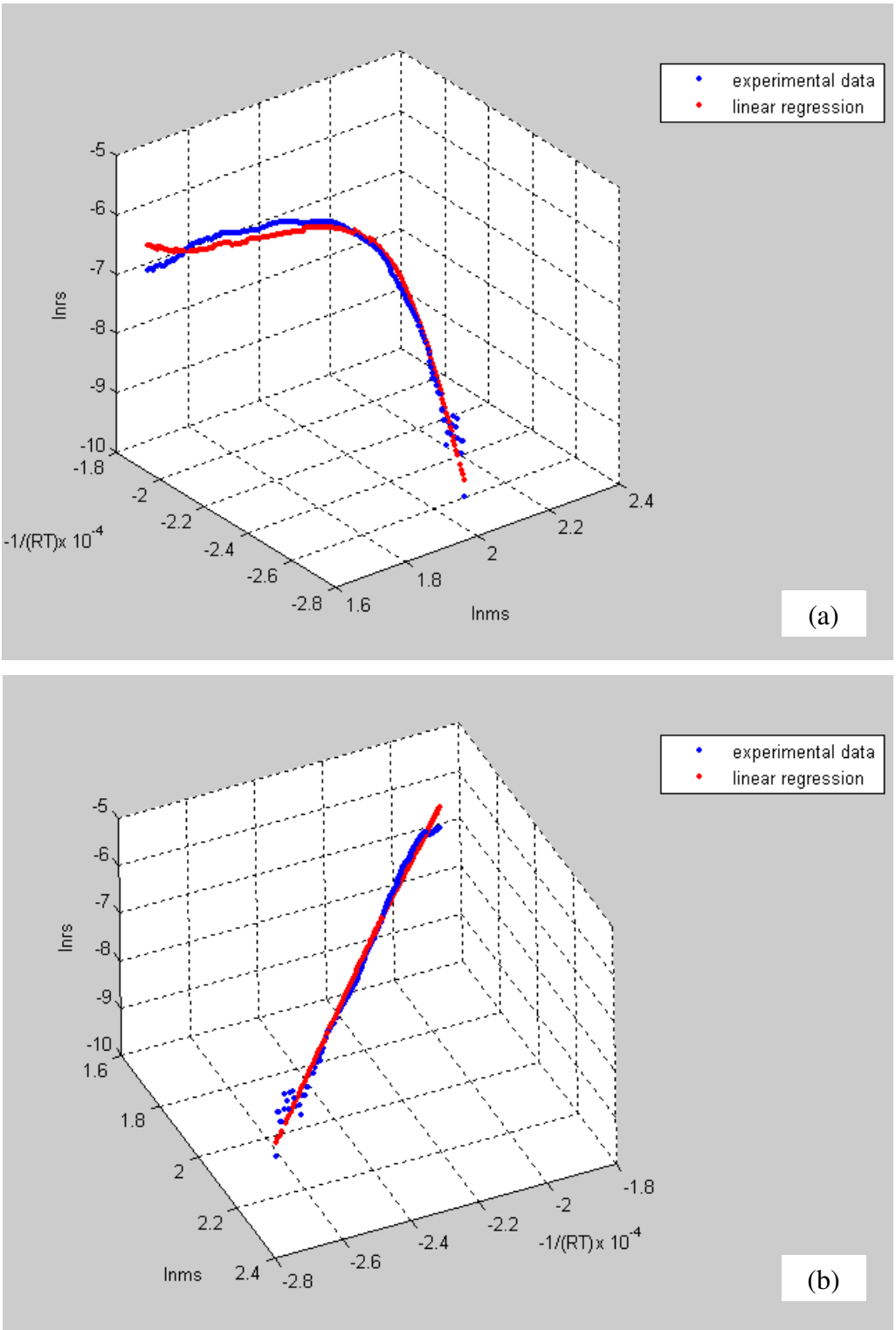

Figure 5.6 Linear regression analysis of the first reaction in test 2 of briquette SRF2 via general order ash rise kinetic model.

Comparing the regression coefficients obtained from the above models, it can be seen that the general order kinetic models were better than the first order kinetic models.

The constant ash model and the ash rise model, however, had very similar regression coefficient.

Figure 5.7 shows the linear regression of the second thermal decomposition zone in the pyrolytic process of briquette SRF2 in test 2 using the first order constant ash model. The curve started from the left side and finished on the right. The activation energy E_a was the slope of the regression line and $\ln k_{S,0}$ was the intercept on axis $\ln \frac{r_S}{m_S}$. Therefore, the kinetic parameters were $E_{a,2} = 86.5$ kJ/mol and $k_{S,0,2} = 2.42 \times 10^3$ s^{-1}, and the regression coefficient R^2_2 was only 84.3%. Similarly, Figure 5.8 shows the linear regression of the second thermal decomposition zone in the pyrolytic process of briquette SRF2 in test 2 using the first order ash rise model, and the kinetic parameters were $E_{a,2} = 86.0$ kJ/mol and $k_{S,0,2} = 2.22 \times 10^3$ s^{-1}, and the regression coefficient R^2_2 was only 84.4%.

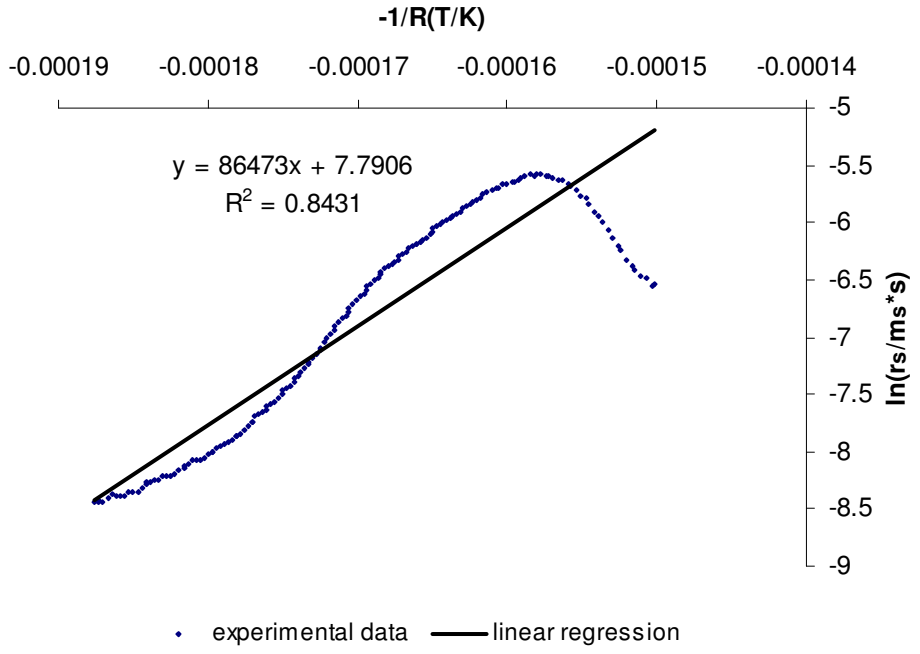

Figure 5.7 Linear regression analysis of the second reaction in test 2 of briquette SRF2 via first order constant ash kinetic model.

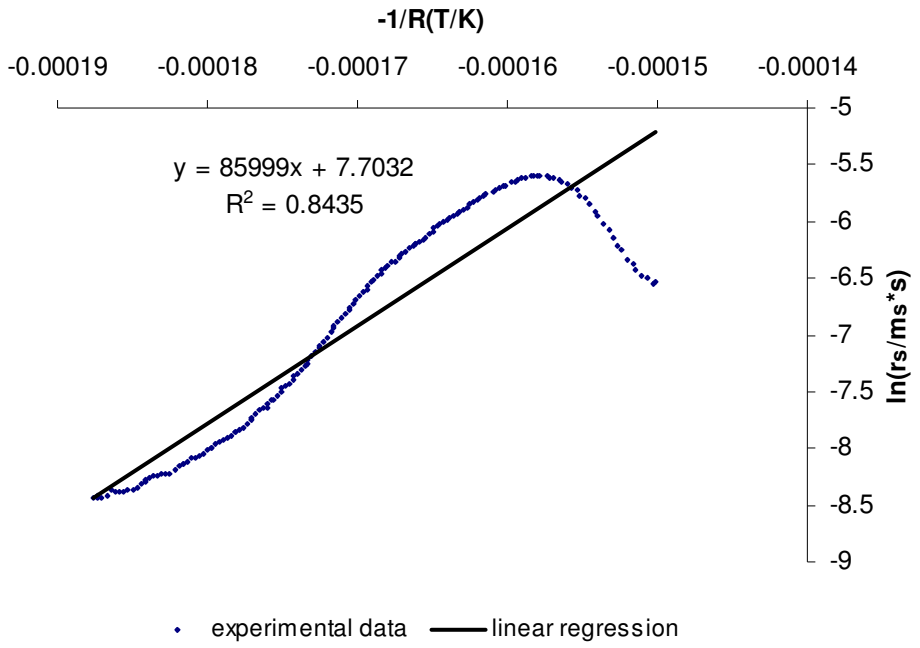

Figure 5.8 Linear regression analysis of the second reaction in test 2 of briquette SRF2 via first order ash rise kinetic model.

Figure 5.9 shows the linear regression of the second thermal decomposition zone in the pyrolytic process of briquette SRF2 in test 2 using the general order constant ash model. In Figure 5.9 (a), the curve started from the bottom right and finished on the left. The reaction order n was the coefficient of the item $\ln m_S$, the activation energy E_a was the coefficient of the item $-\frac{1}{RT}$ and $\ln k_{S,0}$ was the intercept on axis $\ln r_S$. Figure 5.9 shows the linear regression in three-dimension fit the experimental data quite well, and the regression coefficient R^2_2 was 83.9%. The kinetic parameters were $n_2 = 1.7$, $E_{a,2} = 142.6$ kJ/mol and $k_{S,0,2} = 2.21\times10^7$. Similarly in the ash rise model, the kinetic parameters obtained were $n_2 = 1.8$, $E_{a,2} = 142.9$ kJ/mol and $k_{S,0,2} = 1.71\times10^7$, and the regression coefficient R^2_2 was 84.6%.

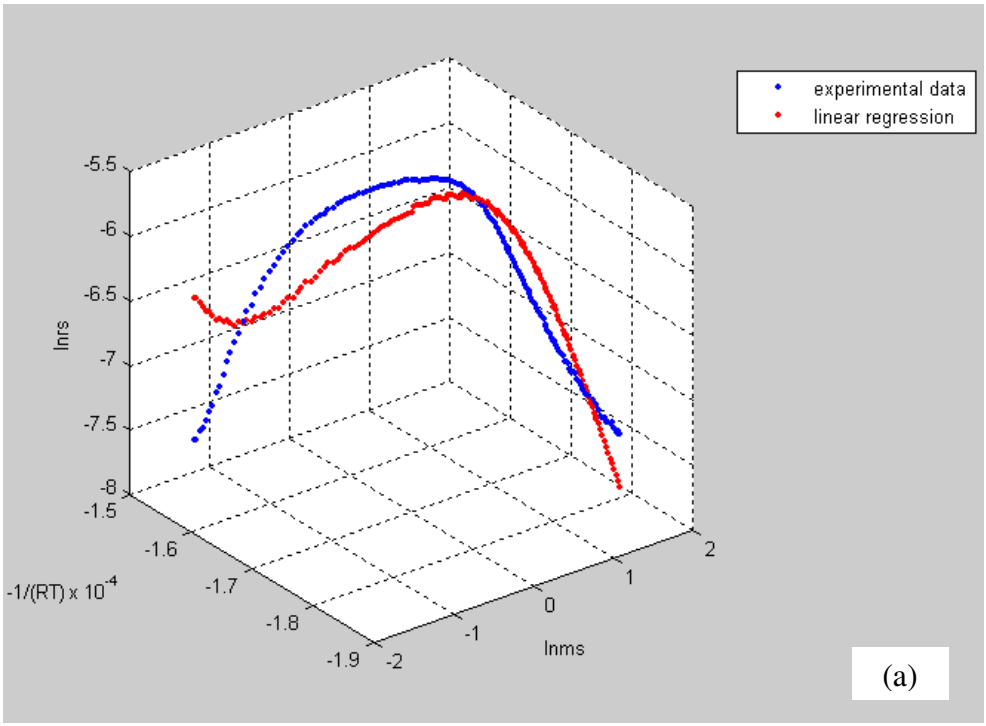

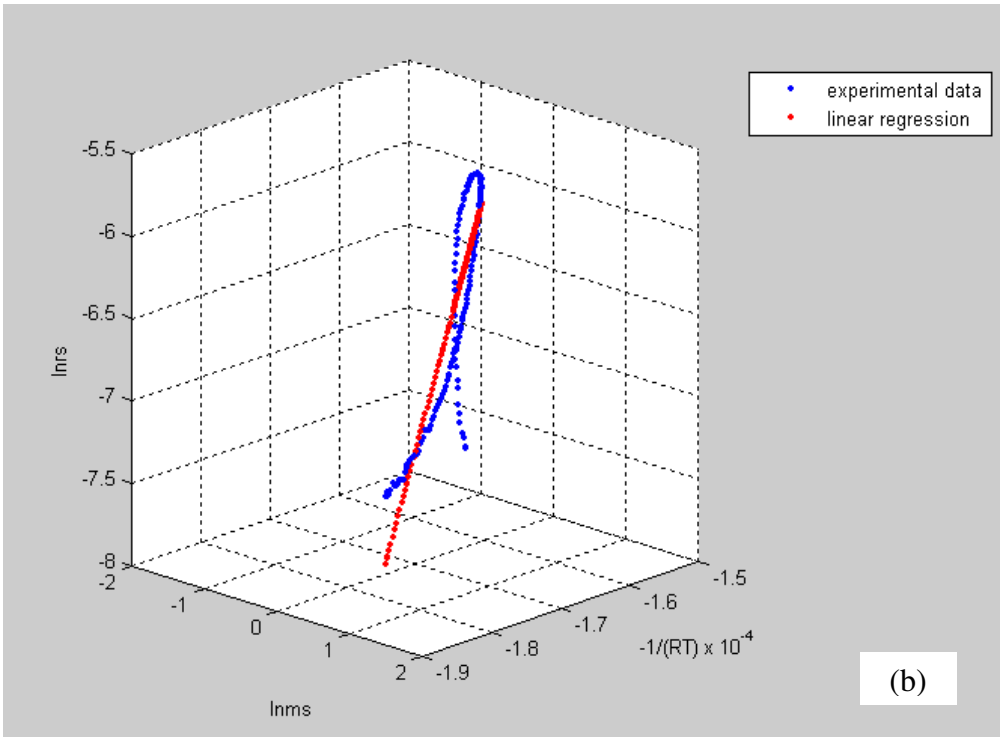

Figure 5.9 Linear regression analysis of the second reaction in test 2 of briquette SRF2 via general order constant ash kinetic model.

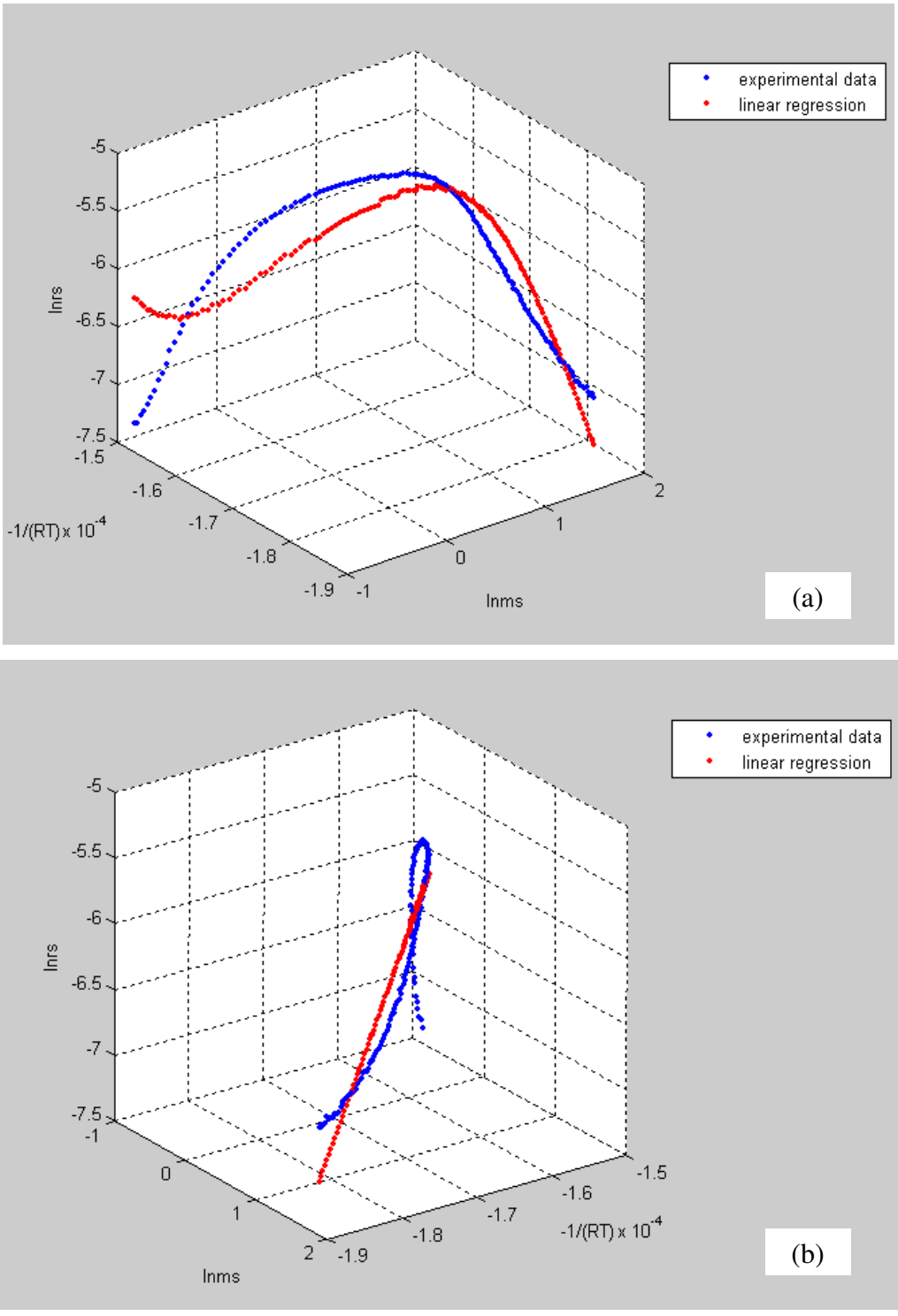

Figure 5.10 Linear regression analysis of the second reaction in test 2 of briquette SRF2 via general order ash rise kinetic model.

Comparing the regression coefficients obtained from the above models, it can be seen again that the general order kinetic models were better than the first order kinetic models, and the ash rise model was better than the constant ash model with a higher regression coefficient.

5.3 Kinetic results

The substantial differences of the kinetic parameters can be observed in literature, which can be due to several factors related to the experimental methods, operating conditions and data analysis, but also to the chemical composition of the raw materials examined in each study [23, 118]. The small contribution of the neighbouring event may also lead to significant errors in the obtained values of the kinetic parameters. This section describes the results of the kinetic parameters obtained from the pyrolysis tests in this research through the general order ash rise kinetic model. Besides kinetic parameters, the peak temperature at which the pyrolytic rate reaches a maximum value on the DTG profile is also presented.

5.3.1 Kinetic results of simulated SRF briquettes

(1) Kinetic results of paper briquette

The DTG profile of the cuboidal paper briquette (0PP) in Figure 4.4 shows one thermal decomposition zone and therefore, the pyrolytic process was treated as one single reaction. Figure 5.11 shows the linear regression analysis, and the results are shown in Table 5.1. In Figure 5.11 (a), the reaction started from the right of the space curve and finished on the left. All space curves were not very linear in three dimensions both in the beginning and in the end of the reaction. This indicated that the neighbouring event effect existed and could lead to errors in the results. The curve in each test was not very close to each other, but the activation energy $E_a = 127$ kJ/mol , the pre-exponential factor $k_{S,0} = 8.7 \times 10^4$ and the reaction order $n_2 = 4.2$ of the pyrolysis of briquette 0PP fell into the range of chemically meaningful values, and the regression coefficient was about 98%. The peak temperature was about 338°C with errors between -9% and 15%.

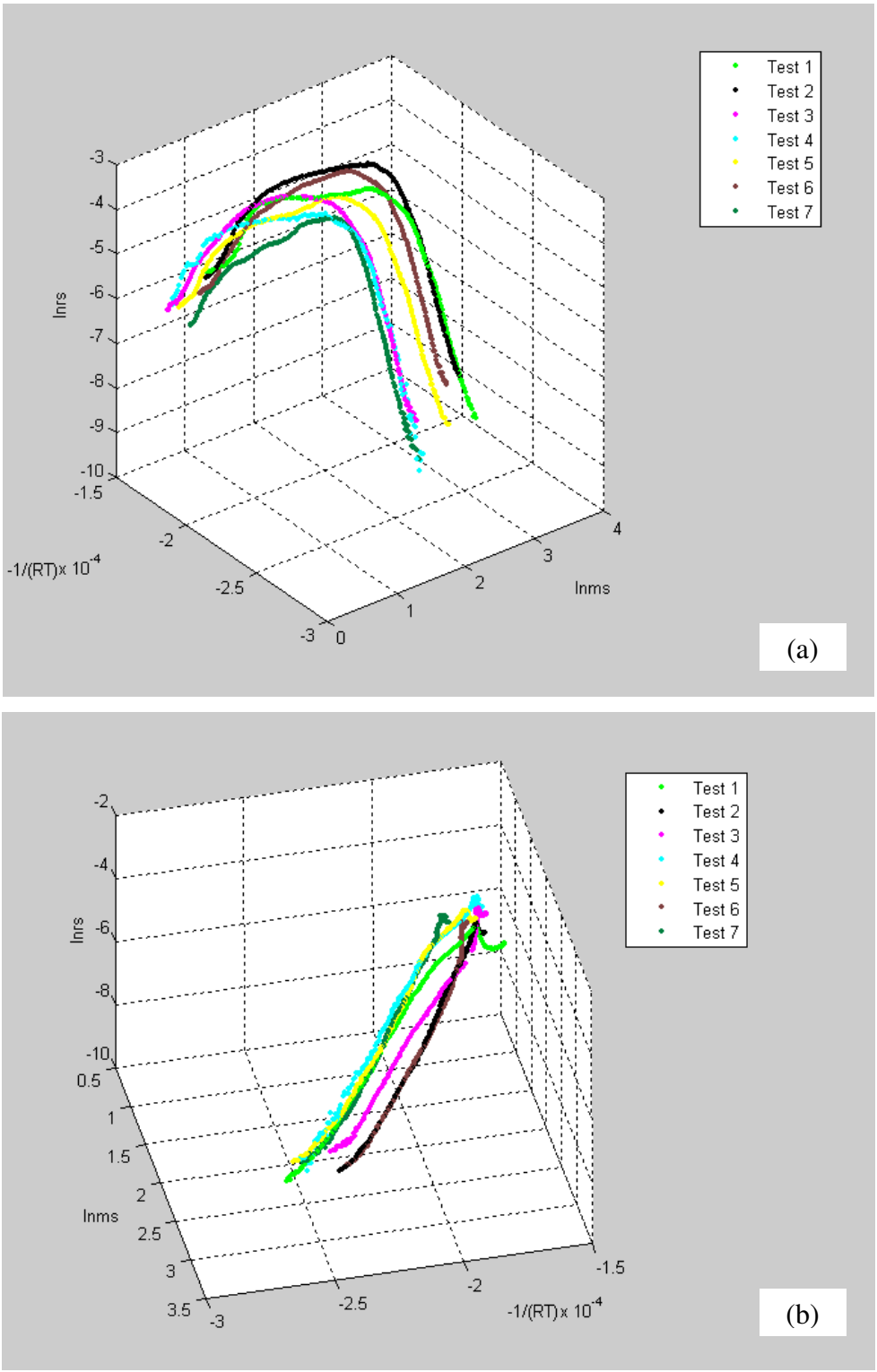

Figure 5.11 Linear regression analysis of the pyrolysis of briquette 0PP.

Table 5.1 Kinetic parameters of briquette 0PP

Test No.	T_p/°C	n	E_a/(kJ/mol)	$k_{S,0}$	R^2
1	306	5.8	128	$2.8\text{x}10^3$	93.2%
2	341	3.8	132	$1.7\text{x}10^5$	98.0%
3	388	3.4	111	$1.1\text{x}10^4$	98.6%
4	328	5.1	136	$2.4\text{x}10^5$	99.1%
5	325	4.4	126	$8.7\text{x}10^4$	96.5%
6	353	3.0	124	$2.9\text{x}10^5$	98.8%
7	323	3.7	131	$1.3\text{x}10^6$	98.9%
Average	*338 (-9%, 15%)*	*4.2*	*127*	*$8.7\text{x}10^4$*	

(2) Kinetic results of briquettes with varying paper/plastic ratios

a. Briquette of 20% PP and 80% paper blend extruded at 125°C (2PP)

Figure 4.11 shows one thermal decomposition zone mainly from hemicellulose and cellulose decomposition and one small thermal decomposition zone mainly from plastic decomposition. The second zone was so small that only the kinetic study of test 3 could be applied. The pyrolytic process was treated as two non-interacting parallel reactions. In tests 1 and 2, two thermal decomposition zones highly overlapped, and therefore the hemicellulose and cellulose decomposition and the plastic decomposition together as well as lignin decomposition were treated as one single reaction. The results of the first and second thermal decomposition zones are shown in Tables 5.2 and 5.3, respectively. When two zones were treated together in tests 1 and 2, the reaction order obtained was smaller than that with the first zone alone, and the activation energy and the pre-exponential factor were significantly small. The results of tests 1 and 2 were only for comparison purpose, and the results of tests 3 – 6 were used for further discussion. The activation energies $E_{a,1} = 109$ kJ/mol and $E_{a,2} = 142$ kJ/mol, the pre-exponential factors $k_{S,0,1} = 3.3\times10^4$ and $k_{S,0,2} = 9.5\times10^6$, and the reaction orders $n_1 = 4.2$ and $n_2 = 2.9$ of the pyrolysis of briquette 2PP fell into the range of chemically meaningful values. The regression coefficient of the second thermal decomposition was lower than that of the first zone. The reaction order of the second zone was smaller than that of the first zone, and both the activation energy and the pre-exponential factor of the second zone were larger than those of the first zone. The peak temperature of the first zone was quite repeatable at 326°C with errors between -3% and 2% and was slightly lower than that of the paper briquette. The peak temperature of the second zone was about 440°C.

Table 5.2 Kinetic parameters of briquette 2PP in the first reaction

Test No.	$T_{p,1}$/°C	n_1	$E_{a,1}$/(kJ/mol)	$k_{S,0,1}$	R^2_1
1	330	2.7	62	3.0	96.9%
2	367	3.1	65	3.3	98.2%
Average	*349 (±5%)*	*2.9*	*64*	*3.2*	
3	330	5.2	107	$1.8\text{x}10^3$	99.8%
4	317	3.8	107	$7.6\text{x}10^4$	97.9%
5	322	3.8	111	$1.4\text{x}10^5$	97.7%
6	333	3.9	112	$6.7\text{x}10^4$	98.5%
Average	*326 (-3%, 2%)*	*4.2*	*109*	*$3.3\text{x}10^4$*	

Table 5.3 Kinetic parameters of briquette 2PP in the second reaction

Test No.	$T_{p,2}$/°C	n_2	$E_{a,2}$/(kJ/mol)	$k_{S,0,2}$	R^2_2
3	440	2.9	142	$9.5\text{x}10^6$	93.6%

b. Briquette of 40% PP and 60% paper blend extruded at 125°C (4PP)

The DTG profile of briquette 4PP in Figure 4.12 shows two thermal decomposition zones and therefore, the pyrolytic process was treated as two non-interacting parallel reactions. Figure 5.12 shows the linear regression analysis of the first thermal decomposition zone which was mainly associated with hemicellulose and cellulose decomposition. In Figure 5.12 (a), the reaction started from the right and finished on the left. The curves were not very linear in the beginning due to the effect of the neighbouring event. Results are shown in Table 5.4 and the kinetic parameters $n_1 = 5.1$, $E_{a,1}$ = 96 kJ/mol and $k_{S,0,1} = 1.3\times10^2$ fell into the range of chemically meaningful values with very good regression coefficient of over 99%. The peak temperature of the first zone was quite repeatable at about 337°C with errors between -3% and 9% and was similar to that of the paper briquette.

Table 5.4 Kinetic parameters of briquette 4PP in the first reaction

Test No.	$T_{p,1}$/°C	n_1	$E_{a,1}$/(kJ/mol)	$k_{S,0,1}$	R^2_1
1	368	5.3	97	93	99.5%
2	337	4.0	79	17	99.3%
3	330	5.4	93	41	99.7%
4	326	3.9	87	$3.0\text{x}10^2$	99.2%
5	326	6.8	125	$2.1\text{x}10^3$	99.3%
Average	*337 (-3%, 9%)*	*5.1*	*96*	*$1.3\text{x}10^2$*	

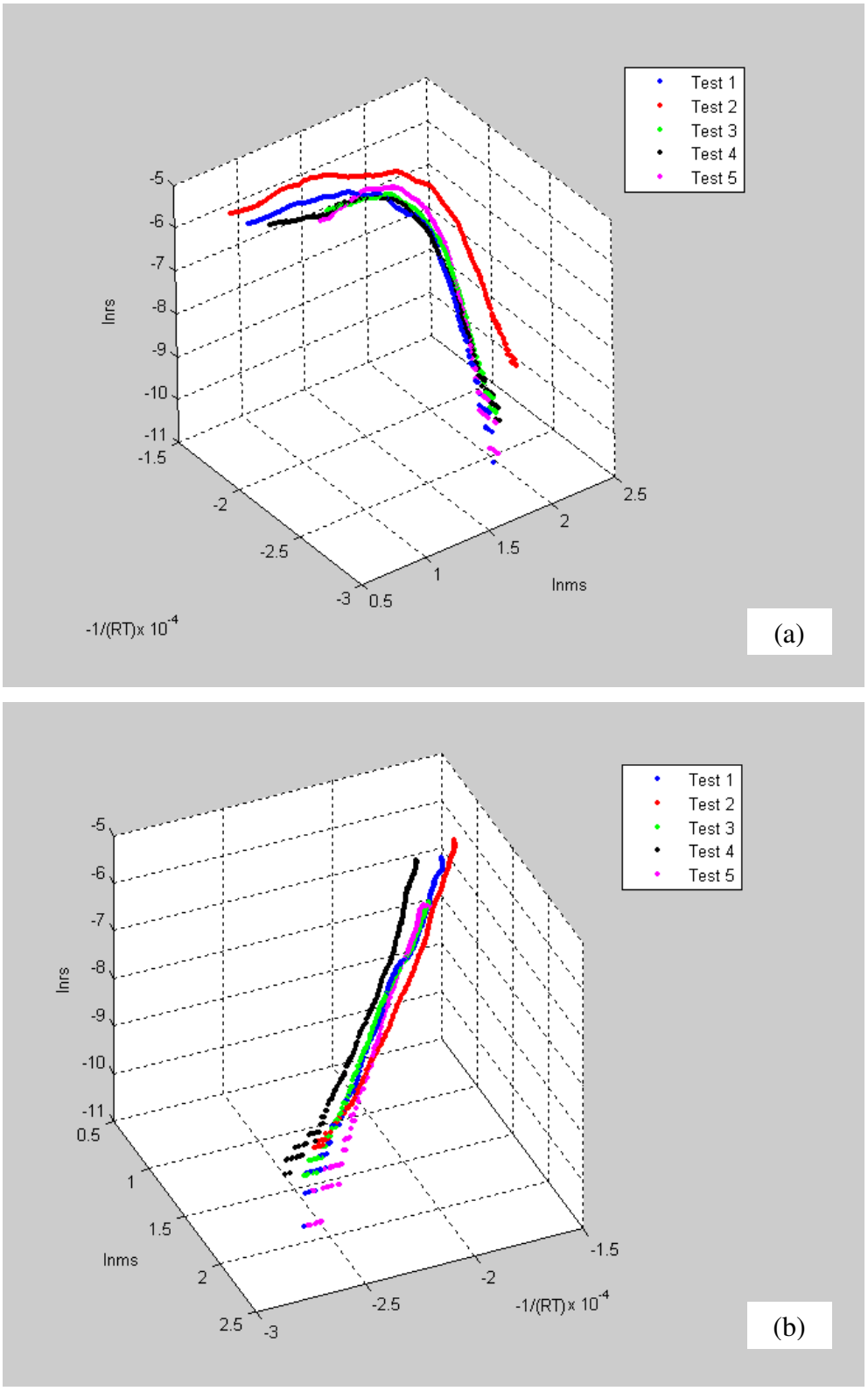

Figure 5.12 Linear regression analysis of the first reaction of briquette 4PP.

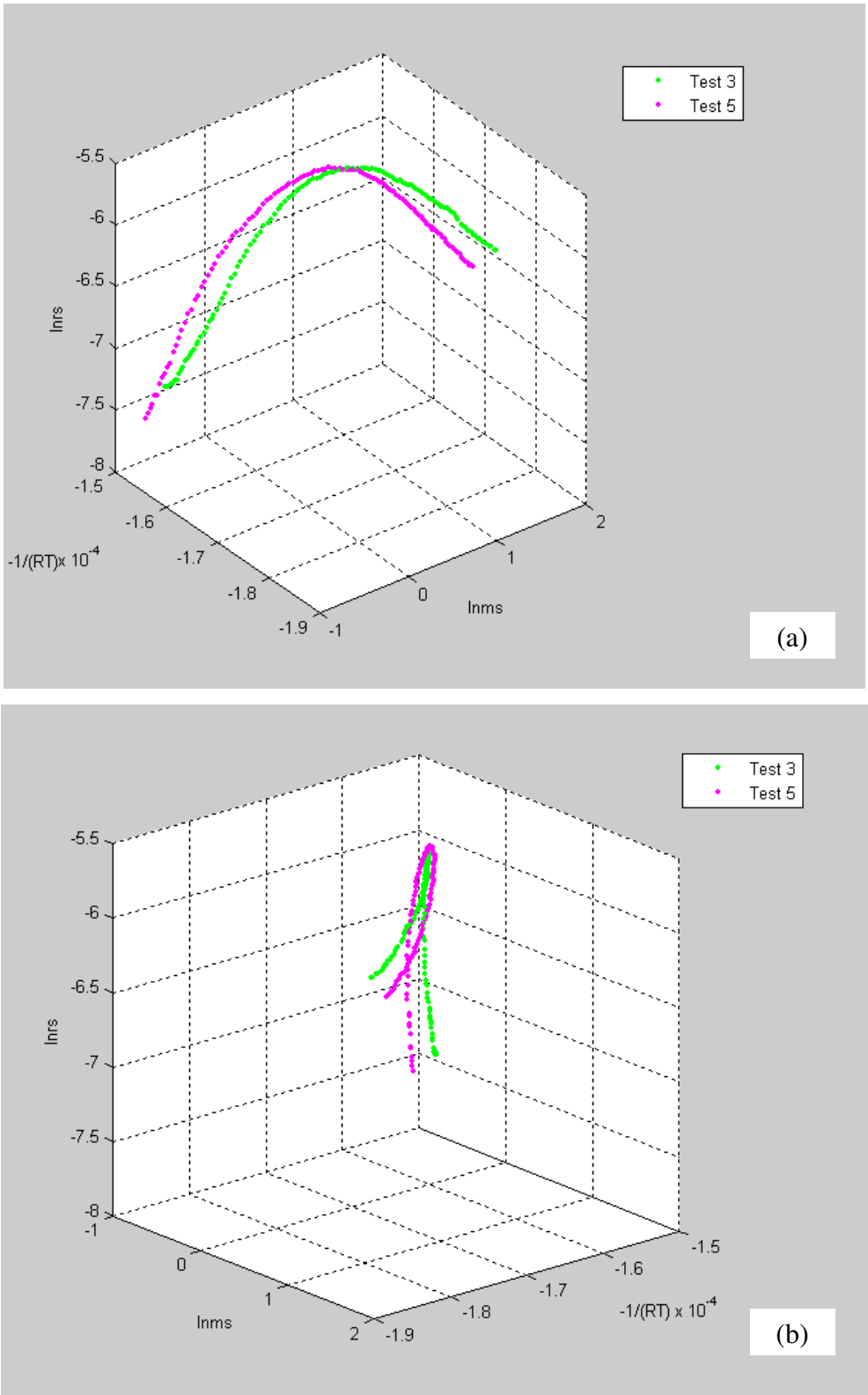

Figure 5.13 Linear regression analysis of the second reaction of briquette 4PP.

Since the second thermal decomposition zone of tests 1, 2 and 4 was not clear in Figure 4.12, only the data from tests 3 and 5 were used to obtain the kinetic parameters of the second thermal decomposition zone. Figure 5.13 shows the linear

regression analysis of the second thermal decomposition zone which was mainly associated with plastic decomposition. Results are shown in Table 5.5 and the kinetic parameters $n_2 = 2.6$, $E_{a,2} = 166$ kJ/mol and $k_{S,0,2} = 7.1\times10^8$ fell into the range of chemically meaningful values. The regression coefficient was 87%, lower than the first thermal decomposition zone. This was mainly due to the existence of lignin decomposition. The effect of the neighbouring event on the second thermal decomposition zone can also be observed in Figure 5.13 (b). The reaction order of the second zone was smaller than that of the first zone, and both the activation energy and the pre-exponential factor of the second zone were larger than those of the first zone. The peak temperature of the second zone was about 448°C with errors of ±1%.

Table 5.5 Kinetic parameters of briquette 4PP in the second reaction

Test No.	$T_{p,2}$/°C	n_2	$E_{a,2}$/(kJ/mol)	$k_{S,0,2}$	R^2_2
3	442	2.8	155	9.6x10^7	87.7%
5	454	2.5	177	5.2x10^9	87.0%
Average	*448 (±1%)*	*2.6*	*166*	*7.1x10^8*	

c. Briquette of 60% PP and 40% paper blend extruded at 125°C (6PPa)

The DTG profile of briquette 4PP in Figure 4.13 shows two thermal decomposition zones and therefore, the pyrolytic process was treated as two non-interacting parallel reactions. The results of the first zone are shown in Table 5.6 and the kinetic parameters $n_1 = 8.2$, $E_{a,1} = 121$ kJ/mol and $k_{S,0,1} = 1.6\times10^2$ fell into the range of chemically meaningful values with very good regression coefficient of 99.5%. The peak temperature of the first zone was about 336°C with errors of ±3%.

Table 5.6 Kinetic parameters of briquette 6PPa in the first reaction

Test No.	$T_{p,1}$/°C	n_1	$E_{a,1}$/(kJ/mol)	$k_{S,0,1}$	R^2_1
1	330	7.0	120	1.3x10^3	99.5%
2	326	10.2	133	1.3x10^2	99.3%
3	345	7.5	106	13	99.6%
4	341	8.1	127	3.6x10^2	99.5%
Average	*336 (±3%)*	*8.2*	*121*	*1.6x10^2*	

The results of the second zone are shown in Table 5.7. The result of test 1 was removed due to the unmeaning values of the activation energy of -200 kJ/mol and the

reaction order of -2.5. The results from other tests $n_2 = 2.5$, $E_{a,2} = 141$ kJ/mol and $k_{S,0,2} = 1.0 \times 10^7$ fell into the range of chemically meaningful values, and the regression coefficient was about 81%, lower than the first zone. The low regression coefficient value was mainly due to the existence of lignin decomposition. The reaction order of the second zone was smaller than that of the first zone, and the activation energy and the pre-exponential factor of the second zone were larger than those of the first zone. The peak temperature of the second zone was about 451°C with errors between -1% and 2%.

Table 5.7 Kinetic parameters of briquette 6PPa in the second reaction

Test No.	$T_{p,2}$/°C	n_2	$E_{a,2}$/(kJ/mol)	$k_{S,0,2}$	R^2_2
2	445	2.5	126	9.7×10^5	78.8%
3	460	2.5	147	2.2×10^7	82.7%
4	448	2.4	150	5.1×10^7	81.4%
Average	*451 (-1%, 2%)*	*2.5*	*141*	*1.0×10^7*	

(3) Kinetic results of briquettes with varying extruding temperatures

a. Briquette of 60% PP and 40% paper blend extruded at 125°C (6PPa)

The results have been shown in Tables 5.6 and 5.7.

b. Briquette of 60% PP and 40% paper blend extruded at 150°C (6PPb)

The results of the first and the second thermal decomposition zones are shown in Tables 5.8 and 5.9, respectively, and the kinetic parameters $n_1 = 13.4$, $n_2 = 1.5$, $E_{a,1} = 137$ kJ/mol, $E_{a,2} = 117$ kJ/mol, $k_{S,0,1} = 0.24$ and $k_{S,0,2} = 3.5 \times 10^5$ fell into the range of chemically meaningful values. The regression coefficient of the first zone was over 99%. However, the second zone had a quite low regression coefficient. The reaction order and the activation energy of the second zone were lower than those of the first zone, and the pre-exponential factor of the second zone was larger than that of the first zone. The peak temperatures of these two zones were quite repeatable at about 318°C with errors between -5% and 4% and 457°C with errors between -1% and 2%, respectively.

Table 5.8 Kinetic parameters of briquette 6PPb in the first reaction

Test No.	$T_{p,1}$/°C	n_1	$E_{a,1}$/(kJ/mol)	$k_{S,0,1}$	R^2_1
1	329	9.4	132	84	99.6%
2	328	12.0	128	0.39	99.4%
3	307	21.0	159	$8.5\text{x}10^{-5}$	99.3%
4	301	12.9	142	1.6	97.7%
5	324	11.6	122	0.20	99.6%
Average	*318 (-5%, 4%)*	*13.4*	*137*	*0.24*	

Table 5.9 Kinetic parameters of briquette 6PPb in the second reaction

Test No.	$T_{p,2}$/°C	n_2	$E_{a,2}$/(kJ/mol)	$k_{S,0,2}$	R^2_2
1	457	1.2	72	$2.1\text{ x}10^{2}$	58.3%
2	464	1.6	139	$9.7\text{x}10^{6}$	59.2%
3	457	1.4	119	$6.6\text{x}10^{5}$	81.2%
4	454	1.3	89	$3.5\text{x}10^{3}$	69.2%
5	452	2.1	166	$1.1\text{x}10^{9}$	85.5%
Average	*457 (-1%, 2%)*	*1.5*	*117*	*3.5x10^{5}*	

c. Briquette of 60% PP and 40% paper blend extruded at 200°C (6PPc)

The results of the first and the second thermal decomposition zones are shown in Tables 5.10 and 5.11, respectively. $n_1 = 7.6$, $n_2 = 2.5$, $E_{a,1} = 119$ kJ/mol , $E_{a,2} = 167$ kJ/mol , $k_{S,0,1} = 1.8\times10^{2}$ and $k_{S,0,2} = 9.4\times10^{8}$. Compared to the pyrolysis tests of the other samples, the regression coefficient of the second zone of briquette 6PPc was quite good, about 92%. The reaction order of the second zone was lower than that of the first zone, and both the activation energy and the pre-exponential factor of the second zone were larger than those of the first zone. The peak temperatures of these two zones were quite repeatable at about 336°C with errors between -2% and 3% and 447°C with errors of ±1%, respectively.

Table 5.10 Kinetic parameters of briquette 6PPc in the first reaction

Test No.	$T_{p,1}$/°C	n_1	$E_{a,1}$/(kJ/mol)	$k_{S,0,1}$	R^2_1
1	336	7.3	113	76	98.7%
2	328	6.7	122	$2.0\text{x}10^{3}$	99.5%
3	348	10.4	131	29	99.4%
4	333	6.1	109	$2.6\text{x}10^{2}$	99.5%
Average	*336 (-2%, 3%)*	*7.6*	*119*	*1.8x10^{2}*	

Table 5.11 Kinetic parameters of briquette 6PPc in the second reaction

Test No.	$T_{p,2}$/°C	n_2	$E_{a,2}$/(kJ/mol)	$k_{S,0,2}$	R^2_2
1	443	2.6	176	$4.5\text{x}10^9$	92.4%
2	453	2.5	161	$2.7\text{x}10^8$	84.8%
3	448	2.4	171	$2.4\text{x}10^9$	92.9%
4	443	2.3	158	$2.6\text{x}10^8$	96.9%
Average	*447 (±1%)*	*2.5*	*167*	*$9.4\text{x}10^8$*	

d. Briquette of 60% PP and 40% paper blend extruded at 250°C (6PPd)

The results of the first and the second thermal decomposition zones are shown in Tables 5.12 and 5.13, respectively. $n_1 = 5.5$, $n_2 = 2.5$, $E_{a,1} = 105$ kJ/mol , $E_{a,2} = 188$ kJ/mol , $k_{S,0,1} = 1.8\times10^3$ and $k_{S,0,2} = 8.7\times10^{10}$. The regression coefficient of the second zone was about 94%, even better than that of briquette 6PPc. When the extruding temperature increases, it could destroy the chemical structure of lignocellulosic materials and reduce the lignin content. As discussed earlier, the existence of lignin decomposition could lower the regression coefficient of the second zone. Therefore, the regression coefficient of the second zone would increase when the extruding temperature increases. Tables 5.12 and 5.13 show that the reaction order of the second zone was lower than that of the first zone, and the activation energy and the pre-exponential factor of the second zone were larger than those of the first zone. The peak temperatures of these two zones were quite repeatable at about 355°C with errors of ±4% and 442°C with errors of 1%, respectively.

Table 5.12 Kinetic parameters of briquette 6PPd in the first reaction

Test No.	$T_{p,1}$/°C	n_1	$E_{a,1}$/(kJ/mol)	$k_{S,0,1}$	R^2_1
1	367	5.8	107	$9.3\text{x}10^2$	99.5%
2	345	4.5	97	$1.3\text{x}10^3$	99.5%
3	354	4.7	89	$1.1\text{x}10^2$	99.0%
4	368	5.5	110	$7.5\text{x}10^3$	99.5%
5	342	6.9	124	$1.9\text{x}10^4$	99.2%
Average	*355 (±4%)*	*5.5*	*105*	*$1.8\text{x}10^3$*	

Table 5.13 Kinetic parameters of briquette 6PPd in the second reaction

Test No.	$T_{p,2}$/°C	n_2	$E_{a,2}$/(kJ/mol)	$k_{S,0,2}$	R^2_2
1	440	2.7	218	$1.1x10^{13}$	98.4%
2	446	2.2	122	$9.5x10^{5}$	80.7%
3	441	1.9	152	$2.6x10^{8}$	99.4%
4	442	3.2	237	$4.4x10^{14}$	94.4%
5	442	2.6	209	$4.2x10^{12}$	95.6%
Average	*442 (0%, 1%)*	*2.5*	*188*	$8.7x10^{10}$	

(4) Summary

The general order ash rise kinetic model with two non-interacting parallel reactions was applied to the pyrolytic kinetic study of the simulated SRF briquettes. The first reaction was mainly associated with the pyrolysis of hemicellulose and cellulose. The peak temperature of the first reaction was quite constant at about 335°C. The peak temperature of the paper briquette pyrolysis was less repeatable than that of the pyrolysis of the paper and plastic blend briquettes. The second reaction was mainly associated with the pyrolysis of plastic. The peak temperature of the second reaction was quite constant at about 448°C. The small and slow pyrolytic process of lignin was associated with both reactions, especially in the second reaction where the regression coefficient was lower than that of the first reaction. The neighbouring event effect existed both in the beginning and in the end of each reaction and led to errors in the results. When these two reactions were treated together as one single reaction, the reaction order, the activation energy and the pre-exponential factor were lower than those of the first reaction alone.

The DTG profiles of the simulated SRF briquettes show that there was no interaction between the pyrolysis of hemicellulose and cellulose and the pyrolysis of plastic. Both reactions were independent of each other and had their own kinetic parameters. The kinetic parameters varied with the composition and the extruding temperature of the briquettes. The above kinetic results of the simulated SRF briquettes are summarised in Table 5.14.

The reaction order of the first reaction was higher than that of the second reaction. The pre-exponential factor of the first reaction was considerably smaller than that of the second reaction. Except briquette 6PPb, the activation energy of the first reaction

was lower than that of the second reaction. The low activation energy of the second reaction of briquette 6PPb could be due to the effect of the low activation energy of lignin pyrolysis. In the pyrolysis tests of briquette 6PPb, the regression coefficient of the second reaction was quite low, and it could be due to the existence of lignin pyrolysis.

Table 5.14 Kinetic parameters of simulated SRF briquettes

Sample	$T_{p,1}$/ °C	n_1	$E_{a,1}$/ (kJ/mol)	$k_{S,0,1}$	$T_{p,2}$/ °C	n_2	$E_{a,2}$/ (kJ/mol)	$k_{S,0,1}$
0PP	338	4.2	127	$8.7x10^4$	/	/	/	/
2PP	326	4.2	109	$3.3x10^4$	440	2.9	142	$9.5x10^6$
4PP	337	5.1	96	$1.3x10^2$	448	2.6	166	$7.1x10^8$
6PPa	336	8.2	121	$1.6x10^2$	451	2.5	141	$1.0x10^7$
6PPb	318	13.4	137	0.24	457	1.5	117	$3.5x10^5$
6PPc	336	7.6	119	$1.8x10^2$	447	2.5	167	$9.4x10^8$
6PPd	355	5.5	105	$1.8x10^3$	442	2.5	188	$8.7x10^{10}$

Table 5.14 shows the following conclusions with which the kinetic parameters of briquettes 6PPa and 6PPb did not comply very well and will be discussed with the kinetic parameters of the SRF briquettes in Section 5.3.2. In the first reaction, when the ratio of plastic/paper increased, the reaction order increased, the activation energy decreased, and the pre-exponential factor decreased. Also in the first reaction, when the extruding temperature increased, the reaction order decreased, the activation energy decreased, and the pre-exponential factor increased. The reaction order of the second reaction was quite constant. In the second reaction, when the ratio of plastic/paper increased, both the activation energy and the pre-exponential factor increased. Also in the second reaction, when the extruding temperature increased, both the activation energy and the pre-exponential factor increased.

5.3.2 Kinetic results of SRF briquettes

(1) Kinetic results of ecodeco briquettes with varying extruding temperatures

a. Ecodeco briquette extruded at 125°C

The results of single briquette segment tests 5 – 8 were studied. The results of the first and the second thermal decomposition zones are shown in Tables 5.15 and 5.16, respectively, and the kinetic parameters $n_1 = 5.9$, $n_2 = 2.0$, $E_{a,1} = 92$ kJ/mol ,

$E_{a,2} = 112$ kJ/mol, $k_{S,0,1} = 74$ and $k_{S,0,2} = 1.1\times10^5$ fell into the range of chemically meaningful values. The regression coefficient of the second thermal decomposition was quite low. The reaction order of the second zone was lower than that of the first zone, and both the activation energy and the pre-exponential factor of the second zone were larger than those of the first zone. The peak temperatures of these two zones were quite repeatable at about 304°C with errors of ±1% and 447°C with errors of ±1%, respectively. The peak temperature of the first zone of briquette SRF1 was lower than that of the paper briquette. This was the effect of the inorganic component. The peak temperature of the second zone of briquette SRF1 was very close to that of the second zone of the simulated SRF briquettes, and this indicated that the plastic component in the ecodeco material was similar to PP.

Table 5.15 Kinetic parameters of briquette SRF1 in the first reaction

Test No.	$T_{p,1}$/°C	n_1	$E_{a,1}$/(kJ/mol)	$k_{S,0,1}$	R^2_1
5	308	6.3	89	3.2	98.3%
6	302	4.9	92	$2.6\text{x}10^2$	96.1%
7	305	7.1	111	$9.3\text{x}10^2$	98.3%
8	302	5.1	76	38	96.2%
Average	*304 (±1%)*	*5.9*	*92*	*74*	

Table 5.16 Kinetic parameters of briquette SRF1 in the second reaction

Test No.	$T_{p,2}$/°C	n_2	$E_{a,2}$/(kJ/mol)	$k_{S,0,2}$	R^2_2
5	450	2.5	124	$3.6\text{x}10^5$	76.6%
6	442	2.3	124	$9.9\text{x}10^5$	88.4%
7	442	1.8	109	$8.7\text{x}10^4$	77.8%
8	453	1.5	90	$4.3\text{x}10^3$	77.0%
Average	*447 (±1%)*	*2.0*	*112*	*$1.1\text{x}10^5$*	

b. Ecodeco briquette extruded at 150°C

The results of single briquette segment tests 2 – 6 were studied. The results of the first and the second thermal decomposition zones are shown in Tables 5.17 and 5.18, respectively, and the kinetic parameters $n_1 = 10.4$, $n_2 = 1.9$, $E_{a,1} = 109$ kJ/mol, $E_{a,2} = 132$ kJ/mol, $k_{S,0,1} = 0.14$ and $k_{S,0,2} = 3.0\times10^6$ fell into the range of chemically meaningful values. The regression coefficient of the second zone was quite low. The reaction order of the second zone was lower than that of the first zone, and both the activation energy and the pre-exponential factor of the second zone were larger than

those of the first zone. The peak temperatures of these two zones were quite repeatable at about 298°C with errors between -4% and 3% and 445°C with errors of ±2%, respectively. The peak temperature of the first zone of briquette SRF2 was lower than that of the paper briquette. This was the effect of the inorganic component. Similar to briquette SRF1, the peak temperature of the second zone of briquette SRF2 was very close to that of the second zone of briquette SRF1, and this indicated that the extruding temperature didn't affect the peak temperature of plastic pyrolysis.

Table 5.17 Kinetic parameters of briquette SRF2 in the first reaction

Test No.	$T_{p,1}$/°C	n_1	$E_{a,1}$/(kJ/mol)	$k_{S,0,1}$	R^2_1
2	286	14.3	129	$4.4\text{x}10^{-3}$	98.0%
3	308	8.4	98	0.95	97.3%
4	303	9.8	105	0.23	97.8%
5	301	6.5	91	2.8	98.8%
6	290	13.2	122	$2.0\text{x}10^{-2}$	97.1%
Average	*298 (-4%, 3%)*	*10.4*	*109*	*0.14*	

Table 5.18 Kinetic parameters of briquette SRF2 in the second reaction

Test No.	$T_{p,2}$/°C	n_2	$E_{a,2}$/(kJ/mol)	$k_{S,0,2}$	R^2_2
2	450	1.8	143	$1.7\text{x}10^{7}$	84.6%
3	455	1.5	99	$1.4\text{x}10^{4}$	74.1%
4	441	1.9	145	$2.3\text{x}10^{7}$	82.3%
5	442	2.2	133	$2.7\text{x}10^{6}$	82.6%
6	437	1.8	141	$1.6\text{x}10^{7}$	80.8%
Average	*445 (±2%)*	*1.9*	*132*	*$3.0\text{x}10^{6}$*	

(2) Kinetic results of briquettes of ecodeco, sawdust and plastic blend

The results of the 80% ecodeco and 20% sawdust blend briquette (SRF3) and the 65% ecodeco, 10% sawdust, 15% paper and 10% PE blend briquette (SRF4) are shown in Tables 5.19 and 5.20. Since briquette SRF3 contained 20% sawdust which had a high lignin content and the activation energy of lignin pyrolysis was very low, therefore the activation energy in both zones of the pyrolysis of briquette SRF3 was quite low, especially in the second zone. Same as the other briquettes, the reaction order of briquettes SRF3 and SRF4 in the second zone was lower than that in the first zone. The peak temperature of the first zone of briquettes SRF3 and SRF4 was lower than that of the paper briquette due to the effect of inorganic component. The peak temperature of the second zone of briquettes SRF3 and SRF4 was higher than that of

the second zone of the simulated SRF briquettes, and this indicated that the peak temperature of PE content in briquettes SRF3 and SRF4 is higher than that of PP.

Table 5.19 Kinetic parameters of briquettes SRF3 & SRF4 in the first reaction

Sample	$T_{p,1}$/°C	n_1	$E_{a,1}$/(kJ/mol)	$k_{S,0,1}$	R^2_1
SRF3	302	7.7	89	$7.1\text{x}10^{-3}$	99.4%
SRF4	300	9.0	100	$5.0\text{x}10^{-3}$	98.8%

Table 5.20 Kinetic parameters of briquettes SRF3 & SRF4 in the second reaction

Sample	$T_{p,2}$/°C	n_2	$E_{a,2}$/(kJ/mol)	$k_{S,0,2}$	R^2_2
SRF3	462	1.9	72	37	65.5%
SRF4	475	1.6	106	$2.5\text{x}10^{4}$	48.9%

(3) Kinetic results of RDF briquette and MBT processed RDF briquette

The DTG profile of the RDF briquette (SRF5) in Figure 4.34 shows that two thermal decomposition zones highly overlapped, and only one zone was presented. Therefore, the pyrolytic process of briquette SRF5 was treated as one reaction, and the reaction order and the activation energy of the pyrolysis of briquette SRF5 were very low. The DTG profile of the MBT processed RDF briquette (SRF6) in Figure 4.34 shows two thermal decomposition zones and therefore, the pyrolytic process of briquette SRF6 was treated as two non-interacting parallel reactions. The results of briquettes SRF5 and SRF6 are shown in Tables 5.21 and 5.22. Both the reaction order and the activation energy of the second zone of briquette SRF6 were lower than those of the first zone, and the pre-exponential factor of the second zone was larger than that of the first zone.

Table 5.21 Kinetic parameters of briquettes SRF5 & SRF6 in the first reaction

Sample	$T_{p,1}$/°C	n_1	$E_{a,1}$/(kJ/mol)	$k_{S,0,1}$	R^2_1
SRF5	338	1.4	30	0.13	95.0%
SRF6	311	6.1	74	$1.1\text{x}10^{-2}$	98.3%

Table 5.22 Kinetic parameters of briquette SRF6 in the second reaction

Sample	$T_{p,2}$/°C	n_2	$E_{a,2}$/(kJ/mol)	$k_{S,0,2}$	R^2_2
SRF6	470	1.3	45	0.78	49.1%

(4) Kinetic results of other SRF briquettes

The DTG profile of the raw MSW briquette (SRF7) in Figure 4.37 shows that two thermal decomposition zones highly overlapped. The DTG profile of the 50% standard dried sewage sludge and 50% tar blend briquette (SRF9) shows that only one thermal decomposition zone was presented. Therefore, the pyrolytic processes of briquettes SRF7 and SRF9 were treated as one reaction. The DTG profile of the RDF and molasses blend briquette (SRF8) in Figure 4.37 shows two thermal decomposition zones and therefore, the pyrolytic process of briquette SRF8 was treated as two non-interacting parallel reactions. The results of briquettes SRF7, SRF8 and SRF9 are shown in Tables 5.23 and 5.24. The reaction order of the single reaction of briquettes SRF7 and SRF9 was not very small, but the activation energy was quite low. The activation energy and the pre-exponential factor of the second zone of briquette SRF8 were larger than those of the first zone. However, different from most of the other briquettes, the reaction order of the second zone of briquette SRF8 was higher than that of the first zone.

Table 5.23 Kinetic parameters of briquettes SRF7, SRF8 & SRF9 in the first reaction

Sample	$T_{p,1}$/°C	n_1	$E_{a,1}$/(kJ/mol)	$k_{S,0,1}$	R^2_1
SRF7	319	3.5	52	0.16	94.6%
SRF8	331	6.1	92	0.31	98.8%
SRF9	264	3.1	41	$4.0\text{x}10^{-2}$	93.7%

Table 5.24 Kinetic parameters of briquette SRF8 in the second reaction

Sample	$T_{p,2}$/°C	n_2	$E_{a,2}$/(kJ/mol)	$k_{S,0,2}$	R^2_2
SRF8	458	8.5	260	$9.0\text{x}10^{9}$	98.9%

(5) Summary

The general order ash rise kinetic model with two non-interacting parallel reactions was applied to the pyrolytic kinetic study of the SRF briquettes. The first reaction was mainly associated with the pyrolysis of hemicellulose and cellulose. The second reaction was mainly associated with the pyrolysis of plastic. The pyrolysis of lignin was associated with both reactions, especially in the second reaction where the regression coefficient was lower than that in the first reaction. When two thermal decomposition zones overlapped, the pyrolytic process was treated as one single

reaction. The reaction order, the activation energy and the pre-exponential factor of the single reaction were lower than those of the first reaction alone. For the 50% standard dried sewage sludge and 50% tar blend briquette (SRF9) the reaction was mainly associated with the pyrolysis of volatiles lighter than cellulose.

The DTG profiles show that there was no interaction between the pyrolysis of hemicellulose and cellulose and the pyrolysis of plastic. Both reactions were independent of each other and had their own kinetic parameters. The kinetic parameters varied with the briquette composition and the briquetting process. The above kinetic results of the SRF briquettes are summarised in Table 5.25.

Table 5.25 Kinetic parameters of SRF briquettes

Sample	$T_{p,1}$/ °C	n_1	$E_{a,1}$/ (kJ/mol)	$k_{S,0,1}$	$T_{p,2}$/ °C	n_2	$E_{a,2}$/ (kJ/mol)	$k_{S,0,1}$
SRF1	304	5.9	92	74	447	2.0	112	$1.1x10^{5}$
SRF2	298	10.4	109	0.14	445	1.9	132	$3.0x10^{6}$
SRF3	302	7.7	89	$7.1x10^{-3}$	462	1.9	72	37
SRF4	300	9.0	100	$5.0x10^{-3}$	475	1.6	106	$2.5x10^{4}$
SRF5	338	1.4	30	0.13	/	/	/	/
SRF6	311	6.1	74	$1.1x10^{-2}$	470	1.3	45	0.78
SRF7	319	3.5	52	0.16	/	/	/	/
SRF8	331	6.1	92	0.31	458	8.5	260	$9.0x10^{9}$
SRF9	264	3.1	42	$4.0x10^{-2}$	/	/	/	/

The peak temperature of the first reaction of the most of the SRF briquettes was lower than that of the paper briquette. However, the peak temperature of the second reaction of the SRF briquettes was not quite constant and most of the briquettes had a higher peak temperature of the second reaction than the simulated SRF briquettes. Since the SRF briquettes contained different types of plastics, this indicated that the pyrolytic behaviours of different types of plastics were similar, but had slightly different peak temperatures. PP pyrolysed at a lower temperature than PE. Table 5.25 shows the reaction order of the first reaction was higher than that of the second reaction, except the RDF and molasses blend briquette (SRF8). The pre-exponential factor of the first reaction was considerably smaller than that of the second reaction. The activation energy of the first reaction was lower than that of the second reaction, except the 80% ecodeco and 20% sawdust blend briquette (SRF3) and the MBT processed RDF briquette (SRF6). These are further discussed with lignin pyrolysis in Section 5.3.4.

The results of the simulated SRF briquettes (6PPa and 6PPb) in Table 5.14 and the results of the SRF briquettes (SRF1 and SRF2) in Table 5.25 show when the extruding temperature increased from 125°C to 150°C, both the reaction order and the activation energy of the first reaction increased, and the peak temperature and the pre-exponential factor of the first reaction decreased. This could be explained by the physical properties of the briquettes, as 150°C was the optimum extruding temperature to produce uniform SRF briquettes as discussed in Chapter Four. Table 5.14 shows that when the extruding temperature increased from 150°C to higher temperature, both the reaction order and the activation energy of the first reaction decreased, and the peak temperature and the pre-exponential factor of the first reaction increased.

As the simple calculation in Chapter Four shows briquette SRF4 contained a higher plastic content and a lower ash content than briquette SRF3, the results of briquettes SRF3 and SRF4 could show that more plastic and less ash in the briquette would increase the activation energy of both reactions. The results of briquettes SRF5 and SRF7 show that in the pyrolysis of the briquettes made from raw waste materials, two reactions overlapped and the pyrolytic process was treated as one single reaction with a low reaction order and a low activation energy. The results of briquettes SRF6 and SRF8 show that the pyrolysis of the briquettes made from waste materials either through an MBT process or blended with a binder could present two thermal decomposition zones in the DTG profile and the kinetic results of both reactions fell into the range of chemically meaningful values. The result of briquette SRF9 shows that the pyrolysis of the standard dried sewage sludge and tar blend briquette had different pyrolytic characteristics from cellulose pyrolysis and plastic pyrolysis.

5.3.3 Kinetic results of pulverised biomass

(1) Kinetic results of wood materials

a. Sawdust

The DTG profiles of the pet shop sawdust (PB1a) and the RWE standard sawdust (PB1b) in Figure 4.42 show two thermal decomposition zones and therefore, the

pyrolytic process was treated as two non-interacting parallel reactions. The first reaction was associated with the pyrolysis of hemicellulose, cellulose and lignin, and the second reaction was associated with the pyrolysis of lignin. In test 6, the second zone was unclear and therefore, the kinetic study of the second reaction was not carried out. The results of the first and the second thermal decomposition zones are shown in Tables 5.26 and 5.27, respectively. The kinetic parameters of these two sawdust materials were similar. The regression coefficient of the second reaction was good and close to 98%. This was because sawdust didn't contain plastic component and the second zone was solely the pyrolysis of lignin. The reaction order $n_2 = 0.6$, the activation energy $E_{a,2} = 60$ kJ/mol and the pre-exponential factor $k_{S,0,2} = 13$ of the lignin pyrolysis in sawdust in the temperature range between 400°C and 550°C were quite low and were lower than those of the first reaction $n_1 = 4.0$, $E_{a,1} = 93$ kJ/mol and $k_{S,0,1} = 4.5 \times 10^4$. The peak temperature of the first reaction of the pyrolysis of the sawdust was lower than that of the paper briquette due to the sample thermal inertia. The peak temperature of the lignin pyrolysis of the sawdust was higher than that of PP in the second reaction of the simulated SRF briquettes.

Table 5.26 Kinetic parameters of samples PB1a & PB1b in the first reaction

Test No.	$T_{p,1}$/°C	n_1	$E_{a,1}$/(kJ/mol)	$k_{S,0,1}$	R^2_1
1	311	4.2	96	$2.7\text{x}10^5$	98.4%
2	315	3.4	91	$1.2\text{x}10^5$	98.2%
3	317	3.6	89	$6.6\text{x}10^4$	98.2%
4	319	4.6	101	$5.2\text{x}10^3$	97.9%
5	306	5.2	108	$1.1\text{x}10^5$	98.9%
6	305	2.8	74	$6.9\text{x}10^2$	98.0%
Average	*312 (±2%)*	*4.0*	*93*	*$4.5\text{x}10^4$*	

Table 5.27 Kinetic parameters of samples PB1a & PB1b in the second reaction

Test No.	$T_{p,2}$/°C	n_2	$E_{a,2}$/(kJ/mol)	$k_{S,0,2}$	R^2_2
1	491	0.5	39	0.32	98.6%
2	460	0.3	24	$2.7\text{x}10^{-2}$	95.2%
3	470	0.5	41	0.64	99.6%
4	466	0.9	122	$5.3\text{x}10^5$	97.8%
5	489	0.6	74	$1.4\text{x}10^2$	97.6%
Average	*475 (±3%)*	*0.6*	*60*	*13*	

b. Pulverised MFC wood

The DTG profile of the pulverised MFC wood (PB2) in Figure 4.43 shows one thermal decomposition zone which was associated with the pyrolysis of hemicellulose, cellulose and lignin. The DTG profile of the pyrolysis of lignin at higher temperature between 400°C and 550°C was too small to form a second zone. Therefore the pyrolytic process of the pulverised wood was treated as one single reaction up to 394°C, and the results are shown in Table 5.28. The reaction order $n_1 = 6.9$, the activation energy $E_{a,1} = 127$ kJ/mol and the pre-exponential factor $k_{S,0,1} = 1.2\times10^6$ of the pyrolysis of the pulverised MFC wood were higher than those of the sawdust. The peak temperature of the pyrolysis of the pulverised MFC wood was lower than that of the first reaction of the pyrolysis of the sawdust.

Table 5.28 Kinetic parameters of sample PB2

Test No.	$T_{p,1}$/°C	n_1	$E_{a,1}$/(kJ/mol)	$k_{S,0,1}$	R^2_1
1	283	7.5	140	1.8x10^7	97.5%
2	285	6.4	115	8.5x10^4	97.3%
Average	*284 (±0%)*	*6.9*	*127*	*1.2x10^6*	

(2) Kinetic results of willow materials

The DTG profiles of the pulverised willow (inger 1) (PB3a) and the pulverised willow (discovery 3) (PB3b) in Figure 4.46 show one single thermal decomposition zone which was mainly associated with the pyrolysis of hemicellulose and cellulose and therefore, the pyrolytic process was treated as one single reaction. The results are shown in Table 5.29 and the kinetic parameters of these two willow materials were similar. The peak temperature was lower than that of the paper briquette.

Table 5.29 Kinetic parameters of samples PB3a & PB3b

Test No.	$T_{p,1}$/°C	n_1	$E_{a,1}$/(kJ/mol)	$k_{S,0,1}$	R^2_1
1	281	4.9	103	2.3x10^4	98.1%
2	309	3.3	94	2.8x10^4	95.9%
3	299	5.0	126	6.6x10^6	98.2%
4	310	4.3	113	9.2x10^5	99.1%
Average	*300 (-6%, 3%)*	*4.4*	*109*	*2.5x10^5*	

(3) Kinetic results of other biomass

The DTG profiles of the pulverised borage meal (PB4), the pulverised oat husk (PB5), the pulverised miscanthus giganteus (PB6), the pulverised miscanthus goliath (PB7), the pulverised rape straw (PB8) and the pulverised wheat straw (PB9) in Figures 4.59 – 4.64 show one single thermal decomposition zone which was mainly associated with the pyrolysis of hemicellulose and cellulose and therefore, the pyrolytic process was treated as one single reaction. The results are shown in Table 5.30. The pyrolytic process of each biomass sample was quite repeatable and the kinetic parameters between different samples were quite different.

Table 5.30 Kinetic parameters of samples PB4, PB5, PB6, PB7, PB8 & PB9

Sample	Test No.	$T_{p,1}$/°C	n_1	$E_{a,1}$/(kJ/mol)	$k_{S,0,1}$	R^2_1
PB4	1	283	7.5	97	27	96.5%
	2	271	7.6	86	1.6	97.4%
	Average	*277 (±2%)*	*7.5*	*91*	*6.6*	
PB5	1	306	5.5	118	$6.3\text{x}10^5$	99.5%
	2	294	4.8	111	$1.1\text{x}10^5$	97.0%
	Average	*300 (±2%)*	*5.2*	*115*	*$2.7\text{x}10^5$*	
PB6	1	281	6.6	127	$6.0\text{x}10^5$	99.1%
	2	283	6.2	133	$3.6\text{x}10^6$	98.6%
	Average	*282 (±0%)*	*6.4*	*130*	*$1.5\text{x}10^6$*	
PB7	1	305	5.0	106	$9.9\text{x}10^4$	98.4%
	2	294	5.8	111	$1.8\text{x}10^5$	98.9%
	Average	*300 (±2%)*	*5.4*	*108*	*$1.3\text{x}10^5$*	
PB8	1	293	3.3	90	$2.8\text{x}10^4$	95.7%
	2	308	2.5	90	$7.9\text{x}10^4$	96.3%
	Average	*301 (±2%)*	*2.9*	*90*	*$4.7\text{x}10^4$*	
PB9	1	297	4.4	113	$1.1\ \text{x}10^7$	97.5%
	2	282	5.8	110	$8.7\text{x}10^5$	98.0%
	Average	*290 (±3%)*	*5.1*	*112*	*$3.0\text{x}10^6$*	

(4) Summary

The biomass materials in this research didn't contain plastic component and therefore, the general order ash rise kinetic model of a single reaction was applied to the pyrolytic kinetic study. The single reaction was mainly associated with the pyrolysis of hemicellulose and cellulose. As the sawdust samples contained higher amounts of lignin than the other samples, the DTG profile of sawdust showed a small second thermal decomposition zone. The general order ash rise kinetic model with two non-interacting parallel reactions was applied to the pyrolytic kinetic study of the sawdust

samples and the second reaction was merely associated with the lignin pyrolysis at the higher temperature. The pyrolysis of hemicellulose and cellulose and the pyrolysis of lignin were independent of each other.

The above kinetic results of the pulverised biomass materials are summarised in Table 5.31. The peak temperature of the pyrolysis of the pulverised biomass was lower than that of the paper briquette due to the sample thermal inertia. The peak temperature of the second reaction of the sawdust indicated that the peak temperature of lignin pyrolysis was slightly higher than that of PP pyrolysis. The lignin pyrolysis had a low reaction order, a low activation energy and a small pre-exponential factor with a good regression coefficient. The kinetic parameters of two sawdust materials were similar and the kinetic parameters of two willow materials were also similar. Different types of biomass had different kinetic parameters. The pyrolysis of the rape straw (PB8), the borage meal (PB4) and the sawdust (PB1a and PB1b) had a low activation energy, and the pyrolysis of the miscanthus giganteus (PB6) and the MFC wood (PB2) had a high activation energy. The pyrolysis of the rape straw (PB8) had a low reaction order, and the pyrolysis of the borage meal (PB4) had a high reaction order.

Table 5.31 Kinetic parameters of pulverised biomass samples

Sample	$T_{p,1}$/ °C	n_1	$E_{a,1}$/ (kJ/mol)	$k_{S,0,1}$	$T_{p,2}$/ °C	n_2	$E_{a,2}$/ (kJ/mol)	$k_{S,0,1}$
PB1a&PB1b	312	4.0	93	$4.5x10^4$	475	0.6	60	13
PB2	284	6.9	127	$1.2x10^6$				
PB3a&PB3b	300	4.4	109	$2.5x10^5$				
PB4	277	7.5	91	6.6				
PB5	300	5.2	115	$2.7x10^5$				
PB6	282	6.4	130	$1.5x10^6$				
PB7	300	5.4	108	$1.3x10^5$				
PB8	301	2.9	90	$4.7x10^4$				
PB9	290	5.1	112	$3.0x10^6$				

5.3.4 Conclusions

Chapter Four shows that there were no interactions between the pyrolysis of hemicellulose and cellulose and the pyrolysis of plastic and therefore, two thermal decomposition zones were independent of each other and had their own kinetic parameters. In this chapter, a general order ash rise kinetic model was successfully

applied to the pyrolytic kinetic study of the simulated SRF briquettes, the SRF briquettes and the pulverised biomass samples. The neighbouring event effect existed and led to errors in the results, especially in the beginning and in the end of the reactions.

Table 5.27 shows a good regression coefficient of the second reaction of the sawdust samples, and this indicated that the second reaction was solely lignin pyrolysis. The lignin pyrolysis had a low reaction order, a low activation energy and a low pre-exponential factor. Similarly, Table 5.24 shows that the regression coefficient of the second reaction of briquette SRF8 was very good, and this indicated that the second reaction of briquette SRF8 was solely plastic pyrolysis and the binder molasses restrained the effect of lignin pyrolysis. The plastic pyrolysis had a high reaction order, a high activation energy and a high pre-exponential factor. The regression coefficients of the second reaction of the other briquette samples were quite low, and this indicated that the reaction consisted of both plastic pyrolysis and lignin pyrolysis. Therefore, the values of the kinetic parameters were between the high value of plastic pyrolysis and the low value of lignin pyrolysis. Due to the effect of lignin pyrolysis, when these two reactions were treated together as one single reaction, the reaction order, the activation energy and the pre-exponential factor were lower than those of the first reaction alone.

In the pyrolysis tests of the simulated SRF briquettes, briquettes 6PPc and 6PPd had quite good regression coefficient shown in Figures 5.10 and 5.12, respectively. This indicated that lignin pyrolysis took place at the high extruding temperature during briquetting process, and the high extruding temperature changed the chemical structure of the lignocellulose content of briquettes 6PPc and 6PPd and reduced the lignin content. Therefore, the second reaction was mainly associated with plastic pyrolysis and briquettes 6PPc and 6PPd had a higher activation energy and a higher pre-exponential factor in the second reaction than the other simulated SRF briquettes.

Table 5.25 shows that briquette SRF6 had a very low activation energy of the second reaction, and this indicated that MBT processed RDF material had a very high lignin content. Except briquette SRF8, the SRF briquettes had a lower activation energy of

the second reaction than the simulated SRF briquettes, and this indicated that waste materials had a higher lignin content than paper material.

Inorganic component shifted the peak temperature of the pyrolysis of hemicelulose, cellulose and lignin to a lower temperature and catalysed the pyrolysis of hemicelulose, cellulose and lignin by lowering the activation energy. But inorganic component didn't shift or catalyse the plastic pyrolysis, and the pyrolytic behaviours of different types of plastics were similar. However, it must be pointed out that the small contribution of the neighbouring event existed and might lead to significant errors in the obtained values of the kinetic parameters especially in the second reaction as shown in Figures 5.6 and 5.10. The kinetic parameters of the second reaction of different samples were quite different due to the varying lignin contents.

Chapter Four shows that the pulverised borage meal sample (PB4) had a high ash content and the pulverised oat husk sample (PB5) and the pulverised miscanthus giganteus sample (PB6) had a relatively high ash content. Compared to the paper briquette, the activation energy of the pyrolysis of sample PB4 was lower by about 36 kJ/mol. However, the activation energies of samples PB5 and PB6 were quite different. The activation energy of the pyrolysis of sample PB5 was lowered by about 12 kJ/mol and the activation energy of the pyrolysis of sample PB6 was hardly lowered. This indicated that besides the catalysis of inorganic component, the activation energy could also be affected by the lignin content. For example, sawdust samples (PB1a and PB1b) had a low ash content but a high lignin content and therefore, their activation energy values were quite low.

The kinetic parameters varied with the briquette composition, the extruding temperature and the briquetting process. Increasing the plastic content of briquettes could increase the reaction order, lower the activation energy and lower the pre-exponential factor of the first reaction. Increasing the extruding temperature of briquettes from 125°C to 150°C could increase the reaction order, increase the activation energy and lower the pre-exponential factor of the first reaction. Further increasing the extruding temperature above 150°C could lower the reaction order, lower the activation energy and increase the pre-exponential factor of the first reaction. In Chapter Six, the pyrolytic characteristics of the simulated SRF briquettes, the SRF

briquettes and the pulverised biomass materials are further discussed with the plastic content and the extruding temperature.

Chapter Six Discussion

In this chapter, the DTG profiles from Chapter Four and the kinetic parameters from Chapter Five are used to further discuss the pyrolytic characteristics of the simulated SRF briquettes, the SRF briquettes and the pulverised biomass materials. It is known that the pyrolytic kinetics is complicated, as it involves a large number of reactions in parallel and series. In this research, each mass loss event corresponded to one pseudo-component and the nature of the volatile species released during the pyrolysis was not determined. The pyrolytic process was treated as one reaction or two non-interacting parallel reactions depending on the number of the thermal decomposition zones from the DTG profile rather than on the pyrolytic process of each pseudo-component.

The pyrolysis of the simulated SRF briquettes consisted of three independent mass loss events, which were hemicellulose and cellulose pyrolysis, plastic pyrolysis and lignin pyrolysis, following a moisture vaporisation event up to 180°C. The hemicellulose pyrolysis and the cellulose pyrolysis were both slightly endothermic, and were associated with the shoulder and the peak of the first reaction of the DTG profile. The peak temperature of the first reaction was at about 330°C. The plastic pyrolysis was endothermic and was associated with the second reaction. The peak temperature of PP pyrolysis was at about 450°C and the pyrolysis was completed by 530°C. The lignin pyrolysis was exothermic and the exothermicity was significant at the temperature range of 300 – 400°C. The lignin pyrolysis started at very low temperature, occurred slowly and took place over a broad temperature range with a small maximum mass loss rate at about 475°C. At the temperature above 700°C, the exothermic decomposition of calcium carbonate took place. The pyrolysis of the SRF briquettes also consisted of hemicellulose and cellulose pyrolysis, plastic pyrolysis and lignin pyrolysis. The pyrolytic behaviours of different types of plastics were similar, but had slightly different peak temperatures. PP pyrolysed at a lower temperature than PE. The pyrolysis of the pulverised biomass only consisted of hemicellulose and cellulose pyrolysis and lignin pyrolysis.

Sample's inorganic component could shift the cellulose pyrolysis to a lower temperature and cause the hemicellulose pyrolysis and the cellulose pyrolysis highly

overlapped. The inorganic component could also catalyse the pyrolysis of hemicellulose, cellulose and lignin by lowering the activation energy and increase the reaction rate. However, the inorganic component didn't shift or catalyse the plastic pyrolysis. The pyrolysis of hemicellulose, cellulose, plastic and lignin proceeded independently. The kinetic parameters of the second reaction couldn't reveal the plastic pyrolysis as the lignin pyrolysis led to significant errors in the obtained values.

The study of the pyrolytic characteristics in this chapter is related to volatile yield, peak height, peak temperature, and activation energy.

6.1 Volatile yield

Producing briquettes with a high volatile yield is an ideal way of reducing the volume of waste and generating volatiles for energy purpose. The volatile yield y can be expressed as

$$y = 1 - x = 1 - \frac{m_{A,t=\infty}}{m_{S,0}} \tag{14}$$

where

x is constant remaining mass fraction as expressed in Equation (7) in Chapter Five,

$m_{A,t=\infty}$ is final ash mass,

$m_{S,0}$ is initial mass of dry sample.

Figures 6.1 – 6.3 show the volatile yields of the simulated SRF briquettes, the SRF briquettes and the pulverised biomass samples, respectively. The values in the bracket indicate the minimum and maximum values of the result.

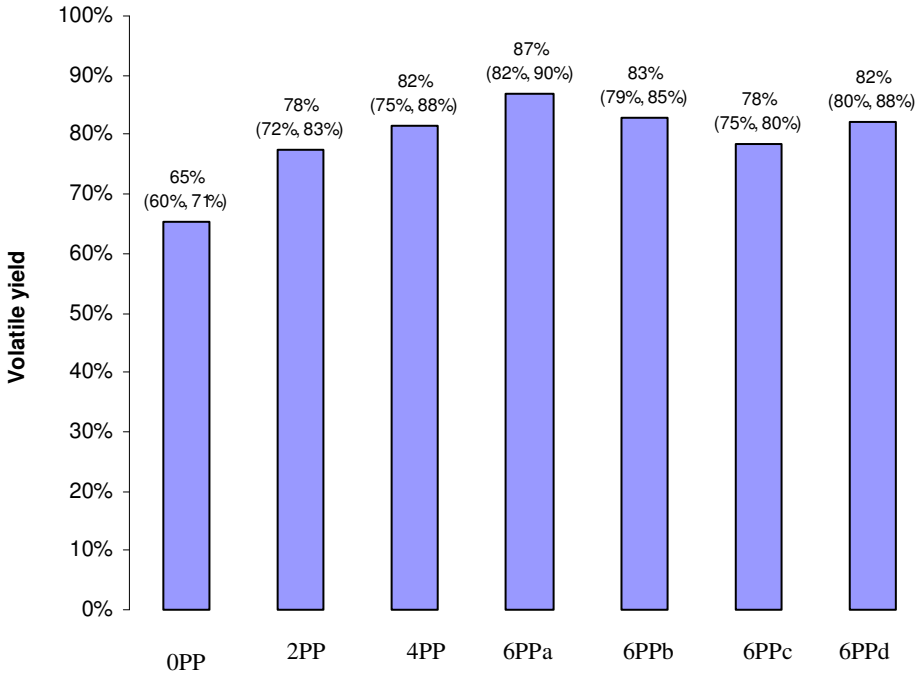

Figure 6.1 Volatile yields of simulated SRF briquettes.

Figure 6.1 shows plastic had a higher volatile content than paper. The briquette with a higher plastic content released more volatiles and produced less ash in pyrolysis. Therefore, the pyrolysis of the briquette with a higher plastic content had less effect of inorganic component. Increasing the plastic content of SRF briquettes could increase the volatile yield and therefore, could improve the quality of the briquettes. Figure 6.1 also shows that, increasing the briquette's extruding temperature didn't increase the volatile yield.

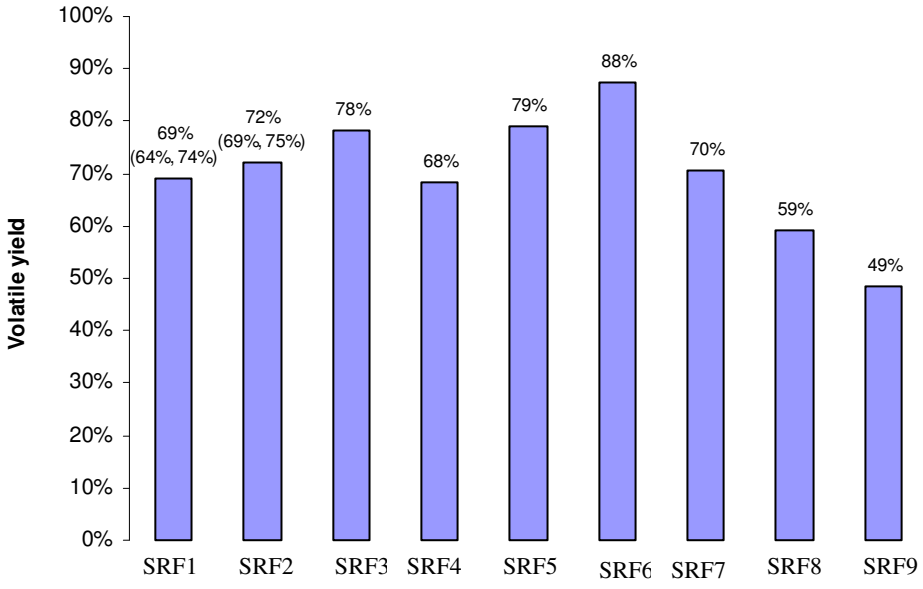

Figure 6.2 Volatile yields of SRF briquettes.

Figure 6.2 shows the 50% standard dried sewage sludge and 50% tar blend briquette (SRF9) had the lowest volatile yield. The RDF and molasses blend briquette (SRF8) had the second lowest volatile yield. The ecodeco briquette extruded at 125°C (SRF1) and the ecodeco briquette extruded at 150°C (SRF2) had the similar volatile yield. The 80% ecodeco and 20% sawdust blend briquette (SRF3) had a higher volatile yield than briquettes SRF1 and SRF2. This indicated that the briquette produced with some biomass materials such as sawdust could have an increased volatile yield. The MBT processed RDF briquette (SRF6) had a higher volatile yield than the RDF briquette (SRF5), and this indicated that the MBT process could increase the volatile yield of SRF briquettes.

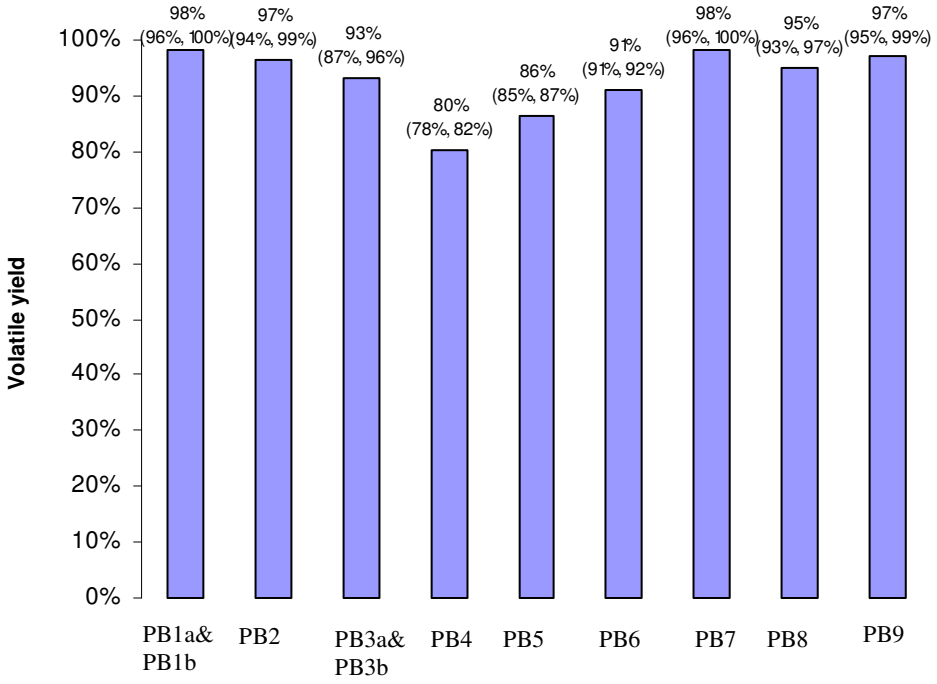

Figure 6.3 Volatile yields of pulverised biomass samples.

Figure 6.3 shows that the pulverised biomass samples had high volatile yields compared to the simulated SRF briquettes and the SRF briquettes. The pulverised borage meal (PB4) and the pulverised oat husk (PB5) had the lowest volatile yields of 80% and 86% among the pulverised biomass samples, respectively.

Comparing Figures 6.1 – 6.3, the following conclusions can be drawn.

• Plastic had a higher volatile yield than paper. SRF briquettes with a higher plastic content could have a higher volatile yield.

• Raw waste materials had low volatile yields. The volatile yield of standard dried sewage sludge and tar was very low and only about 49%.
• Biomass materials had very high volatile yields. The volatile yields of borage meal and oat husk were lower than that of the other biomass.
• SRF briquettes with different extruding temperatures had similar volatile yields.
• Adding biomass into SRF briquettes could increase the briquette's volatile yield.
• An MBT process prior to briquetting could increase the SRF briquette's volatile yield.

6.2 Derivative thermogravimetric profile

The pyrolysis tests in this research were quite repeatable, especially the tests of the pulverised biomass samples.

6.2.1 Peak height

The DTG profiles of the simulated SRF briquettes show that the peak height of the first thermal decomposition zone was proportional to the paper content of the briquette and the peak height of the second thermal decomposition zone was proportional to the plastic content of the briquette. Since the briquettes were not very uniform, the peak height in each test was slightly different.

For each sample, the DTG peak height is directly proportional to the pyrolytic reactivity of each component. Compared with hemicellulose and cellulose pyrolysis and plastic pyrolysis, lignin pyrolysis occurred slowly over a broad temperature range and therefore, lignin was the least reactive pseudo-component in the pyrolytic process. For all samples, the DTG peak height is also directly proportional to the pyrolytic reactivity of each sample [119]. Since the sample size might affect the peak height, the briquette samples and the pulverised samples are discussed separately.

Taking into account of the DTG peak height of all briquette samples, all simulated SRF briquettes (0PP, 2PP, 4PP, 6PPa, 6PPb, 6PPc and 6PPd), the ecodeco briquette extruded at 125°C (SRF1), the ecodeco briquette extruded at 150°C (SRF2) and the 65% ecodeco, 10% sawdust, 15% paper and 10% PE blend briquette (SRF4) had the

biggest peak height and therefore were most reactive in pyrolysis, followed by the 80% ecodeco and 20% sawdust blend briquette (SRF3), the MBT processed RDF briquette (SRF6), the raw MSW briquette (SRF7) and the RDF and molasses blend briquette (SRF8). The RDF briquette (SRF5) was second least reactive. And the 50% standard dried sewage sludge and 50% tar blend briquette (SRF9) was least reactive. It can be seen that the simulated SRF briquettes were more reactive than the SRF briquettes. The briquettes of raw waste materials were not reactive. The raw MSW briquette was slightly more reactive than the RDF briquette. The MBT processed RDF briquette and the RDF and molasses blend briquette were slightly more reactive than the RDF briquette. The peak height of briquettes SRF1, SRF2 and SRF3 indicated that adding sawdust into SRF briquettes couldn't increase the peak height. The peak height of briquettes SRF3 and SRF4 indicated that adding plastic into SRF briquettes could increase the peak height.

Taking into account of the DTG peak height of all pulverised samples, the pulverised wheat straw sample (PB9) had the biggest peak height and therefore was most reactive. The pulverised rape straw sample (PB8) was second most reactive, followed by the pulverised willow samples (PB3a and PB3b), the pulverised oat husk sample (PB5), the pulverised miscanthus giganteus sample (PB6) and the pulverised miscanthus goliath sample (PB7). The sawdust samples (PB1a and PB1b), the pulverised MFC wood sample (PB2) were not quite reactive. And the pulverised borage meal sample (PB4) was least reactive. Therefore borage meal and wood were least and second least reactive among the biomass materials, respectively

The peak height alone cannot be used to assess the reactivity of the samples, as it doesn't involve the pyrolytic temperature and the kinetic parameters. In the following, the peak temperature and the activation energy are discussed.

6.2.2 Peak temperature

Peak temperature is another important factor to indicate sample's reactivity to the pyrolysis and it is inversely proportional to the reactivity [119]. The peak temperature of hemicellulose and cellulose pyrolysis was over 110°C lower than that of plastic pyrolysis and therefore, hemicellulose and cellulose component was more reactive in

pyrolysis than plastic component. Different types of plastics had slightly different peak temperatures. The peak temperature of PP pyrolysis was lower than that of PE pyrolysis and therefore, PP was more reactive in pyrolysis than PE. The peak temperature of lignin pyrolysis was at about 475°C and higher than that of PP pyrolysis. Therefore, lignin component was less reactive than PP.

Since inorganic component shifted and catalysed cellulose pyrolysis, the pyrolytic characteristics of hemicellulose and cellulose were quite different among the samples. However, inorganic component didn't affect plastic pyrolysis. In this section, only the peak temperature of the first reaction is discussed. Due to the different thermal inertia, the briquette samples and the pulverised samples are discussed separately.

The peak temperature of the briquette samples from Tables 5.14 and 5.25 shows that all simulated SRF briquettes (0PP, 2PP, 4PP, 6PPa, 6PPb, 6PPc and 6PPd), the RDF briquette (SRF5), the RDF and molasses blend briquette (SRF8) and the raw MSW briquette (SRF7) were least reactive in the hemicellulose and cellulose pyrolysis. The MBT processed RDF briquette (SRF6) was quite reactive. The ecodeco briquette extruded at 125°C (SRF1), the ecodeco briquette extruded at 150°C (SRF2), the 80% ecedeco and 20% sawdust blend briquette (SRF3) and the 65% ecodeco, 10% sawdust, 15% paper and 10% PE blend briquette (SRF4) were reactive. The 50% standard dried sewage sludge and 50% tar blend briquette (SRF9) was most reactive, but the reaction was the pyrolysis of light volatiles other than hemicellulose and cellulose.

The peak temperature of the pulverised samples from Table 5.31 shows that the sawdust samples (PB1a and PB1b) were least reactive in the hemicellulose and cellulose pyrolysis. The willow (PB3a and PB3b), the oat husk (PB5), the miscanthus goliath (PB7) and the rape straw (PB8) were quite reactive. The wheat straw (PB9) was reactive. The MFC wood (PB2), the miscanthus giganteus (PB6) and the borage meal (PB4) were most reactive.

6.3 Activation energy

Activation energy is an energy barrier that reactants must get over in order to become products. The pyrolysis with a high activation energy means sample needs high energy from surroundings to start the reaction and therefore, the pyrolysis with a high activation energy highly relies on the temperature. The starting temperature of the pyrolysis of each pseudo-component in the DTG profile could specify the activation energy of the pyrolysis of each pseudo-component. Lignin pyrolysis started at the very low temperature and therefore, it had a very low activation energy, followed by hemicellulose and cellulose pyrolysis. Plastic pyrolysis started at the high temperature and therefore, it had a high activation energy.

The inorganic component could catalyse the hemicellulose and cellulose pyrolysis by lowering the activation energy, and this could explain why the activation energy of the first reaction of some samples was quite low besides the effect of the lignin pyrolysis. In the second reaction, the activation energy obtained was due to both the activation energy of the plastic pyrolysis and that of the lignin pyrolysis. The inorganic component didn't catalyse the plastic pyrolysis and therefore, it didn't lower the activation energy of the plastic pyrolysis. The activation energy of the second reaction lower than that of the plastic pyrolysis was due to the effect of the lignin pyrolysis. In the following, the effects of the inorganic content and the lignin content on the activation energy are discussed.

In this research, since the ecodeco material had a higher inorganic content than the sawdust, paper and plastic materials, and the sawdust had a higher lignin content than the ecodeco, the paper and the plastic, the 80% ecodeco and 20% sawdust blend briquette (SRF3) had a higher inorganic content and a higher lignin content than the 65% ecodeco, 10% sawdust, 15% paper and 10% PE blend briquette (SRF4). Therefore, the activation energy values of the first and the second reactions of the pyrolysis of briquette SRF3 were lower than those of briquette SRF4, and this agreed with the results shown in Table 5.25.

Table 5.14 shows that the activation energy of the first reaction of the simulated SRF briquettes varied between 96 and 137 kJ/mol, which was mainly associated with the hemicellulose and cellulose pyrolysis. Table 5.25 shows that the activation energy of the first reaction of the SRF briquettes was lower than that of the simulated SRF briquettes. This indicated that inorganic component widely existed in all waste materials and catalysed the hemicellulose and cellulose pyrolysis of the SRF briquettes, or the waste materials contained a high lignin content. Except briquettes SRF5, SRF7 and SRF9 whose DTG profiles showed one pyrolytic reaction, the MBT processed RDF briquette (SRF6) had the lowest activation energy of the first reaction among the SRF briquettes. This indicated that the MBT process couldn't restrain the catalysis of inorganic component or the effect of lignin pyrolysis. As discussed in Section 4.2.4, the binder molasses could restrain the curve shifting effect of the inorganic component. Therefore, the RDF and molasses blend briquette (SRF8) had a higher activation energy of the first reaction than briquette SRF6, and the activation energy of the first reaction was lowered merely due to the effect of the lignin pyrolysis. As discussed in Section 5.3.4, however, the binder molasses could restrain the lignin pyrolysis in the second reaction. Therefore, the binder molasses could restrain lignin pyrolysis at the high temperature, but not at the low temperature.

6.4 Activation energy and peak temperature

The lignin pyrolysis started at a very low temperature and had a low activation energy, but it didn't mean that lignin was very reactive. This was because the lignin pyrolysis was a slow process and its peak temperature was quite high. Using both the activation energy and the peak temperature together is a reliable tool to assess the sample's reactivity. The activation energy and the peak temperature were both inversely proportional to the reactivity. The sample with a low activation energy and a low peak temperature was highly reactive.

In this research, when two thermal decomposition zones highly overlapped, the pyrolysis was treated as one single reaction and therefore, the activation energy obtained was very small. This didn't mean that the briquettes were reactive, because this was the significant errors caused by the lignin pyrolysis. In this section, only the

pyrolysis of the briquettes with two clear thermal decomposition zones and the pyrolysis of all biomass samples are discussed.

Figure 6.4 shows the samples' activation energies and peak temperatures. The data of the first reaction were on the left around 310°C and were quite close to each other mainly associated with the hemicellulose and cellulose pyrolysis. The data of the second reaction were on the right around 460°C and were not quite close to each other. The data of the second reaction of the sawdust samples (PB1a and PB1b) were associated with the lignin pyrolysis with a very low activation energy. The data of the second reaction of the RDF and molasses blend briquette (SRF8) were associated with the plastic pyrolysis with a high activation energy. The data of the second reaction of the other samples were highly influenced by the lignin pyrolysis and therefore, they couldn't reveal the sample's reactivity of the plastic pyrolysis. In fact, the inorganic component didn't affect the plastic pyrolysis, and the reactivity of the plastic pyrolysis was proportional to the plastic content. In this section, only the data of the first reaction are discussed to reveal the sample's reactivity, and the briquette samples and the pulverised samples are discussed separately.

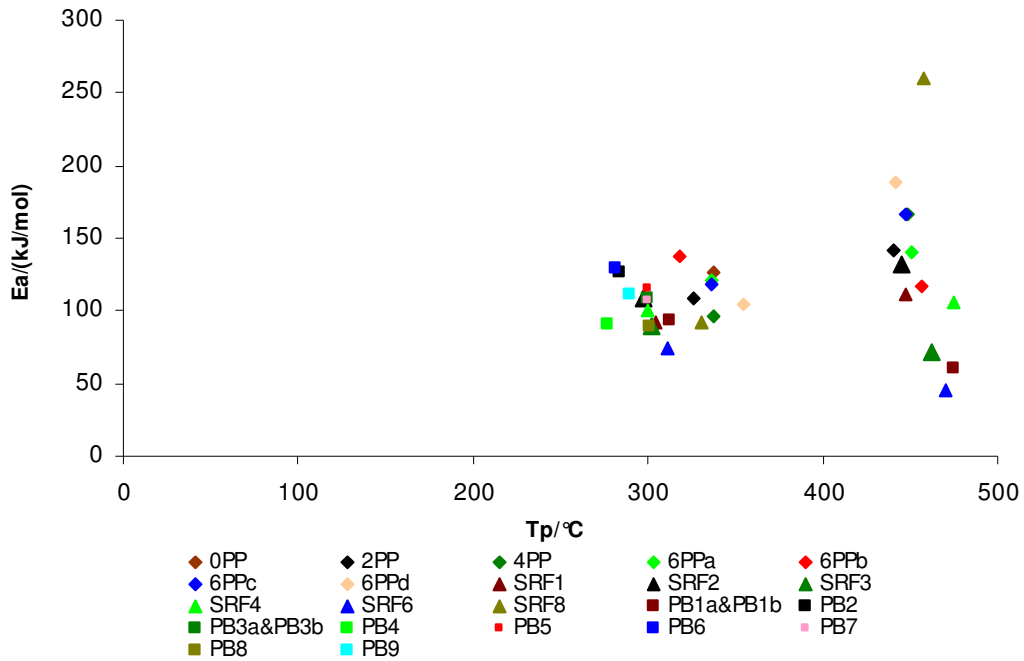

Figure 6.4 Samples' activation energies & peak temperatures.

For the briquette samples, Figure 6.4 shows that the MBT processed RDF briquette (SRF6) with the lowest activation energy and low peak temperature in the first

reaction was most reactive. The 80% ecodeco and 20% sawdust blend briquette (SRF3), the ecodeco briquette extruded at 125°C (SRF1), the 65% ecodeco, 10% sawdust, 15% paper and 10% PE blend briquette (SRF4) and the ecodeco briquette extruded at 150°C (SRF2) were also reactive. The RDF and molasses blend briquette (SRF8) was a little more reactive than the simulated SRF briquettes (0PP, 2PP, 4PP, 6PPa, 6PPb, 6PPc and 6PPd). The simulated SRF briquettes with high activation energies and high peak temperatures of the first reaction were not very reactive. The 60% PP and 40% paper blend briquette extruded at 250°C (6PPd) with the highest peak temperature and a high activation energy was least reactive.

For the pulverised samples, Figure 6.4 shows that the pulverised borage meal sample (PB4) with the lowest peak temperature and a low activation energy was most reactive. The pulverised rape straw sample (PB8) was second most reactive, followed by the sawdust samples (PB1a and PB1b), the pulverised miscanthus goliath sample (PB7), the pulverised willow samples (PB3a and PB3b), the pulverised wheat straw sample (PB9), the pulverised oat husk sample (PB5), the pulverised MFC wood sample (PB2) and the pulverised miscanthus giganteus sample (PB6).

6.5 Summary

An optimum SRF briquette is the briquette with a high volatile yield and high reactivity and therefore, a desirable SRF briquette should have a high volatile yield, a big DTG peak height, a low peak temperature and a low activation energy. The SRF briquettes in this research overall had a relatively low volatile yield, a small peak height, a low peak temperature, and a low activation energy. Therefore, it is necessary to increase the briquette's volatile yield and peak height.

To increase the volatile yield, SRF briquettes could be produced with a high plastic content, and the extruding temperature couldn't affect the volatile yield. Biomass has a very high volatile content and adding biomass into the SRF briquettes could increase the volatile yield. Sawdust, miscanthus goliath, MFC wood, wheat straw and rape straw have very high volatile contents. MBT process could highly improve the volatile yield.

The biomass samples had a big peak height, but adding biomass into the SRF briquettes couldn't increase the peak height. Adding plastic or molasses binder and an MBT process could improve the peak height. However, when the molasses binder is used, the curve shifting effect of the inorganic component could be restrained and therefore, the peak temperature could be increased.

The ecodeco briquettes (SRF1 and SRF2) had a quite big peak height, a low peak temperature and a low activation energy, but the volatile yield was only about 70%. Therefore, it is necessary to increase the volatile yield in order to produce SRF briquettes from ecodeco. The ecodeco and sawdust blend briquette (SRF3) showed an increased volatile yield. The RDF briquette (SRF5) had a quite low volatile yield of 79% and a very small peak height because two thermal decomposition zones highly overlapped. Therefore, it is necessary to separate these two zones to increase the peak height, and increase the volatile yield in order to produce SRF briquettes from RDF. The MBT processed RDF briquette (SRF6) had a high volatile yield of 88%, an improved peak height compared to briquette SRF5, a low peak temperature and a low activation energy. The raw MSW briquette (SRF7) had a low peak temperature and a low activation energy, but it had a low volatile yield of 70% and a low peak height. Therefore, it is necessary to increase the volatile yield and the peak height in order to produce SRF briquettes from MSW. The RDF and molasses blend briquette (SRF8) had a low activation energy, but it had a very low volatile yield of 59% and a low peak height, and its peak temperature was as high as the paper briquette. Therefore, it is necessary to increase the volatile yield and the peak height and lower the peak temperature in order to produce SRF briquettes from RDF with the molasses binder. The 50% standard dried sewage sludge and 50% tar blend briquette (SRF9) had a single peak with a very low peak height and had a very low volatile yield of 49%. Therefore, it is necessary to increase the peak height and increase the volatile yield in order to produce SRF briquettes from standard dried sewage sludge and tar.

Chapter Seven Conclusions and Further Recommendation

In this final chapter, the first section provides a short discussion and summarises the conclusions and contributions of the thesis. In the second section, suggestions for future work are listed.

7.1 Short discussion and conclusions

Throughout the entire course of this research project, an extensive amount of simulated SRF briquettes, SRF briquettes and pulverised biomass samples have been investigated in a pyrolytic process using laboratory scale. The whole process including moisture vaporisation, hemicellulose and cellulose pyrolysis, plastic pyrolysis, lignin pyrolysis and calcium carbonate decomposition has been described. A general order ash rise kinetic model has been developed to obtain the kinetic parameters. Results have been compared with literature data and generally good order-of-magnitude agreement has been found. The pyrolytic characteristics of all samples have been studied, and the main conclusions and contributions in this thesis are summarised below.

The overall pyrolysis of SRF briquettes consists of five events. The first event is moisture vaporisation up to 180°C. The second event is hemicellulose and cellulose pyrolysis with an activation energy between 96 – 137 kJ/mol and a peak temperature at about 330°C, and slightly endothermic. Inorganic component which is widely present in waste could shift the cellulose pyrolysis to a lower temperature and catalyse the hemicellulose and cellulose pyrolysis by lowering the activation energy. The third event is plastic pyrolysis with an activation energy of 260 kJ/mol and endothermic. The inorganic component couldn't shift the plastic pyrolysis to a lower temperature or catalyse the plastic pyrolysis. The pyrolysis of different types of plastics is similar, but takes place at slightly different temperatures. The peak temperature of PP pyrolysis is at about 450°C and the process completes by 530°C. The fourth event is

lignin pyrolysis with an activation energy between about 30 – 70 kJ/mol and a peak temperature at about 475°C. The lignin pyrolysis starts at a very low temperature, occurs slowly and takes place over a broad temperature range. It is exothermic and the exothermicity is significant at the temperature range of 300 – 400°C. The inorganic component could also catalyse the lignin pyrolysis by lowering the activation energy. The fifth event is decomposition of calcium carbonate which takes place at the temperature above 700°C and is exothermic. This mass loss event was not considered in the kinetic model in this research. These five events are independent of each other and have their own kinetic parameters. The kinetic parameters obtained in the pyrolysis are an additive function of each contributing fraction associated with the process. The neighbouring event effect exists and leads to errors in the results, especially in the beginning and in the end of the events. Secondary reactions, heat transfer and mass transfer are important, but they are beyond the scope of this research.

The pyrolysis of SRF briquettes could be quite repeatable. SRF briquettes extruded at 150°C could be quite uniform and perform good repeatability of the pyrolytic process. 150°C is the desirable extruding temperature and could prevent from breaking down the lignocellulose content especially lignin in the briquetting process at high temperatures over 200°C. Waste materials have poor thermal conductivity and by increasing the extruding temperature to 150°C, the thermal conductivity of SRF briquettes could be improved.

SRF briquettes overall have a relatively low volatile yield, a small DTG peak height, a low peak temperature, and a low activation energy. Therefore, it is necessary to increase the volatile yield and the DTG peak height in order to produce high quality SRF briquettes. Raw waste couldn't be used directly to produce SRF briquettes and SRF briquettes made from different waste have different pyrolytic characteristics. For example, MSW briquette is slightly more reactive than RDF briquette. The volatile yield of the standard dried sewage sludge and tar briquette is only 49%. To produce SRF briquettes from RDF, it needs to separate the hemicellulose and cellulose pyrolysis and the plastic pyrolysis into two temperature zones in order to increase the peak height, and increase the volatile yield. To produce SRF briquettes from MSW, it needs to increase the volatile yield and the peak height. To produce SRF briquettes

from ecodeco, it needs to increase the volatile yield. Biomass and plastic could be added into the briquettes to increase the volatile yield, but the extruding temperature couldn't affect the volatile yield.

Biomass has a very high volatile content. Adding biomass into SRF briquettes could increase the volatile yield. Sawdust, miscanthus goliath, MFC wood, wheat straw and rape straw have very a high volatile content. Borage meal and oat husk have a relatively low volatile content. For the biomass with a higher hemicellulose and cellulose content, the pyrolytic rate is faster. While the biomass with a higher lignin content gives a slower pyrolytic rate. Biomass has a big peak height, but adding biomass into SRF briquettes couldn't increase the peak height of SRF briquettes.

Plastic is not present in biomass and it has a higher volatile content than paper. Plastic as a rich source of hydrocarbons could play a vital role by enhancing the repeatability of the pyrolysis. Different plastics have slightly different pyrolytic characteristics. PP pyrolyses at a lower temperature than PE. Increasing the plastic content of SRF briquettes could increase the volatile yield, the peak height and the repeatability of the pyrolysis, and could also increase the reaction order, lower the activation energy and lower the pre-exponential factor in the hemicellulose and cellulose pyrolysis. The reactivity of the plastic pyrolysis is proportional to the plastic content in SRF briquettes.

Inorganic component could have a positive effect by acting as catalysts. Binder molasses could improve the DTG peak height, restrain the curve shifting effect of the inorganic component on hemicellulose and cellulose pyrolysis and restrain the effect of lignin pyrolysis at high temperatures on plastic pyrolysis. An MBT process couldn't restrain the catalysis of inorganic component or the effect of lignin pyrolysis. An MBT process could highly improve the volatile yield and the peak height of SRF briquettes.

Waste has a higher lignin content than paper, and wood materials contain relatively high lignin. The obtained kinetic parameters of plastic pyrolysis are strongly affected by lignin pyrolysis and therefore, binder molasses which could restrain the effect of

the lignin pyrolysis at high temperatures is recommended to be added into SRF briquettes.

7.2 Recommendation for further work

To optimise the conversion efficiency of SRF briquettes and biomass to energy using gasification, further work would help. Such work may include:

(1) Analysis of pyrolytic products in detail to ascertain variations with pyrolytic temperatures and product compositions at specified temperatures;
(2) Identification of catalytic effects of inorganic component on hemicellulose and cellulose pyrolysis;
(3) Parametric study of briquette composition for optimum pyrolytic kinetic parameters;
(4) Experiments in the presence of oxygen and at higher heating rates;
(5) Checking the applicability of model parameters with different sample size;
(6) Introducing thermodynamic analysis;
(7) Taking into account of ultimate analysis and introducing inorganic components as catalysts;
(8) Large-scale gasification testing and process evaluation.

References

1. *UK meets 2010 Landfill Directive target and responds to landfill consultations*, Defra, http://ww2.defra.gov.uk/news/2010/09/08/landfill-directive-target, Accessed 8th September 2010.
2. *Report on the Landfill Allowances Scheme (LAS) Wales 2009-10*. September 2010, Environment Agency Wales.
3. *Council tax could rise if European Union landfill targets are missed*, The Telegraph, http://www.telegraph.co.uk/earth/earthnews/3411174/Council-tax-could-rise-if-European-Union-landfill-targets-are-missed.html, Accessed 3rd December 2010.
4. *Design and Testing of Secondary Refuse Fuel Briquettes to Enable Hydrogen Production and Energy Recovery via Gasification (HyPERG)*. May 2004, EB Nationwide Ltd and Progressive Energy Ltd.
5. Vamvuka, D., et al., *Pyrolysis characteristics and kinetics of biomass residuals mixtures with lignite.* Fuel, 2003. **82**(15-17): p. 1949-1960.
6. Pyle, D.L. and C.A. Zaror, *Heat transfer and kinetics in the low temperature pyrolysis of solids.* Chemical Engineering Science, 1984. **39**(1): p. 147-158.
7. *Hydrogen Production and Energy Recovery via Gasification (HyPERG)*, *First Interim Report*. June 2005, EB Nationwide Ltd, Shanks First Funding for the Environment, Progressive Energy Ltd, Cardiff University and University of Glamorgan.
8. Garcia, A.N., M.M. Esperanza, and R. Font, *Comparison between product yields in the pyrolysis and combustion of different refuse.* Journal of Analytical and Applied Pyrolysis, Pyrolysis 2002 Conference issue, 2003. **68-69**: p. 577-598.
9. Emery, A., et al., *Environmental and economic modelling: A case study of municipal solid waste management scenarios in Wales.* Resources, Conservation and Recycling, 2007. **49**(3): p. 244-263.
10. *How can BMW be diverted from landfill*, Environment Agency, http://www.environment-agency.gov.uk/business/topics/waste/104645.aspx, Accessed 4th December 2010.

11. Demirbas, A., *Pyrolysis of municipal plastic wastes for recovery of gasoline-range hydrocarbons.* Journal of Analytical and Applied Pyrolysis, 2004. **72**(1): p. 97-102.
12. Zevenhoven, R., et al., *Laboratory scale characterization of plastic-derived fuels*. 1995, Borealis Polymer Oy: Borga, Finland.
13. York, R., E.A. Rosa, and T. Dietz, *The Ecological Footprint Intensity of National Economies.* Journal of Industrial Ecology, 2004. **8**(4): p. 139-154.
14. Dasappa, S., et al., *Biomass gasification--a substitute to fossil fuel for heat application.* Biomass and Bioenergy, 2003. **25**(6): p. 637-649.
15. Zainal, Z.A., et al., *Prediction of performance of a downdraft gasifier using equilibrium modeling for different biomass materials.* Energy Conversion and Management, 2001. **42**(12): p. 1499-1515.
16. Wu, C.-H., et al., *Thermal treatment of coated printing and writing paper in MSW: pyrolysis kinetics.* Fuel, 1997. **76**(12): p. 1151-1157.
17. Saitzyk, S., *ART HARDWARE: The Definitive Guide to Artists' Materials*. June 1987: Watson-Guptill Publications.
18. Devi, L., K.J. Ptasinski, and F.J.J.G. Janssen, *A review of the primary measures for tar elimination in biomass gasification processes.* Biomass and Bioenergy, 2003. **24**(2): p. 125-140.
19. Yaman, S., *Pyrolysis of biomass to produce fuels and chemical feedstocks.* Energy Conversion and Management, 2004. **45**(5): p. 651-671.
20. Liang, X.H. and J.A. Kozinski, *Numerical modeling of combustion and pyrolysis of cellulosic biomass in thermogravimetric systems.* Fuel, 2000. **79**(12): p. 1477-1486.
21. Hall, D., F. Rosillo-Calle, and J. Woods. in *Proceedings of the Sixth E.C. Conference in Biomass for Energy. Industry and Environment*. 1991. London.
22. Bapat, D., S. Kulkami, and V. Bhandarkar. in *Proceedings of the 14th International Conference in Fluidized Bed Combustion*. 1997. Vancouver, BC, Canada: ASME.
23. Vamvuka, D., et al., *Pyrolysis characteristics and kinetics of biomass residuals mixtures with lignite.* Fuel, 2003. **82**(15-17): p. 1949-1960.
24. Williams, A., M. Pourkashanian, and J.M. Jones, *Combustion of pulverised coal and biomass.* Progress in Energy and Combustion Science, 2001. **27**(6): p. 587-610.

25. L.Klass, D., *Biomass for renewable energy, fuels, and chemicals*. 1998: San Diego : Academic Press.
26. Bridgeman, T.G., et al., *Torrefaction of reed canary grass, wheat straw and willow to enhance solid fuel qualities and combustion properties.* Fuel, 2008. **87**(6): p. 844-856.
27. Ptasinski, K.J., M.J. Prins, and A. Pierik, *Exergetic evaluation of biomass gasification.* Energy, 2007. **32**(4): p. 568-574.
28. *Ullmann's Encyclopedia of Industrial Chemistry*. 5th ed. Vol. A5. 1986, Germany.
29. Saiz-Jimenez, C., *Production of Alkylbenzenes and Alkylnaphthalenes upon Pyrolysis of Unsaturated Fatty Acids A Model Reaction to Understand the Origin of some Pyrolysis Products from Humic Substances?* Naturwissenschaften, 1994. **81**(10): p. 451-453.
30. Overend, R.P., T.A. Milne, and L.K. Mudge, *Fundamentals of thermochemical biomass conversion*. 1985, Amsterdam: Elsevier.
31. Caballero, J.A., et al., *Pyrolysis kinetics of almond shells and olive stones considering their organic fractions.* Journal of Analytical and Applied Pyrolysis, 1997. **42**(2): p. 159-175.
32. Corella, J. and A. Sanz, *Modeling circulating fluidized bed biomass gasifiers. A pseudo-rigorous model for stationary state.* Fuel Processing Technology, 2005. **86**(9): p. 1021-1053.
33. Blesa, M.J., et al., *Effect of the pyrolysis process on the physicochemical and mechanical properties of smokeless fuel briquettes.* Fuel Processing Technology, 2001. **74**(1): p. 1-17.
34. Rogner, H. and A. Popescu, *An introduction to energy*, in *World Energy Assessment: Energy and the Challenge of Sustainability*, J. Goldemberg, Editor. 2000, UNDP / UN-DESA / World Energy Council: New York.
35. Nieminen, J. and M. Kivela, *Biomass CFB gasifier connected to a 350 MWth steam boiler fired with coal and natural GAS-Thermie demonstration project in lahti in Finland.* Biomass and Bioenergy, The International Biomass Gasification Utility Scale Projects Meeting, 1998. **15**(3): p. 251-257.
36. Mory, A. and T. Zotter, *Eu-demonstration project BioCoComb for biomass gasification and co-combustion of the product-gas in a coal-fired power plant*

in austria. Biomass and Bioenergy, The International Biomass Gasification Utility Scale Projects Meeting, 1998. **15**(3): p. 239-244.

37. De Lange, H.J. and P. Barbucci, *The thermie energy farm project.* Biomass and Bioenergy, The International Biomass Gasification Utility Scale Projects Meeting, 1998. **15**(3): p. 219-224.
38. Faaij, A., et al., *Characteristics and availability of biomass waste and residues in The Netherlands for gasification.* Biomass and Bioenergy, 1997. **12**(4): p. 225-240.
39. Olivares, A., et al., *Biomass Gasification: Produced Gas Upgrading by In-Bed Use of Dolomite.* Ind. Eng. Chem. Res., 1997. **36**(12): p. 5220-5226.
40. Hall, D. and J. House. *Biomass: an environmentally acceptable fuel for the future*. in *12th European Conference and Technology Exibition on Biomass for Energy, Industry and Climate Protection*. 2002. Amsterdam, Netherlands.
41. Palz, W. and A. Kyramarios. *Bioenergy perspectives in developing countries*. in *Proceedings of the First World Conference on Biomass for Energy and Industry*. 2000. Sevilla, Spain.
42. Skutsch, M. and J. Van Rijn. *Biomass: the fuel of the future*. in *12th European Conference and Technology Exibition on Biomass for Energy, Industry and Climate Protection*. 2002. Amsterdam, Netherlands.
43. Strehler, A. *Potential and global aspects of bioenergy application*. in *Proceedings of the First World Conference on Biomass for Energy and Industry*. 2000. Sevilla, Spain.
44. Bridgwater, A.V., *Renewable fuels and chemicals by thermal processing of biomass.* Chemical Engineering Journal, 2003. **91**(2-3): p. 87-102.
45. Ding, W.B., et al., *Depolymerization of waste plastics with coal over metal-loaded silica-alumina catalysts.* Fuel Processing Technology, Coal and Waste, 1996. **49**(1-3): p. 49-63.
46. Feng, Z., et al., *Direct liquefaction of waste plastics and coliquefaction of coal-plastic mixtures.* Fuel Processing Technology, Coal and Waste, 1996. **49**(1-3): p. 17-30.
47. Lee, K.-H. and D.-H. Shin, *Characteristics of liquid product from the pyrolysis of waste plastic mixture at low and high temperatures: Influence of lapse time of reaction.* Waste Management, 2007. **27**(2): p. 168-176.

48. Bockhorn, H., et al., *Environmental engineering: Stepwise pyrolysis of plastic waste.* Chemical Engineering Science, 1999. **54**(15-16): p. 3043-3051.
49. Dornburg, V. and A.P.C. Faaij, *Optimising waste treatment systems: Part B: Analyses and scenarios for The Netherlands.* Resources, Conservation and Recycling, 2006. **48**(3): p. 227-248.
50. Saha, B. and A.K. Ghoshal, *Thermal degradation kinetics of poly(ethylene terephthalate) from waste soft drinks bottles.* Chemical Engineering Journal, 2005. **111**(1): p. 39-43.
51. Finnveden, G., et al., *Life cycle assessment of energy from solid waste--part 1: general methodology and results.* Journal of Cleaner Production, Environmental Assessments and Waste Management, 2005. **13**(3): p. 213-229.
52. Katami, T., et al., *Formation of PCDDs, PCDFs, and coplanar PCBs from polyvinyl chloride during combustion in an incinerator.* Environmental Science and Technology, 2002. **36**(6): p. 1320-1324.
53. Choy, K.K.H., et al., *Process design and feasibility study for small scale MSW gasification.* Chemical Engineering Journal, 2004. **105**(1-2): p. 31-41.
54. Hasselriis, F., *Optimization of combustion conditions to minimize dioxin emissions.* Waste Management & Research, 1987. **5**(3): p. 311-326.
55. McKay, G., *Dioxin characterisation, formation and minimisation during municipal solid waste (MSW) incineration: review.* Chemical Engineering Journal, 2002. **86**(3): p. 343-368.
56. Brunner, C.R., *Handbook of Hazardous Waste Incineration*. 2nd ed. 1993, New York, NY: McGraw-Hill.
57. Narayan, P., *Analysing thesis for the fulfillment of the Master of Science in Environmental Management and Policy*. 2001: Lund, Sweden.
58. USEPA, *Report to the US Congress - Resource Recovery and Source Reduction.* February 1978.
59. LEE, C.C. and G.L. Huffman, *Thermodynamics Used In Environmental Engineering*, in *Handbook of Environmental Engineering Calculations*, C.C. LEE and S.D. Lin, Editors. 1999, McGRAW-HILL.
60. Hester, R.E. and R.M. Harrison, *Waste Incineration and the Environment*. 1994: Royal Society of Chemistry.
61. McKendry, P., *Energy production from biomass (part 3): gasification technologies.* Bioresource Technology, 2002. **83**(1): p. 55-63.

62. Liu, G.-S. and S. Niksa, *Coal conversion submodels for design applications at elevated pressures. Part II. Char gasification.* Progress in Energy and Combustion Science, 2004. **30**(6): p. 679-717.
63. Bjorklund, A., M. Melaina, and G. Keoleian, *Hydrogen as a transportation fuel produced from thermal gasification of municipal solid waste: an examination of two integrated technologies.* International Journal of Hydrogen Energy, 2001. **26**(11): p. 1209-1221.
64. Leung, D.Y.C., X.L. Yin, and C.Z. Wu, *A review on the development and commercialization of biomass gasification technologies in China.* Renewable and Sustainable Energy Reviews, 2004. **8**(6): p. 565-580.
65. Lapuerta, M., J.J. Hernandez, and J.J. Rodriguez, *Kinetics of devolatilisation of forestry wastes from thermogravimetric analysis.* Biomass and Bioenergy, 2004. **27**(4): p. 385-391.
66. Sheng, G.X., *Biomass gasifiers: from waste to energy production.* Biomass, 1989. **20**(1-2): p. 3-12.
67. Kurkela, E., et al., *Development of simplified IGCC-processes for biofuels: Supporting gasification research at VTT.* Bioresource Technology, 1993. **46**(1-2): p. 37-47.
68. Hos, J.J. and M.J. Groeneveld, *Biomass gasification*, in *Biomass regenerable energy*, D.O. Hall and R.P. Overend, Editors. April 1987, John Wiley & Sons Inc: New York. p. 37-55.
69. Overend, R.P., et al. *Fundamentals of thermochemical biomass conversion*. 1985. London; New York; New York, NY, USA: Elsevier Applied Science Publishers ; Sole distributor in the USA and Canada, Elsevier Science Pub. Co.
70. Rao, M.S., et al., *Stoichiometric, mass, energy and exergy balance analysis of countercurrent fixed-bed gasification of post-consumer residues.* Biomass and Bioenergy, 2004. **27**(2): p. 155-171.
71. Koukouzas, N., et al., *Co-gasification of solid waste and lignite - A case study for Western Macedonia.* Waste Management, 2008. **28**(7): p. 1263-1275.
72. Feng, W., H.J. van der Kooi, and J. de Swaan Arons, *Biomass conversions in subcritical and supercritical water: driving force, phase equilibria, and thermodynamic analysis.* Chemical Engineering and Processing, 2004. **43**(12): p. 1459-1467.

73. Lee, D.H., et al., *Prediction of gaseous products from biomass pyrolysis through combined kinetic and thermodynamic simulations.* Fuel, 2007. **86**(3): p. 410-417.
74. Babu, B.V. and A.S. Chaurasia, *Pyrolysis of biomass: improved models for simultaneous kinetics and transport of heat, mass and momentum.* Energy Conversion and Management, 2004. **45**(9-10): p. 1297-1327.
75. Walendziewski, J., *Engine fuel derived from waste plastics by thermal treatment.* Fuel, 2002. **81**(4): p. 473-481.
76. Buekens, A.G. and H. Huang, *Catalytic plastics cracking for recovery of gasoline-range hydrocarbons from municipal plastic wastes.* Resources, Conservation and Recycling, 1998. **23**(3): p. 163-181.
77. Murata, K., et al., *Basic study on a continuous flow reactor for thermal degradation of polymers.* Journal of Analytical and Applied Pyrolysis, 2002. **65**(1): p. 71-90.
78. Vasile, C., et al., *Thermal and catalytic decomposition of mixed plastics.* Journal of Analytical and Applied Pyrolysis, 2001. **57**(2): p. 287-303.
79. Di Blasi, C., *Heat, momentum and mass transport through a shrinking biomass particle exposed to thermal radiation.* Chemical Engineering Science, 1996. **51**(7): p. 1121-1132.
80. Fisher, T., et al., *Pyrolysis behavior and kinetics of biomass derived materials.* Journal of Analytical and Applied Pyrolysis, 2002. **62**(2): p. 331-349.
81. Horne, P.A. and P.T. Williams, *Influence of temperature on the products from the flash pyrolysis of biomass.* Fuel, 1996. **75**(9): p. 1051-1059.
82. Raveendran, K. and A. Ganesh, *Heating value of biomass and biomass pyrolysis products.* Fuel, 1996. **75**(15): p. 1715-1720.
83. Meier, D. and O. Faix, *State of the art of applied fast pyrolysis of lignocellulosic materials -- a review.* Bioresource Technology, 1999. **68**(1): p. 71-77.
84. Agblevor, F.A. and S. Besler, *Inorganic Compounds in Biomass Feedstocks. 1. Effect on the Quality of Fast Pyrolysis Oils.* Energy & Fuels, 1996. **10**(2): p. 293-298.
85. Zanki, R., K. Sjostrom, and E. Bjornbom. *Rapid pyrolysis of biomass at high temperature at the initial stage in gasification*. in *Proceedings of the First*

World Conference on Biomass for Energy and Industry. 2000. Sevilla, Spain: James & James (Science Publishers) Ltd.

86. Tromp, P.J.J., F. Kapteijn, and J.A. Moulijn, *Characterization of coal pyrolysis by means of differential scanning calorimetry. 2. Quantitative heat effects in a H2 and in a CO2 atmosphere.* Fuel Processing Technology, 1989. **23**(1): p. 63-74.
87. Gawlik, B.M., et al., *Quality management organisation, validation of standards, developments and inquiries for solid-recovered fuels--An overview on the QUOVADIS-Project.* Energy Policy, 2007. **35**(12): p. 6293-6298.
88. Ndiema, C.K.W., P.N. Manga, and C.R. Ruttoh, *Influence of die pressure on relaxation characteristics of briquetted biomass.* Energy Conversion and Management, 2002. **43**(16): p. 2157-2161.
89. Wamukonya, L. and B. Jenkins, *Durability and relaxation of sawdust and wheat-straw briquettes as possible fuels for Kenya.* Biomass and Bioenergy, 1995. **8**(3): p. 175-179.
90. Chin, O.C. and K.M. Siddiqui, *Characteristics of some biomass briquettes prepared under modest die pressures.* Biomass and Bioenergy, 2000. **18**(3): p. 223-228.
91. Singh, R.N., *Equilibrium moisture content of biomass briquettes.* Biomass and Bioenergy, 2004. **26**(3): p. 251-253.
92. Singh, R.N., P.R. Bhoi, and S.R. Patel, *Modification of commercial briquetting machine to produce 35 mm diameter briquettes suitable for gasification and combustion.* Renewable Energy, 2007. **32**(3): p. 474-479.
93. Richards, S.R., *Physical testing of fuel briquettes.* Fuel Processing Technology, 1990. **25**(2): p. 89-100.
94. Sugawara, K., et al., *Effect of heating rate and temperature on pyrolysis desulfurization of a bituminous coal.* Fuel Processing Technology, 1994. **37**(1): p. 73-85.
95. Kaliyan, N. and R. Vance Morey, *Factors affecting strength and durability of densified biomass products.* Biomass and Bioenergy, 2009. **33**(3): p. 337-359.
96. Yaman, S., et al., *Production of fuel briquettes from olive refuse and paper mill waste.* Fuel Processing Technology, 2000. **68**(1): p. 23-31.
97. Yaman, S., *Fuel briquettes from biomass-lignite blends.* Fuel Processing Technology, 2001. **72**(1): p. 1-8.

98. Gueret, C., M. Daroux, and F. Billaud, *Methane pyrolysis: thermodynamics.* Chemical Engineering Science, 1997. **52**(5): p. 815-827.

99. Conesa, J.A., et al., *KINETIC STUDY OF THE PYROLYSIS OF SEWAGE SLUDGE.* Waste Management & Research, 1997. **15**(3): p. 293-305.

100. Biagini, E., et al., *Devolatilization rate of biomasses and coal-biomass blends: an experimental investigation.* Fuel, 2002. **81**(8): p. 1041-1050.

101. Hagge, M.J. and K.M. Bryden, *Modeling the impact of shrinkage on the pyrolysis of dry biomass.* Chemical Engineering Science, 2002. **57**(14): p. 2811-2823.

102. Varhegyi, G., et al., *Kinetic modeling of biomass pyrolysis.* Journal of Analytical and Applied Pyrolysis, 1997. **42**(1): p. 73-87.

103. C. A. Koufopanos, et al., *Modelling of the pyrolysis of biomass particles. Studies on kinetics, thermal and heat transfer effects.* The Canadian Journal of Chemical Engineering, 1991. **69**(4): p. 907-915.

104. Branca, C., A. Albano, and C. Di Blasi, *Critical evaluation of global mechanisms of wood devolatilization.* Thermochimica Acta, 2005. **429**(2): p. 133-141.

105. Di Blasi, C., *Modeling chemical and physical processes of wood and biomass pyrolysis.* Progress in Energy and Combustion Science, 2008. **34**(1): p. 47-90.

106. Narayan, R. and M.J. Antal, *Thermal Lag, Fusion, and the Compensation Effect during Biomass Pyrolysis.* Industrial & Engineering Chemistry Research, 1996. **35**(5): p. 1711-1721.

107. Kastanaki, E., et al., *Thermogravimetric studies of the behavior of lignite-biomass blends during devolatilization.* Fuel Processing Technology, 2002. **77-78**: p. 159-166.

108. Milosavljevic, I., V. Oja, and E.M. Suuberg, *Thermal Effects in Cellulose Pyrolysis: Relationship to Char Formation Processes.* Industrial & Engineering Chemistry Research, 1996. **35**(3): p. 653-662.

109. C. A. Koufopanos, A. Lucchesi, and G. Maschio, *Kinetic modelling of the pyrolysis of biomass and biomass components.* The Canadian Journal of Chemical Engineering, 1989. **67**(1): p. 75-84.

110. Ramiah, M.V., *Thermogravimetric and differential thermal analysis of cellulose, hemicellulose, and lignin.* Journal of Applied Polymer Science, 1970. **14**(5): p. 1323-1337.

111. Gronli, M.G., G. Varhegyi, and C. Di Blasi, *Thermogravimetric Analysis and Devolatilization Kinetics of Wood.* Industrial & Engineering Chemistry Research, 2002. **41**(17): p. 4201-4208.

112. Ranzi, E., et al., *Kinetic modeling of polyethylene and polypropylene thermal degradation.* Journal of Analytical and Applied Pyrolysis, 1997. **40-41**: p. 305-319.

113. Lattimer, R.P., *Pyrolysis field ionization mass spectrometry of polyolefins.* Journal of Analytical and Applied Pyrolysis, 1995. **31**: p. 203-225.

114. Erdoğan Kiran and J. K. Gillham, *Pyrolysis-molecular weight chromatography: A new on-line system for analysis of polymers. II. Thermal decomposition of polyolefins: Polyethylene, polypropylene, polyisobutylene.* Journal of Applied Polymer Science, 1976. **20**(8): p. 2045-2068.

115. Ishaq, M., et al., *Pyrolysis of some whole plastics and plastics-coal mixtures.* Energy Conversion and Management, 2006. **47**(18-19): p. 3216-3223.

116. Garcia, A.N., A. Marcilla, and R. Font, *Thermogravimetric kinetic study of the pyrolysis of municipal solid waste.* Thermochimica Acta, 1995. **254**: p. 277-304.

117. Gani, A. and I. Naruse, *Effect of cellulose and lignin content on pyrolysis and combustion characteristics for several types of biomass.* Renewable Energy, 2007. **32**(4): p. 649-661.

118. Ghetti, P., L. Ricca, and L. Angelini, *Thermal analysis of biomass and corresponding pyrolysis products.* Fuel, 1996. **75**(5): p. 565-573.

119. Vamvuka, D., S. Troulinos, and E. Kastanaki, *The effect of mineral matter on the physical and chemical activation of low rank coal and biomass materials.* Fuel, 2006. **85**(12-13): p. 1763-1771.

120. Rapagna, S. and A. Latif, *Steam gasification of almond shells in a fluidised bed reactor: the influence of temperature and particle size on product yield and distribution.* Biomass and Bioenergy, 1997. **12**(4): p. 281-288.

121. Suarez-Garcia, F., A. Martinez-Alonso, and J.M.D. Tascon, *Pyrolysis of apple pulp: effect of operation conditions and chemical additives.* Journal of Analytical and Applied Pyrolysis, 2002. **62**(1): p. 93-109.

122. Demirbas, A., *Utilization of Urban and Pulping Wastes to Produce Synthetic Fuel via Pyrolysis.* Energy Sources, Part A: Recovery, Utilization, and Environmental Effects, 2002. **24**(3): p. 205 - 213.

123. Lanzetta, M. and C. Di Blasi, *Pyrolysis kinetics of wheat and corn straw.* Journal of Analytical and Applied Pyrolysis, 1998. **44**(2): p. 181-192.

124. Raveendran, K., A. Ganesh, and K.C. Khilar, *Influence of mineral matter on biomass pyrolysis characteristics.* Fuel, 1995. **74**(12): p. 1812-1822.

125. Marsh, R., A.J. Griffiths, and K.P. Williams, *Measurement of heat transfer and change in compressive strength of waste derived solid fuels due to devolatisation.* Fuel, 2008. **87**(8-9): p. 1724-1733.

126. Guo, J. and A.C. Lua, *Kinetic study on pyrolytic process of oil-palm solid waste using two-step consecutive reaction model.* Biomass and Bioenergy, 2001. **20**(3): p. 223-233.

127. Ahuja, P., S. Kumar, and P.C. Singh, *Model for primary and heterogeneous secondary reactions of wood pyrolysis.* Chemical Engineering & Technology, 1996. **19**(3): p. 272-282.

128. Shuangning, X., et al., *Devolatilization characteristics of biomass at flash heating rate.* Fuel, 2006. **85**(5-6): p. 664-670.

129. Cetin, E., et al., *Influence of pyrolysis conditions on the structure and gasification reactivity of biomass chars.* Fuel, 2004. **83**(16): p. 2139-2150.

130. Rostami, A.A., M.R. Hajaligol, and S.E. Wrenn, *A biomass pyrolysis sub-model for CFD applications.* Fuel, 2004. **83**(11-12): p. 1519-1525.

131. Shen, D.K., et al., *Modeling pyrolysis of wet wood under external heat flux.* Fire Safety Journal, 2007. **42**(3): p. 210-217.

132. Cai, J., et al., *Thermogravimetric analysis and kinetics of coal/plastic blends during co-pyrolysis in nitrogen atmosphere.* Fuel Processing Technology, 2008. **89**(1): p. 21-27.

133. Yu, Y.H., et al., *Kinetic studies of dehydration, pyrolysis and combustion of paper sludge.* Energy, 2002. **27**(5): p. 457-469.

134. Sutcu, H., *Pyrolysis by thermogravimetric analysis of blends of peat with coals of different characteristics and biomass.* Journal of the Chinese Institute of Chemical Engineers, 2007. **38**(3-4): p. 245-249.

Appendix Risk Assessment

UNIVERSITY OF GLAMORGAN
PRIFYSGOL MORGANNWG

RISK ASSESSMENT

Department	**Engineering**	Location/Room No	**G116**
Brief Summary of Work Activity	**Electric tube furnace:** **Used to heat specimens to temperatures up to 1000*C**		
List Significant Hazards	The specimen will be very hot up to 1000*C when coming out of the furnace and will cause burns if it comes into contact with skin or eyes Some specimens may give off harmful fumes at high temperatures		
List Who might be exposed to the Hazards	**The people operating the equipment**		
List Existing Control Measures	Only people with training may operate this equipment. Protective clothing must be worn, to protect eyes and hands and any other exposed body parts Local extraction is also available *Signage.*		
Residual Risk - High, Medium or Low	**low**		

Are risks adequately controlled? YES *☐ NO ☐

If NO list additional controls/action required below to eliminate risk or reduce so that it is LOW and who is responsible for implementation

Additional Control Measures	Action to be taken by	Implementation Date

Signature of Assessor		**Date:** 7/7/09

Are risks adequately controlled (LOW) following implementation of control measures? YES ☐ NO ☐

Signature of Head of Department	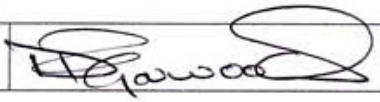	**Date:** 17/7/09

Date for Review (maximum 12 months from date of assessment)	